ESSO EXPLORATION JUBA S.A.

AIRBORNE MAGNETOMETER SURVEY 1984
SOMALI DEMOCRATIC REPUBLIC

Hunting

HUNTING GEOLOGY AND GEOPHYSICS LIMITED

R 755A

Hunting Copy

HUNTING GEOLOGY AND GEOPHYSICS LIMITED

A division of Hunting Surveys and Consultants Limited

ELSTREE WAY - BOREHAM WOOD - HERTS - WD6 1SB - ENGLAND
(Registered Office)

Telephone: 01-953 6161 Telex: 23517 HUNBOR G Cables: ASTEREO BOREHAMWOOD

Applied Geological and Geophysical Services

ESSO EXPLORATION INC.,
P.O. Box 146,
Houston,
Texas 77001,
United States of America.

Attention: O.Fox, R. Brotherton.

31st May, 1985

Subject: **Extra Work - Somalia**
Aeromagnetic Interpretation

Comparison of Hunting's magnetic interpretation and ESSO's preliminary seismic data, has suggested that a review of magnetic interpretation would be useful, within two localities in particular. For this purpose ESSO provided Hunting with two seismic sections, SO-4B-30 and SO-4A-80, upon which ESSO has marked interpreted acoustic basement. A shot-point location map has also been provided. Assuming that acoustic and magnetic basements are identical (although not necessarily true, both 'basement' surfaces can be reasonably expected to parallel each other) Hunting's task was to remodel magnetic profiles 1035/A, 126/1 and JJ' constrained by the basement structure indicated by the seismic data. The re-modelled profiles and intermediate modelling stages are attached to this report. Points at which depths are constrained, that is, at intersections (or points of close proximity) with the seismic sections, are ticked in red. Modelled profile JJ' lies in the west of Block 2 and intersects seismic line SO-4B-30. Modelled profiles 1035/A and 126/1 lie within the northern half of Block 1 and intersect seismic line SO-4A-80.

The initial models for both JJ' and 1035/A have been performed assuming constant susceptibility. Clearly the gross disparity of modelled and observed data in both cases suggests that basement is of non-uniform magnetic composition. It appears likely that this situation is the norm rather than the exception for the survey area as a whole.

PROFILE JJ'

Initial Non-uniform magnetic basement composition is indicated by the gross disparity of observed and modelled profiles.

Interim 1 The northwest end of the profile is lengthened using dummy observed values. A banding of magnetic susceptibilities is introduced. For a best fit, contacts are required to dip to the northwest.

Directors D. T. SINKER, BA, FCA, Chairman D. B. MORRIS, MSc, Managing P. A. RANKIN, DFC, BSc, C.Eng, FIMM D. B. TIPPER, BSc, C.Eng, FIMM W. A. WILLOX, BSc, C.Eng, FIMM
Associate Directors J. P. CROOK, BSc, C.Eng, FIMM E. R. PETERS, BSc, MIMM J. G. POTTS, Ph.D, C.Eng, FIMM
Consultant P. H. A. MARTIN-KAYE, Ph.D, FIMM

Registered Number 458841 England

Interim 2 Addition of further magnetic band.

Interim 3 The southeast of the profile is lengthened using dummy observed values. To obtain a more satisfactory fit in the southeast, a more graduated magnetic composition appears necessary. Further magnetic banding is therefore added in the southeast.

Interim 4 Magnetic susceptibilities are raised 'all round' and banding widened in the southeast to approach a better fit.

Interim 5 A further magnetic band is added in the southeast, and with re-adjusted susceptibilities, results in a very satisfactory fit.

Final A small drop of susceptibility values 'all round' improves the fit.

Seismically constrained modelling of profile JJ' suggests therefore, that basement is of a highly graduated magnetic composition and in the vicinity of the basin (northwestern half), is generally of high magnetic susceptibility. A change to a significantly less magnetic basement is suggested at the southeast of the profile in order to explain the steep magnetic gradient in this region.

PROFILE 1035/A

Initial Non-uniform magnetic basement composition is indicated by the gross disparity of observed and modelled profiles.

Interim 1 A banding of magnetic susceptibilities is introduced. For best fit, contacts are found to require southeastward dip.

Interim 2 Addition of further magnetic bands.

Interim 3 Vertically sided low susceptibility body in the northwest results in best fit of the steep gradient in this region. Susceptibility values are adjusted.

Interim 4 Further susceptibility adjustments generate better fit in the northwest.

Interim 5 Addition of fault, present on the seismic section disrupts the fit slightly.

Final Retaining the fault but reducing susceptibilities 'all round' by 0.0001 cgs (thereby reducing the vertical sided body in the northwest to zero susceptibility) produces the best overall fit.

Seismically constrained modelling of profile 1035/A therefore suggests that basement composition is magnetically highly graduated, though apparently not quite as marked as basement in the vicinity of profile JJ', Block 2. Basement susceptibility appears to increase steadily from northwest to southeast, from 0 to 0.0032 cgs (ignoring the end units which are regarded with less certainty). The sharper characteristics of the re-modelled profile with respect to the observed suggests that in this case, acoustic basement may lie at a significantly shallower depth than magnetic basement.

PROFILE 126/1

Profile 126/1 intersects 1035/A within the interpreted 0.0025 cgs unit. This value, the corresponding depth on 1035/A and the seismic depth at the intersection with 126/1 have been used to constrain the re-modelling of profile 126/1.

Original Already, the depth match at the intersection with profile 1035/A, is close.

Interim 1 Susceptibility value of model is changed to 0.0025 cgs.

Interim 2 Possibility of no fault at the 1035/A intersection is entertained.

Final Fault reappears to the northeast of original position which allows very good fit with both profile 1035/A and intersecting seismic line SO-4A-80.

The original interpretation across the proposed Hiran Graben is therefore not compromised. Basement high H1 however must be regarded as spurious as a result of the re-modelling of 1035/A. In the absence of H1, magnetic basement depth may now be re-contoured to reflect the Hiran Graben structure directly.

Vestone

V. Stone,
Geophysicist.

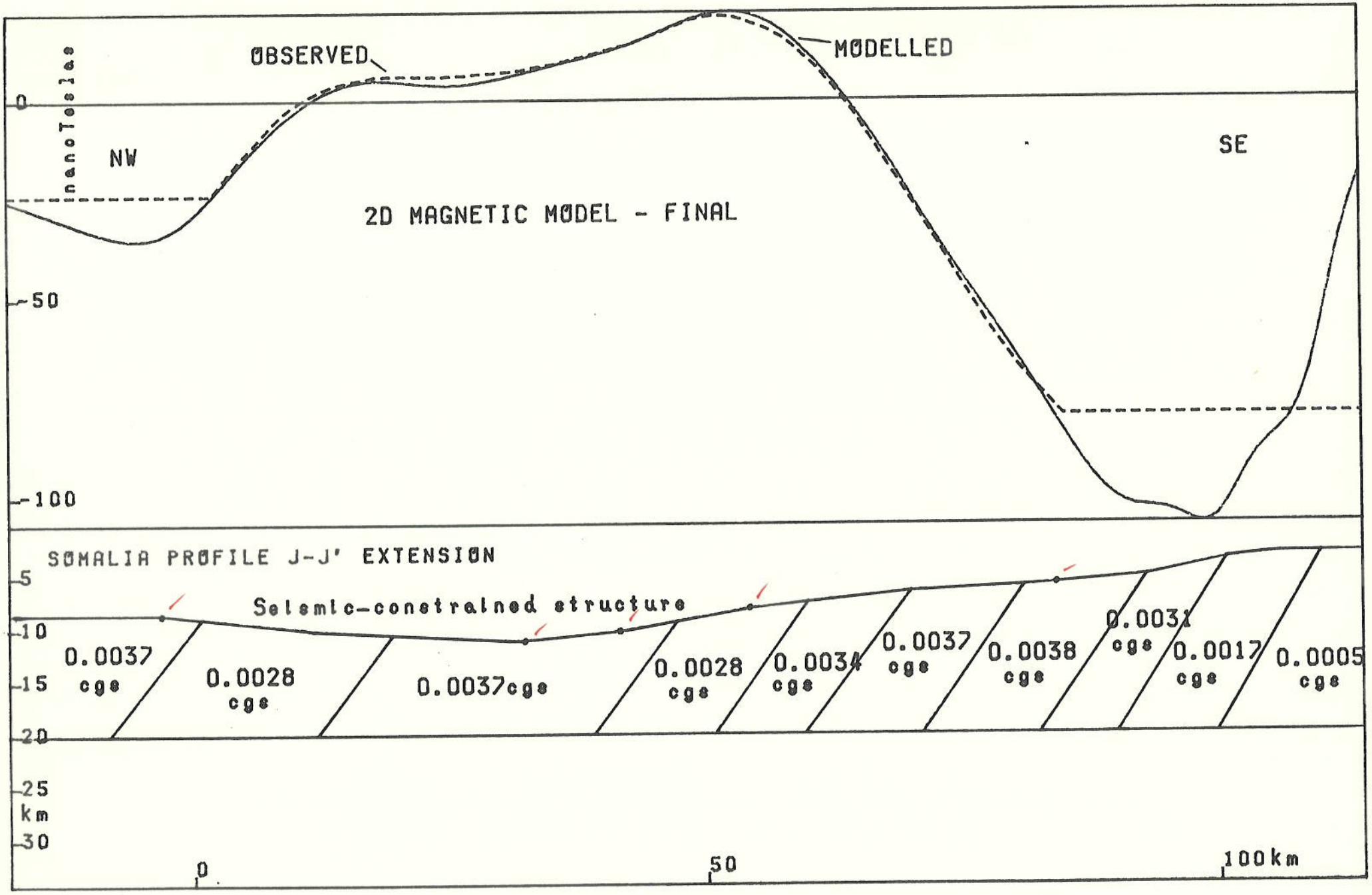
OBSERVED
MODELLED
nanoTeslas
0
NW
SE
2D MAGNETIC MODEL - FINAL
-50
-100
SOMALIA PROFILE J-J' EXTENSION
5
Seismic-constrained structure
10
15
20
25
km
30
0.0037 cgs
0.0028 cgs
0.0037cgs
0.0028 cgs
0.0034 cgs
0.0037 cgs
0.0038 cgs
0.0031 cgs
0.0017 cgs
0.0005 cgs
0
50
100km

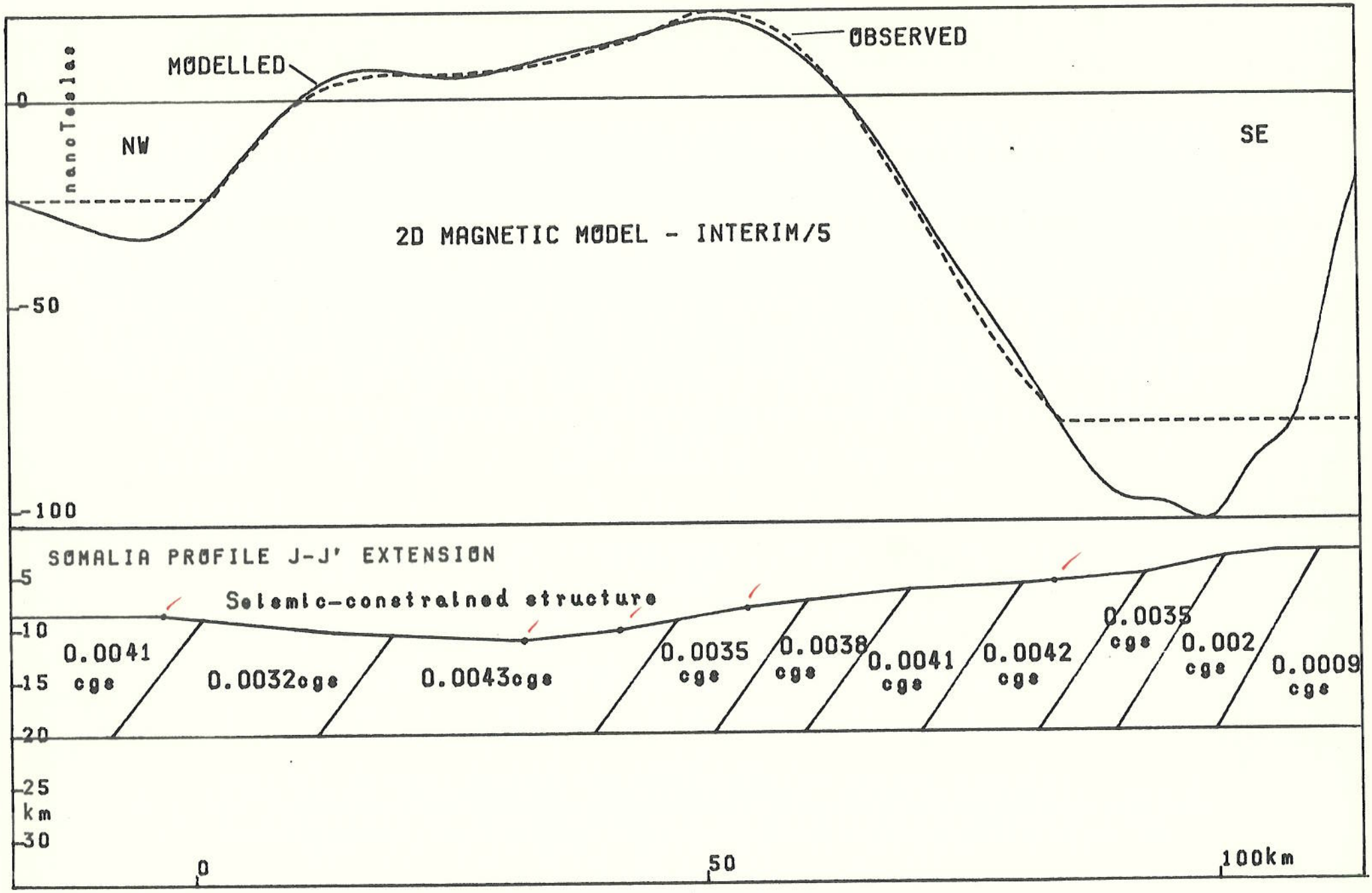
MODELLED
OBSERVED
nanoTeslas
0
NW
SE
2D MAGNETIC MODEL - INTERIM/5
-50
-100
SOMALIA PROFILE J-J' EXTENSION
Seismic-constrained structure
5
10
15
20
25
km
30
0.0041 cgs
0.0032cgs
0.0043cgs
0.0035 cgs
0.0038 cgs
0.0041 cgs
0.0042 cgs
0.0035 cgs
0.002 cgs
0.0009 cgs
0
50
100km

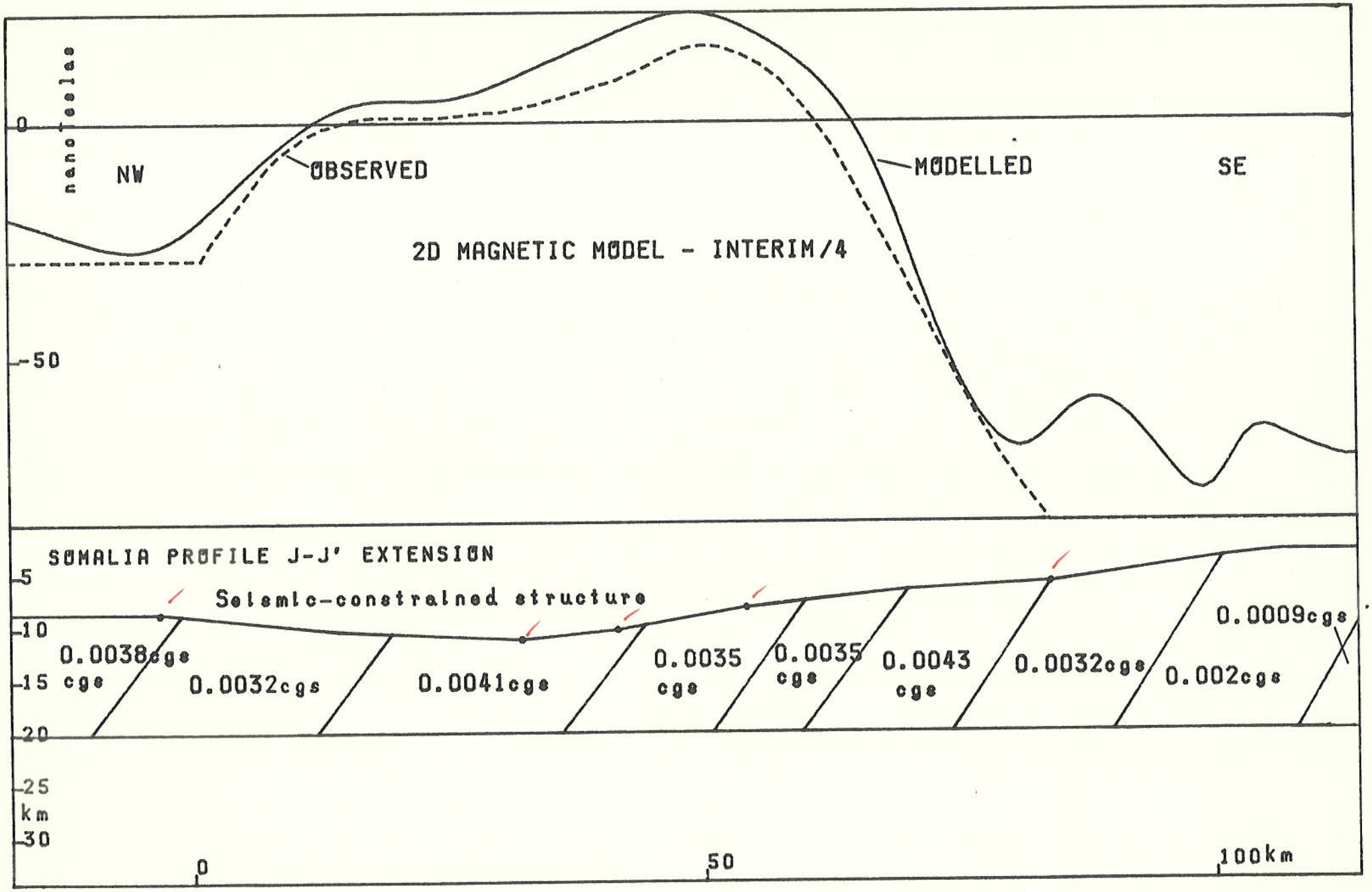
nanoteslas
0
-50
NW
OBSERVED
MODELLED
SE
2D MAGNETIC MODEL - INTERIM/4
SOMALIA PROFILE J-J' EXTENSION
Seismic-constrained structure
5
10
15
20
25
km
30
0.0038cgs
cgs
0.0032cgs
0.0041cgs
0.0035
cgs
0.0035
cgs
0.0043
cgs
0.0032cgs
0.002cgs
0.0009cgs
0
50
100km

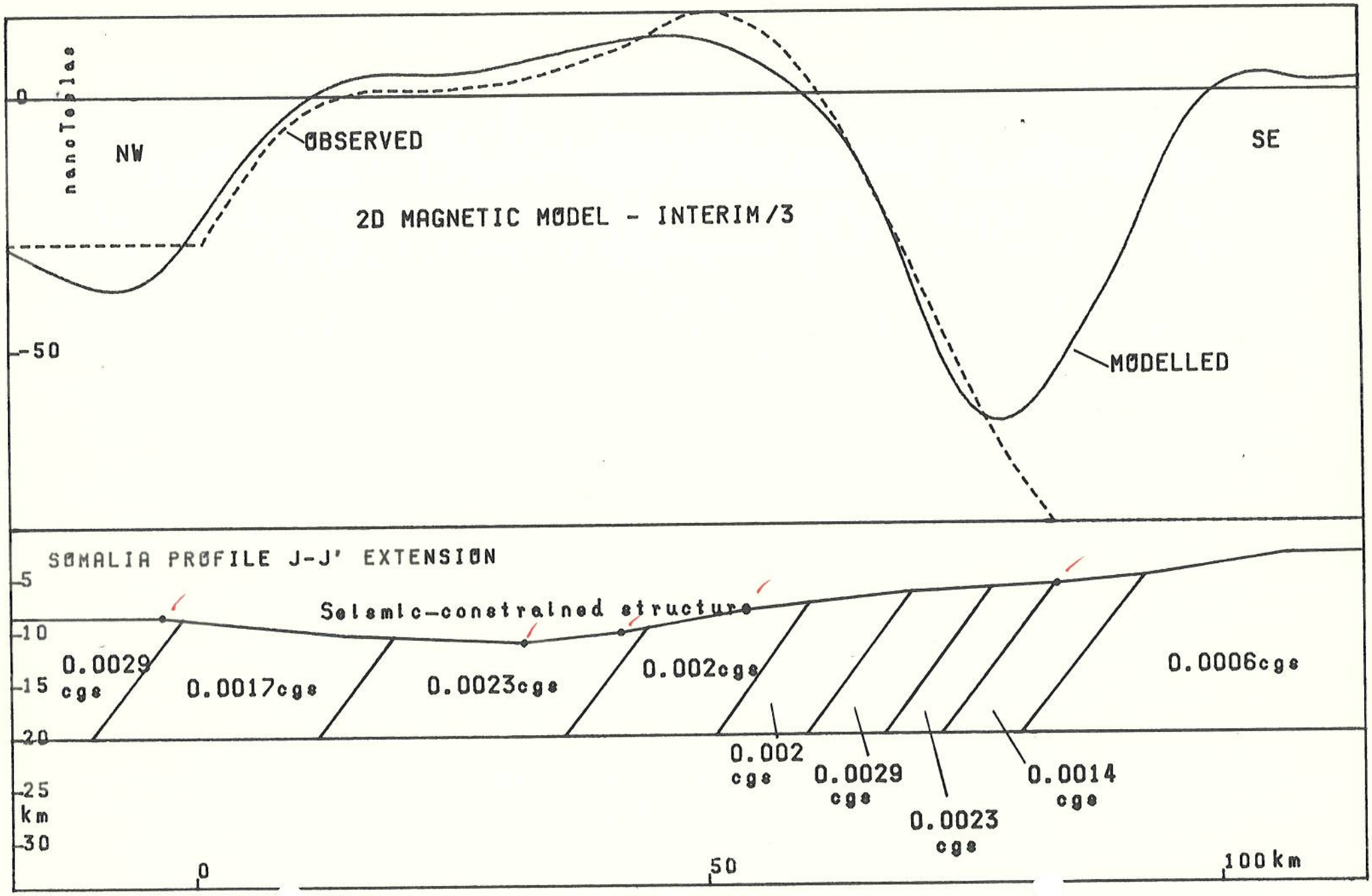
nanoTeslas
0
-50
NW
SE
OBSERVED
MODELLED
2D MAGNETIC MODEL - INTERIM/3
SOMALIA PROFILE J-J' EXTENSION
Seismic-constrained structure
-5
-10
-15
-20
-25
km
-30
0.0029 cgs
0.0017cgs
0.0023cgs
0.002cgs
0.0006cgs
0.002 cgs
0.0029 cgs
0.0023 cgs
0.0014 cgs
0
50
100km

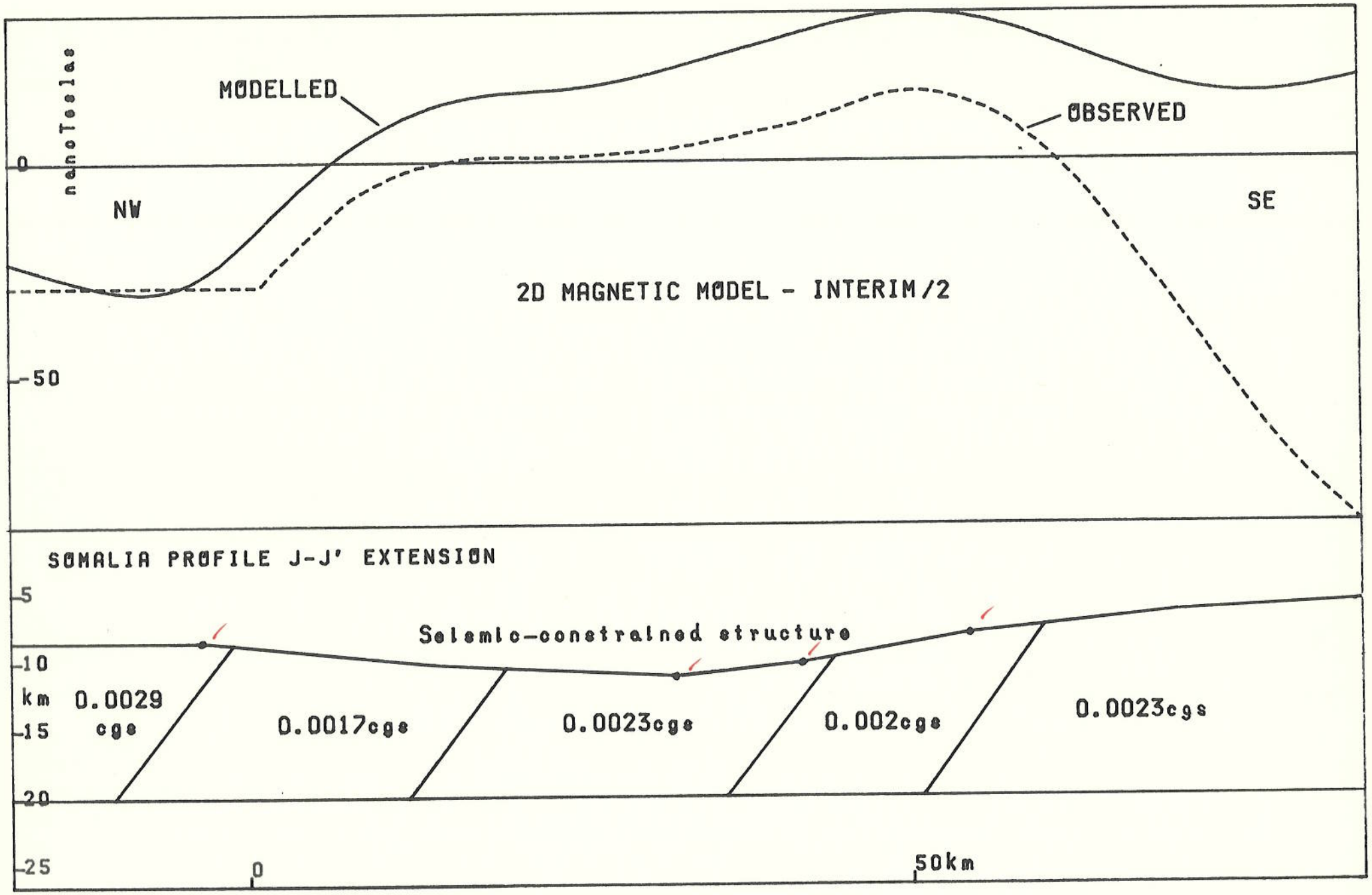
nanoTeslas
MODELLED
OBSERVED
0
NW
SE
2D MAGNETIC MODEL - INTERIM/2
-50
SOMALIA PROFILE J-J' EXTENSION
5
Seismic-constrained structure
10
km
15
20
25
0.0029
cgs
0.0017cgs
0.0023cgs
0.002cgs
0.0023cgs
0
50km

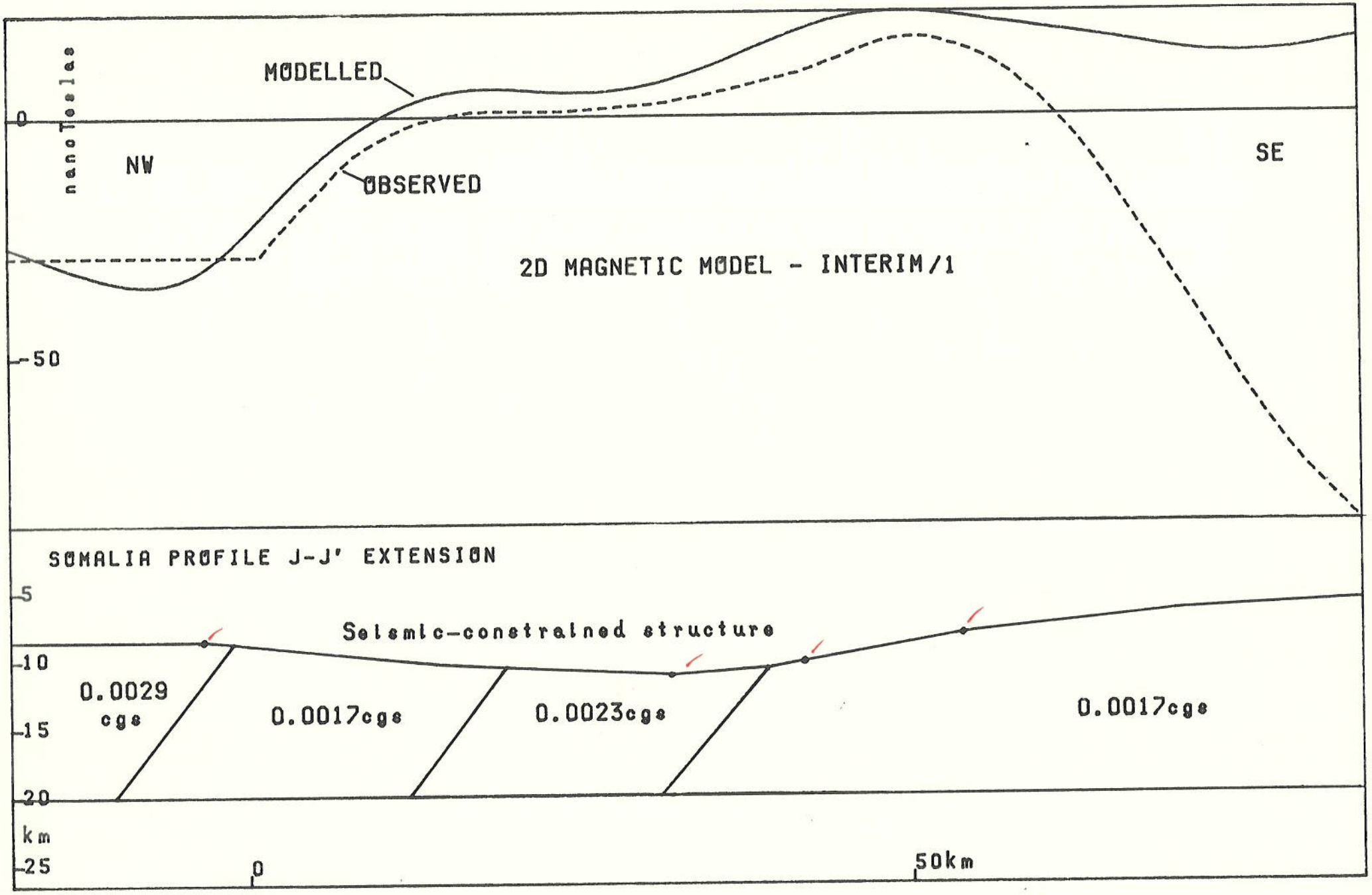
MODELLED
OBSERVED
nanoTeslas
0
-50
NW
SE
2D MAGNETIC MODEL - INTERIM/1
SOMALIA PROFILE J-J' EXTENSION
Seismic-constrained structure
5
10
15
20
km
25
0.0029
cgs
0.0017cgs
0.0023cgs
0.0017cgs
0
50km

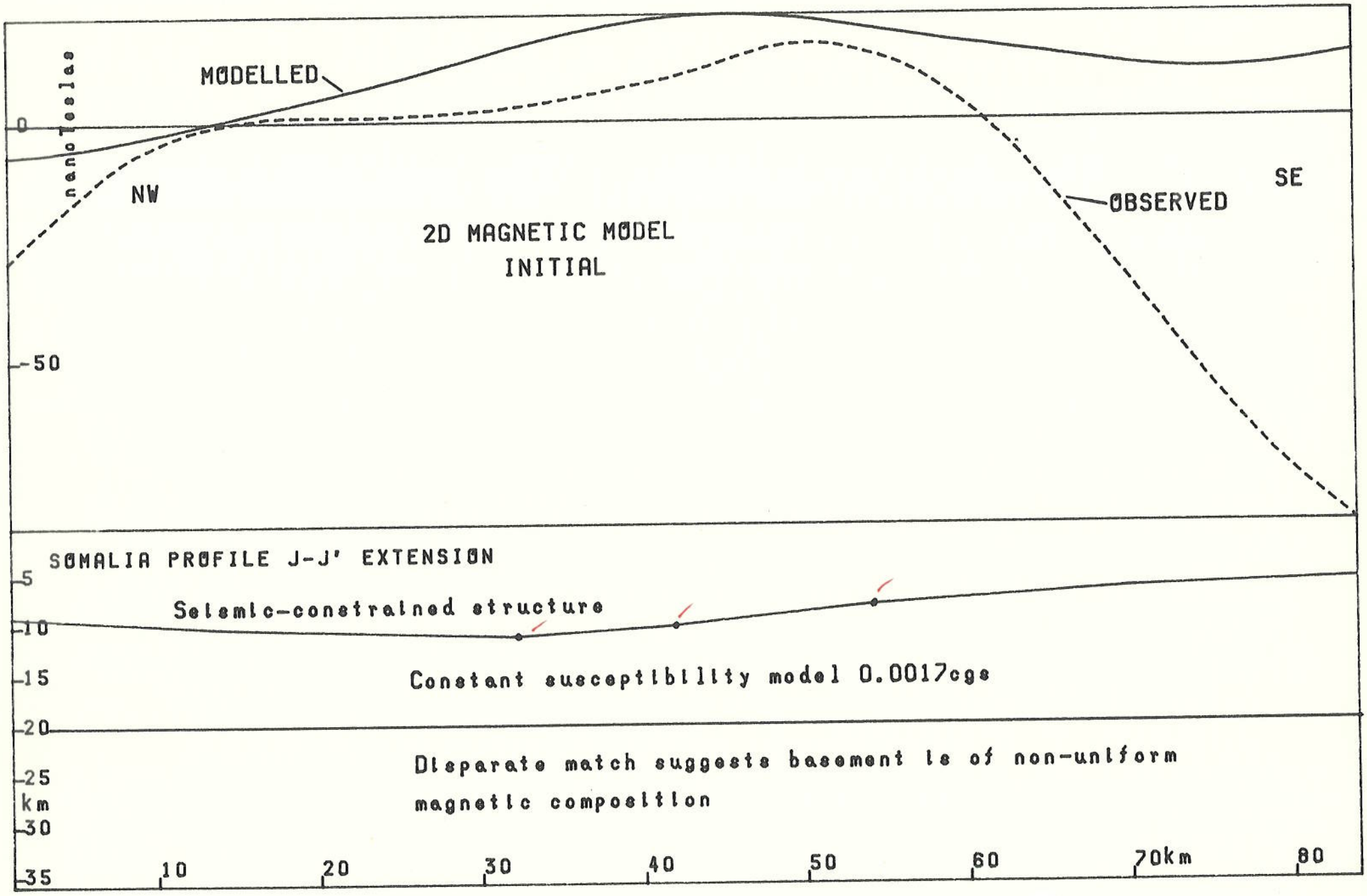
MODELLED
nanoTeslas
0
NW
SE
OBSERVED
2D MAGNETIC MODEL
INITIAL
-50
SOMALIA PROFILE J-J' EXTENSION
5
Seismic-constrained structure
10
15
Constant susceptibility model 0.0017cgs
20
Disparate match suggests basement is of non-uniform
25
km
magnetic composition
30
35
10
20
30
40
50
60
70km
80

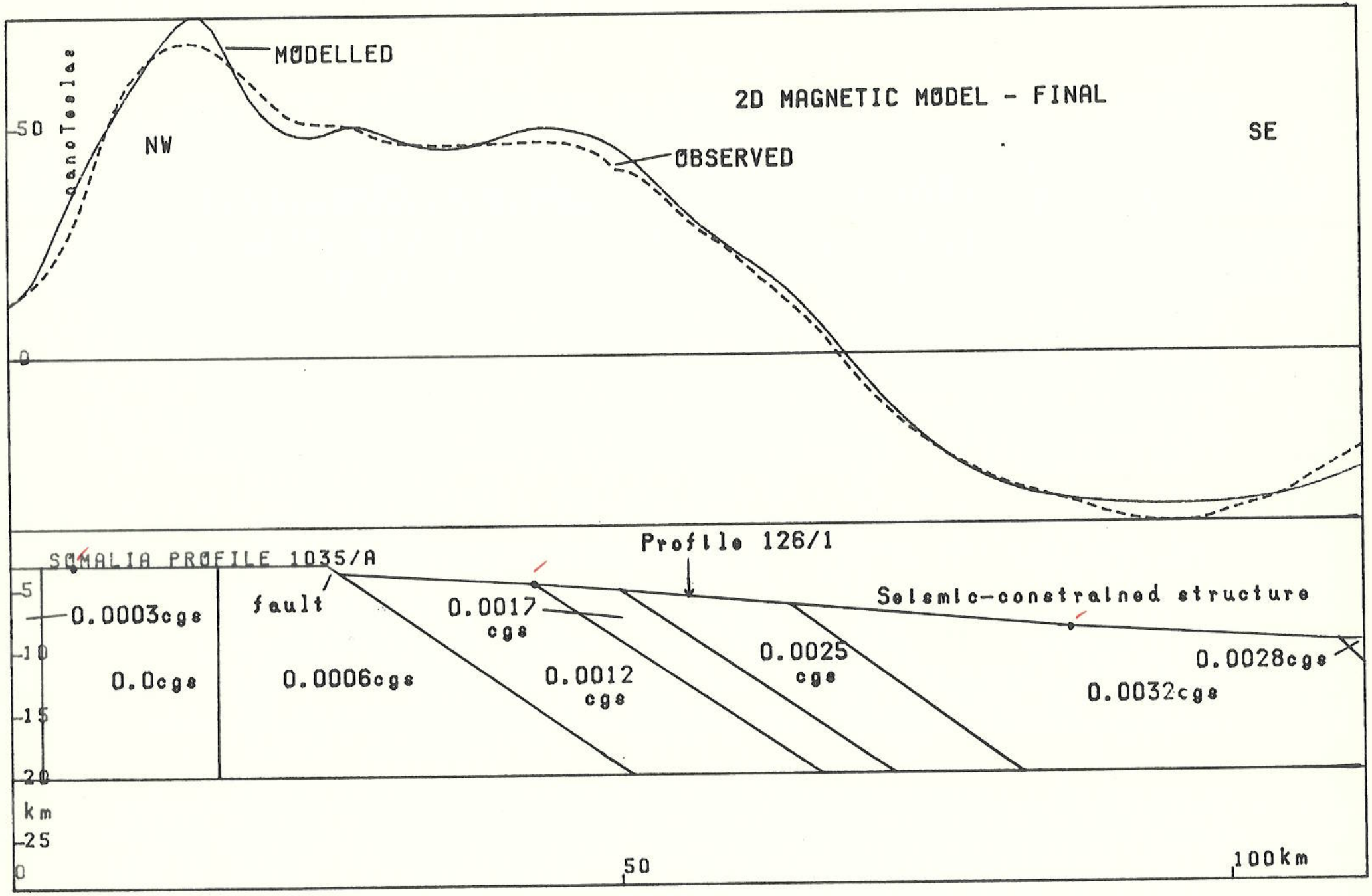
MODELLED
2D MAGNETIC MODEL - FINAL
nanoTeslas
50
NW
SE
OBSERVED
0
SOMALIA PROFILE 1035/A
Profile 126/1
Seismic-constrained structure
5
0.0003cgs
fault
0.0017
cgs
10
0.0cgs
0.0006cgs
0.0012
cgs
0.0025
cgs
0.0028cgs
0.0032cgs
15
20
km
25
0
50
100km

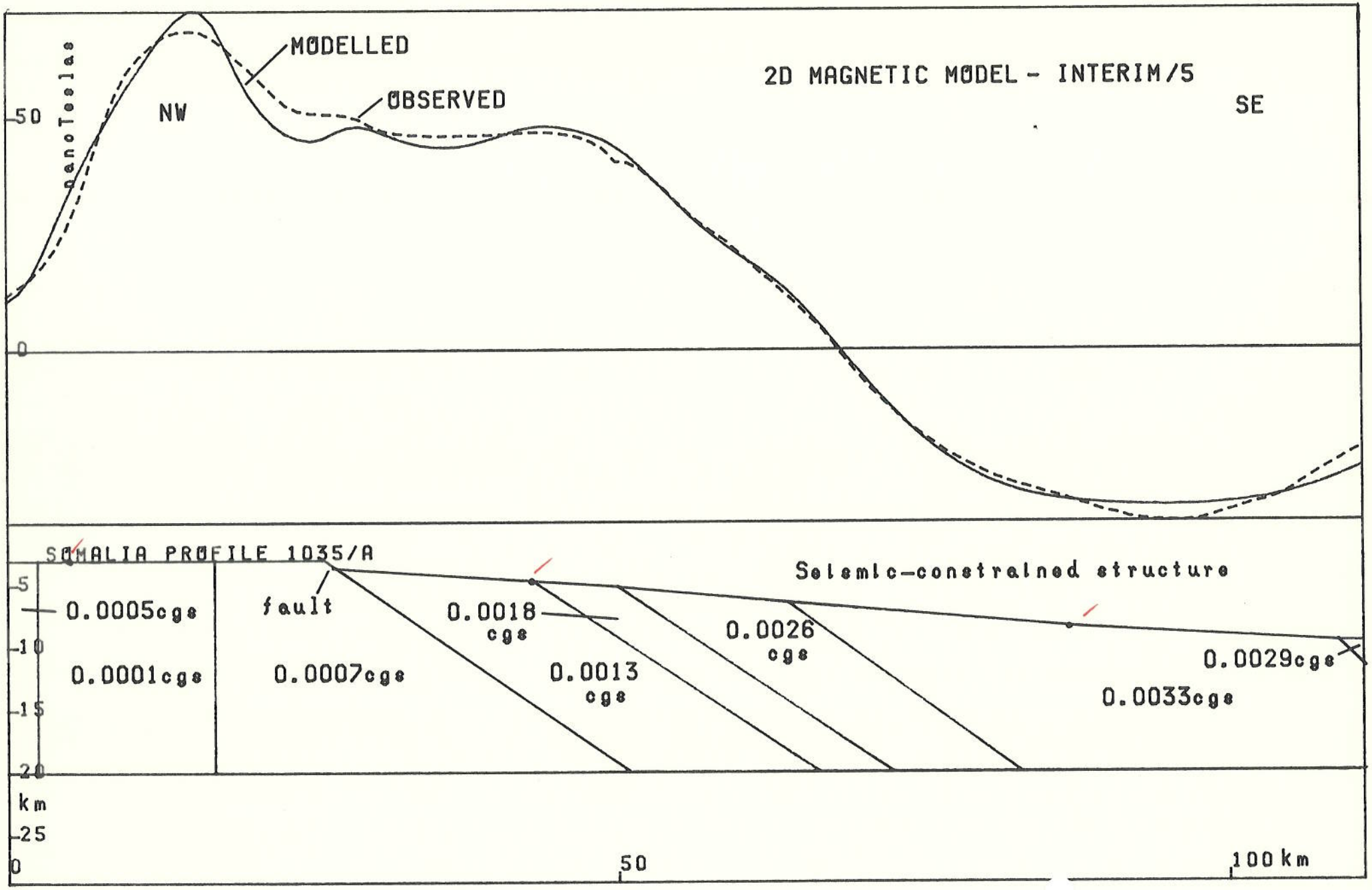
2D MAGNETIC MODEL - INTERIM/5
MODELLED
OBSERVED
NW
SE
nanoTeslas
50
0
SOMALIA PROFILE 1035/A
Seismic-constrained structure
fault
0.0005cgs
0.0001cgs
0.0007cgs
0.0018 cgs
0.0013 cgs
0.0026 cgs
0.0029cgs
0.0033cgs
5
10
15
20
km
25
0
50
100 km

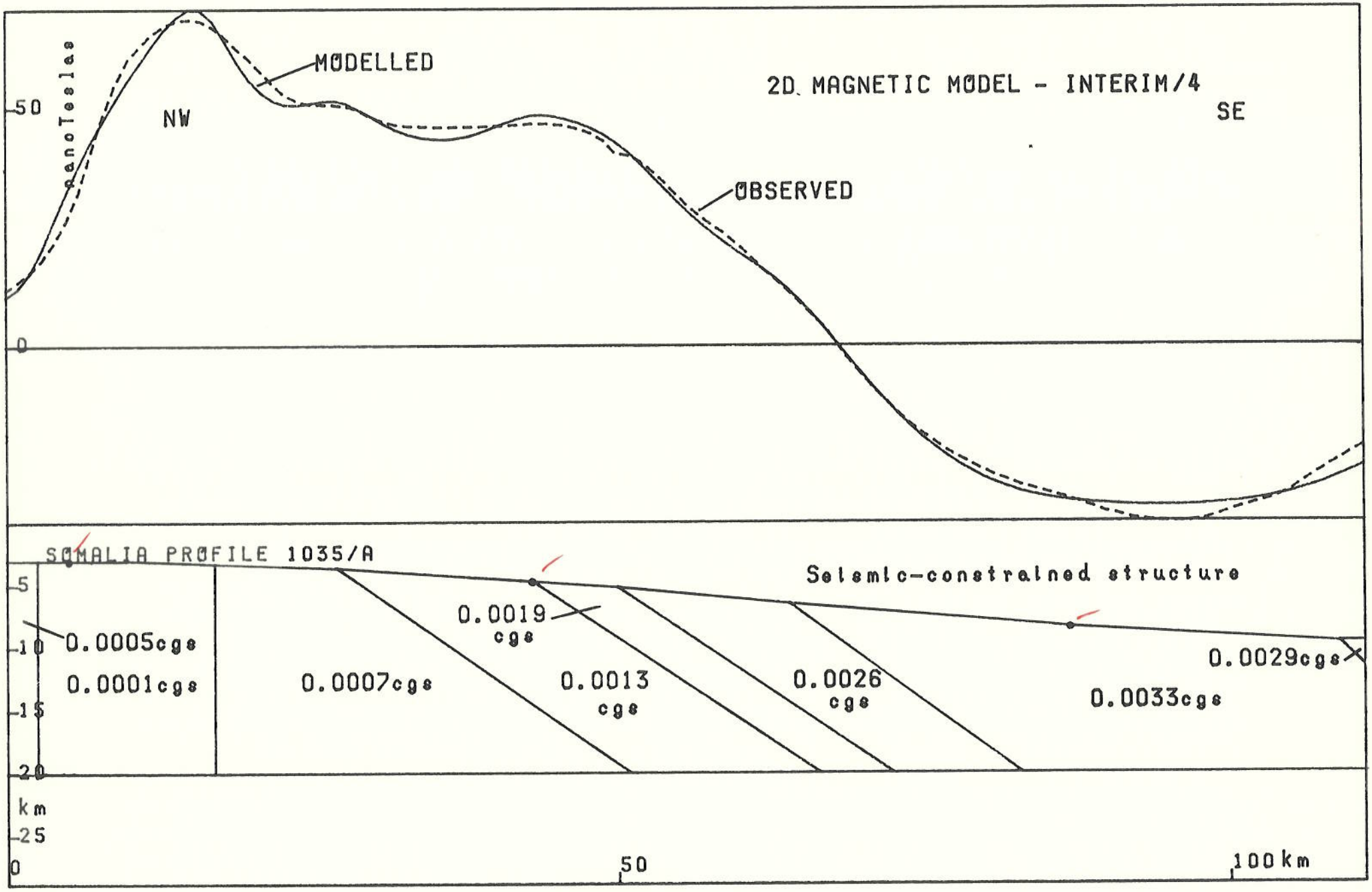
2D MAGNETIC MODEL - INTERIM/4
MODELLED
OBSERVED
NW
SE
nanoTeslas
50
0
SOMALIA PROFILE 1035/A
Seismic-constrained structure
0.0005cgs
0.0001cgs
0.0007cgs
0.0019 cgs
0.0013 cgs
0.0026 cgs
0.0033cgs
0.0029cgs
5
10
15
20
km
25
0
50
100km

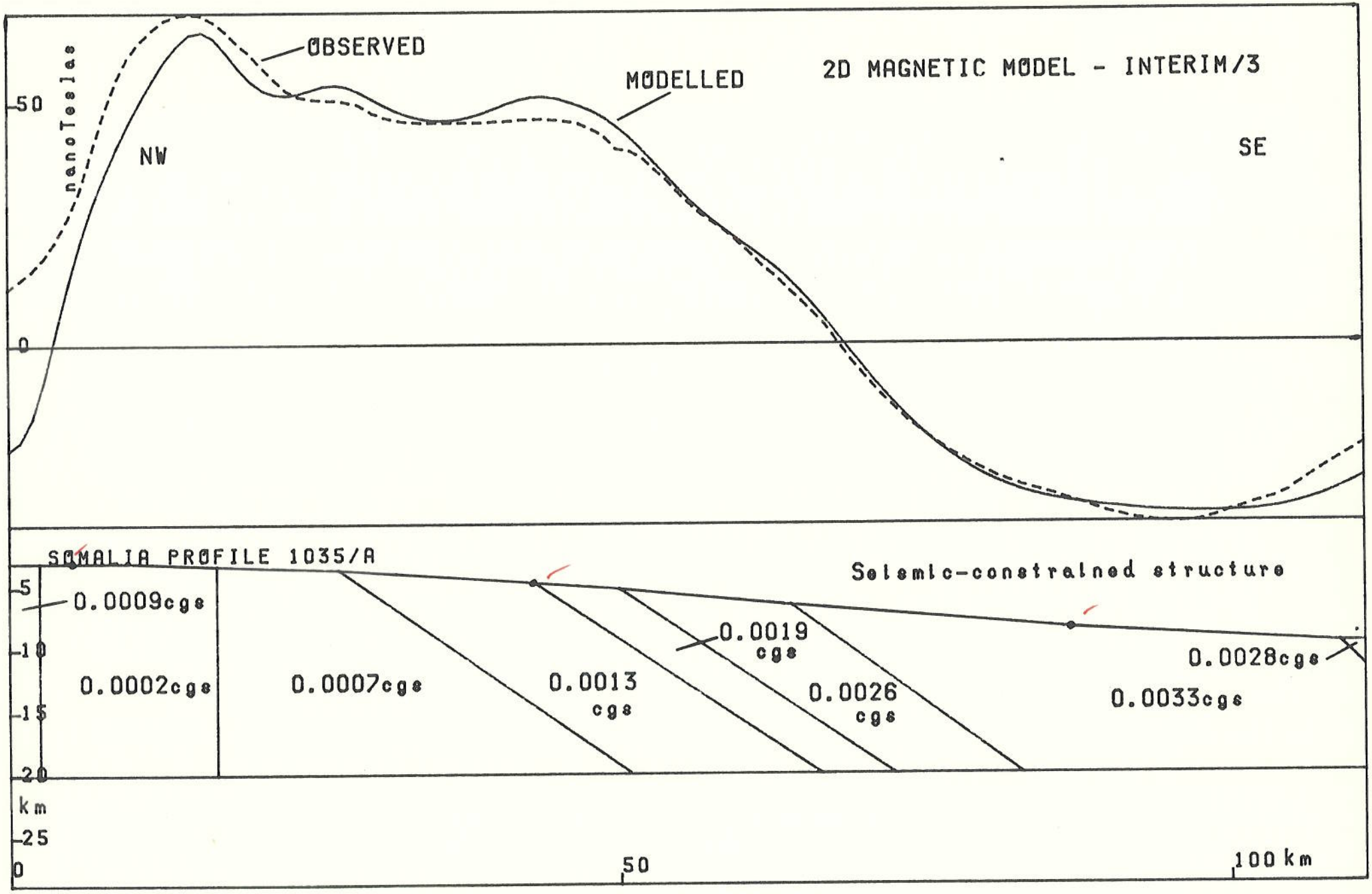
2D MAGNETIC MODEL - INTERIM/3
OBSERVED
MODELLED
NW
SE
nanoTeslas
50
0
SOMALIA PROFILE 1035/A
Seismic-constrained structure
0.0009cgs
0.0002cgs
0.0007cgs
0.0013 cgs
0.0019 cgs
0.0026 cgs
0.0028cgs
0.0033cgs
5
10
15
20
km
25
0
50
100 km

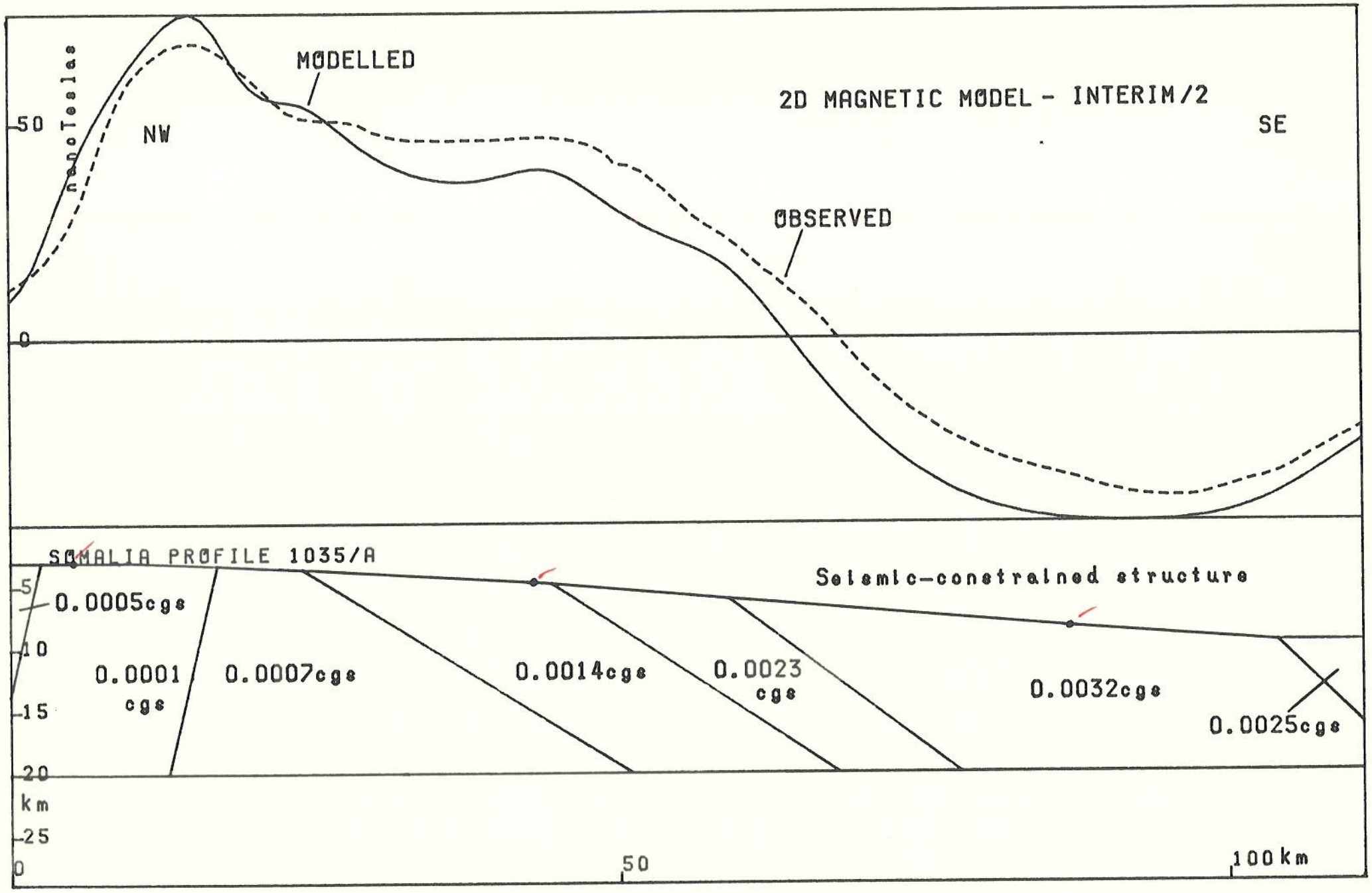
2D MAGNETIC MODEL - INTERIM/2
MODELLED
OBSERVED
NW
SE
nanoTeslas
50
0
SOMALIA PROFILE 1035/A
Seismic-constrained structure
0.0005cgs
0.0001 cgs
0.0007cgs
0.0014cgs
0.0023 cgs
0.0032cgs
0.0025cgs
5
10
15
20
km
25
0
50
100km

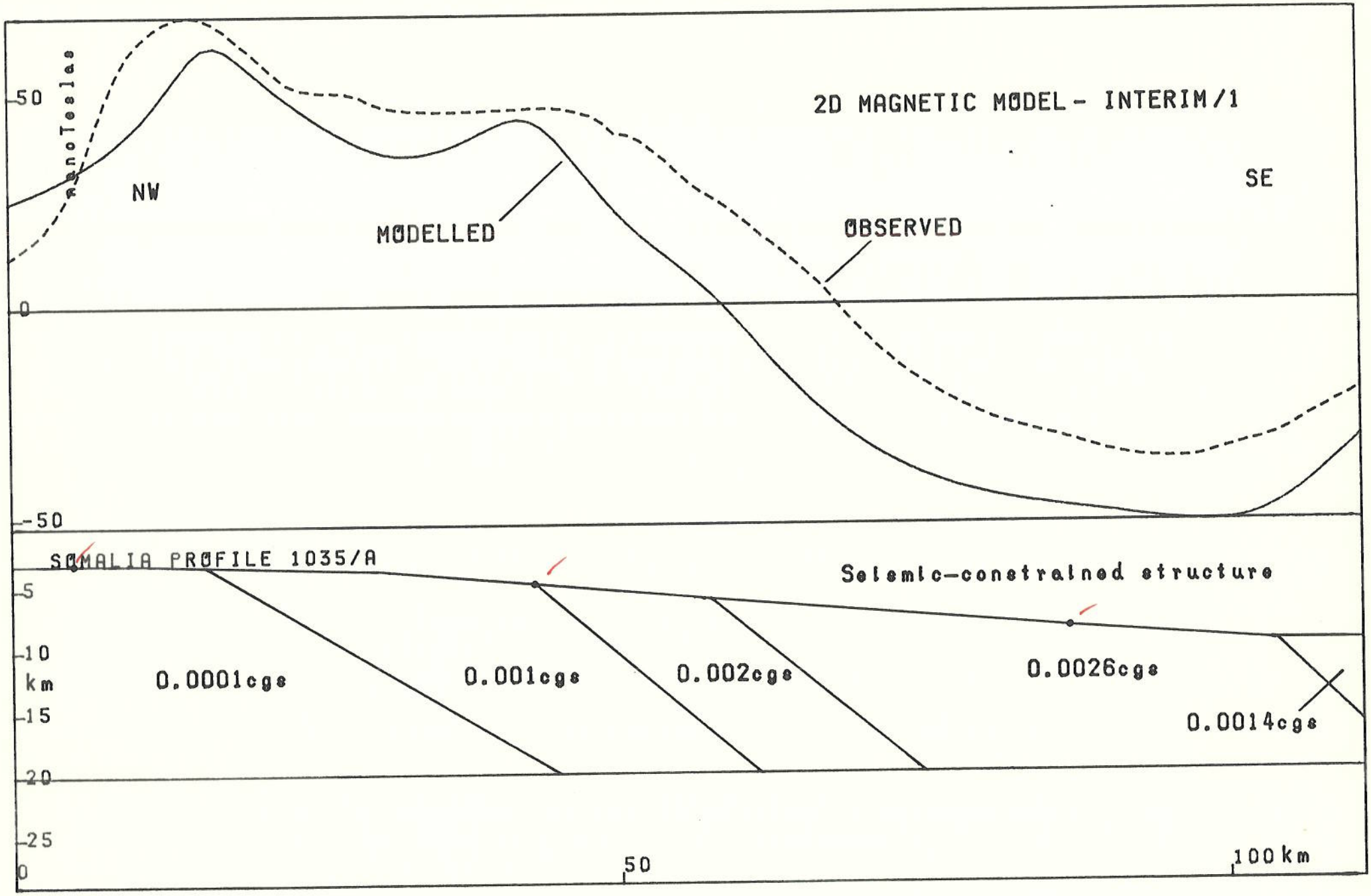
2D MAGNETIC MODEL - INTERIM/1
nanoTeslas
50
0
-50
NW
SE
MODELLED
OBSERVED
SOMALIA PROFILE 1035/A
Seismic-constrained structure
5
10
km
15
20
25
0
50
100 km
0.0001cgs
0.001cgs
0.002cgs
0.0026cgs
0.0014cgs

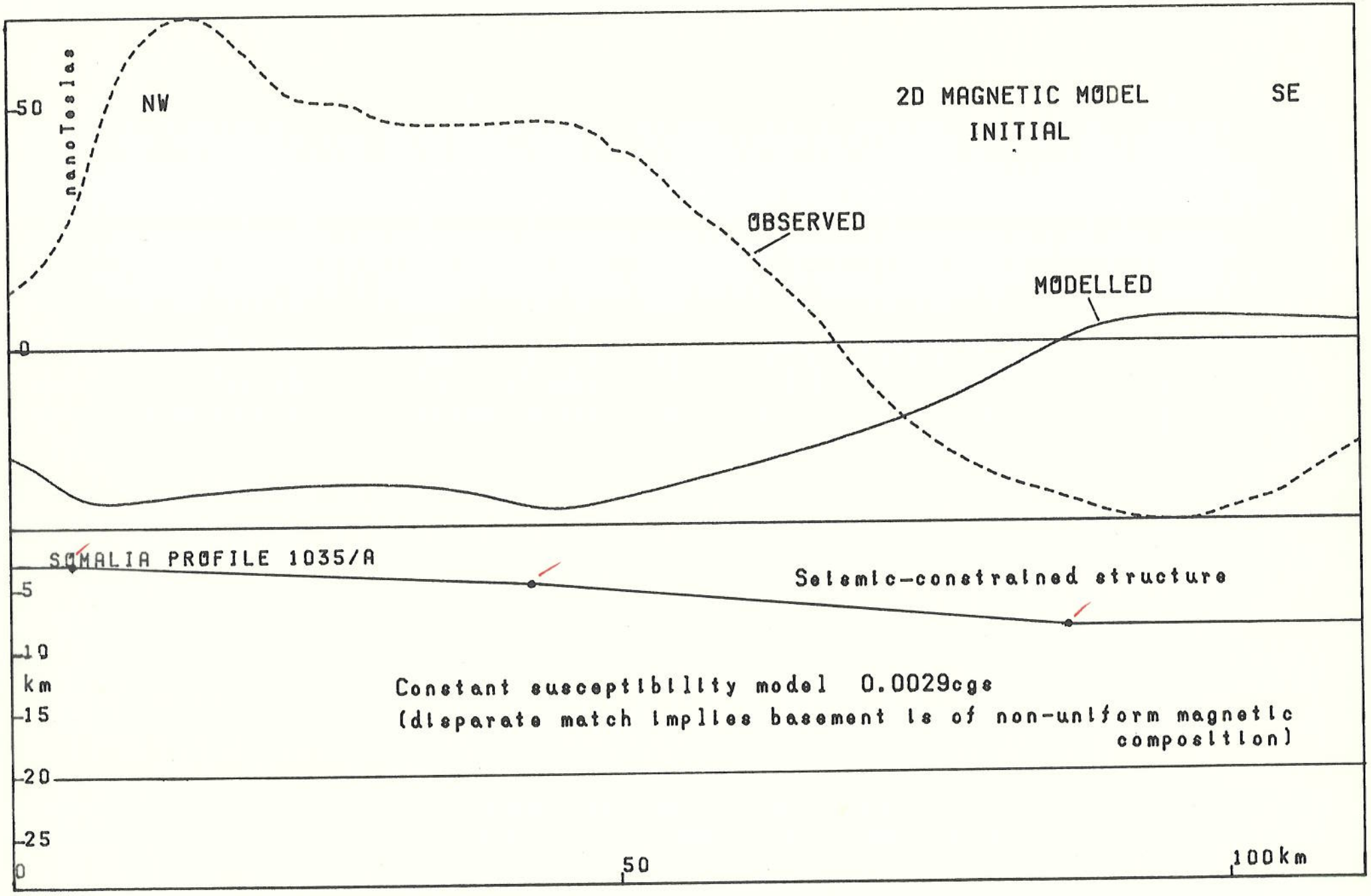
2D MAGNETIC MODEL
INITIAL
NW
SE
nanoTeslas
50
0
OBSERVED
MODELLED
SOMALIA PROFILE 1035/A
Seismic-constrained structure
5
10
km
15
20
25
0
50
100km
Constant susceptibility model 0.0029cgs
(disparate match implies basement is of non-uniform magnetic composition)

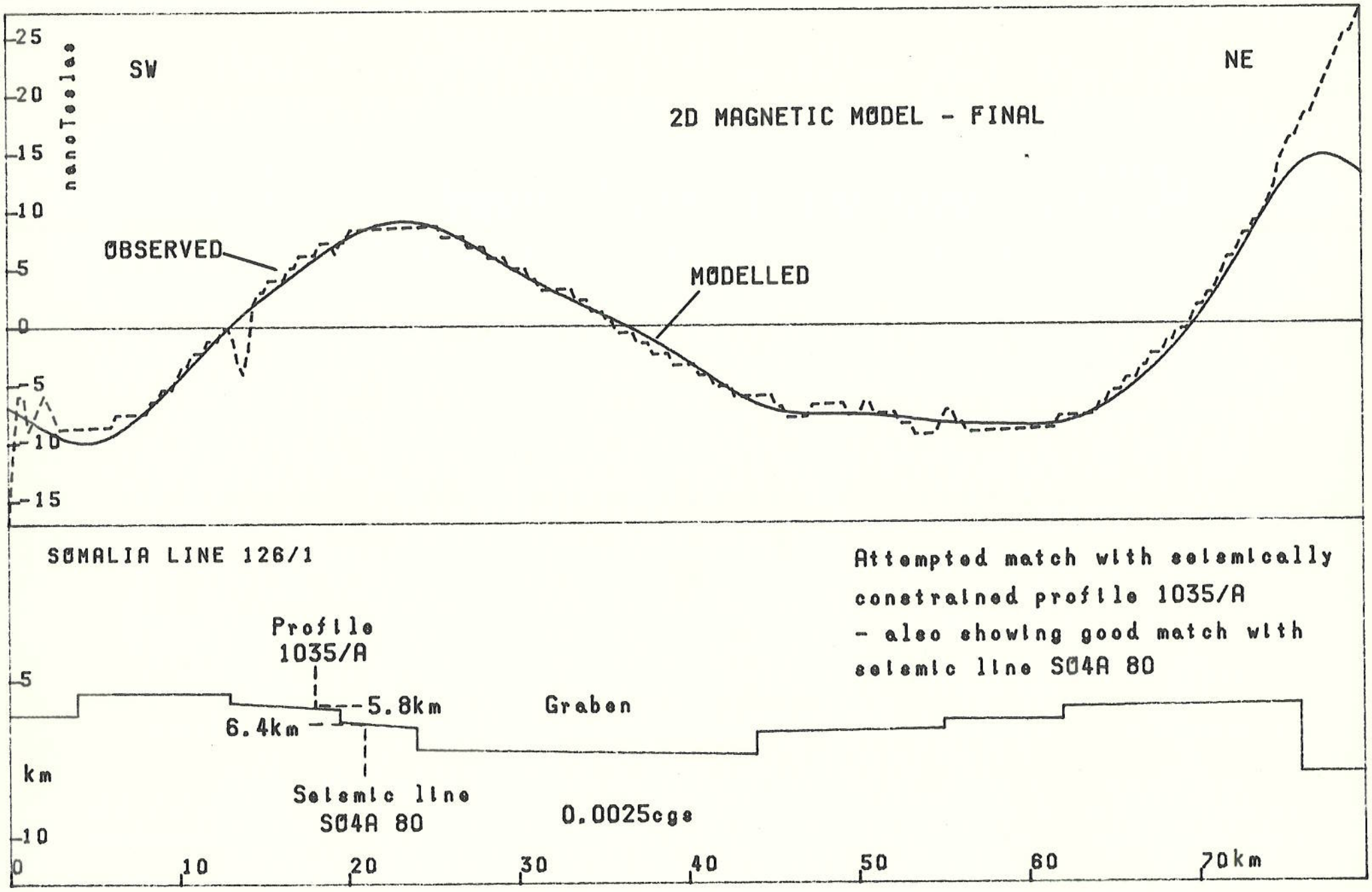
SW
NE
2D MAGNETIC MODEL - FINAL
nanoTeslas
25
20
15
10
5
0
-5
-10
-15
OBSERVED
MODELLED
SOMALIA LINE 126/1
Attempted match with seismically constrained profile 1035/A
- also showing good match with seismic line S04A 80
Profile
1035/A
5.8km
6.4km
Graben
km
Seismic line
S04A 80
0.0025cgs
0
10
20
30
40
50
60
70km

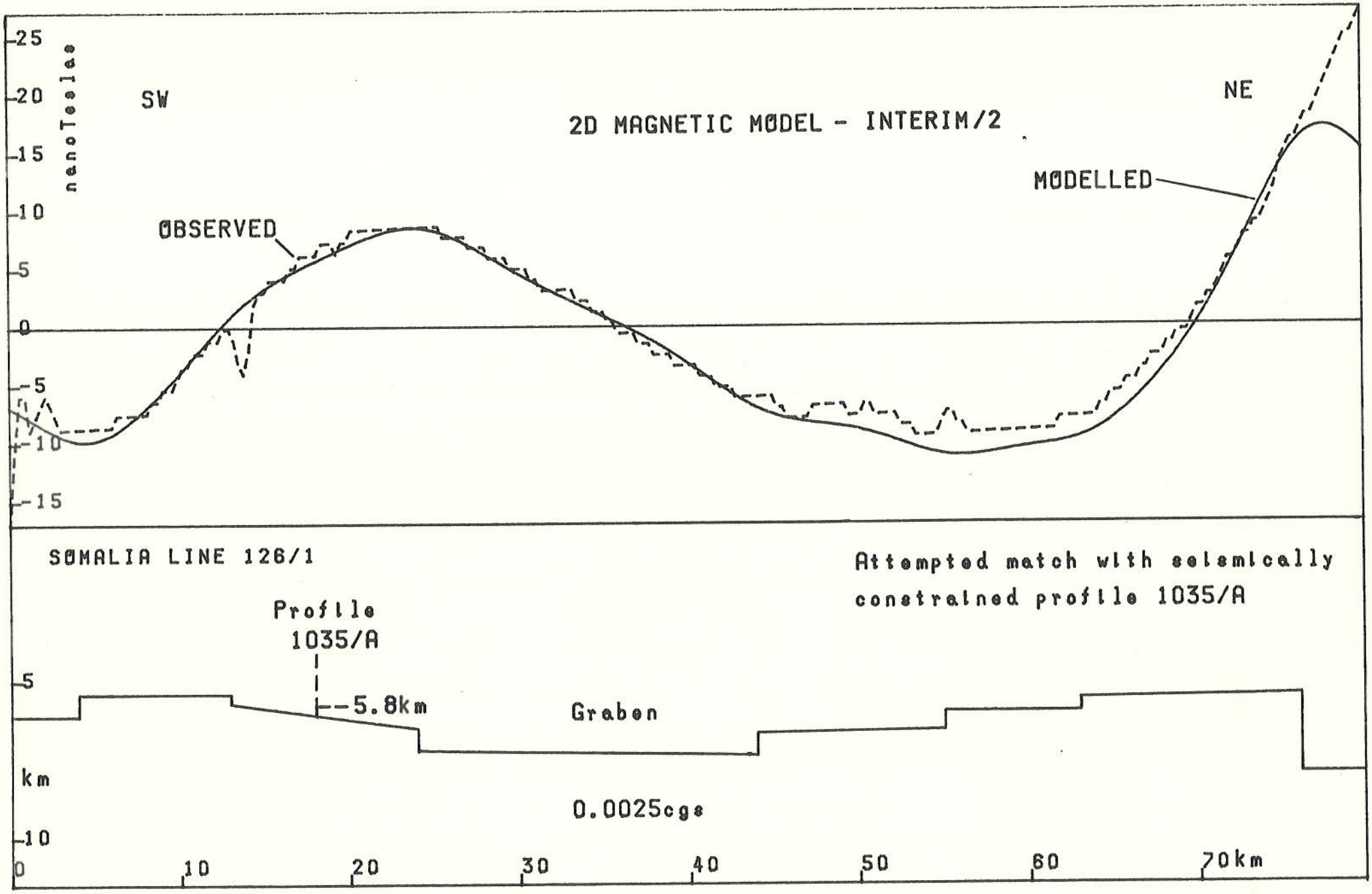
2D MAGNETIC MODEL - INTERIM/2
SW
NE
nanoTeslas
25
20
15
10
5
0
-5
-10
-15
OBSERVED
MODELLED
SOMALIA LINE 126/1
Attempted match with seismically constrained profile 1035/A
Profile 1035/A
5.8km
Graben
0.0025cgs
km
5
-10
0
10
20
30
40
50
60
70km

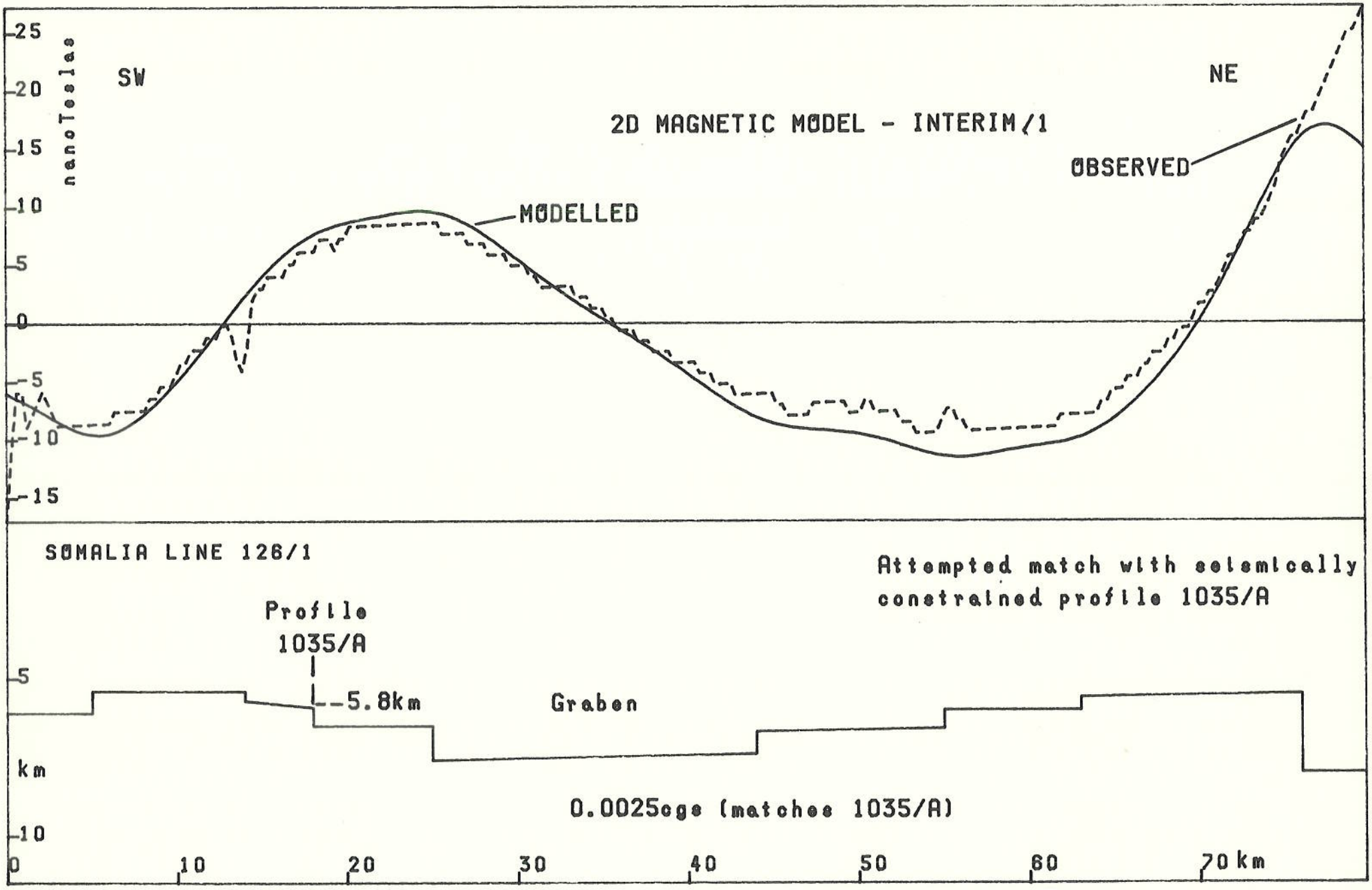
2D MAGNETIC MODEL - INTERIM/1
SW
NE
nanoTeslas
25
20
15
10
5
0
-5
-10
-15
MODELLED
OBSERVED
SOMALIA LINE 126/1
Attempted match with seismically constrained profile 1035/A
Profile 1035/A
5.8km
Graben
km
5
-10
0.0025cgs (matches 1035/A)
0
10
20
30
40
50
60
70 km

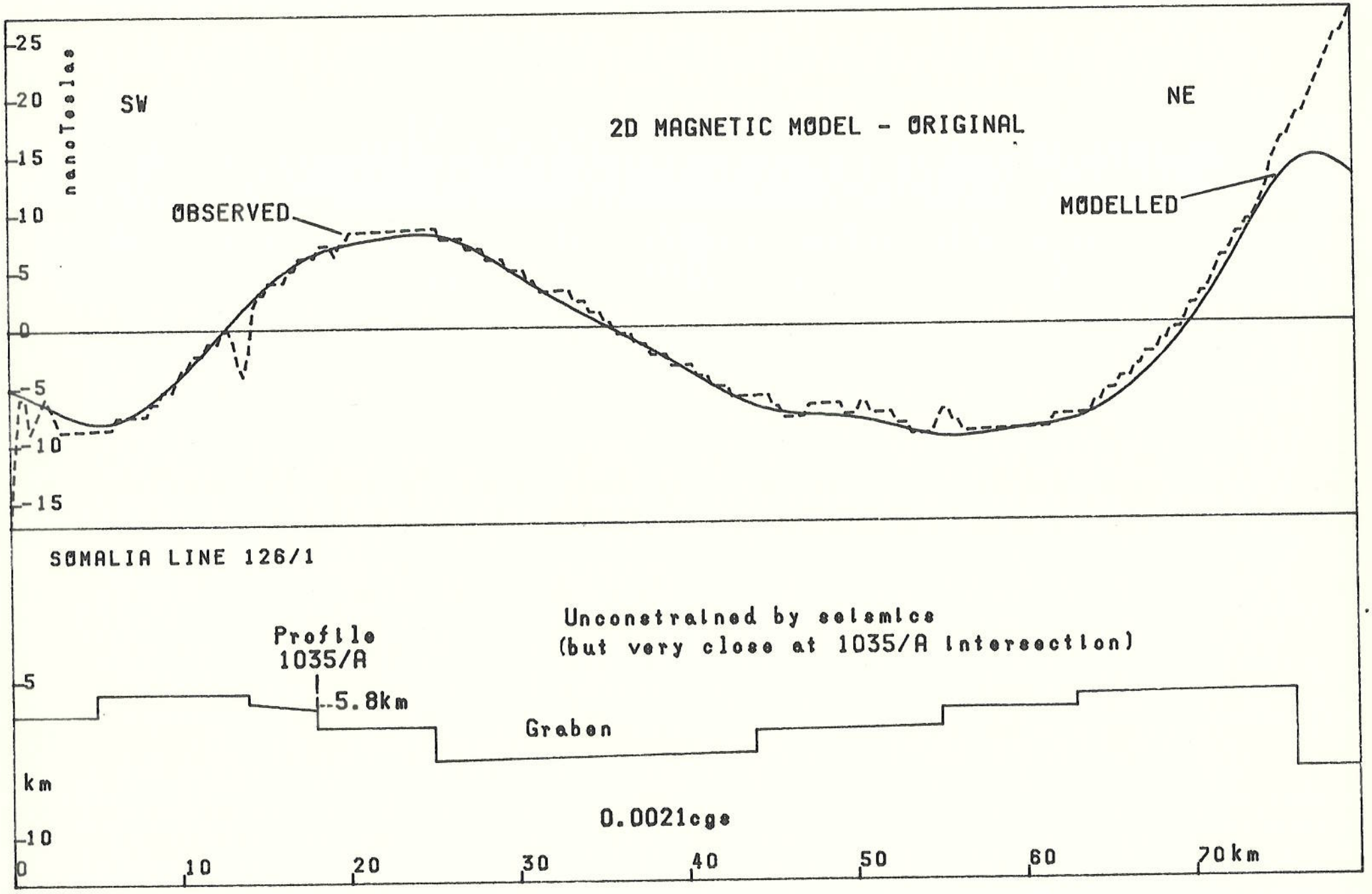
2D MAGNETIC MODEL - ORIGINAL
SW
NE
nanoTeslas
25
20
15
10
5
0
-5
-10
-15
OBSERVED
MODELLED
SOMALIA LINE 126/1
Unconstrained by seismics
(but very close at 1035/A intersection)
Profile
1035/A
5.8km
Graben
km
5
10
0.0021cgs
0
10
20
30
40
50
60
70km

ESSO EXPLORATION JUBA S.A.

INTERPRETATION

OPERATIONS AND PROCESSING

REPORTS

OF AN

AIRBORNE MAGNETOMETER SURVEY

IN SOMALIA

Hunting Geology and Geophysics Limited,
Elstree Way,
Borehamwood,
Herts, WD6 1SB
England.

Telephone: (01) 953 6161
TELEX: 23517 HUNBOR G
Cables: ASTEREO BOREHAMWOOD

MAY 1985
Project No: 210 293

INTERPRETATION

INTERPRETATION REPORT

C O N T E N T S

		PAGE
	SUMMARY	i
1.	INTRODUCTION	1
2.	GEOLOGICAL BACKGROUND	3
	2.1 Physiography	3
	2.2 Basement	3
	2.3 Sedimentary Section	3
	2.4 Volcanic Rocks	4
	2.5 Structure	4
3.	INTERPRETATION METHODS	6
	3.1 Introduction	6
	3.2 Model Anomalies	7
	3.3 Quantitative Interpretation - Methods for Estimation of Anomaly Source Depth	7
	3.3.1 Approximate Methods	7
	3.3.2 More Accurate Methods	8
	3.4 Spectral Analysis	9
	3.5 Computer Modelling	9
	3.6 Comments	9
4.	INTERPRETATION - BLOCK 1	11
	4.1 Introduction	11
	4.1.1 Long Wavelength Zone	11
	4.1.2 Short Wavelength Zone	11
	4.1.3 Medium Wavelength Zone	12
	4.2 Structure	12
	4.2.1 Structure Trends	12
	4.2.1.1 NE-SW	12
	4.2.1.2 ENE-WSW to E-W	12
	4.2.1.3 N-S	13
	4.2.1.4 NNW-SSE to NW-SE	13
	4.2.2 H1 - structural high	14
	4.2.3 L1 or Hiran Graben - structural low	15
	4.2.4 L2 - structural low	17
	4.2.5 L3 - structural low	17

4.3 Volcanics and Associated Intrusives 18

4.3.1 Western Volcanic Region 18
4.3.2 Southern Volcanic Region 20
4.3.3 Eastern Volcanic Region 22
4.3.4 Other Intrusives 23

5. INTERPRETATION - BLOCK 2 25

5.1 Introduction 25

5.1.1 Long Wavelength Zone 25
5.1.2 Short Wavelength Zone 26
5.1.3 Medium/Short Wavelength Zone 26

5.2 Structure 27

5.2.1 Structural Trends 28

5.2.1.1 NE-SW 28
5.2.1.2 ENE-WSW to E-W 29
5.2.1.3 N-S 30
5.2.1.4 NW-SE 31

5.2.2 The Oddur Arch - regional structural high 32
5.2.3 L6 and L16 - structural lows 33
5.2.4 L9 - structural low 33
5.2.5 L7 - structural low 34
5.2.6 L10 - structural low 34
5.2.7 L8 - structural low 35
5.2.8 L11 - structural low 35
5.2.9 H9 - structural high 36
5.2.10 L12 - structural low 36
5.2.11 H6 - structural high 37
5.2.12 H7 - structural high 37
5.2.13 H8 - structural high 38
5.2.14 L13 and L15 - structural lows 39
5.2.15 L14 - structural low 39

5.3 Basement Zones and Associated Intrusives 40

5.4 Volcanics and Associated Intrusives 43

5.4.1 Tertiary Volcanics - Arcuate Zone 43
5.4.2 Jurassic Volcanics - Southern Zone 45

6. CONCLUSIONS 48

6.1 Block 1 48
6.2 Block 2 49
6.2.1 Western Deep Basement 49
6.2.2 Eastern Deep Basement 50
6.2.3 Shallow Basement 50

7. ACKNOWLEDGEMENTS 52

BIBLIOGRAPHY 53

FIGURES

		FOLLOWING PAGE
FIGURE		
1A.	Location Diagram	i
1B.	Sheet Layout Diagram	i
2.	Two-Dimensional Model Anomalies	7
3.	Spectral Plot (example) of Unfiltered Magnetic Data	9
Computer Modelled Magnetic Profiles		
4.	Profile 1021/1	17
5.	Profile 1035/1	17
6.	Profile AA'	17
7.	Profile BB'	17
8.	Profile 126/1	17
9.	Profile 2070/1	42
10.	Profile 2086/1	42
11.	Profile FF'	42
12.	Profile JJ'	42
13.	Profile KK'	42
14.	Profile 2261/1	42
15.	Profile 2292/1	42
16.	Profile GG'	42
17.	Profile 227/1	42
18.	Profile EE'	42
19.	Profile 2285/1	42
20.	Profile 4003/1	42
21.	Profile 2082/1	42
22.	Profile II'	42
23.	Profile 2145/1	42
24.	Profile HH'	42

APPENDICES

Appendix 1 — Sheet by Sheet Spectral Analyses of Block 2.
Sheet by Sheet Spectral Analysis Classification.

Appendix 2 — Tabulation of Bur Acaba Basement Rock Magnetic Susceptibilities.

INTERPRETATION MAP WORKSHEETS AT 1:500 000 SCALE
(at rear of report)

Map 1	Block 1 Qualitative
Map 2	Block 1 Depths
Map 3	Block 2 Qualitative
Map 4	Block 2 Depths

SUMMARY

A 76,617 line kilometre airborne magnetic survey was performed in the Somali Democratic Republic over a petroleum exploration concession held by Esso Exploration Juba SA. The data were subsequently processed, compiled into maps and profiles, and finally interpreted. Interpretation reveals numerous features of both economic and academic interest.

LOCATION MAP

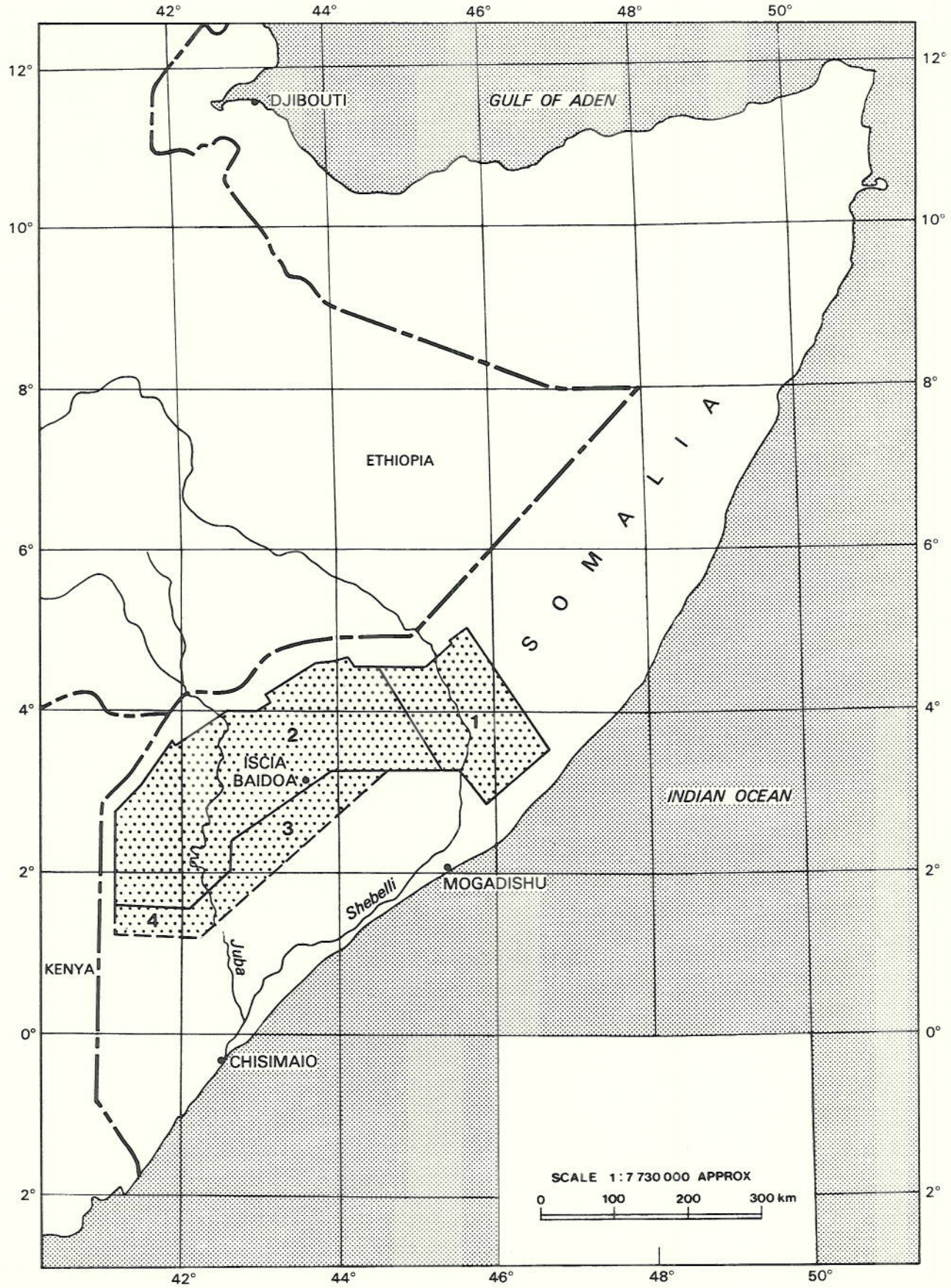

SHEET LAYOUT DIAGRAM SHOWING 1:100 000 SHEETS

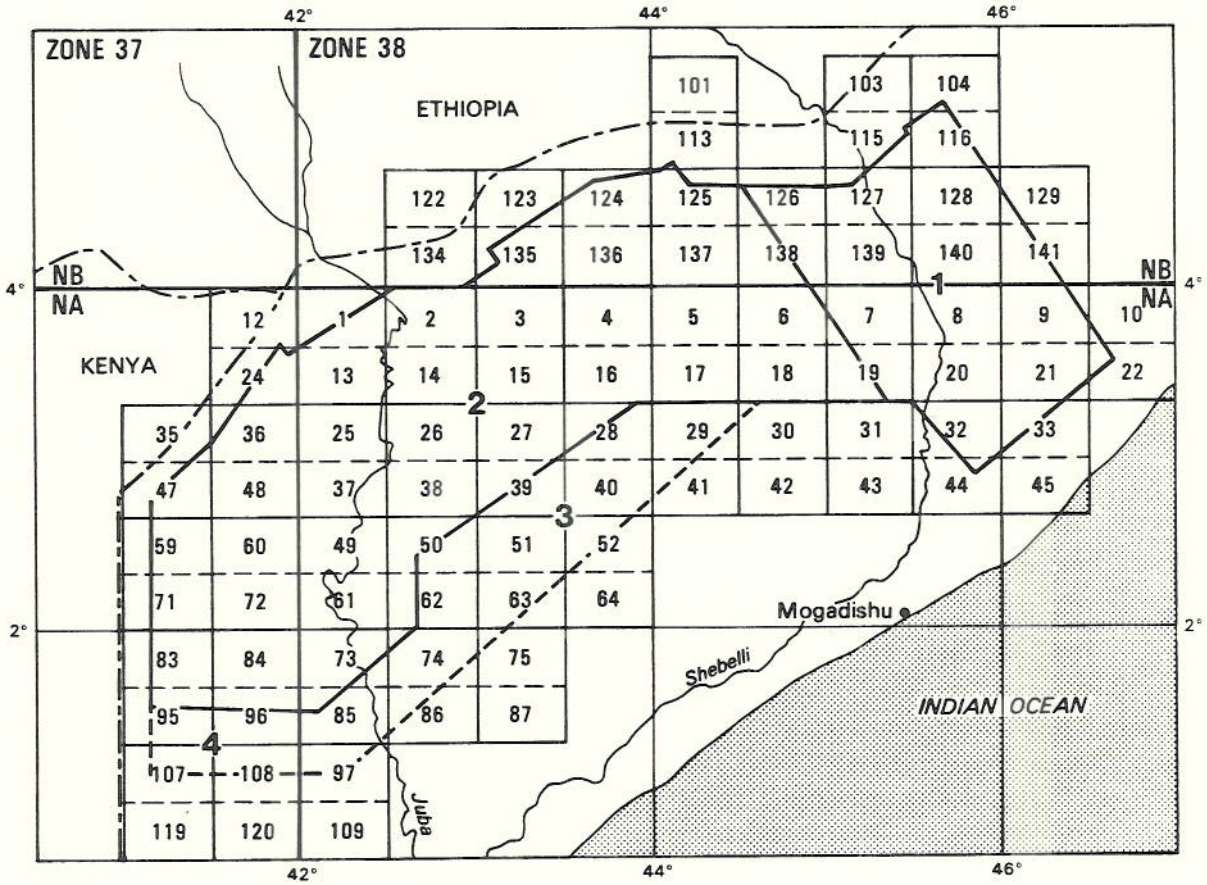

1. INTRODUCTION

During the months of May to August 1984, Hunting Geology and Geophysics Limited carried out an aeromagnetic survey over an oil exploration concession in the Somali Democratic Republic on behalf of Esso Exploration Juba S.A., a division of Esso Exploration Incorporated, Houston, Texas. A total of 76,617 line kilometres of data were acquired. Productive flying commenced on 21st May 1984, was interrupted for 29 days due to Force Majeure on 25th May and was completed on 19th August 1984. The aim of the survey and subsequent interpretation was to provide structural, basement depth and intra-sedimentary volcanic information to assist planning of the 1984-85 seismic programme. Two separate presentations of the Block 1 and Block 2 interpretations were made by Hunting at Esso's Houston head office, in December 1984 and April 1985 respectively.

This report describes the interpretation of the aeromagnetic data. The flying operations, data acquisition, compilation and processing procedures are described in the accompanying Operations and Processing Reports. All depths quoted in this text are defined below sea level unless stated otherwise. Depths annotated in the computer model text figures are defined with respect to sensor. Numerical annotation of qualitative features on the interpretation map sheets, generally increases in value from east to west across the survey area.

Figure 1A shows the location of the survey area and Figure 1B the layout of 1:100 000 scale map sheets. A summary of survey parameters and statistics is as follows:

Productive flying commenced	21st May 1984
Temporary halt of operations due to Force Majeure	25th May
Recommencement of operations	24th June
Flying completed	19th August
Total productive line kms flown	76,617 km
Block 1	21,508 km
Block 2 (including reconnaissance areas)	55,109 km
Flight line direction (both Blocks)	N147 deg - N327 deg
Tie line direction " "	N57 deg - N237 deg
Flight line spacing " "	2 km
Tie line spacing " "	6 km
Bur Acaba reconnaissance area-Block 3:	
Flight line direction	N147 deg - N327 deg
Doublet spacing	2 km
Southern reconnaissance area-Block 4:	
Flight line direction	N 0 deg - N180 deg
Doublet spacing	2 km

Survey altitude above sea level:

Block 1	1500	feet
Block 2	3000	feet
Block 3 and 4 (reconnaissance areas)	3000	feet

2. GEOLOGICAL BACKGROUND

2.1 Physiography

The survey covers an area of southwestern Somalia extending from close proximity to the Kenyan and Ethiopian borders in the north and west, to the area of basement outcrop commonly known as the Bur Acaba Uplift in the south and to approximately longitude 46 degrees east. This area is of generally low relief, the topography rising and falling gently between 200 and 500 metres above sea level, interspersed with granite hills (known locally as burs), rising sharply from the plain.

2.2 Basement

Basement outcrops in the Bur Acaba region to the south of the main survey area (but over-flown by reconnaissance lines). This region is one of only two major basement exposures in Somalia (the other lying along the coast of northern Somalia). The Bur Acaba basement rocks range from Precambrian to lower Palaeozoic and consist of metamorphics (gneiss, schist, quartzite and marble) intruded by granite or granodiorite.

There appear to be as many as three superimposed structural trends within the exposure of the Bur Acaba uplift, northwest-southeast, northeast-southwest and north-south. Daniels (1965) presents a photogeological interpretation of the region in which he suggests that the northwest-southeast trend represents a period of folding pre-dating the northeast-southwest folding which appears to the extreme southwest of the uplift. The north-south trend is part of a larger possibly related structure commonly known as the Oddur Arch which strikes northwards through the survey area.

2.3 Sedimentary Section

It is widely believed that by the end of the Palaeozoic, the whole of Somalia was effectively a peneplain, probably comprising large exposures of ancient crystalline/metamorphic rocks with smaller outliers of Palaeozoic sedimentation. During the Jurassic a marine transgression occurred from the east probably as a result of the commenced separation of Madagascar from East Africa. The associated process of sedimentation was complicated by secondary regressions and transgressions causing major facies changes within the mainly limestone deposits of this time. Closely following this cyclic deposition was a period of what is thought to be epeirogenic uplift in the Late Jurassic. Further cyclic marine transgressions occurred within the Cretaceous followed by a second period of epeirogenic uplift. Apart from minor Eocene marine transgressions in the coastal areas, Somalia appears to have remained essentially above sea level since the Cretaceous.

Within the survey area the sedimentary section is summarised by Merla, Abate, Azzaroli, Bruni, Canuti, Fazzuoli, Sagri and Tacconi, 1973, (see Bibliography) as follows:

Upper Cretaceous to Lower Eocene	Auradu Limestones
Upper Cretaceous	Yessoma Sandstone Belet Uen Limestone Ferfer Gypsum Mustahil Limestone
Lower Cretaceous	Main Gypsum Formation
Jurassic	Garbeharre Sandstone Gabredarre and Uegit formation (oolitic limestones, marls and gypsum) Warandab and Anole formations (gypsiferous clays and marls) Hamanler and Iscia Baidoa formations (organogenic and oolitic limestones).

2.4 Volcanic Rocks

Basalt flows are seen at outcrop within the survey area and have been described by Stefanini (1925) as thick flows of Late Tertiary age, underlain by volcanic ash and tuff.

2.5 Structure

Palaeozoic peneplanation has probably been responsible for the disappearance of much pre-Jurassic structure in Somalia. Following the Palaeozoic, significant basin development occurred during the marine sedimentation of the Jurassic. It is generally understood that basin development was caused principally by the differential isostatic response to sedimentation. Rejuvenated structural highs, subject to erosion, fed adjacent developing sedimentary basins and in this way widely varying thicknesses of Jurassic sediment were generated. This process also occurred during the Cretaceous period.

The thickness of Jurassic sediments at the centre of the Mandera-Lugh Basin has been estimated by Barnes (1976) at 2-3 km. Total depth to basement here has been estimated at 7.5 km by Merla et al (1973). According to Barnes, the basin developed in association with Jurassic faulting adjacent to the Bur Acaba Uplift to the southeast. (Barnes 1976 account of structure in this region is however persistently confused by descriptive directional inconsistencies).

A system of normal NE-SW faults controls the southern boundary of the Bur Acaba Uplift region. These faults generally show eastward downthrow and in turn structurally control almost the full length of the eastern Somalia coastline. Major movement along this fault system

appears to have occurred in the Jurassic with reactivation in the Tertiary. The throw of the fault at the southeast boundary of the Bur Acaba exposure is thought by Beltrandi and Pyre (1973) to be in excess of 4 km.

Lying within central Somalia is a large embayment of Mesozoic marine sediments. This regional feature, which is observed only in the subsurface, is recognised as comprising three basinal components, the Central Somalia Coastal Basin, the Obbia Basin, and the Mudugh Basin which fringes the northeastern region of Block 1.

The north-south trending Oddur Arch structure which lies centrally within the survey area, effectively separates the Mandera-Lugh and Mudugh basins. These basins coalesce north of the arch to form the Ogaden Basin of Ethiopia.

3. INTERPRETATION METHODS

3.1 Introduction

The interpretation presented in this report is based on an analysis of the following data:

(a) Total magnetic intensity contour maps, levelled with International Geomagnetic Reference Field (IGRF) subtracted and a constant of 5000nT added (to remove negative values), at scales of 1:100 000 and 1:500 000.

(b) Total magnetic intensity contour maps, upward continued to 3000 feet above sea level within Block 1, at a scale of 1:100 000.

(c) Total magnetic intensity contour maps, matched-filtered for removal of volcanics within Block 2, at a scale of 1:100 000.

(d) Shallow component residual magnetic contour maps of Block 2 at a scale of 1:100 000 produced by subtraction of (c) from (a).

(e) Computer plotted 1:100 000 scale Calcomp profiles of processed total magnetic intensity data containing the following channels:

Block 1

(i) Total magnetic intensity, levelled with IGRF subtracted and a constant of 5000nT added.

(ii) Horizontal gradient of the above.

(iii) Corresponding diurnal data.

(iv) Barometric altimeter trace.

(v) Pseudo-topography trace (barometric minus radar altimeter trace).

Block 2

Differs from Block 1 in so far as an extra channel is included, showing the matched-filtered version of total magnetic intensity.

The horizontal gradient for Block 2 profiles is based on the filtered total magnetic intensity channel.

(f) The original in-flight analogue records.

(g) Radially averaged plots of spectral analysis (of pre-filtered data) on a sheet by sheet basis.

(h) Available geological information (see Bibliography).

(i) LANDSAT imagery.

The following procedures were involved:

(a) Qualitative examination of magnetic contour maps to ascertain the nature of discrete anomalies and significant residual features, to recognize distinctive magnetic zones, to recognize indirect evidence of faulting and to select anomalies for quantitative interpretation. See the following Section 3.2.

(b) Manual depth estimation of magnetic basement and volcanic horizons using Calcomp profiles of all lines flown, subtraction of sensor height above sea level, application of measured obliquity corrections, and more-detailed analysis of particularly significant anomalies.

(c) Plotting the results of (a) and (b) on interpretation worksheet overlays at 1:100 000 and 1:500 000 scales.

(d) Computer modelling of selected anomalies, to resolve ambiguities and to fill in areas where sensible application of manual depth estimating methods is difficult due to the nature of the data.

(e) Reassessment of the data, including application of appropriate filters and further computer modelling, to finalise the interpretation.

3.2 Model Anomalies

In magnetic interpretation it is important that the interpreter is familiar with the shapes and relative amplitudes of a range of anomalies pertaining to simple but geologically sensible bodies.

Figure 2 shows computer modelled anomalies generated to facilitate this, where induced magnetisation has been assumed over a suite of two-dimensional magnetic bodies for an ambient field strength of 34,500 nT and an inclination of -20 degrees. A magnetic susceptibility contrast of 0.001 (c.g.s. units) has been used in each case as this lies well within the range for common igneous/sedimentary rock contrasts. Profiles were calculated for bodies striking east-west, northeast-southwest / northwest-southeast and north-south. In each case the profile is at 90 degrees to the strike of the body.

3.3 Quantitative Interpretation - Methods for Estimation of Anomaly Source Depth

3.3.1 Approximate Methods

Peters' half-slope method.

In this method (Peters, 1949) the horizontal distance between half-slope points either side of the chosen inflection point is used as a depth index. This depth index is then divided by a number dependant on the assumed depth-to-width ratio of the anomalous body, thus giving the depth to source estimate. For a dyke having a width-to-depth ratio of 2, for example, the value of this divisor is

FIGURE 2

TWO DIMENSIONAL MODEL ANOMALIES

inducing field inclination i = − 20° (mean)
total field value = 34,500 nT (mean)
susceptibility contrast = 0·001 cgs
width/throw = 3
depth = 2 km

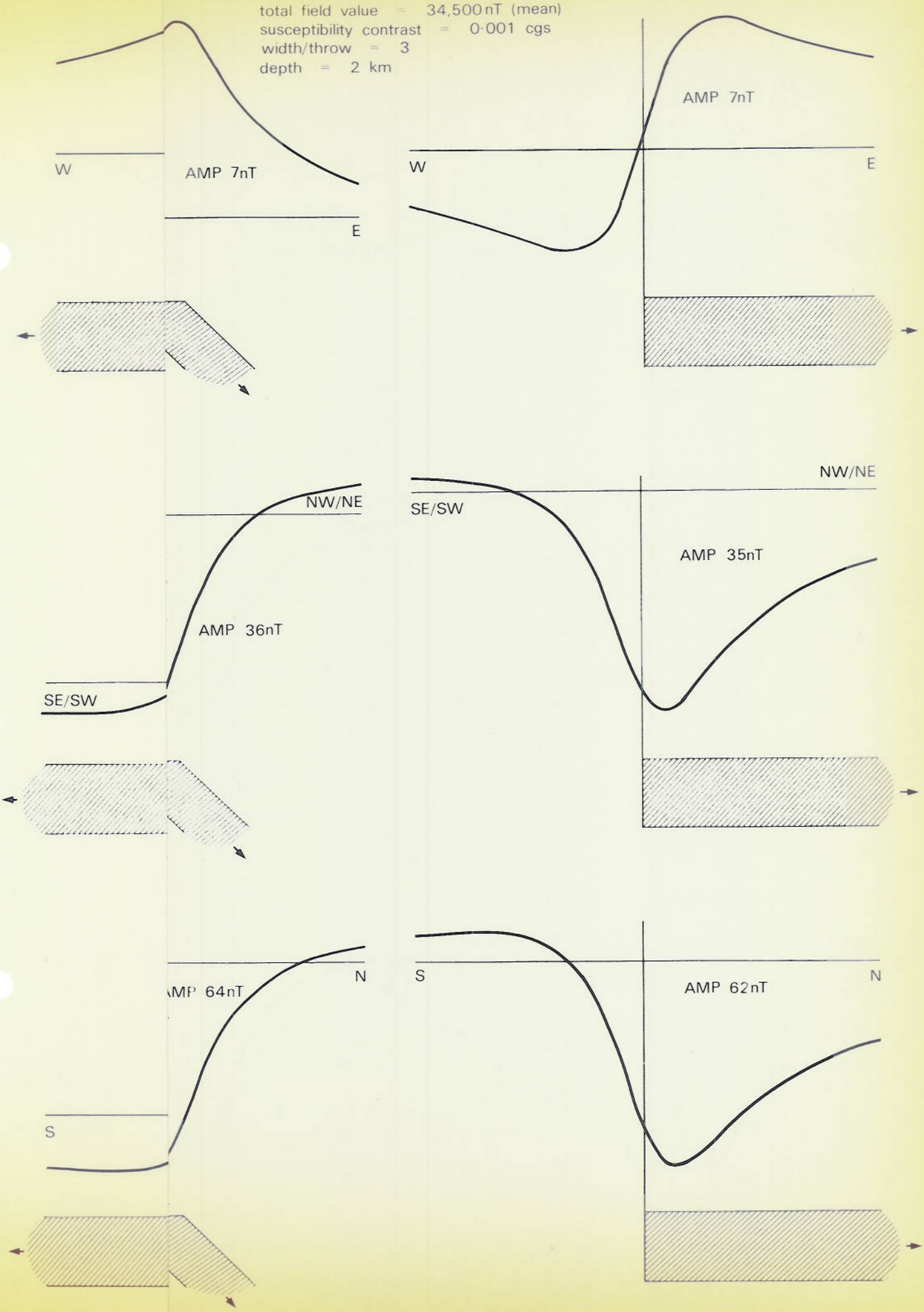

1.6. For narrower bodies with respect to depth, a divisor of 1.2 is appropriate, and for wide bodies and basement contacts the divisor is 2.0 (Am 1972).

Sokolov's method.

This method uses the horizontal distance between the intersections of the chosen inflection tangent (at the centre of an anomaly) with the tangents to the point of maximum and minimum field value. Source depth is estimated by applying a divisor to this index distance, usually 2.0.

Straight Slope (Vacquier) method.

This method uses as a depth index the horizontal length of the straight slope of the anomaly's flank. Where the anomaly amplitude is greater than a few tens of nanoTesla (nT) and the straight slope occupies about half the total amplitude, the depth extent is probably large relative to depth in which case the index is divided by 1.1 to obtain actual depth (Vacquier, Steenland, Henderson and Zietz, 1951, see Bibliography). For anomalies of lower amplitude the depth index is divided by 0.7, the model implicit in this case being a depth-limited prism or plate (Steenland, 1965). This method must be used with caution as spurious inflections due to interfering bodies may be misleading.

3.3.2 More Accurate Methods

Bean's method.

This method devised by Bean (1966) uses both flanks of an anomaly and gives estimates of inclination, magnetisation and susceptibility in addition to depth. Ratios of horizontal distances relating to half-slope and inflection points are calculated and depth estimates obtained from nomograms. Assumed models are faults and vertical dykes. Different nomograms are used depending on thickness-to-depth ratios. The method is accurate and rapid to use.

Modified Peter's method.

This is a refinement of the half-slope method and uses the half maximum slope separation on both major limbs of asymmetric anomalies in addition to the ratio of gradients of the two slopes.

50-75 or Koefoed method.

The horizontal distances between the half and three-quarter slope positions are used in a manner similar to the Bean method. The assumed geological model is a step or contact and nomograms are used for steps having a vertical step-distance/depth-to-top ratio >10 (the contact model), approximately unity (the thick plate model) and < 1/10 (the thin plate model). This tends to be the most useful manual method, being for example less restricted in its use than Bean which generally requires that both limbs of the anomaly are available.

3.4 Spectral Analysis

Preliminary spectral analysis was carried out on specific lines to obtain a general indication of basement depths and presence of intra-sedimentary horizons. Further spectral analysis was subsequently carried out over the whole of Block 2 on an (radially averaged) area basis in order to obtain a representative high frequency cut off for filtering of high frequency volcanic response. A general example of spectral analysis can be seen in Figure 3. Specific plots of analyses for the area can be found in Appendix 1. In an ideal situation (flat-lying horizons) each straight line segment of the spectral plot is contributed by a separate magnetic horizon, the corresponding gradient of which is proportional to the depth of the horizon according to the equation below. The use of this equation, even in a less than ideal situation, may give useful general values for depths if the data set is sensibly restricted in area:

$$h = \frac{p_f}{} \times \frac{D}{4}$$ where h = depth to the magnetic horizon in km below sensor

where p_f = gradient of the straight line segment of the plot

D = size of the grid in km (actually 0.5 km)

The equation specific to the scales at which the power spectra are plotted and displayed in Appendix 1 is:

h = 1.592 tan km (below sensor)

where = angle of corresponding segment with respect to the x axis

3.5 Computer Modelling

This was carried out over numerous selected profiles to augment manual interpretation. Computer modelling also enabled sensible depth estimates to be derived within magnetic areas not readily susceptible to manual methods (see the following section). Both 2D and 3D models were generated using Hunting software and the in-house Perkin-Elmer 3240 mini-computer via an HP 2647A graphics terminal.

3.6 Comments

Note that in the absence of intrasedimentary volcanics, intrusions and other magnetic horizons, qualitative and quantitative magnetic interpretation relate to the one surface - magnetic basement. Interpreted faulting will in this case not necessarily imply extension of the feature through the overlying sedimentary section. Magnetic basement does not necessarily coincide with 'economic' basement or with the deepest seismic marker horizon.

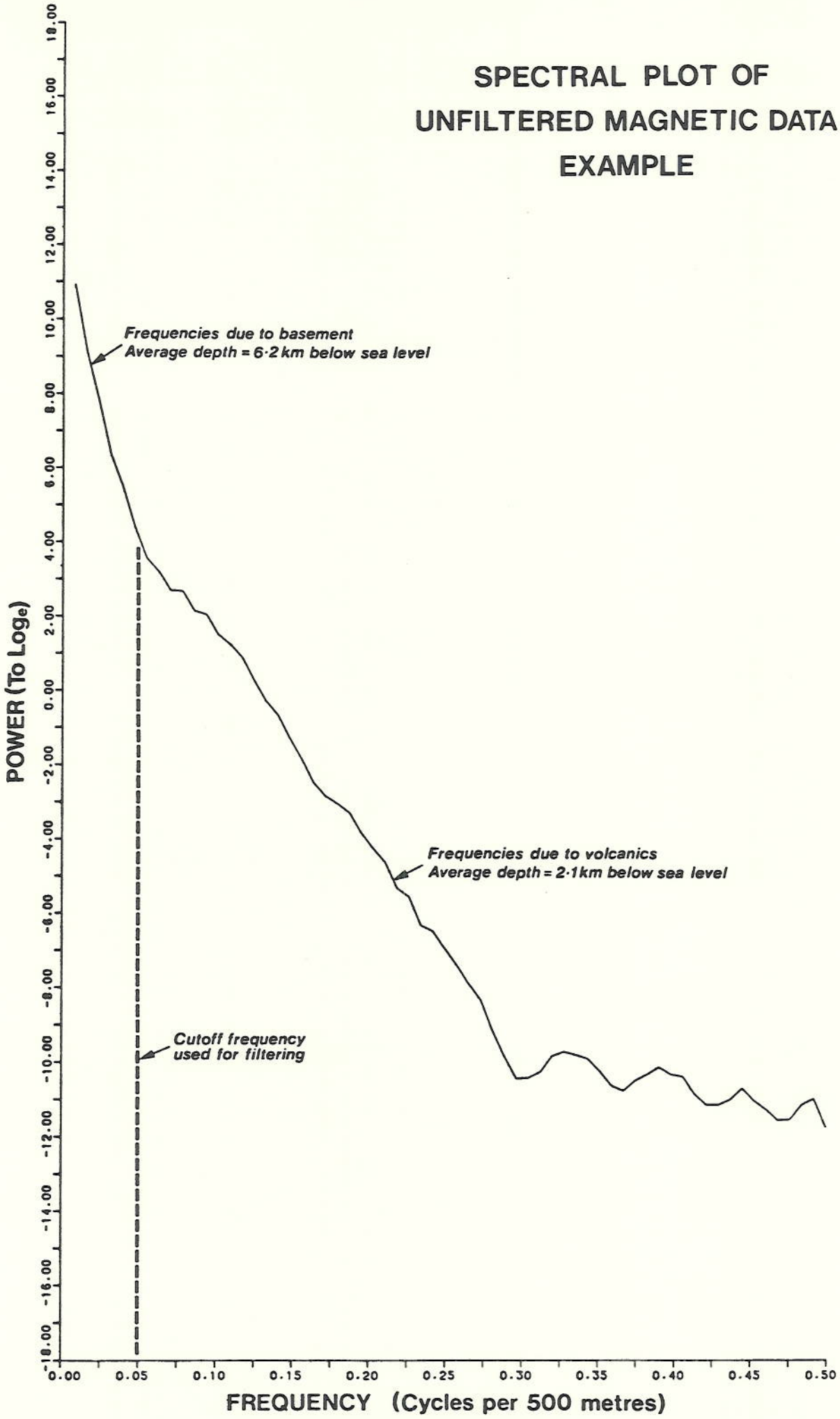
SPECTRAL PLOT OF
UNFILTERED MAGNETIC DATA
EXAMPLE
Frequencies due to basement
Average depth = 6·2 km below sea level
Frequencies due to volcanics
Average depth = 2·1 km below sea level
Cutoff frequency
used for filtering
POWER (To Log$_e$)
18.00
16.00
14.00
12.00
10.00
8.00
6.00
4.00
2.00
0.00
-2.00
-4.00
-6.00
-8.00
-10.00
-12.00
-14.00
-16.00
-18.00
0.00
0.05
0.10
0.15
0.20
0.25
0.30
0.35
0.40
0.45
0.50
FREQUENCY (Cycles per 500 metres)

In this report 'two-dimensionality' and 'three-dimensionality' are properties reflecting the relative strike length of the contoured magnetic anomaly. Two-dimensionality is generally ascribed to those anomalies whose strike length is at least ten times the anomaly width. In order that a practical number of anomalies are amenable to two-dimensional computer modelling, this rule is often relaxed (to say five times). Three-dimensional anomalies are those features with little or no discernible strike length and in contour form are therefore roughly equidimensional.

Application of manual depth estimating methods (as described in Sections 3.3.1 and 3.3.2) to the important long wavelength zones, particularly of Block 1, have frequently generated unreasonably deep basement depths. Two explanations may account for this (i) that numerous adjacent magnetic basement features interfere, often unresolvably on account of their relatively small separation in comparison to their large depth , and (ii) that interpretations are attempted in regions where the basement is of graduated rather than of effectively uniform magnetic composition. Computer modelling will generally highlight such problem areas and in many instances will suggest reasonable interpretations. In any given geologic situation other equally sensible alternative models will generally exist. In the absence however of other information or constraints only the simplest model can sensibly be considered.

The numerous computer modelled profiles within both Blocks 1 and 2 have provided the necessary structural framework upon which, especially in Block 1, a more reliable manual interpretation has been based.

4. INTERPRETATION - BLOCK 1

4.1 Introduction

Block 1 interpretation has been performed on the 1500 feet above sea level (asl) data set. A 3000 feet asl upward continued data set was generated for the purposes of matching Block 1 magnetic contours with those of Block 2.

Block 1 may be categorized into three principal magnetic zones on the basis of wavelength.

4.1.1 Long Wavelength Zone

This, the largest zone, comprises 80 percent of the block and contains low amplitude, long wavelength features, clearly indicating the likelihood of deep basement.

Three major features are immediately observed:

(i) A broad rectilinear positive anomaly of ENE-WSW strike and approximately 40 nT amplitude near the southern boundary of the block.

(ii) A broad negative anomaly of NE-SW strike and approximately 40 nT amplitude across the centre of the block.

(iii) A 144 nT peak to peak dipolar anomaly, clearly related to a limited strike length, broad NW-SE body, close to the block's eastern boundary in the north.

The positive anomaly in the south and the central negative anomaly are connected by a broad zone of relatively uniform magnetic gradient, within which manual depth estimating methods are not particularly useful. A broad NW-SE residual anomaly can however be recognized superimposed upon this gradient which has been interpreted as a feature of structural significance (see Section 4.2.3).

4.1.2 Short Wavelength Zone

This zone which extends well into Block 2 contains relatively high amplitude, short wavelength features, a characteristic often associated with shallow volcanics. The zone closely follows the western boundary of Block 1 in a 20-40 km wide band and is indeed confirmed as volcanics by exposure over its northern extent. The zone continues along the block's southern boundary and reaches the eastern boundary via a narrow, arcuate short wavelength feature extending through the long wavelength zone. At the eastern boundary, the zone trends northwestward along the eastern boundary. It is assumed that this volcanic zone continues into the adjacent concession. See Section 4.3 for a full description of volcanic zones.

4.1.3 Medium Wavelength Zone

This zone lies in the extreme northwest corner of Block 1 and continues into Block 2. Comprising medium amplitude, (up to 50 nT) medium wavelength features, this zone may in principal relate either to shallower basement or to significant thicknesses of deeper intrasedimentary volcanics. Spectral analysis of Block 2 data within the joint Block 1/Block 2 Sheet 126/138, together with the corresponding qualitative interpretation, suggests that the shallow basement interpretation is more probable.

4.2 Structure

4.2.1 Structural Trends

Four major structural trends dominate Block 1.

4.2.1.1 NE-SW

NE-SW appears to be a fundamental structural trend within both Blocks 1 and 2 and may be related to the Precambrian orogeny associated with the Bur Acaba Uplift, the exposed metamorphic core of which lies immediately south of Block 2. This is the dominant magnetic trend in the northern half of Block 1 and it is associated with the following interpreted structural features:

(i) A possible extension of the Bur Acaba uplift whose axis is annotated H1 (see Sheets 7/19 and 128/140 and Section 4.2.2).

(ii) A parallel trough L3, 30 km to the north, controlled on its northern edge by the parallel fault F73. Probably a continuation of the Mudugh Basin to the east (see Sheets 127/139 and 128/140 and Sections 4.2.3 and 4.2.5).

(iii) 30 km further north, a less extensive parallel structural high H3 (see Sheets 127/139 and 104/116 and Section 4.2.5).

Surface mapping shows very little NE-SW trend in this region. Having disappeared as a magnetic trend south of fault F8 (see next sub-section) NE-SW reappears as a surface mapped geological trend in the extreme south, and south and east of Block 1. Here numerous NE-SW faults together with unmapped parallel counterparts appear to control much of the Somali coastline. These faults probably originated during the Jurassic at the time of the East African/Madagascar break-up.

4.2.1.2 ENE-WSW to E-W

The NE-SW trend essentially disappears south of the interpreted fault F8 and is replaced here by a dominant trend varying between ENE-WSW to sub E-W. In Section 4.2.3 it is suggested that basement structures north and south of fault F8 are unrelated. Interpreted structural features south of F8 in the ENE-WSW to E-W direction are:

(i) Fault F8 (see Sheets 7/19, 8/20 and 9/21, and Sections 4.2.3, 4.3.1 and 4.3.3).

(ii) An intruded shear zone B4 immediately south of F8 (see Sheet 9/21 and Section 4.3.3).

(iii) A short distance further to the south, a long deep trough L2 related to fault F9, proposed to account for the very long and broad positive magnetic anomaly across the southern part of the block. (See Sheets 8/20 and 9/21, and Section 4.2.4).

(iv) Minor faulting across the eastern volcanic zone namely F56, F57 and F58 (see Sheet 9/21 and Section 4.3.3).

(v) The intrusions D6 and D7 in the extreme southern corner of Block 1, probably associated with a fault bounding the volcanic zones V15 and V17 to the south. This fault is possibly a continuation of the NE-SW fault F28 to the east which separates the southern and eastern volcanic zones (see Sheets 32/44, 33/45, 9/21 and 10/22, and Section 4.3.2).

(vi) Possible anticline H5 reflected in the depths to volcanics within zones V15 and V16 (see Sheet 32/44 and Section 4.3.2).

4.2.1.3 N-S

Numerous N-S magnetic dislocations, presumed fault-associated, occur within the volcanic zone of western Block 1 and in some cases form well defined boundaries of this zone. Their strike is parallel to the structure of the nearby Oddur Arch within Block 2 (an apparent northward extension of the Bur Acaba Uplift) and might be reasonably regarded therefore as associated eastern flank faulting. Similar evidence of abundant N-S faulting occurs in Block 2 directly over the Oddur Arch region. The accepted Late Tertiary age of the volcanics within which the N-S features are recognized implies reactivation. Some N-S fractures, notably associated with the features D9 and D15/D16/D17 have clearly been subjected to relatively recent basic intrusion.

4.2.1.4 NNW-SSE to NW-SE

The main magnetic features with this trend lie to the south of the structural high H1 and occur as residuals superimposed upon the stronger regional NE-SW Precambrian magnetic trend. The simplest and most credible interpretation of this residual magnetic pattern is a series of parallel or sub-parallel faults intersecting basement, the interpreted displacements of which define a graben. Computer modelling confirms the plausibility of this interpretation and ascribes significant depths and throws to those parts of the proposed graben modelled. For the purpose of this report, this structure has been called the Hiran Graben. This graben in common with many other NW-SE trough-like structures across Northeast Africa, is likely to be at least Cretaceous in age. The discussion in the last paragraph of

Section 4.2.3 explains how the structure may in fact date back to the Palaeozoic.

Other features with this trend are the interpreted volcanic zones on the western and eastern boundaries of the block. While the overall strike of the western zone (jointly V1 V5, V7, V8, V9, V10) may arguably be coincidental, the western boundary of volcanic zone V21 in the east is most certainly controlled by NW-SE faulting along F14.

4.2.2 H1 - structural high

A major feature of Block 1 is the broad NE-SW negative magnetic anomaly contained within Sheets 8/20 and 128/140. In Sheet 128/140, the anomaly interferes with the southern negative component of the large dipolar anomaly associated with the intrabasement body B1. Two flight line profiles, 1021/1 and 1035/1, were computer modelled to determine the likely nature of the anomaly. Using magnetic susceptibility values for the basement from 0.0001 to 0.002 cgs units (guided by measured susceptibilities on a wide range of rock samples from the Bur Acaba exposure) an intrabasement model with no basement surface relief gave an unacceptable fit of 'computed' versus 'observed'. With the added dimension of surface relief, however, acceptable fits were obtained on both profiles using a smooth dome shaped model cross-section (see Figures 4 and 5). Further computer modelling along tie line 126/1 served to define more satisfactorily the northern limit of the structure (see Figure 8).

The broad ridge thus defined by modelling is annotated H1 and is interpreted as an effective extension of the Bur Acaba uplift, the exposed metamorphic core of which lies immediately south of Block 2, roughly colinear with the high axis H1. The axis is approximately 19 km north of the corresponding magnetic low. At its shallowest, the uplift appears to be within 1.8 km of sea level on profile 1021/1. The northern flank appears steeper than the south, reaching a depth of roughly 5-6 km over a 20 km distance as compared to a depth of 3-4 km over the same distance to the south. The steepness of the northern slope appears to be due to a closely adjacent basement low L3, also of NE-SW strike and which may be continuous with the Mudugh Basin to the east. The 'Bulo Berti' drill-hole, annotated number 3 (see joint boundary between Sheets 127/139 and 128/140) lies on the northern flank of the high. Drilled to a depth of 2.0 km , basement was not intersected. This is consistent with interpreted basement depths in this area.

The modelling depicted in Figures 4 and 5 along profiles 1021/1 and 1035/1 respectively should, as with all large scale modelling exercises, be treated with some caution due to the assumption of a large area of magnetically homogeneous basement rock. Gradual lateral variation in susceptibility as might be expected if the core of the uplift is markedly metamorphic, could contribute significantly to the nature of the anomaly, ignorance of which could result in underestimated depths. Basement contours over this structural high are depicted discontinuously due to the superimposed NW-SE structure of the proposed Hiran Graben which intersects it (see Section 4.2.3).

It would be reasonable to expect that any major structure post-dating the split during the Jurassic of Africa and Madagascar, would exhibit mappable features at surface, for example the Lamu Trough to the west of Block 2 in Kenya. The geological maps/texts available for this study , however, contain no evidence for the proposed H1 structure. The implication therefore is that H1 is probably Palaeozoic. The proposed shallow depth of the uplifted basement at H1 and the generalized assumption of full peneplanation by the end of the Palaeozoic conflicts, suggesting either that this interpretation is incorrect or that peneplanation may locally have been incomplete. Any topographic features like H1 remaining above the peneplain, would have possessed a mature (that is, smoothly eroded) cross-section. This interpretation though consistent with the smooth computer modelled cross-section for H1, remains somewhat uncertain.

4.2.3 L1 or Hiran Graben - structural low

Immediately south of the uplift H1, is a wide band of magnetic contours, with relatively uniform gradient, apparently containing no magnetic anomaly amenable to basement depth estimation. Closer inspection , however, reveals a 25 km wide NW-SE dipolar residual anomaly, roughly 45 km long and of roughly 10 nT peak to peak amplitude, superimposed upon both the southern flank of H1's negative anomaly and upon the adjacent negative component of body B1. Further inspection reveals that the feature extends north of H1 where the dipolar anomaly redevelops, presumably in the absence of magnetic interference from H1 and B1. This extends its probable length to over 90 km. A magnetic feature of this length and width (approximately 25 km) is likely to be very significant indeed.

Three magnetic profiles were chosen for computer modelling, approximately at right angles to the residual anomaly: tie line 126/1 in the north and residually extracted profiles AA' and BB' in the south. The result of computer modelling on these profiles is shown in Figures 6, 7 and 8. Using susceptibility values for basement in accord with measurements on samples from the Bur Acaba exposure, the only model giving an acceptable fit of 'computed' versus 'observed' in all three cases, was that of a graben, slightly steeper on its western flank , of 2 km relief from central axis to shoulder and of the order of 7 km in depth. The axis of this feature is annotated L1. For the purpose of this report, this feature has been named the Hiran Graben, running as it does through the greater part of Hiran Province. The graben is likely to be at least Cretaceous in age. Absence of any mappable surface evidence, however, like H1 suggests the possibility of an earlier origin. The last paragraph of this section pursues this possibility.

Using the computer-modelled information and observed magnetic lineations to define its path, the Hiran Graben, north of fault F8, follows a sinuous path. In the south its strike is NW-SE while in the north it strikes in a more west-northwesterly direction apparently deflected by the unyielding nature of the interpreted intra-basement body B1. The northwesterly striking part of the structure (that is, in the south) is defined by faults F1 and F3 on the west and F2 and F4 on the east. The west-northwesterly part (in the north) is defined by faults F1, F11 and F10 on the west and F2, F4 and F15 on the east.

ML1 and ML2 are small-amplitude, magnetic, linear features or form lines, probably related to the graben and which are used in the interpretation to orientate the strike of the structure in the north. The computer modelling suggests that the graben structure is bounded by the faults F5 and F12 in the west, and F6 in the east, which in effect provide the graben with horst-like shoulders.

At its northernmost limit in sheet 127/139, the Hiran Graben appears to intersect the interpreted trough L3. The existence of this trough becomes clear only on studying basement depth estimates. It is perhaps of interest to note that near the intersection of the western graben fault F1 and the L3 axis lies a circular low amplitude magnetic anomaly B3. It is conjectured that this might be an alkaline intrusive or kimberlite. The same fault F1 appears to have a marked controlling effect on a 12 km section of the Webi Shebeli River in this region. This is the only occasion that the river appears controlled by graben related structure.

Computer modelling suggests that in vertical extent the graben's basement surface relief is an almost constant 2 km (from floor to shoulder). Modelling also indicates , however, that the structure as a whole is shallower across AA' than across profile 126/1 in the north and particularly BB' in the south. This is consistent with the position of the intersecting uplift H1 which probably pre-dates the structure. Modelling indicates a maximum basement depth of (working north): 7.7 km along BB', 6.0 km along AA', and 6.4 km along profile 126/1. Direct magnetic evidence for the graben disappears south of the proposed fault F8. There are two possible explanations for this: (i) that south of F8, basement magnetic susceptibility decreases markedly with respect to overlying sediment, or (ii) a more credible explanation, that graben structure simply disappears. The arcuate zone of volcanics immediately south of F8 in Sheet 9/21 indicates, however, that at least minor extensions of graben faulting may occur south of F8. The faults, which appear to be displaced eastwards along F8 by approximately 2 km, are F6, F4 and F2 and are revealed as discontinuities in the magnetic signature of the NE-SW striking body B4. Furthermore, the intrusive bodies D1, B14, D13 and the associated volcanic zone V20 lie immediately west of fault F2 (colinear in the case of D13) and so may directly relate to minor southward extensions of the graben's axial faults. This correlation may , however, be coincidental as implied by the following paragraph in which contradictory observations are discussed which strictly limit the Hiran Graben to the region north of fault F8.

Seemingly good though ultimately misleading evidence for a reappearance of a trough-like structure occurs southeast of interpreted fault F28. Here, outside the survey area, one can observe from the 1:1 000 000 scale UNDP geology map several NE-SW surface mapped faults possessing a coaxial, coastward directed convexity suggesting an imposed NW-SE structure; perhaps the unbroken interior sag structure of a graben. Fault F28' is the northernmost and is the counterpart of magnetic fault F28 (see the 1:500 000 scale worksheet interpretation included in this report). Unfortunately the direction of downthrow on these faults is known to be to the south and, therefore, assuming normal southward dipping fault planes, the implied possibility is not of a trough but of a positive linear structure. No

structure either positive or negative can be interpreted directly from the magnetic data north of F28. However, the interpretation of the Western and Southern Volcanic regions described in Sections 4.3.1 and 4.3.2, indicates in both instances the possibility of underlying colinear positive structure. One might similarly entertain the possibility of a linear positive structure extending northwestwards along the axis of the surface mapped faults south of Block 1 and then into the block along the NW-SE component of the arcuate volcanic zone in Sheet 9/21. Juxtaposed as this feature would ultimately be against the Hiran Graben structure across fault F8, the implication is that F8 may be a major strike-slip fault, of such displacement that fundamental basement structure does not correlate across. According to this hypothesis, the Hiran Graben must pre-date fault F8 and would therefore appear to be Palaeozoic. To suggest that the interpreted deep trough L2, south of F8, may represent an ancient subducted trench, may perhaps be taking hypothesis too far. (If true however, this would suggest that F8 is an inter-plate suture therefore belonging to the same category of fault as the San Andreas, in which case both F8 and L2 would presumably have very significant strike-lengths. This is one of the few plausible means of explaining both the relatively profound depth of trough L2 and its apparent occlusion of the interpreted Hiran Graben to the north). If the interpreted position of F8 is relocated near to the southern boundary of B4, the validity of the interpreted graben-related faults F6, F4, and F2 across body B4 need not be compromised. The computer modelled profiles 1021/1 and 1035/1 (Figures 4 and 5) are not particularly consistent, however, with the interpretation of F8. Shortcomings are (i) the position of F8 with respect to the southernmost contact and (ii) the angle of this contact. Subsequent metamorphism from the developing H1 structure in the north, however, may have disrupted the earlier magnetic picture. (See Section 4.2.4).

4.2.4 L2 - structural low

The broad positive 40nT magnetic anomaly that strikes ENE-WSW across the southern region of the block is clearly of particular significance. Computer modelled profiles 1021/1 and 1035/1 (Figures 4 and 5) indicate that it is probably due to a trough L2, possibly formed in conjunction with faulting along F9 in half graben fashion, and situated within a broader basement trough. On both modelled profiles, L2 attains maximum modelled depths of around 11.5 km and so appears to represent the deepest structural low within Block 1. In Section 4.2.3 it is suggested that L2 may mark the position of an ancient, probably Palaeozoic, subducted trench. In this case L2 would be expected to have a significantly long strike-length and would extend westwards immediately south of the exposed Bur Acaba Uplift.

4.2.5 L3 - structural low

The existence of the trough L3 only clearly emerges on contouring the basement depth estimates. The trough, which strikes NE-SW directly north of feature H1 across Sheets 127/135 and 128/140 , is not as well defined magnetically as the trough L2 for example in the south. The linear positive magnetic trend corresponding to the proposed fault F73

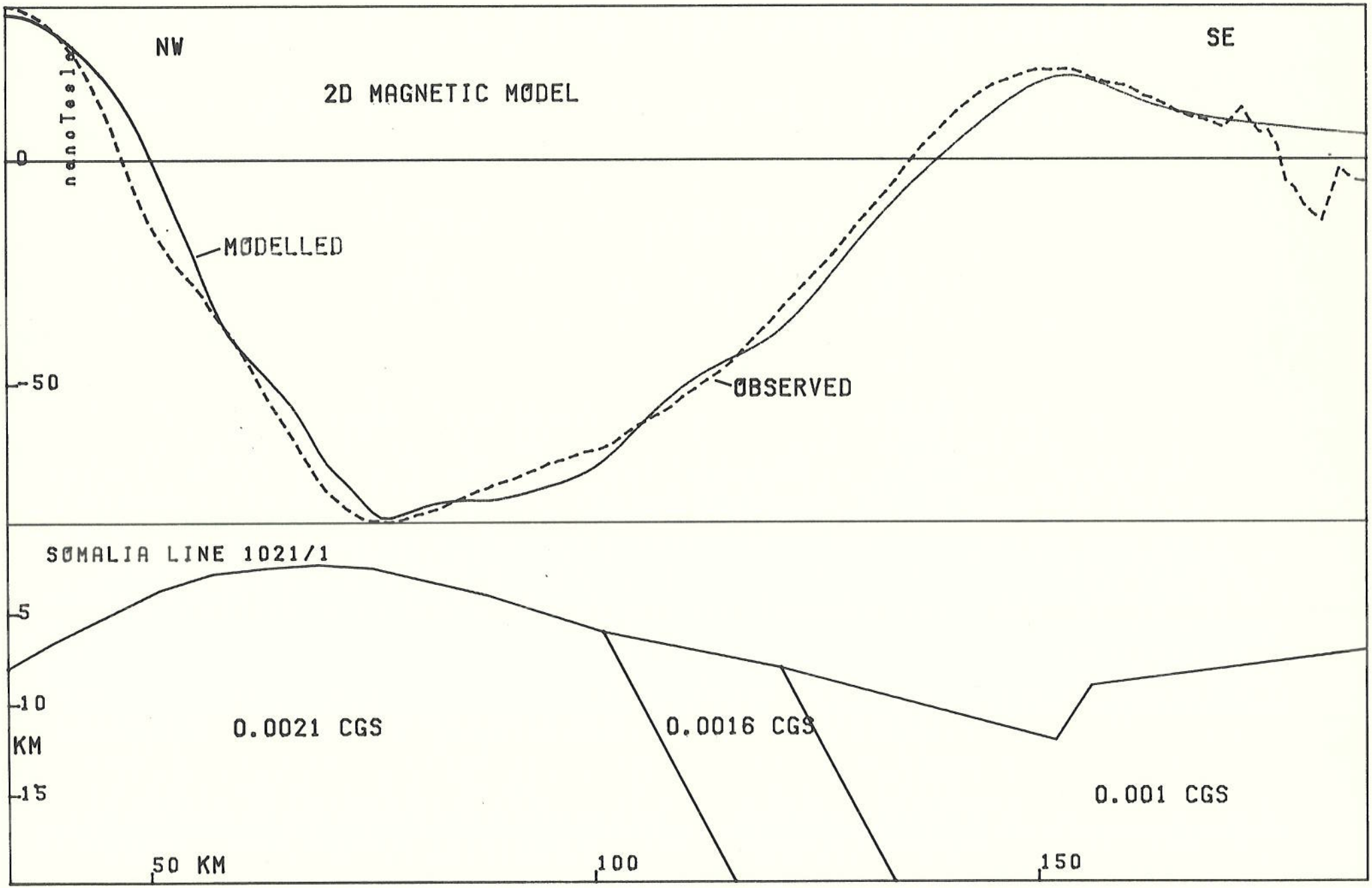
NW
SE
2D MAGNETIC MØDEL
nanoTesla
0
-50
MØDELLED
ØBSERVED
SØMALIA LINE 1021/1
5
10
KM
15
0.0021 CGS
0.0016 CGS
0.001 CGS
50 KM
100
150

FIGURE 4

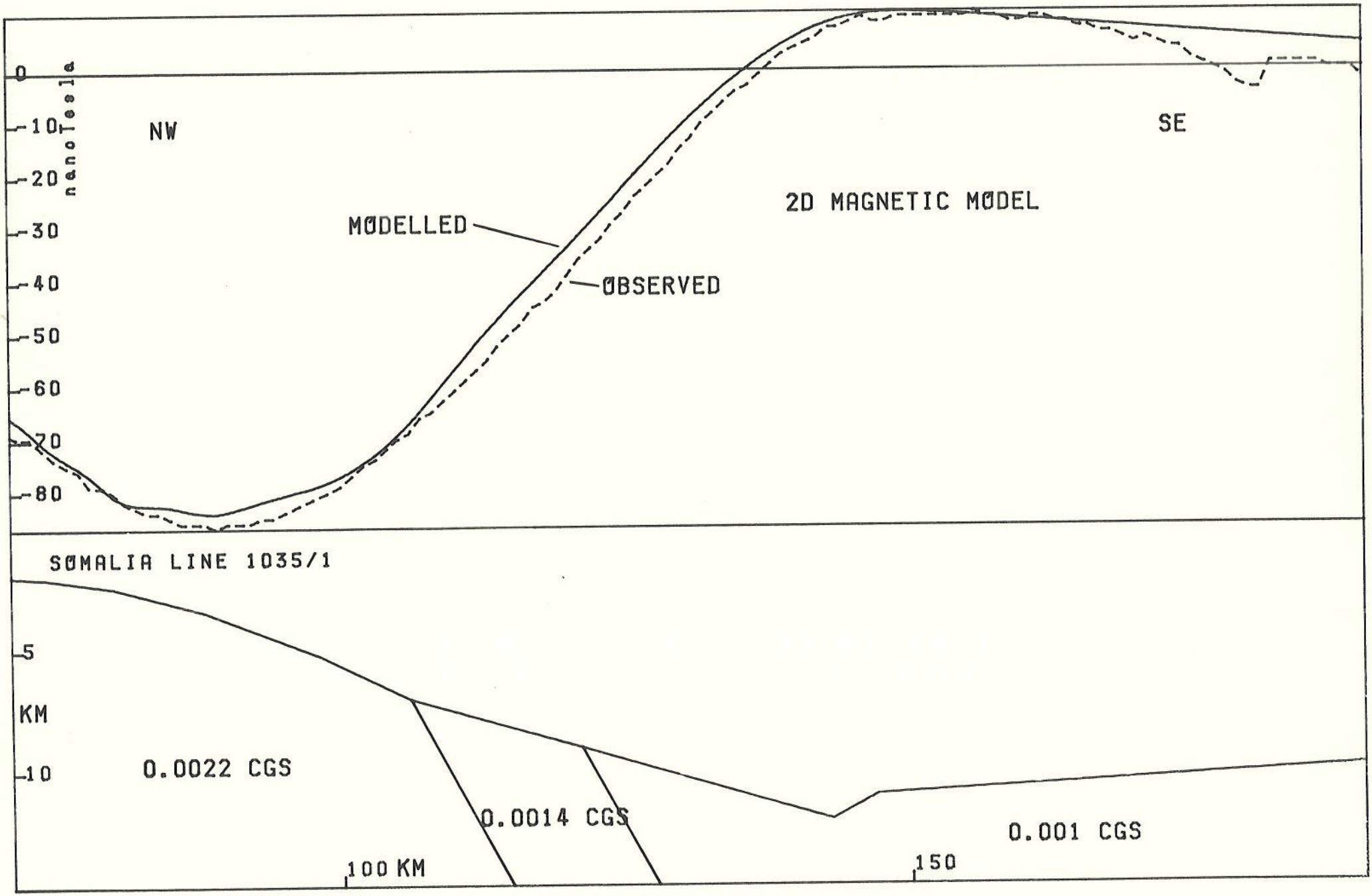
0
-10
-20
-30
-40
-50
-60
-70
-80
nanoTesla
NW
SE
2D MAGNETIC MODEL
MODELLED
OBSERVED
SOMALIA LINE 1035/1
5
KM
10
0.0022 CGS
0.0014 CGS
0.001 CGS
100 KM
150

FIGURE 5

FIGURE 6

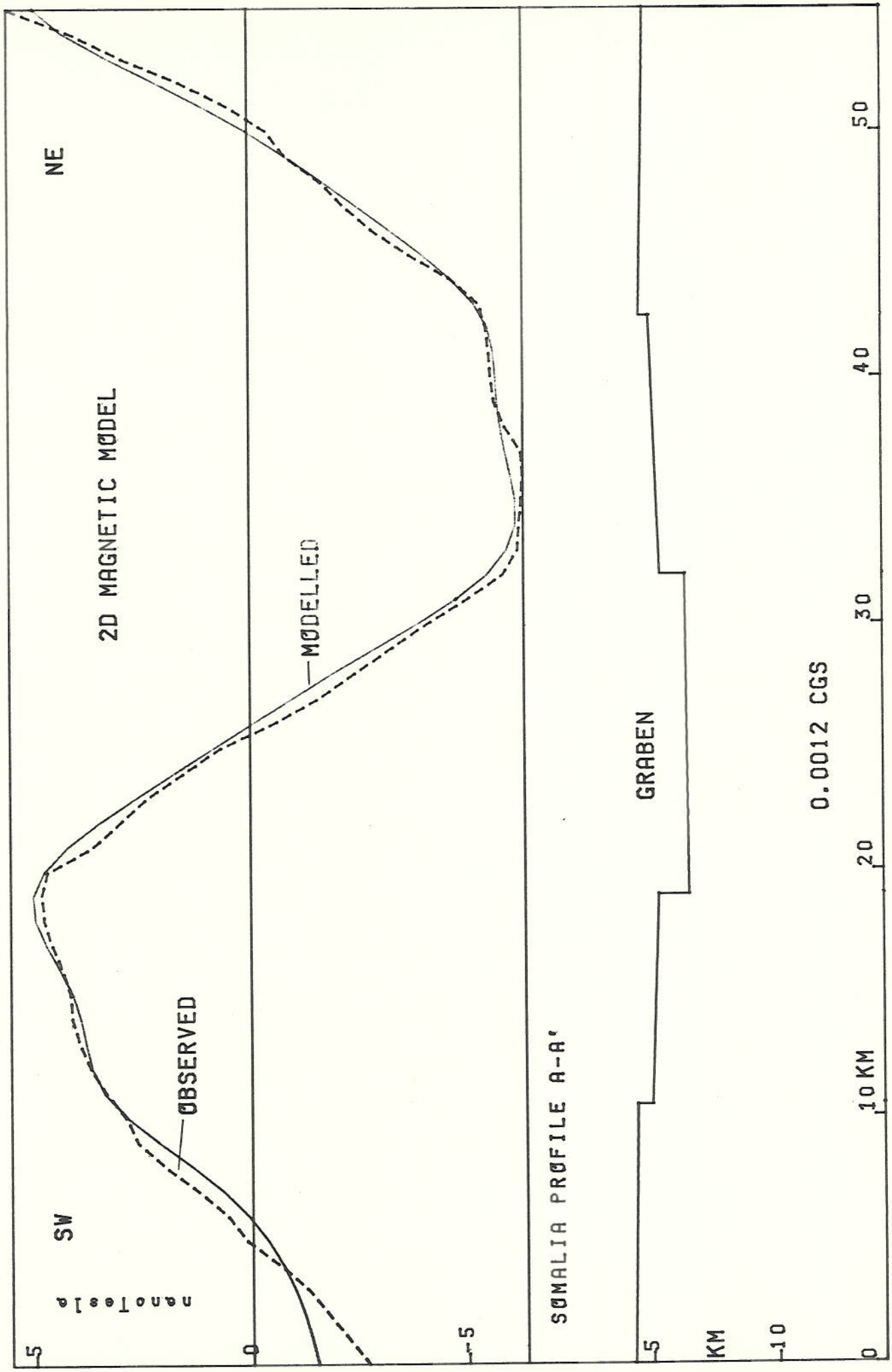
2D MAGNETIC MODEL
NE
SW
nanoTesla
5
0
-5
MODELLED
OBSERVED
SOMALIA PROFILE A-A'
GRABEN
0.0012 CGS
5
KM
-10
0
10 KM
20
30
40
50

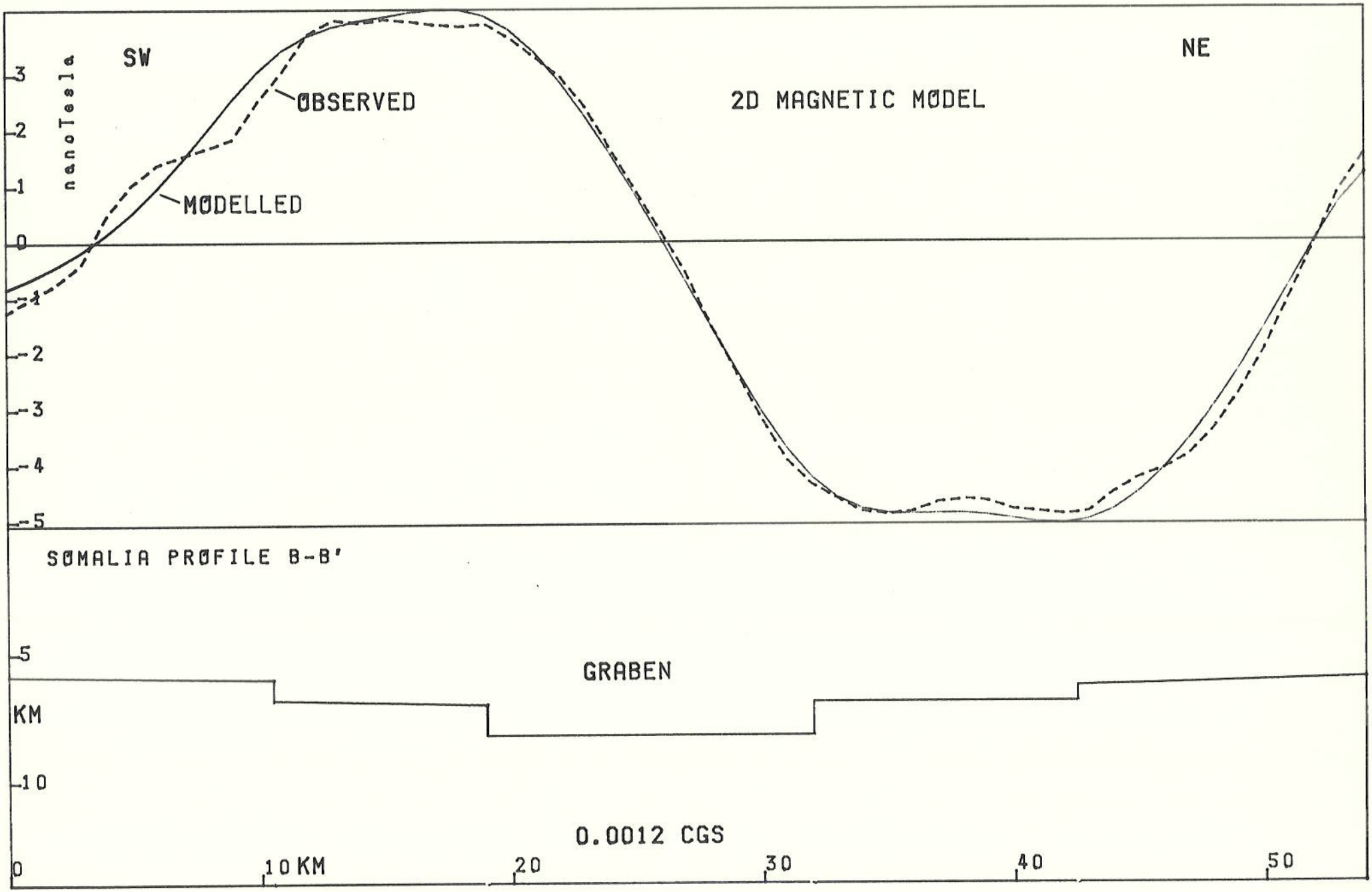
SW
NE
nanoTesla
3
2
1
0
-1
-2
-3
-4
-5
OBSERVED
MODELLED
2D MAGNETIC MODEL
SOMALIA PROFILE B-B'
5
GRABEN
KM
10
0.0012 CGS
0
10 KM
20
30
40
50

FIGURE 7

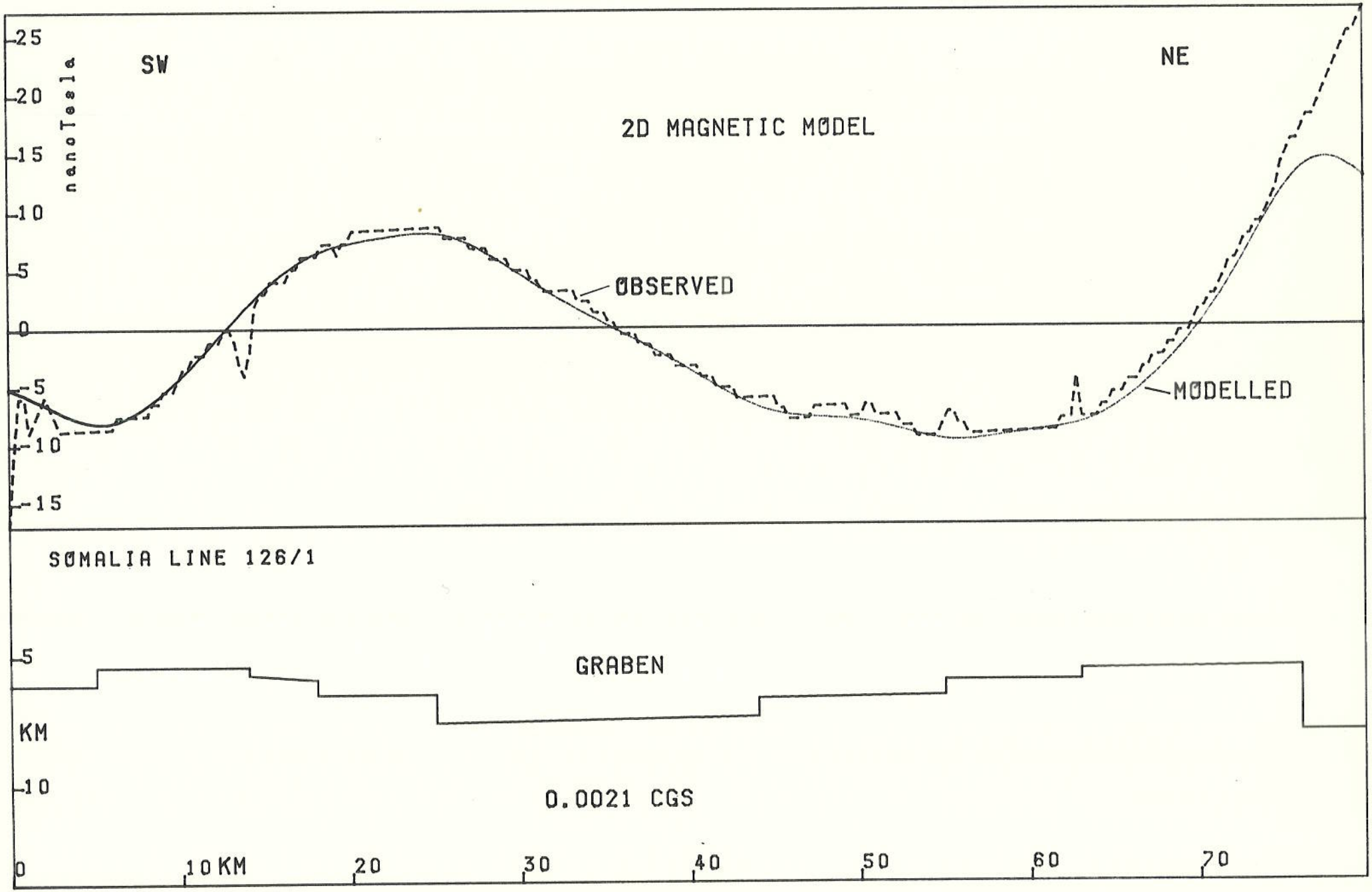
SW
NE
2D MAGNETIC MØDEL
nanoTesla
25
20
15
10
5
0
-5
-10
-15
ØBSERVED
MØDELLED
SØMALIA LINE 126/1
GRABEN
KM
5
10
0.0021 CGS
0
10 KM
20
30
40
50
60
70

FIGURE 8

within Sheet 127/139 probably defines the effective northern boundary of this feature. The structural high H1 forms the southern limit. It is necessary to attribute a change of magnetic susceptibility (higher to the south) across the positive magnetic trend associated with F73 if it is to be fully explained.

L3 is approximately 100 km in length, is narrowest in the middle region, about 20 km wide, where it intersects the Hiran Graben L1, and widens towards the west and east where the widths are nominally 25 and 40 km respectively. The structure appears to terminate near the northern limit of the western volcanic zone and is probably bounded in the west by the fault F41. In the east L3 broadens considerably and strikes eastwards out of Block 1 probably connecting with the Mudugh Basin, suggesting that L3 may be of late Jurassic or Cretaceous age. Maximum depth is attained (i) at the intersection with the Hiran Graben L1 in Sheet 127/139 where the estimated depth is about 6.5 km and (ii) near the eastern boundary of Block 1 where the depth is again probably 6.5 km. A NW-SE re-entrant is formed by the extension of L3 into a short trough L5 which extends across the corner of Sheet 104/116 into Sheets 128/140 and 103/115. The extent of L3 is limited in the extreme northeastern corner of Block 1 by the proposed ridge H4 which attains a minimum estimated depth of 2.5 km.

Immediately north of L3, over its western extent in Sheet 127/139, basement appears to level out over a large region centred upon body B7, extending as far west as faults F45 and F46. The broad NE-SW structural high so defined is annotated H3. With the exception of the B2 region, where basement appears to rise locally to 1 km depth, estimates indicate a markedly small range of basement depths in this region, between 2.2 and 2.9 km.

4.3 Volcanics and Associated Intrusives

The magnetic data suggest that a significant proportion of Block 1 is overlain or intruded by basic volcanic material. This is distributed almost continuously along the western and southern margins of the block, joining the eastern margin via an arcuate zone interpreted as mainly intrusive, in the southeast of the block within Sheet 9/21

4.3.1 Western Volcanic Region

This NW-SE trending region of mainly sub-outcrop volcanics, exposed portions of which are known to be of Late Tertiary age, is 20-40 km in overall width and 120 km in length. In view of the interpreted structural uplift H2 immediately to the north, the Western Volcanic Region too may be associated with a long established, underlying coaxial uplift. Such a structure might be expected to have been contemporaneous with the parallel Hiran Graben to the east and may indeed have contributed to the subsequent 'fill' of the graben. The component zones of the Western Volcanic Region are characterised by high frequencies and a range of high to low value amplitudes. Zoning has been performed mainly on the basis of mean amplitude. The most active zone is V1 where amplitudes average 300 nT peak to peak. V7 follows with up to 200 nT mean amplitude, Zone V8 100 nT, Zones V2, V4

and V5 50 nT, Zones V9 and V11 30 nT, Zone V10 10 nT, Zones V3 and V6 5 nT and Zones V12-V14 less than 5 nT.

The northern extent of the Western Volcanic Region, which is largely exposed, corresponds to the highest magnetic amplitude, and is known to be of Late Tertiary age, consisting of volcanic ash and tuff capped by a thick flow of basalt. Concealment by thin Quaternary cover occurs in the vicinity of the interpreted fault F8. The magnetic grain of the volcanics north and south of this fault differs in character, trending generally NW-SE within (and indeed parallel to) Zone V1 to the north, and essentially ENE-WSW, parallel to F8 within Zone V5 to the south. This might be explained by the possible absence of basalt cap south of fault F8 revealing the different, generally lower amplitude, magnetic signature of older volcanic ash and tuffs beneath. An implication of this is that in this region F8 has experienced Late Tertiary reactivation, probably simply upthrown to the south.

Outside of Zone V5, the Western Volcanic Region is dominated (as is the eastern half of Block 2) by N-S magnetic discontinuities which are assumed to be faults. These faults, which in places control the boundary of this volcanic region , are parallel to the Oddur Arch structure within Block 2 and considering the recent age of the volcanics are probably reactivated faults controlling the Oddur Arch's eastern flank. These features are particularly common in the north of the volcanic region. Those defining volcanic zone boundaries are: the fault associated with the interpreted dyke D19, F41, F33, F34, F35, F36, F39, F30, F32, F29 and F31. The very distinctive N-S fault F41, probably downthrown to the east, clearly defines the western boundary of this volcanic region in Sheets 126/138 and 6/18, and extends into Block 2. Faults F33, F34, F35, F36 and F39 cause numerous offsets in the northern volcanic boundary, and each can be followed large distances southwards into the volcanic zone itself. Faults F30 and F32 are distinctive, defining the eastern boundary of the particular volcanic zones V9 and V7/V1 respectively in Sheet 7/19. Faults F29 and F31 appear to bound the narrow N-S volcanic zone V2/V3 in the south of Sheet 7/19.

Study of the 1:500 000 scale magnetic contours in particular, suggests that faults F29 and F31, together with intrusives D15-D17, are continuations of N-S faulting in Sheets 127/139 and 7/19, notably - F30, possibly F33 and also the fault associated with the distinctive interpreted dyke D19. Lack of intervening continuity, may be due to the strong superimposed NW-SE trend of the volcanic zones V1 and V7. Assuming this is so, the 100 km long feature so defined represents the longest N-S feature in Block 1. It is terminated in the north by the circular, probably intrusive feature B3. Other smaller intrusives B17 and B5 occur to the south on the dyke D19. (See Section 4.3.4).

In the southern half of this volcanic region prevalent directions of magnetic discontinuities/faults are roughly NE-SW/ENE-WSW and E-W.

(a) The former, NE-SW/ENE-WSW strikes correspond to faults F52, F53, F65 and the westward extensions of F8 and F9. They occur in a confined group in the south of the adjacent Sheets 7/19 and 8/20 and would appear to be eastward

extensions of faults originating within the Bur Acaba Uplift region south of Block 2. The strike of these faults follows the same general direction as the magnetic grain in the northern half of volcanic zone V5. It is likely that these faults are reactivations of Precambrian fracturing which accompanied the orogeny associated with the Bur Acaba Uplift. Fault pairs F52/F53 and F85/F86 appear to define horst blocks striking northeastwards from Block 2 into the Western Volcanic Zone of Block 1. This interpretation is confirmed by computer modelling. See Figures 9 and 10 in Section 5 (Block 2) of this report.

(b) Faults with E-W strike all lie north of fault F8 within Sheets 7/19 and 8/20 and are F37, F63, F64 and F66. These may represent more recent faulting within the basalt flow horizon thought to exist only north of fault F8. To the north of fault F37, E-W strike appears to vary through WNW-ESE strike at fault F38, to the NW-SE strike of faults F21, F47/F23 and F24 in the north of Sheets 7/19 and 8/20. Faults F24 and F21 are particularly significant defining part of the eastern boundary of Zones V7 and V1 respectively.

The elliptical feature D18 on the boundary between Sheets 7/19 and 127/139 is interpreted as a ring dyke. The region encircled by this feature appears magnetically identical to volcanic Zone V10 to the north. Immediately to the south of D18, B6 is interpeted as an intrusive body, one of a number of extrusive lava sources likely to exist in this region.

V12 and V14, V6 and V13 are narrow low amplitude volcanic zones on the eastern and western boundaries respectively of this volcanic region . They probably represent thin marginal bands of eroded volcanogenic material.

4.3.2 Southern Volcanic Region

This magnetic region, within Sheets 32/44, 33/45, 9/21 and 10/22, is a continuation of the Western Zone's concealed volcanics. The region comprises five amplitude-defined volcanic zones, V15, V16, V17, V18 and V20, all lying south of the colinear features D6, D7 and F28.

Zones V15, V16 and V17 lying mainly within Sheet 32/44, define a particularly distinct block of volcanics in the west, intersected by approximately N-S magnetic discontinuities, interpreted as faults, and containing a high proportion of interpreted intrusives. V17 lies at an average depth of 0.3 km with a mean peak to peak amplitude of 30 nT. V15 to the east lies at an average depth of 0.6 km with a mean peak to peak amplitude of 15 nT (excluding effect of intrusion D6), and Zone V16 comprising the southern half of the region immediately south of D10 exhibits a southward dip from about 0.2 km to 1.0 km with a mean peak to peak amplitude of 10 nT peak to peak. The northern colinear boundaries of Zones V17 and V15 are defined by dyke-like bodies D6 and D7 whose ENE-WSW strike lies at right angles to the eastern edge of the Western Volcanic Zone. D6 is interpreted as

dipping northwards and is consistent with information from the 'Gal Tardo' drill hole located a kilometre or so to the north. Information from the 'Bio Addio' drill-hole which lies in the south of the volcanic zone confirms the underlying volcanic nature of this region.

Intrusive D7, in common with two others in this region D8 and D9, exhibits the reversal effect of remanent magnetization and therefore may not be contemporaneous with those intrusives in the region showing normal induced magnetization, D6, D10 and D24. Chemical differences may of course also account for varying degrees of remanence.

Interestingly, depth estimates to the volcanic surface in this region suggest an approximately E-W positive hinge-line H5 near the centre of the region; and like the Western Volcanics, the Southern Volcanic Region may possibly be associated with an underlying uplift. Apparently associated with this structure, dipping in opposite directions either side of the axis, are the dyke-like intrusions D6 to the north and D10 to the south. This suggests the possibility that D6 and D10 may at one time have been part of one (sub-)horizontal volcanic sill, subsequently arched upwards along axis H5 and peneplaned back exposing detached northern and southern dippng dyke-like bodies. The central intrusions D9 and D8, which are remanently magnetized, are possible volcanic feeders for this region but may pre- or post-date the proposed structure. It is suggested that the basaltic sill encountered at a depth of 1.6 km in the 'Bio Addio' drill-hole corresponds to the interpreted intrusive D10.

A particularly striking aspect of the volcanic region defined by zones V15, V16 and V17 is the strong evidence for approximately N-S faulting. These features, which are observed as magnetic discontinuities across the general ENE-WSW grain of the region, are: F18, F19, F20, F25 and F26. The dyke-like intrusions D6 and D7 along the northern boundary of the volcanic region and D8 and D9 in particular, appear markedly dislocated by these features. Their N-S strike, like those N-S faults of the Western Volcanic Region, suggests a possible association with the Oddur Arch structure to the west. The undoubtedly deep basement structure immediately north of the Southern Volcanic Region is probably controlled in part by northward extensions of faults F18 and F19 in particular. For it is in this region that long wavelength magnetic contours, of the high associated with the trough L2, turn abruptly N-S. It is possible that F20 is similarly extended northwards. Lack of direct magnetic evidence for these faults outside the volcanic zone is in part due to the very low amplitude anomaly generated by N-S magnetic features. Low amplitude residual anomalies north of fault F8 may mark the path of fault F18 extending almost as far as Bulo Berti, along and possibly controlling a 25 km extent of the Webi Shebeli River.

The strong ENE-WSW trend of features D6,D7,D8 and D9 lends confidence to the interpretation of weaker linear interpreted features of the same trend in the south of Block 1 (such as F8,F9 and L2), as nowhere is an ENE-WSW trend recognised at the surface.

Zone V18 within Sheet 33/45 is a low amplitude region interposed between Zones V15, V16 and V17 in the west and the volcanic Zone V20

in the east. Zone V18 whose mean peak to peak amplitude is about 5 nT, probably represents a region of thinner volcanic deposits, possibly tuffs. To the east, V20 is comparable in peak to peak amplitude to Zone V15 and both zones are probably of like composition. Depth estimates suggest that the volcanics of Zone V20 south of F28 lie between 0.5 and 0.7 km.

Volcanics undoubtedly continue south of the Block 1 survey area.

4.3.3 Eastern Volcanic Region

This region comprises two zones separated by fault F8: (i) The very distinctive arcuate, intrusive-dominated zone in the south, and (ii) the eastern boundary volcanic Zone V21 of Sheets 9/21 and 129/141 to the north.

The arcuate zone may perhaps be more conveniently described as comprising a faulted NE-SW component body B4 immediately south of the eastern end of fault F8, connected in the west to a broader southeasterly striking, somewhat sinuous component approximately on strike with the Hiran Graben L1 to the north.

The NE-SW component comprises a cross-faulted, linear, tripolar anomaly 30 km long, and with a general peak to peak amplitude of 60 nT. The feature is probably dominated by remanent magnetization which may explain the difficulty in obtaining a sensible computer modelled profile of this feature. The feature might be caused by a dipping dyke-like intrusion with associated short sill-like bodies to north and south, dislocated by faulting along the plane of intrusion. Dislocations along this feature namely F2, F4, F7 and F6 are interpreted as NW-SE cross-faulting, thought to be related to the eastern flanking faults of the interpreted Hiran Graben to the north. This association suggests that the Hiran Graben may once have extended south of F8. Considerations at the end of Section 4.2.3 , however, throw some doubt on this. A sinistral strike-slip movement has been ascribed to F8 in this region to match the apparent offsets of the dislocations across B4 and the extrapolated modelled Hiran Graben faults to the north. Strictly, however , the true sense and magnitude of movement on F8 is somewhat uncertain. An alternate position for F8 is near the southern boundary of B4. The directions of throw on the cross faults F4 and F6 in particular (also note F7) are probably to the west and east respectively, as implied by their assumed counterparts to the north on the eastern flank of the Hiran Graben. The corresponding offsets along B4 in turn imply that the dyke-like component associated with B4, dips to the north. It is suggested that the intrusive body B4 may represent an intruded shear zone. It is accompanied to the north by Zone V20, which probably represents a thin section of volcanics.

The NW-SE trending component of the arcuate zone is 40 km long and appears to comprise numerous intrusions, namely B12, D1, B14, D25, D2, D3, D13, D5 and B13 lying within the volcanic Zone V20. Mean peak to peak amplitude is less than that of the NE-SW component, 40 nT north of F56 and about 15 nT in the south where there is a lower incidence of intrusives. Depths, mainly computed on the intrusions, vary from

about 0.3 km in the north, 0.1 km in the central region and 0.5 km in the south. One suggestion is that most intrusive features in this region are associated with extended faulting of the Hiran Graben's central floor. Section 4.2.3, however, suggests that the observed colinearity with the extrapolated axis of the Hiran Graben may be purely coincidental. Like B4, many of the intrusions along the NW-SE component are probably remanently magnetized. Interpreted faults F56, F57 and F58 parallel the ENE-WSW fault F9 close-by. V20 broadens as it connects with the southern volcanic zone.

Considering the preceding observations, the arcuate zone probably corresponds to a zone of intrusion-dominated, fissure-type volcanics.

The narrow, eastern boundary volcanic Zone V21 of Sheets 129/141 and 9/21 shows a mean peak to peak amplitude of 60 nT. This zone exhibits a well defined, linear NW-SE trending western boundary. This is almost certainly fault associated, namely with fault F14, and constitutes the clearest direct evidence of NW-SE (Hiran Graben related) faulting (albeit probably reactivated) in Block 1. An extension of F14 to the north may define the eastern boundary of the large intrabasement body B1 in Sheet 128/140. V21 is acccompanied by a lower amplitude marginal Zone V20 south of the interpreted NE-SW fault F61, probably related to thinner volcanics. The volcanic zone V21 undoubtedly continues eastwards outside Block 1.

4.3.4 Other Intrusives

Virtually all the major intrusives of Block 1 that lie outside the volcanic zones, occur north of the Western Volcanic Region, mainly within Sheets 126/138, 127/139 and 103/115. The exception to this is the interpreted intrabasement and apparently very rigid block B1 within Sheet 128/140. See Section 4.2.3 for further description of B1.

West of the line defined by faults F45, F46 and F41, all of which are downthrown to the east, the intrusives are probably wholly intrabasement, lying within the shallower basement (just under 1 km in average depth) which extends eastwards from Block 2. These features, which are all contained within Sheet 121/138 are: bodies B7 and B8 apparently offset by fault F69 and probably dipping to the south and dyke-like body D22 apparently offset by fault F70.

East of faults F45, F46 and F41, the intrusives lie within deeper basement. In the case of B2, which probably dips to the north, there appears to be a corresponding shallowing of basement, 1 km in a region generally of over 2 km depth. No such association is observed with body B7 to the north.

However, B3 to the east of B2 is most certainly an intrusion, the top of which very nearly reaches the surface according to depth estimates. B3 corresponds to a low amplitude, somewhat incoherent, circular anomaly and lies on axis with the interpreted dyke D19 along which there appear to be other minor three-dimensional intrusions, B17 and B5. Study of the 1:500 000 scale magnetic contours shows particularly well that this collection of intrusions, terminated by B3 in the

north, is probably part of a larger linear zone of intrusion extending southwards through Zones V9, V7 and V1 of the Western Volcanic Region and along dykes D15, D16 and D17 contained within the N-S faults F29 and F31 at the south of Sheet 7/19. This composite N-S intrusive feature is about 100 km in strike length and represents the longest N-S feature in Block 1. In length it is rivalled by the NW-SE Hiran Graben to the east and by the NE-SW trough L3 in the north. It is of interest to observe that B3 lies on the intersection of the modelled Hiran Graben fault F1 and the northward extension (presumably the controlling fault) of D19. B17 similarly lies at the intersection of D19 and the modelled Hiran Graben related fault F10. It is suggested that B3 may represent an alkaline volcanic (or even a Kimberlite) intrusion. (See Section 4.3.1).

5. INTERPRETATION - BLOCK 2

5.1 Introduction

Block 2 is approximately three times the area of Block 1 and shows a much more complex magnetic anomaly pattern. This complexity clearly derives from a relatively shallow basement in the region of the N-S Oddur Arch structure, superimposed upon which, it is proposed, are zones of intrasedimentary volcanics.

Although the Oddur Arch is clearly a dominant structural feature, magnetically it does not dominate, due mainly to its N-S strike (giving rise to very little induced amplitude). Lying in the eastern half of Block 2, the structure is revealed at surface by the arcuate disposition of Jurassic sedimentary units north of the Bur Acaba Uplift. The axis of the Oddur Arch intersects the northernmost point of the Bur Acaba outcrop and extends directly northwards to the northern margin of the survey area. (See Section 5.2.2.)

West of the Oddur Arch (the Juba River provides an equally appropriate reference) the magnetic character of Block 2 reverts to the broader, long wavelength pattern observed in Block 1.

A matched filter was applied to the data of Block 2 in order to remove the high frequency magnetic response of suspected widespread shallow volcanics from that of deeper basement. This was achieved by conducting a sheet by sheet spectral analysis of the entire Block 2 data set. These results were then used to design a suitable low pass filter. (See Section 3.4.) Magnetic contour maps of both the filtered and residual "shallow" component data have been very useful, largely in three ways (i) to distinguish zones of intrasedimentary volcanics (of relatively low amplitude and therefore difficult to separate visually from stronger superimposed intrusive and basement anomalies), (ii) to delineate linear, probably fault-related features and (iii) to enable better determination of obliquities for depth estimation correction.

5.1.1 Long Wavelength Zone

Two long wavelength zones occur in Block 2. Both probably correspond to deep basement. Together they comprise just under half the area of Block 2.

(i) The smaller region lies in the extreme east of the block along the boundary with Block 1, within Sheets 6/18, 7/19, 30/42 and 31/43. This region is characterized by relatively open magnetic contours showing strong NE-SW trends of up to 12 nT amplitude in the east and 22 nT amplitude in the west. This region appears to be an extension of the deep basement region of Block 1.

(ii) The larger second region lies in the west of the block and undoubtedly corresponds to a region of deep basement, the northern part of which is generally regarded (see Barnes) as part of the Mandera-Lugh Basin. For the most part this

region is closely bounded to the east by the N-S course of the Juba River. Unlike the long wavelength region of Block 1, this region contains many distinct anomalies resulting in a more satisfactory distribution of manually estimated depths. This region appears to contain various structural trends of comparable significance and may therefore have been subject to more than one tectonic episode.

The predominant magnetic trend in the region is NE-SW. Magnetic features showing this trend appear to be mainly structurally associated (see Sections 5.2.8, 5.2.10 and 5.2.11), to lie within the northern two thirds of the region and to have amplitudes ranging from approximately 15 to 25 nT.

Following in significance is the NW-SE trend. Magnetic features showing this trend lie within the southern third of the region and have amplitudes ranging from approximately 5 to 30 nT. This trend, although secondary, is related to a long NW-SE interpreted horst, the details of which are described in Section 5.2.13.

Reconnaissance area Block 4, which forms part of this region, is dominated by a large negative E-W trending anomaly of 90 nT amplitude, which in Section 5.2.12 is ascribed a rather fundamental significance.

Several three-dimensional, dipolar magnetic anomalies are observed in this region, of which the major three have peak to peak amplitudes of between 160 and 180 nT. (See Section 5.3)

5.1.2 Short Wavelength Zone

The principal short wavelength region of Block 2 extends westwards as an apparent continuation of the Western Volcanic Region of Block 1, in a narrow 7-20 km wide, 280 km long, arcuate band across the northern region of Block 2. This is the most distinctive magnetic feature of Block 2 and undoubtedly reflects the presence of extensive, probably fissure-type, sub-outcrop volcanics. Coinciding with the region's western extremity is a large exposure of basalts dated as Late Tertiary. Other less extensive regions of short wavelength magnetics, also coinciding with basalt outcrop, occur along the eastern bank of the Juba River. (See Section 5.4 for full description of volcanic zones.)

5.1.3 Medium/Short Wavelength Zone

The remainder of Block 2 may be described as a complex region of medium to short wavelength anomalies, distinct from the wholly short wavelength arcuate region of the previous section.

Particularly short wavelength regions are observed within a 20 to 40 km band around the northern boundary of the Bur Acaba basement

exposure. This magnetic signature can probably be attributed to shallow basement. North of this band, spectral analysis suggests the existence of two distinct magnetic horizons, the shallower presumably being an intrasedimentary layer of volcanics. This is certainly consistent with the complex patchy nature of the mid-region caused, it is suggested, by an erosional unconformity at the level of the volcanics. It should be noted that although numerous intrusive (vertical/sub-vertical) bodies appear throughout this region tending to degrade spectral plot sharpness, the spectral analysis appears to have satisfactorily determined those sheets likely to contain two horizons. (See Appendix 1).

5.2 Structure

Contours of estimated basement depths clearly show a relatively steep, essentially N-S striking gradient which shallows eastwards to the medium to short wavelength region of the Oddur Arch. West of this gradient, which may be associated with the long, interpreted N-S faults F232, F231 and F227, lies the long wavelength deep basement region a large part of which corresponds to the region known commonly as the Mandera-Lugh Basin. This boundary closely follows the course of the Juba River for a significant distance clearly suggesting that the river is structurally controlled. Surface elevation is in general significantly lower to the west of the Juba River within the deep basement region. This region lies on average less than 500 feet above sea level. East of the river, topography is smoother, on average greater than 1000 feet above sea-level rising eastwards to the crest of the Oddur Arch.

In the western deep basement region , interpreted basement depths suggest a regional undulation of basement surface between NE-SW and E-W in trend, between 6 and 10 km in depth and with a peak to trough separation varying between 25 to 75 km. Some significant NW-SE cross-structure has been interpreted. The northern half of the deep basement region largely corresponds to the Mandera-Lugh Basin as described by Barnes (1976). According to Barnes, this basin appears to extend southwards as far as the position of the interpreted basement ridge H6 (see Section 5.2.11). Magnetic depth estimates, however, indicate that deep basement extends regionally from the north of the block past ridge H6 to the south as far as the interpreted E-W basement ridge H7. If this magnetic interpretation is correct, the Mandera-Lugh Basin appears to be a more extensive feature.

In the shallow basement region, interpreted basement depths clearly support the simple broad structure of the Oddur Arch, showing it to be gently deepening from the Bur Acaba outcrop in the south to a maximum of just over 4 km depth at the intersection with L9 in the north. Other features of low relief have been interpreted over the Oddur Arch.

Many interpreted faults within the shallow basement region have been deduced from subtle features such as alignment of short strike-length magnetic anomalies and discontinuities. Depending on the nature of the basement, faults revealed in this fashion are often of indeterminate significance. If for example an interpreted fault,

particularly of E-W strike (which in principle should give rise to a maximum response) is only indirectly revealed, it may be assumed to be of relatively small throw if the basement is known to be relatively magnetic and magnetically homogeneous. If however basement is known to be particularly inhomogeneous magnetically and at the same time relatively shallow, even a fault of moderate throw will not necessarily give rise to a directly attributable coherent magnetic response. Therefore, within a region such as the medium to short wavelength zone of Block 2, whose basement is relatively shallow and composition probably chaotic (see the geology and magnetics over the Bur Acaba outcrop and models JJ' and KK' - Figures 12 and 13) indirectly revealed faults tend to remain indeterminate both in displacement and magnitude.

5.2.1 Structural Trends

Within the deep basement region the principle interpreted trends lie within the range NE-SW through to E-W. A secondary but quite significant trend is NW-SE. The principal interpreted trend within the shallow basement region is N-S. Secondary trends are NE-SW and approximately E-W.

The range of interpreted trends within the western deep basement region is essentially the same as that of the shallow region, except for the notable absence of N-S. This difference is attributed to the Oddur Arch whose structural influence becomes apparent only east of the Juba River. Faults F231 and F227, and perhaps adjacent minor faults to the west define a N-S band within which the western deep basement region appears to have been decoupled from movements associated with the developing Oddur Arch to the east. (See Section 5.2.12).

5.2.1.1 NE-SW

This trend, as previously suggested, is probably related to the Bur Acaba Uplift. It is most strongly evident in the long wavelength, deep basement regions in the west and east of the block. More subtle though persistent evidence for this trend also occurs within the medium to high frequency complex in a band of between 15-30 km along the northern boundary of the Bur Acaba Uplift.

The major interpreted structural features are:

(i) L6, a trough/graben located within the eastern deep basement region. 65 km long and 7 to 10 km wide, this feature is defined by the major faults F85 and F52 to north and south respectively. Associated parallel faulting to north and south, F86 and F53, provides L6 with horst-like shoulders. A parallel trough L16 lies a short distance to the north. (See Sheets 6/18, 7/19, 30/42, 31/43 and Section 5.2.3).

(ii) H6, a ridge located within the western deep basement region. This 145 km long feature spans the full width of the deep basement region. H6 corresponds to a major linear negative

anomaly and may form the southern boundary of a deeper pre-Jurassic component of the Mandera-Lugh Basin. (See Sheets 59/71, 60/72, 49/61 and Section 5.2.11).

(iii) L12, a relatively broad trough north of ridge H6. Existence of this feature only clearly emerges on contouring the basement depth estimates, as it appears to give rise to little direct magnetic response. L12 would appear to be a major structural component of the Mandera-Lugh Basin. (See Sheets 59/71, 60/72, 49/61, 25/37 and Section 5.2.10).

(iv) L11, a relatively short, 55 km long trough comprising part of the Mandera-Lugh Basin region. L11 strikes parallel to an interpreted regional basement contact a short distance to the south. (See Sheets 25/37, 1/13 and Section 5.2.8).

(v) F96 and F191, two very long parallel faults, probably downthrown to the north, lying within the shallow basement zone. These indirectly revealed faults are 320 km and 130 km in length respectively and parallel the northern boundary of the Bur Acaba outcrop. (See Sheets 49/61, 50/62, 26/38, 27/39, 28/40, 4/16, 5/17 and 6/8).

5.2.1.2 ENE-WSW to E-W

This range of trends is found throughout Block 2. The major interpreted structural features are:

(i) L10, a linear 190 km ENE-WSW trough which lies at the extreme north of the western deep basement zone extending eastwards into the shallow basement region of the Oddur Arch. Its western half represents a major structural component of the Mandera-Lugh Basin. (See Sheets 12/24, 1/13, 2/14, 3/15 and Section 5.2.6).

(ii) L9, a trough of similar relief and overall length as L10. It continues eastwards from a position approximately 30 km north of the eastern end of L10 within the shallow basement zone. Near its midway point L9 makes a transition in strike from E-W to NW-SE. L9 and L10 together form an almost unbroken arcuate trough running from the western boundary across the top of Block 2 to the southern boundary in the east. Intersection of L9 with the graben L7 may form a sub-basin. This might have explained the presence of two nearby evaporite outliers, but for a significant positional discrepancy. (See Sheets 123/135, 124/136, 125/137, 5/17, 6/18 and Section 5.2.4).

(iii) Faults F160,F161, F162 and F168. These indirectly revealed faults lie south of L9 within the shallow basement zone and are almost exactly E-W. F168 appears to mark the southern boundary of intrasedimentary volcanics. The other faults may or may not be of structural significance. (See Sheets 3/15, 4/16, 5/17 and 6/18).

(iv) F115, an essentially E-W fault, 35 km long, with an interpreted downthrow to the north and lying 28 km east of trough L10 within the shallow basement zone. This fault, which coincides with a mapped geological boundary, exhibits dislocations interpreted as evidence of the N-S graben L7. F114 and F113 to the east may be related faults. (See Sheets 4/16, 5/17 and Section 5.2.5).

(v) F193, another essentially E-W fault lying in the south west of the shallow basement region, 70 km long and with an interpreted downthrow to the north. Like F115, F193 also exhibits marked dislocations which in turn suggests the presence of a broad N-S graben L8. (See Sheets 35/42, 36/48, 25/37 and Section 5.2.7).

(vi) H9, a 120 km long E-W ridge spanning the full width of the deep western basement region. Effectively separating trough L10 from L12, H9 constitutes a structural component of the southwardly extended Mandera-Lugh Basin. (See Sheets 35/42, 36/48, 25/37 and Section 5.2.9).

(vii) L14, a relatively short 60 km long ENE-WSW/sub E-W trough located in the south of the western deep basement region. (See Sheets 83/95, 84/96 and Section 5.2.15).

(viii) H7, an 80 km long E-W ridge. This is the southernmost feature of the deep basement area flown and is interpreted from reconnaissance data only. This feature may represent a westward extension of the Bur Acaba Uplift. (See Sheets 108/120, 97/109, 73/85 and Section 5.2.12).

5.2.1.3 N-S

This trend is observed only east of the Juba River, essentially within the shallow basement region of the Oddur Arch. The major structural features are:

(i) F227 and F231, two long, parallel faults probably downthrown to the west but with strike-slip components, interpreted from both "deep" and "shallow" component data sets. In the north these faults show a controlling effect on the volcanic zones. Together with fault F232 (and other possible nearby faults) F227 and F231 appear to define the western limit of the shallow basement region, that is, the Oddur Arch structure. (See Sheets 2/14, 26/38, 50/62, 49/61 and Section 5.2.12).

(ii) Fault F41, accompanied by other minor parallel faults nearby, is one of the most significant N-S Oddur Arch related faults of the eastern flank. F41 strongly controls the western boundaries of volcanic zones V1, V23 and particularly V8 within Block 2 and Block 1. (See Sheets 6/18, 126/138, 127/139 and Sections 4.3.1 and 5.2.3)

(iii) Faults F146, F140, F135, F134, F131, F130, F128, F127, F126, F124. These faults define a N-S fracture zone within the shallow basement region, whose relatively high density of fracturing would imply proximity to a significant linear structural feature. This structure is clearly the Oddur Arch, and is confirmed by the interpreted basement depth contours. Closer study of these indirectly revealed faults shows however, by their relationship with various other interpreted features, that they define a N-S trending structural low, L7, coaxial with the Oddur Arch. (See Sheets 124/136, 125/137, 4/16, 5/17 and Section 5.2.5).

(iv) Faults F204, F203, F182, F181, F198 and F197. These relatively short interpreted faults together allude to the presence of a 60 km long N-S structural low L8. These faults are indirectly revealed by discontinuities along the essentially E-W fault F193, which is interpreted as downthrown to the north. (See Sheets 3/15, 27/39 and Section 5.2.7).

5.2.1.4 NW-SE

Evidence for this trend is strongest in the western deep basement region. The major interpreted structural features are:

(i) H8, a structural high over 100 km in length, lying within the western deep basement region. This feature is controlled by faults F244, F243 and F242. Intersecting structural high H6 appears to give rise to a high closure at this point. (See Sheets 59/71, 60/72, 84/96 and Section 5.2.13).

(ii) L13 and L15 are structural highs to east and west of the interpreted intrusion B42 lying within the western deep basement region. Depth estimates suggest that B42, which is approximately 16 km long and 10 km wide, intrudes well into the sedimentary section of what may otherwise have been an undisturbed sedimentary basin. (See Sheets 60/72, 84/96, 73/85, 49/61 and Section 5.2.14).

(iii) F237, an 85 km long fault downthrown to the NE, within the western deep basement zone. This fault which is indirectly revealed in the south but gives rise to direct magnetic response to the north, is accompanied by two much shorter faults to the west, F238 and F239. Together these faults may form a short 18 km wide horst. (See Sheets 36/48, 60/72 and 49/61).

(iv) L9, a trough within the shallow basement region, (see previous section) the eastern section of which trends NW-SE along the eastern flank of the Oddur Arch. (See Sheets 5/17, 6/18 and Section 5.2.4).

(v) Faults F108, F110 and F111. These faults which occur on the eastern flank of the Oddur Arch, are interpreted directly

from NW-SE magnetic anomalies which appear in both the "deep" and "shallow" component data sets. Downthrow is indicated to the east and as such the faults appear to strongly control the eastern flank of the Oddur Arch structure. Magnetic amplitude is significantly higher to the west of these faults, which in principle could indicate shallower intrasedimentary volcanics or merely shallower basement or indeed both. (See Sheets 5/17, 6/18 and Section 5.2.2).

(vi) F50, a long indirectly revealed fault within the shallow basement region. This persistent fault appears to be at least 130 km in length, but association with the approximately colinear intrusions D34 and D35 may increase its length to 210 km. (See Sheets 7/19, 6/18, 5/17, 125/137, 124/136 and Section 5.4.1.)

5.2.2 The Oddur Arch - regional structural high

Lying in the eastern half of Block 2, the Oddur Arch is clearly revealed at surface by the pronounced northward convexity of Jurassic sedimentary units 'younging' to the north.

Although the Oddur Arch is a dominant structural feature of Block 2, magnetically it does not dominate, due to its N-S strike (generating little amplitude) and also due to its significant width which in effect distributes an already barely detectable amplitude over a very wide region which in turn is overprinted by many other magnetic features. Nevertheless, magnetic depth estimates of intrabasement features within the region clearly reflect the N-S structure of the arch. Contouring of these depths shows the arch intersecting the northernmost point of the Bur Acaba outcrop and extending directly northwards through Sheets 5/17 and 125/137 as an effective extension of the Bur Acaba Uplift, attaining an interpreted depth of just over 4 km at the intersection with feature L9. Accepting that Somalia was essentially a peneplain prior to re-sedimentation in the Jurassic, at least part of the Oddur Arch structure post-dates the Jurassic. In the absence of evidence to the contrary, it is suggested that a related proto-arch feature existed prior to the Jurassic. The appearance of volcanics during the Late Tertiary across the north of the arch suggests that some updoming and related fissuring may have occurred as recently as Late Tertiary. (See Section 5.4.1).

F108, F110 and F111 are directly revealed NW-SE trending faults lying on the eastern flank of the arch. Downthrown to the east as their magnetic signatures indicate, suggests that these faults are important structural elements of the Oddur Arch.

A plausible association of the N-S trending Oddur Arch structure with the Cretaceous N-S trending Cap St. Andre Uplift of northern Madagascar is suggested. Although the positions of the two structures may not necessarily have been exactly colinear prior to the East Africa/Madagascar break-up, they nevertheless share the same unusual N-S trend and may therefore exploit a common pre-Jurassic regional zone of weakness.

5.2.3 L6 and L16 - structural lows

These essentially NE-SW sedimentary troughs comprise the smaller deep basement region in the east of Block 2. Their existence is a consequence of faulting F52, F85 and F86 implied by two-dimensional computer modelling along profiles 2070/1 and 2086/1. See Figures 9 and 10. Model 2070/1 in particular probably represents the best fit of any model within Block 2.

The southernmost trough L6 is fault controlled on both sides and appears to extend into the Western Volcanic Region of Block 1. Along profile 2070/1 the trough attains a maximum modelled depth of 5.2 km and a shoulder to floor relief of about 1 km. Along profile 2086/1 the maximum modelled depth is 4.4 km and shoulder to floor relief is again about 1 km. L6 therefore appears to plunge to the northeast.

Trough L16, which may be fault controlled to the south only, attains a maximum modelled depth along profile 2070/1 of 5.1 km and a shoulder to floor relief of 1 km. Along profile 2086/1, Figure 10, the maximum modelled depth is again 5.1 km, however shoulder to floor relief is somewhat indeterminate due to magnetic interference.

The NE-SW faults controlling L6 and L16 are probably Jurassic reactivations of older faults related to the Bur Acaba orogeny. L6 and L16 are possibly truncated by rising basement northeast of the Bur Acaba outcrop.

Unlike the larger deep basement zone in the west, the structure here appears remarkably simple with little observable cross-structure. The intersecting interpreted N-S faults F41 and F39 however are probably more significant than their minor magnetic responses would suggest, for even major N-S striking structures generate very little magnetic response.

5.2.4 L9 - structural low

L9 is an approximately 40 km wide, possibly up to 190 km long, sedimentary trough, defined by manual basement depth estimates. The trough trends E-W across the north and then NW-SE along the eastern flank of the shallow basement region. The continuity of L9 is somewhat uncertain due to poor distribution of estimated basement depths, especially east of the 124/136 and 125/137 sheet boundary. A maximum depth of about 4.5 km is attained within Sheet 124/136. Maximum structural relief occurs along the E-W section, of about 1 km to the south and 1.5 km to the north. L9 may ultimately connect trough L16.

The E-W axis of L9 coincides closely with the shallow intrasedimentary volcanic zones V44, V33 and V32 and may therefore have played a significant role in localizing/retaining volcanics in this region. Also coincident with L9 are two small E-W trending evaporite outliers/basins (see UNDP geology map, unit Klmg) which occur over the very crest of the Oddur Arch. The exposure of the unit J3an (shale, marl, marly limestone) within which these basins lie, widens

considerably over the crest of the Oddur Arch in apparent accommodation of these basins. (See Section 5.4.1).

5.2.5 L7 - structural low

This N-S feature which is perhaps 100 km long and at least 65 km wide in the north, is implied by the indirectly revealed fractures/faults F146, F140, F135, F134, F131, F130, F128, F127, F126 and F124, within Sheets 124/136, 125/137, 4/16 and 5/17. Lying within the shallow basement region, this the highest density of N-S fracturing in the survey area, suggests proximity or indeed coincidence with the Oddur Arch axis. The estimated basement depth contours suggest that this indeed is the case.

Close study of these faults shows that their relationship with the intersecting fault/geological boundary F115 (interpreted as downthrown to the north) and northward dipping intrusions D36, D35, D33, D32 to the north (see Section 5.4.1) implies a broad N-S structural low L7, close to the Oddur Arch axis. It is assumed that the fault plane of F115 dips northward, consistent with normal faulting.

L7 indeed has the appearance of a graben, suggesting therefore that the Oddur Arch structure has been associated with doming followed by tensionally induced coaxial rifting.

The amount of structural relief across L7 is very difficult to assess magnetically. Computer modelling cannot be applied due to the inherent insensitivity of induced magnetic response to N-S trending features. Direct dip measurement of the fault plane at the fault/geological boundary F115, together with the displacements of this fault determined magnetically along the intersecting N-S faults, would go some way to quantifying the relief at the southern end of the graben. If the dip of F115 is not significantly less than 60 degrees (to the north) then structural relief should not be insignificant. Certainly, if L7 is of sufficient relief, then a significant negative closure or sub-basin may occur in the region of its intersection with sedimentary trough L9 within Sheet 124/136. It is debatable whether the evaporite filled basins in this locality (see unit Klmg UNDP geology map) are the result of such sub-basin formations.

5.2.6 L10 - structural low

L10 is a 190 km long, funnel-shaped sedimentary trough extending east-northeastwards from the extreme north of the western deep basement region, into the shallow basement region of the Oddur Arch. Within the deep basement region, interpretation of this feature is based on computer modelling. For the remainder (greater part) of the feature, interpretation is based on manually estimated basement depths.

A maximum depth of 9.6 km is attained in the west, across the broad positive magnetic anomaly computer modelled as profile FF', (Figure 11). Computer modelling here and also along profiles JJ' and KK'

(Figures 12 and 13) suggests that trough L10 enlarges southwards into a broad basin bounded by interpreted basement ridge H9 to the south and accompanied by another interpreted trough L11 to the east. This basin appears to comprise the northern region of the deep Mandera-Lugh Basin. (See Section 5.2.9.) Modelling at the north of profile FF' suggests that basement shallows quickly on the northern flank of L10 and may be controlled by fault F241. A contact at this position would however be difficult to distinguish from a fault.

As trough L10 extends eastwards into the shallow basement region it naturally shallows and at its easternmost point attains a depth of 4 to 4.5 km.

The eastern half of L10 coincides closely with the large, shallow intrasedimentary volcanic Zone V44 within Sheets 2/14 and 3/15. L10 therefore, like L9, may have played a significant role in localizing volcanics in this region. Zone V44 extends from L10 towards the region of L9 via a 'neck' about 12 kms south of the L10 axis. This narrowed region of volcanics may correspond to a complementary structural high axis separating troughs L9 and L10.

L9 and L10 together form an almost unbroken arcuate trough running from the western boundary across the top of Block 2 to the southern boundary in the east.

5.2.7 L8 - structural low

This N-S trough, perhaps 60 km in length and lying within the shallow basement region is implied by the indirectly revealed faults F204, F203, F182, F198, F197, F194, F196 and F195, within Sheets 3/15, 26/38 and 27/39. The interpretation of L8 is less certain than that of the similar feature L7 to the northeast because: (i) there is not quite the same degree of supporting evidence and (ii) the existence of a trough/graben in this position is less easy to understand.

Many of the faults defining L8 occur as dislocations in the directly interpreted E-W fault F193, which appears from its magnetic response to be downthrown to the north. The interpretation of throw on the dislocations/cross-faults is based on the assumption that the fault plane of F193 dips northward, consistent with normal faulting. Faults F204 and F203 are interpreted as downthrown to the east and west respectively, in containment of the interpreted volcanic zone V57.

The amount of structural relief which may exist across L8 is difficult to assess magnetically. As in the case of L7, computer modelling cannot be applied due to the minimal magnetic response of N-S features.

5.2.8 L11 - structural low

L11 is a relatively short 55 km long NE-SW structural low or trough which, together with the eastern half of L10 probably forms the northern region of the Mandera-Lugh Basin (see Section 5.2.9). The interpretation of L11 is based on the computer modelled profiles JJ'

(Figure 12) and KK' (Figure 13) across a very long linear magnetic high striking NE-SW through Sheets 2/14, 1/13 and 25/37.

Realistic modelling across profiles JJ' and KK' was difficult, due to the distinctive broad magnetic gradient which accompanies the magnetic high to the southeast. In order to obtain a satisfactory match with the observed data, it appears that along both profiles, basement assumes a graduated (but not unrealistic) magnetic composition. Shallower basement to the south also appears necessary. The resulting models suggest that the trough L11 attains a maximum uniform depth of 9.1 km and that (i) to the northwest, basement appears to extend across to trough L10 without a significant rise in basement level and (ii) to the southeast, basement of non-uniform susceptibility shallows rapidly, reaching a depth of 4 kms over a distance of 23 km.

The greatest change in basement susceptibility for both computer modelled profiles, occurs near to the observed magnetic high, abruptly rising by about 0.002 cgs units to the southeast. This interpreted change in susceptibility possibly signifies a major change of basement composition and has thus been interpreted as a contact, one which can be followed magnetically over a greater NE-SW extent than L11 itself. (See Sheets 2/14, 1/13, 25/37, 36/48 and possibly 59/71).

5.2.9 H9 - structural high

H9 is an E-W basement ridge whose interpretation derives solely from contouring of manually estimated basement depths. As no individual magnetic anomaly corresponds coherently with this feature, its existence is regarded with less certainty than for example, L11 of the previous section. H9 appears to form the southern boundary of the Mandera-Lugh Basin component formed by troughs L10 and L11.

According to basement depth estimates, H9 is a saddle region, the ridge in the west and east appearing to be shallower, at 3.5 and 4.5 km respectively, than the central region at 6.8 km.

Depths at the western end of H9 are supported by the computer model HH'. This model was conducted three-dimensionally over the high amplitude (at least 180 nT) dipolar anomaly B44, lying incompletely defined on the northwestern boundary of Block 2 within Sheet 35/47. The modelled body lies at an interpreted depth of 3.6 km and is probably a basement intrusion. (See Section 5.3). This interpretation might in turn imply that deeper E-W intrabasement igneous activity is responsible for the uplift along H9. Almost bisecting H9 is a broad, low amplitude, N-S trending, positive anomaly. This is interpreted as a deep intrabasement intrusion, B43. Its N-S trend is however curious if it is to be related to the suggested deep igneous activity along the E-W axis of H9.

5.2.10 L12 - structural low

South of H9 lies the southern extension of the Mandera-Lugh Basin, of which L12 appears to be the northernmost component. This feature is a broad ENE-WSW, 120 km long, trough whose interpretation derives

solely from contouring of manually estimated basement depths. As no individual magnetic anomaly corresponds coherently with this feature, L12 like H9 must be regarded with less certainty. L12 attains a maximum estimated depth of 8.6 km within Sheet 60/72, although depths elsewhere along the axis appear to vary little from this. The amount of structural relief with respect to H9 to the north is roughly between 4.5 and 1.7 km, and with respect to H6 to the south (see Section 5.2.11) is between 1.7 and 0.9 km.

L12 appears intersected in the west by three significant NW-SE trending faults F242, F243 and F244. These , which are downthrown to the east, east and west respectively, have been determined by computer modelling along the nearby profile GG' (Figure 16) and together may be regarded as comprising a horst (see Section 5.2.13). In the east L12 is intersected by the long NW-SE fault, F237. This fault, probably downthrown to the northeast, is in the north directly interpreted from a residual low amplitude positive anomaly, striking NW-SE through the northeast corner of Sheet 60/72 into Sheets 36/48 and 49/61. F237 and possible faults F238 and F239 to the west may constitute another shorter horst on the northern flank of L12.

5.2.11 H6 - structural high

H6 is a linear structural high or ridge lying approximately 28 km south of trough L12 of the same basic ENE-WSW trend and spans the full width of the deep basement region. H6 follows a linear negative magnetic anomaly, up to 30-40 nT in amplitude, trending through Sheets 49/61, 60/72 and 59/71. Two computer modelled profiles along flight lines 2261/1 and 2292/1 (Figures 14 and 15) accompany a relatively high density of manual depth estimates along this feature. The southern slope of H6 suggests that basement deepens still further to the south. Shallowest estimated depths along H6 occur (i) along the eastern third of the feature, at just under 7 km, and (ii) in the west at the intersection of the interpreted horst defined by the three NW-SE faults F242, F243 and F244, again at just under 7 km. Elsewhere axial depth is deeper at about 7.5 km.

North of H6 basement structure appears to consist of a rather simple linear undulation between NE-SW and E-W in trend. To the south, however, this simplicity is lost. H6 appears therefore, to mark a distinction between a deep basement region of relatively uncomplicated structural history to the north and a relatively complex one to the south. The Mandera-Lugh Basin which appears hitherto to have been regarded as lying north of the H6 position, may be a more extensive feature extending south of H6, indeed as far as the interpreted ridge H7. (See the following section).

5.2.12 H7 - structural high

This 85 km long feature H7 is based on computer modelling along the N-S reconnaissance profile 4003/1 (see Figure 20) across a broad E-W magnetic low of approximately 90 nT amplitude. Modelling suggests that H7, which lies near the southern boundary of the deep basement

region, may be an E-W basement ridge lying at a depth of approximately 5.2 km.

Ridge H6, described in the previous section, and H7, appear to partially enclose a region of generally depressed basement containing the interpreted features L14, L13 and L15. (See Sections 5.2.14 and 5.2.15). It is suggested that H7 or indeed H6 may be of particularly fundamental significance, for according to the magnetic data one or the other may represent a westward, though displaced, extension of the Bur Acaba Uplift. Although the Bur Acaba Uplift is a feature of regional tectonic significance and likely therefore to extend further west than the present-day outcrop, there is no magnetic evidence for this, unless a N-S displacement directly west of the outcrop is invoked, in which case either feature H6 or H7 may represent the extension. Assuming that the proposed westward extension of the Bur Acaba Uplift does not immediately attain great depth close to the Bur Acaba basement outcrop, then H7 which is both significantly shallower and further from the Bur Acaba basement outcrop than H6, is the more likely candidate. The implied N-S displacement is therefore probably the result of pre-Jurassic sinistral strike-slip movement along the interpreted N-S fault F231 and/or its counterparts F227 and F232 extended southwards.

5.2.13 H8 - structural high

The 100 km long interpreted structural high H8 is the result of approximately NW-SE faulting F242, F243 and F244, interpreted as downthrown to the east, east and west respectively. This horst-like feature intersects L12, H6 and the short ENE-WSW trough L14 to the south.

The interpretation of a structural high in this position is based on the recognition of interference across the linear NE-SW negative anomaly associated with feature H6 in the southwest corner of Sheet 60/72. Profiles GG' and 227/1, lying either side of H6 were chosen for two-dimensional computer modelling along which in both cases a long wavelength, low amplitude NW-SE residual anomaly can be observed. The results, seen in Figure 16 (profile GG') and Figure 17 (profile 227/1) show that the anomaly may be simply explained on both profiles, as the effect of three long faults within a basement of uniform magnetic susceptibility. In relation to the outer parallel faults F242 and F244, the inner fault F243 appears to be slightly rotated anti-clockwise, giving the horst a much broader top surface in the south than in the north.

The horst is of highest structural relief in the south. Across profile 227/1 relief is about 2.6 km, the largest throws occurring along the outer opposing faults F242, 1.7 km and F244, 2.0 km. The throw of the inner fault F243 is about 0.7 km. In the north along profile GG' total structural relief is about 1.5 km. As the largest throws appear to occur along the two eastern faults F243, 1.0 km and F242, 1.3 km and the throw on the remaining fault F244, is about 0.5 km or less, (a lesser throw would not markedly change the modelled fit) H8 in the north is approximately half-horst in form. The increasing structural relief to the south is accompanied by increasing

depth to upper surface. In the north along GG' this reaches 7.1 km and in the south 8.0 km along profile 227/1.

A structural high/closure at the 7 km level, may occur at the intersection of H8 with H6. (See the estimated basement depth contours across the 59/71 and 60/72 Sheet boundary.)

5.2.14 L13 and L15 - structural lows

The structural lows L13 and L15 trend approximately NW-SE and comprise a large area of the continued deep basement region south of ridge H6. L13 appears to be at least 60 km in length and L15 about 30 km. L13 and L15 have no recognizable direct magnetic responses. L13 is however considerably better defined by manual estimated depths than is L15, whose somewhat tentative position is suggested by the disposition of unsatisfactorily controlled basement depth contours on the very edge of the survey area. Were it not for the presence of the interpreted intrusion B42, features L13 and L15 would not appear discretely but be part of a larger interpreted basin. According to computer modelling along profile EE', Figure 18, the intrusion B42 extends above the regional basement level in the southwest, by over 5 km.

Basement attains a maximum estimated depth along L13 of 10.6 km. This depth appears to be approximately maintained along its full length. L13 together with L14 in the west (see following section) attain the greatest estimated depths of the entire survey area. Until now, deepest basement was expected within the Mandera-Lugh Basin proper, that is, north of H6. The profound depth along L13 is consistent with depths derived from adjacent computer modelling on profiles 227/1 and 2261/1.

5.2.15 L14 - structural low

L14 is an approximately E-W, 60 km long, structural low, lying west of L13. Its interpretation is based on computer modelling across a sub E-W, positive residual anomaly of 20nT amplitude, along profile 2285/1. (See Figure 19). Modelling suggests that L14 is a trough with a flat floor of 15 km width, lying at a (obliquity corrected) depth of 10 km. The southermost depth 10.6 km on the adjacent computer modelled profile 2292/1, Figure 15, conforms well with this interpretation.

Features H8, L13 and L14 together generate a complex structural pattern in this region. L14 together with L13 appear to be the deepest structural lows within the survey area. This region, like the Mandera-Lugh Basin in the north, is certain to be underlain by thick Palaeozoic sediments. L14, which appears to be continuous with L13, may extend further west than indicated.

5.3 Basement Zones and Associated Intrusives

The majority of magnetic zones or bodies that can be associated directly with basement reside within a 20 to 40 km band around the northern boundary of the Bur Acaba basement outcrop. Here, the basement is shallow and apparently free of overlying volcanics. These zones are of a relatively high amplitude/high frequency nature and although they may be observed in the unfiltered and filtered "deep" component magnetic contours, are most easily discriminated via the "shallow" component contours.

The prefix 'P' has been used in annotation of basement zones, in reference to its Precambrian age.

Within Sheets 50/62, 27/39, 28/40 and 29/41¼, spectral analysis clearly distinguishes only one magnetic horizon, that is, basement. (See Appendix 1.) Generally in all regions except those known to contain non-magnetic basement, the deepest or solitary spectrally determined magnetic horizon, is considered magnetic basement. North of these sheets spectral analysis indicates at least two horizons which implies the possibility of intrasedimentary volcanics. These volcanics probably lie directly north of the interpreted E-W fault F168. (See Section 5.4.2.)

The largest basement zone P12, occurs within Sheets 27/39, 28/40, 50/62, 51/63 and 52/64. Its eastern boundary appears to lie within the reconnaissance Block 3 (within the Bur Acaba outcrop region) bounded by an easily recognized N-S line separating relatively high magnetic amplitudes in the west from low amplitudes in the east. It is suggested that basement within the Bur Acaba outcrop to the east of this boundary is essentially gneiss-dominated and that to the west within zone P12, basement is essentially dominated by high susceptibility granite. (See Appendix 2 for a tabulation of basement rock susceptibilities sampled from the Bur Acaba outcrop). Two dyke-like intrusives D64 and D65 are interpreted from particularly strong magnetic responses within zone P12. D64 is a narrow, straight, 25 km long intrusive undoubtedly associated with the NE-SW indirectly revealed fault F191. Fault F191 and undetected counterparts, undoubtedly control the adjacent northern boundary of the Bur Acaba outcrop. D65 is a wider, sinuous 40 km long feature with no apparent associated faulting.

The relatively high susceptibility associated with Zone P12 is part of a regional high susceptibility zone extending northwards from the southwestern end of Zone P12 towards an interpreted E-W basement contact directly east of volcanic Zone V52 (within Sheets 25/37 and 26/38). This contact is part of a recumbent U-shaped basement contact whose interpretation derives from a curious, similarly disposed combination of negative (in the north and west) and positive (in the south) magnetic anomalies. The observed polarities of these anomalies implies that the region immediately outside of the 'U' corresponds to a higher susceptibility than within. This is consistent with the relative position of P12. The U-shaped contact appears to be part of a longer contact which: (i) in the north extends northwards along the intersecting fault F227 and then eastwards into Sheet 27/39 along the northern boundary of basement zone P9, and (ii) in the south, extends

westwards to the interpreted N-S fault F230, then following the northern boundary of basement zone P13 and then P12 itself. All basement immediately east of this essentially arcuate line of contact may be regarded as of low magnetic susceptibility.

East of P12 are the basement zones P14 and the larger P15, both of which probably relate to basement of similar composition. The "shallow" component magnetic contours suggest that the western boundary of zone P15 is controlled by the essentially N-S fault F232, offset near the centre by the interpreted E-W fault F233. Fault F232 together with F231 and F227 appear to reflect a fundamental N-S zone of magnetic discontinuity observed best in the "deep" component magnetic contours. This zone is thought to involve sinistral strike-slip movement and may have de-coupled the tectonics associated with the Oddur Arch from the deep basement region to the west. (See Section 5.2.12.)

Within zone P15 on the western boundary of Sheet 50/62, lies a prominent three-dimensional dipolar anomaly of approximately 170 nT peak to peak amplitude. This anomaly has been computer modelled along the profile II', Figure 22, and appears to correspond to a highly magnetic, 0.0029 cgs, southerly dipping intrusion whose upper surface lies at a depth of 3.6 km. According to magnetic susceptibility measurements carried out by Hunting on basement samples supplied by the UNDP, Mogadishu (see Appendix 2) a susceptibility of 0.0029 cgs is consistent with a body of biotite gneiss. The disposition of the modelled body however suggests it is more likely to be of volcanic origin.

Northeast of P12 lie the basement zones P11, P10 and P9. Zone P11 is particularly easy to discriminate on account of its characteristic strong NW-SE grain. Zones P9 and P11 exhibit relatively low amplitude compared to P10, suggesting an alternative route for the granitic/gneissic contact northwards from the Block 3 reconnaissance area, that is, initially following the northern boundary of zone P10 and then P12. Direct evidence for the effectively E-W fault F193 is observed within Zone P9. This fault is interpreted as downthrown to the north and appears subject to N-S/NE-SW dislocations, presumed faults. Section 5.2.7 explains how this observation leads to the inference of the structural low L8.

East of P9 and P10 lies a small group of basement zones, P3, P5, P6, P7 and P8. Clearly magnetic basement composition here is chaotic.

Further east lie the basement zones P4 and P1 separated by a relatively non-magnetic NW-SE band. P4 is generally of higher amplitude which probably indicates a difference in composition, as depths to basement appear comparable at roughly 2.0 km. Directly south of zone P4 lies a dipolar magnetic anomaly of 150 nT peak to peak amplitude, lying just within the Bur Acaba basement outcrop region. This anomaly has been computer modelled along profile 2145/1, Figure 3, and appears to be due to a highly magnetic, 0.0026 cgs, basement block whose upper surface lies at a depth of between 1.5 and 1.7 km. According to measured susceptibility values, a susceptibility of 0.0026 cgs is consistent with a body of biotite gneiss, however, volcanic intrusive material cannot be ruled out. Computer modelling

further suggests that basement of 0.0005 cgs susceptibility occurs either side of this body, consistent with "medium grained" granite or possibly amphibolite. The southern boundary of the 0.0017 cgs modelled unit at the northeast of the profile corresponds well with the qualitatively determined southern boundary of basement zone P4. Probably the most significant aspect of this modelling is that the modelled body(ies) clearly occurs well below the surface of the basement outcrop suggesting that basement, over this part of the Bur Acaba uplift at least, may be as inhomogeneous vertically as laterally.

Zone P1 contains two dyke-like zones of intrusion, D38 and D39. D38 is interpreted as a broad WNW-ESE trending magnetically remanent dyke-like body of about 50 km length. This feature is evident in the "deep" component magnetic contours but virtually absent in the "shallow" component which, considering the proximity to surface of basement in this region, implies that the intrusion D38 lies well below the basement surface. This reinforces the suggestion already put forward, that Bur Acaba basement appears significantly inhomogeneous both laterally and vertically. D39 is a small ENE-WSW probably volcanic dyke.

Northwest of Zone P9, mainly within Sheet 2/14, lies a large circular interpreted body B37. Evidence for this body is not immediately obvious, deriving not from a direct magnetic response but rather from a possible association with an interpreted palaeo-topographic high. Perhaps the most obvious suggestion of a large palaeo-topographic high in this position derives from the observed westward deviation of the southern and northern extremities of the essentially N-S colinear basalt exposures V48 and V49 respectively. Other circumferential limitation of volcanics implying this feature occurs in the form of zones V50 in the southeast and V44 (part of the Late Tertiary arcuate zone) in the northeast. Particularly convincing evidence for the eastern boundary of B37 is observed in the "shallow" component magnetic contours near the eastern boundary of Sheet 2/14. Here, a relatively high frequency zone of magnetics with a pronounced WNW-ESE grain (essentially volcanic zone V57) disappears abruptly along an arcuate line joining V50 in the south and V44 in the north. In short therefore, if viewed on a sufficiently regional basis, the circular region B37 is easily recognized. The underlying cause of the palaeo-topographic high may be a non-magnetic granite batholith. Computer modelled profile KK', Figure 13, is not inconsistent with this interpretation as the southern quarter of the profile corresponds to an interpreted low magnetic susceptibility of 0.0005 cgs.

B31 which lies 50 km ESE of the western boundary of B37 directly along the dyke-like feature D62, may correspond to a smaller granite batholith. D62 therefore may represent a coaxial intrusion of a connecting saddle region.

Assuming that B37 is correctly interpreted as a batholith and has at some stage been the cause of significant palaeo-topographic relief, associated structure within the sedimentary section may not simply be limited to the western boundary (where as we have already seen basement deepens sharply towards the deep basement region) but may extend around the full circumference of the feature. Although

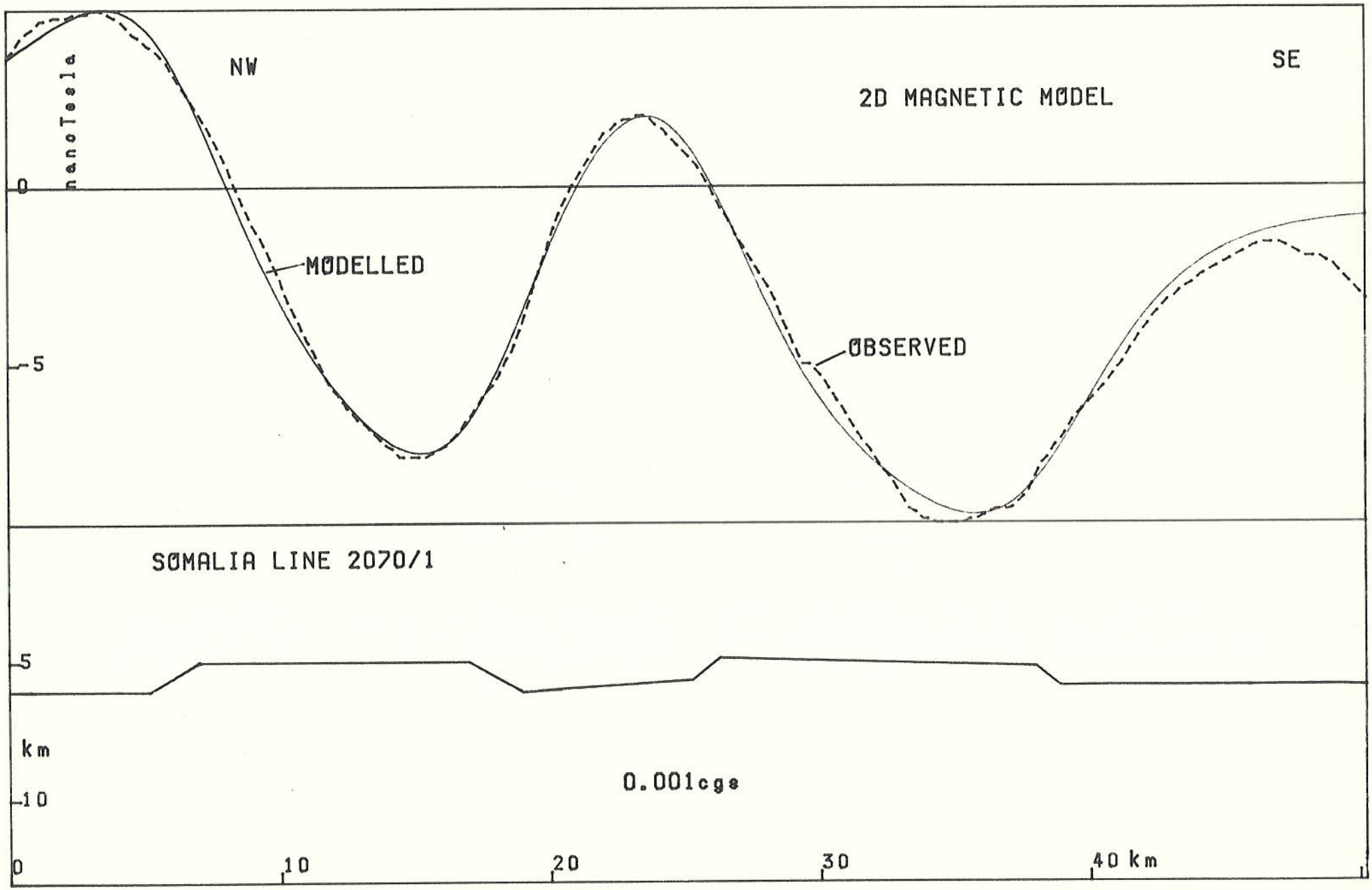
NW
SE
2D MAGNETIC MØDEL
nanoTesla
0
-5
MØDELLED
ØBSERVED
SØMALIA LINE 2070/1
5
km
-10
0.001cgs
0
10
20
30
40 km

FIGURE 9

FIGURE 10

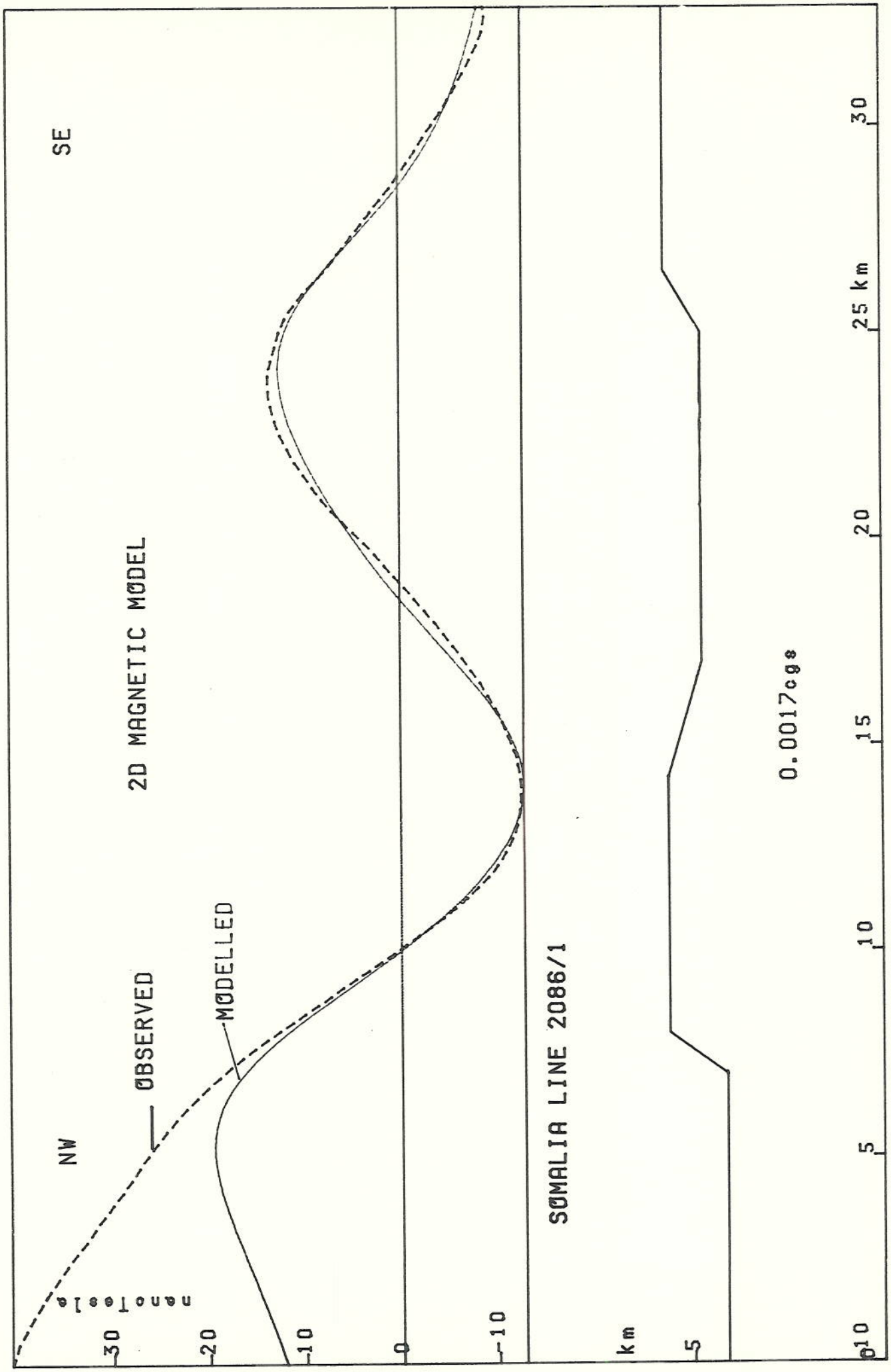
SE
NW
2D MAGNETIC MODEL
OBSERVED
MODELLED
SOMALIA LINE 2086/1
0.0017cgs
nanotesla
30
20
10
0
-10
km
5
10
15
20
25 km
30

FIGURE 11

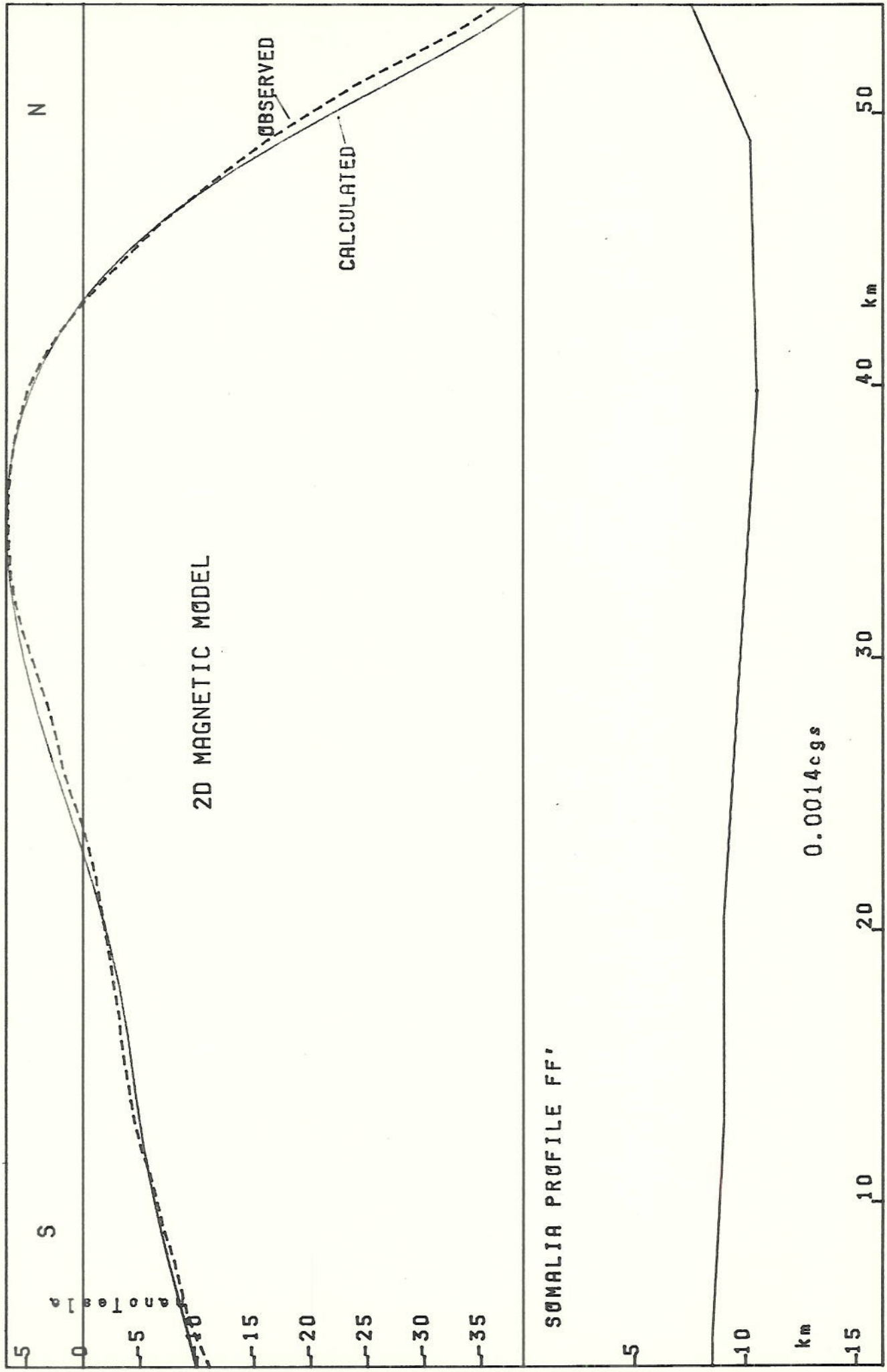
N
S
OBSERVED
CALCULATED
2D MAGNETIC MODEL
SOMALIA PROFILE FF'
0.0014cgs
km
km
5
0
5
10
15
20
25
30
35
5
10
15
10
20
30
40
50

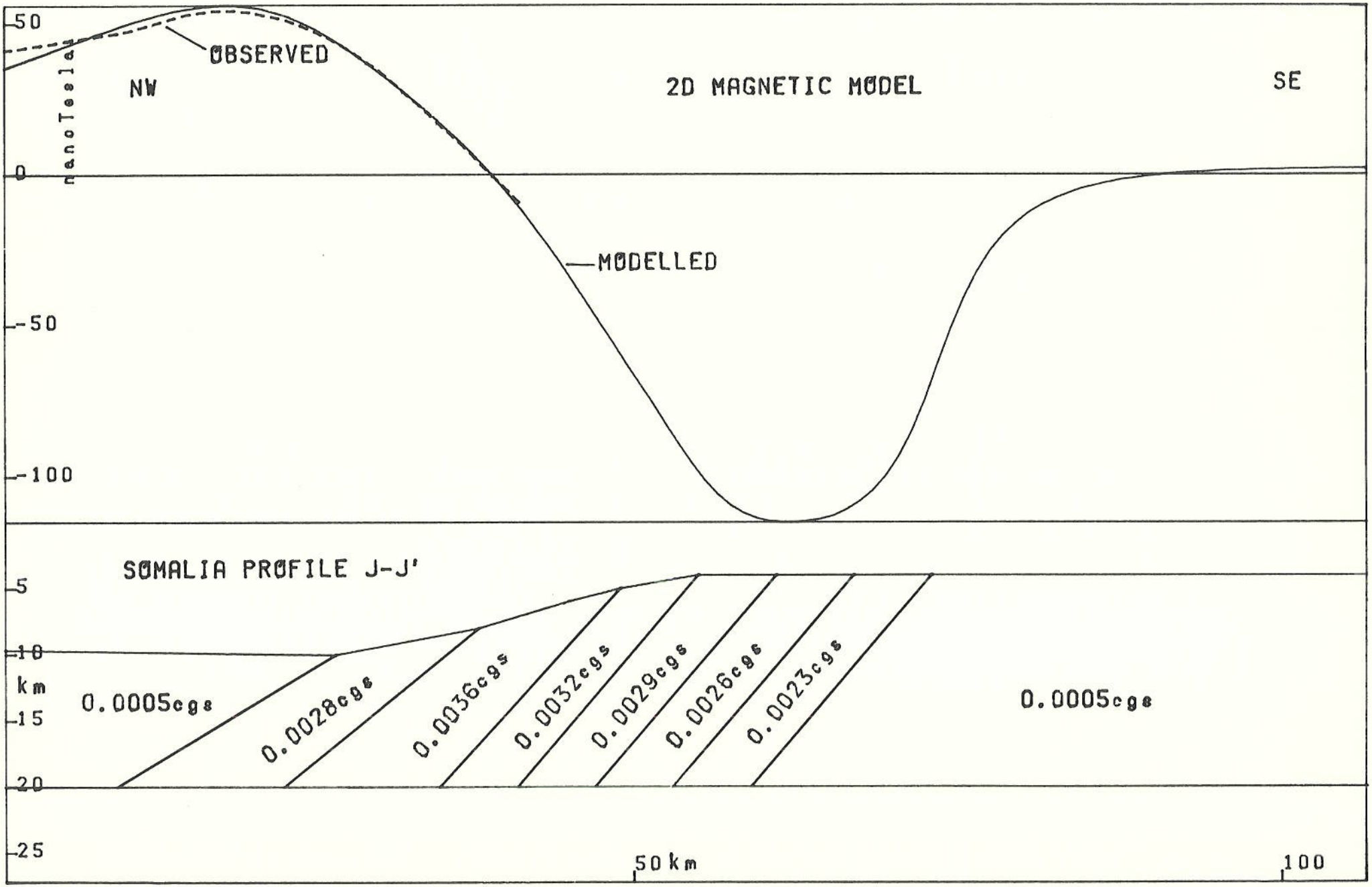
50
0
-50
-100
nanoTesla
NW
OBSERVED
2D MAGNETIC MODEL
SE
MODELLED
SOMALIA PROFILE J-J'
5
10
km
15
20
25
0.0005cgs
0.0028cgs
0.0036cgs
0.0032cgs
0.0029cgs
0.0026cgs
0.0023cgs
0.0005cgs
50 km
100

FIGURE 1

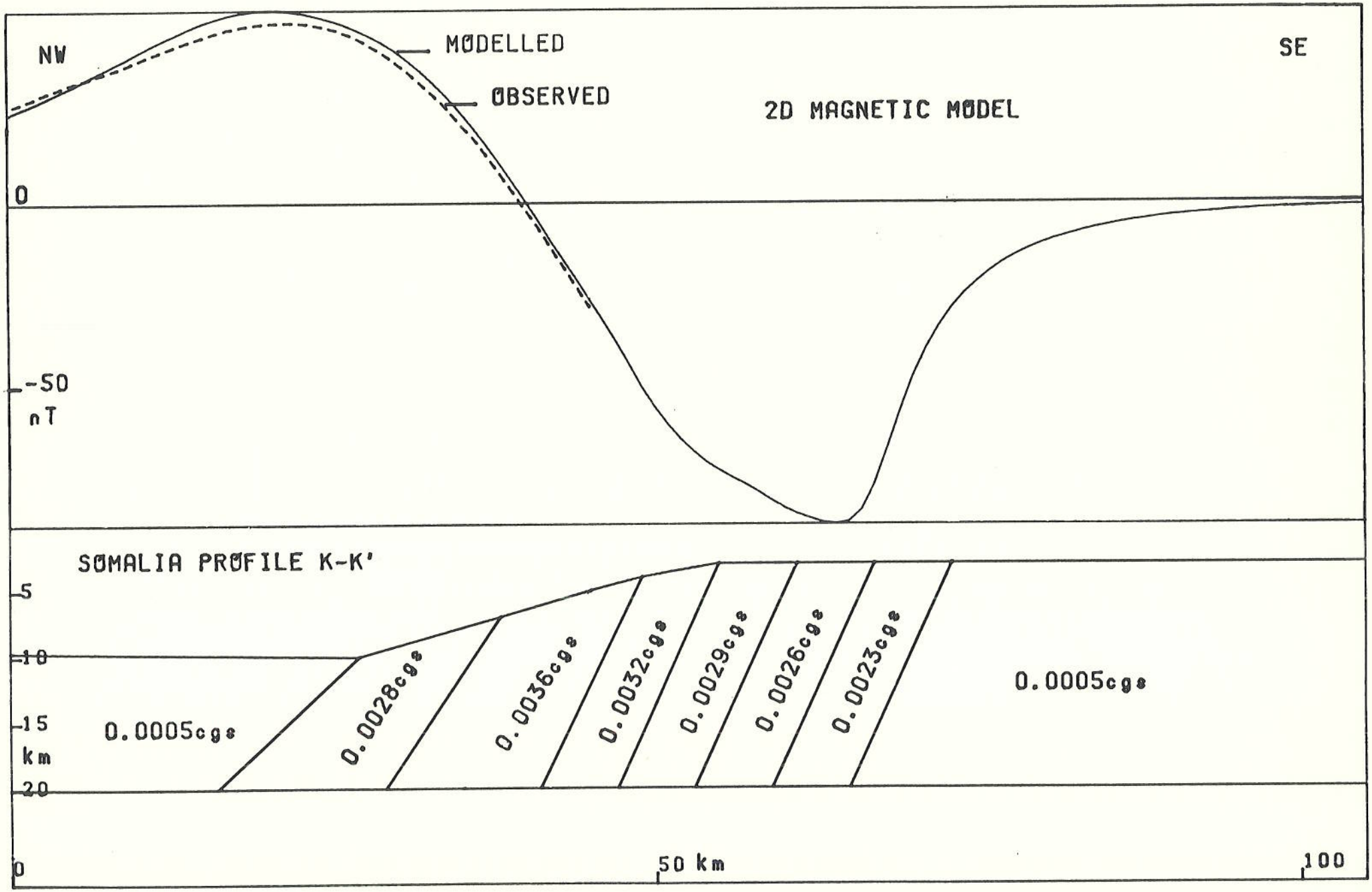
NW
SE
MODELLED
OBSERVED
2D MAGNETIC MODEL
0
-50
nT
SOMALIA PROFILE K-K'
5
10
15
km
20
0.0005cgs
0.0028cgs
0.0036cgs
0.0032cgs
0.0029cgs
0.0026cgs
0.0023cgs
0.0005cgs
0
50 km
100

FIGURE 1

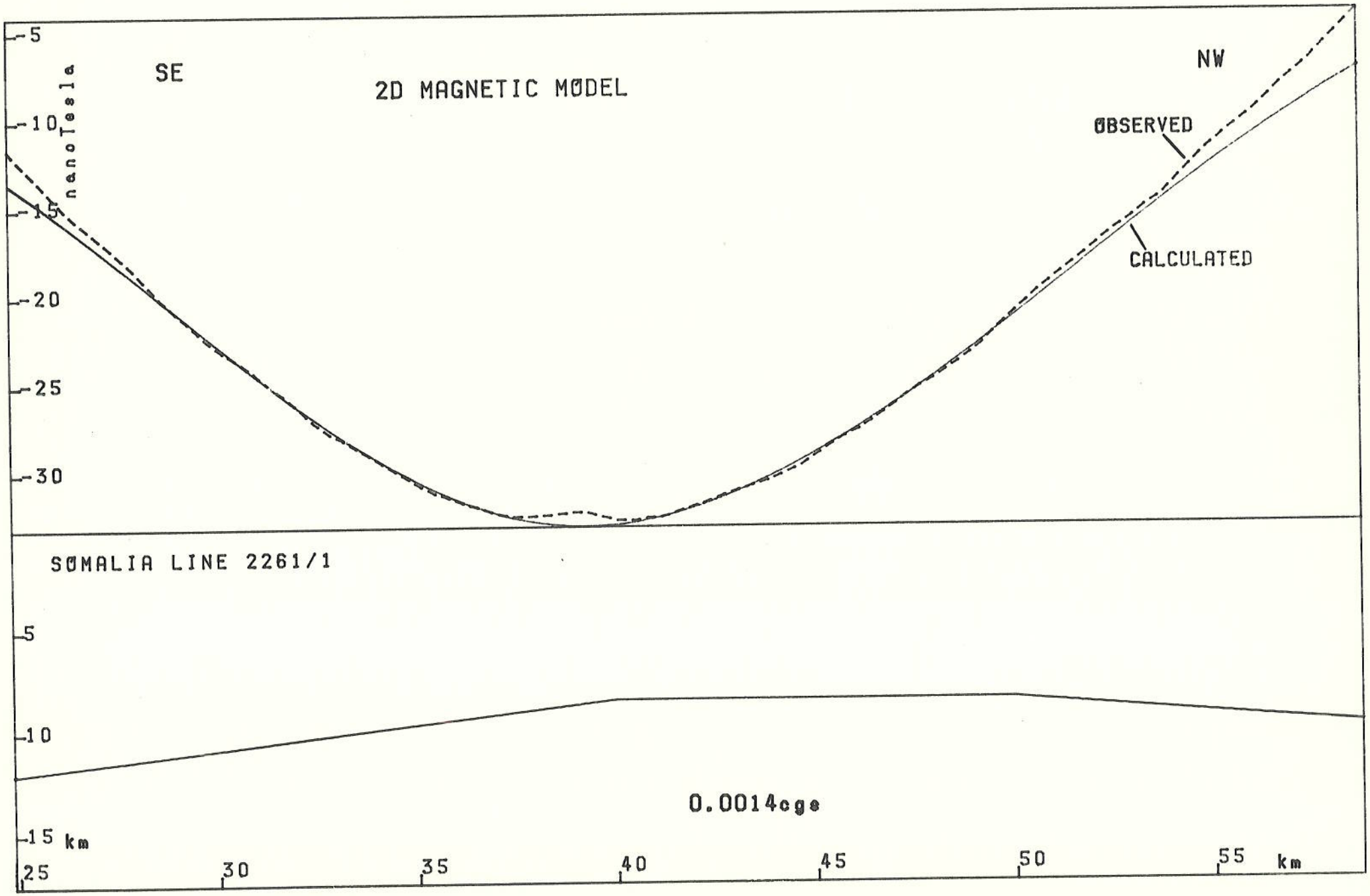
2D MAGNETIC MODEL
SE
NW
nanoTesla
OBSERVED
CALCULATED
-5
-10
-15
-20
-25
-30
SOMALIA LINE 2261/1
5
10
15 km
0.0014cgs
25
30
35
40
45
50
55 km

FIGURE 14

FIGURE 15

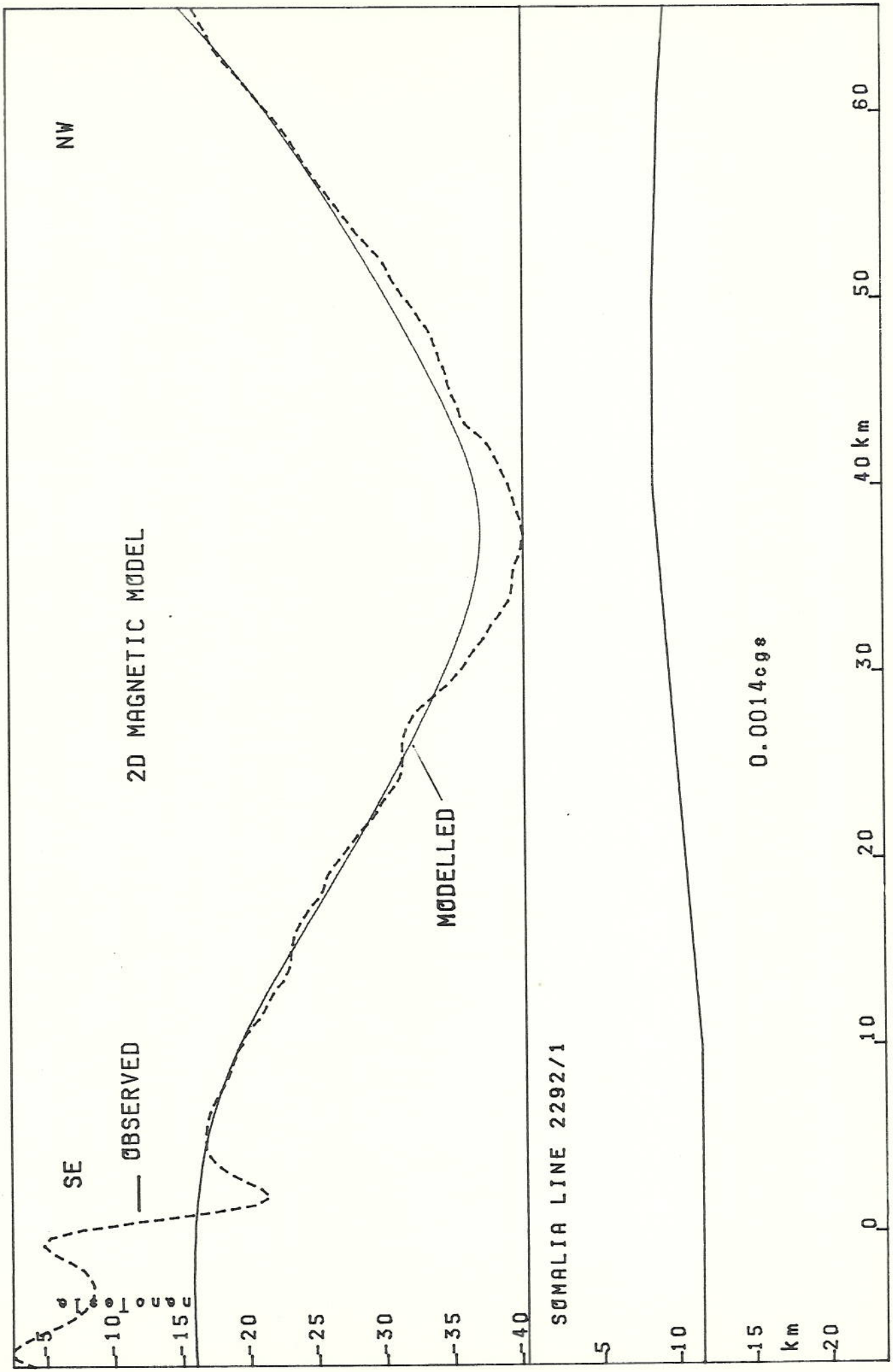
NW
SE
2D MAGNETIC MODEL
OBSERVED
MODELLED
SOMALIA LINE 2292/1
0.0014cgs
-5
-10
-15
-20
-25
-30
-35
-40
5
10
15
20
km
0
10
20
30
40 km
50
60

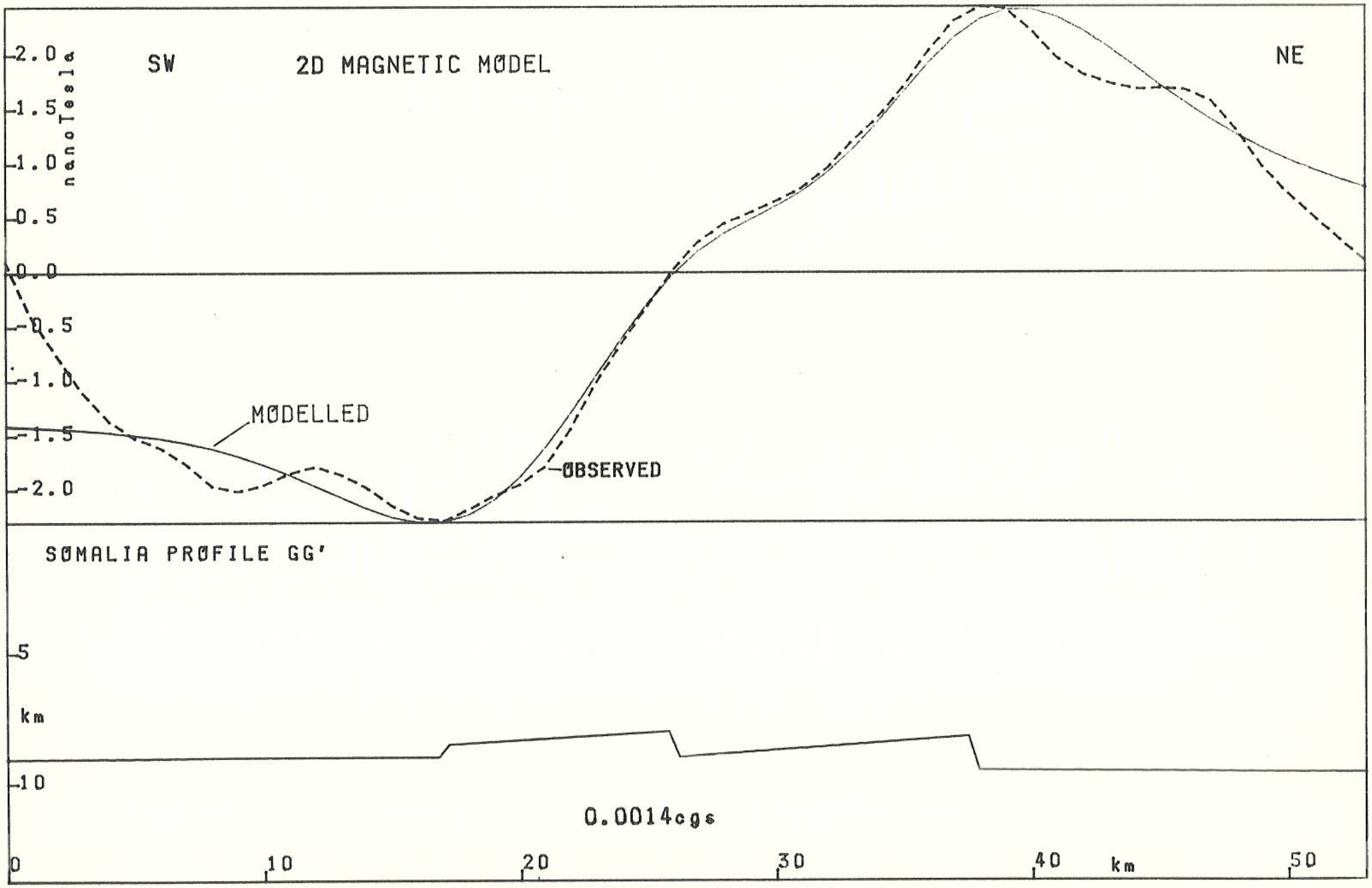
SW
2D MAGNETIC MØDEL
NE
nanoTesla
2.0
1.5
1.0
0.5
0.0
-0.5
-1.0
-1.5
-2.0
MØDELLED
ØBSERVED
SØMALIA PRØFILE GG'
5
km
10
0.0014cgs
0
10
20
30
40
km
50

FIGURE 16

FIGURE 17

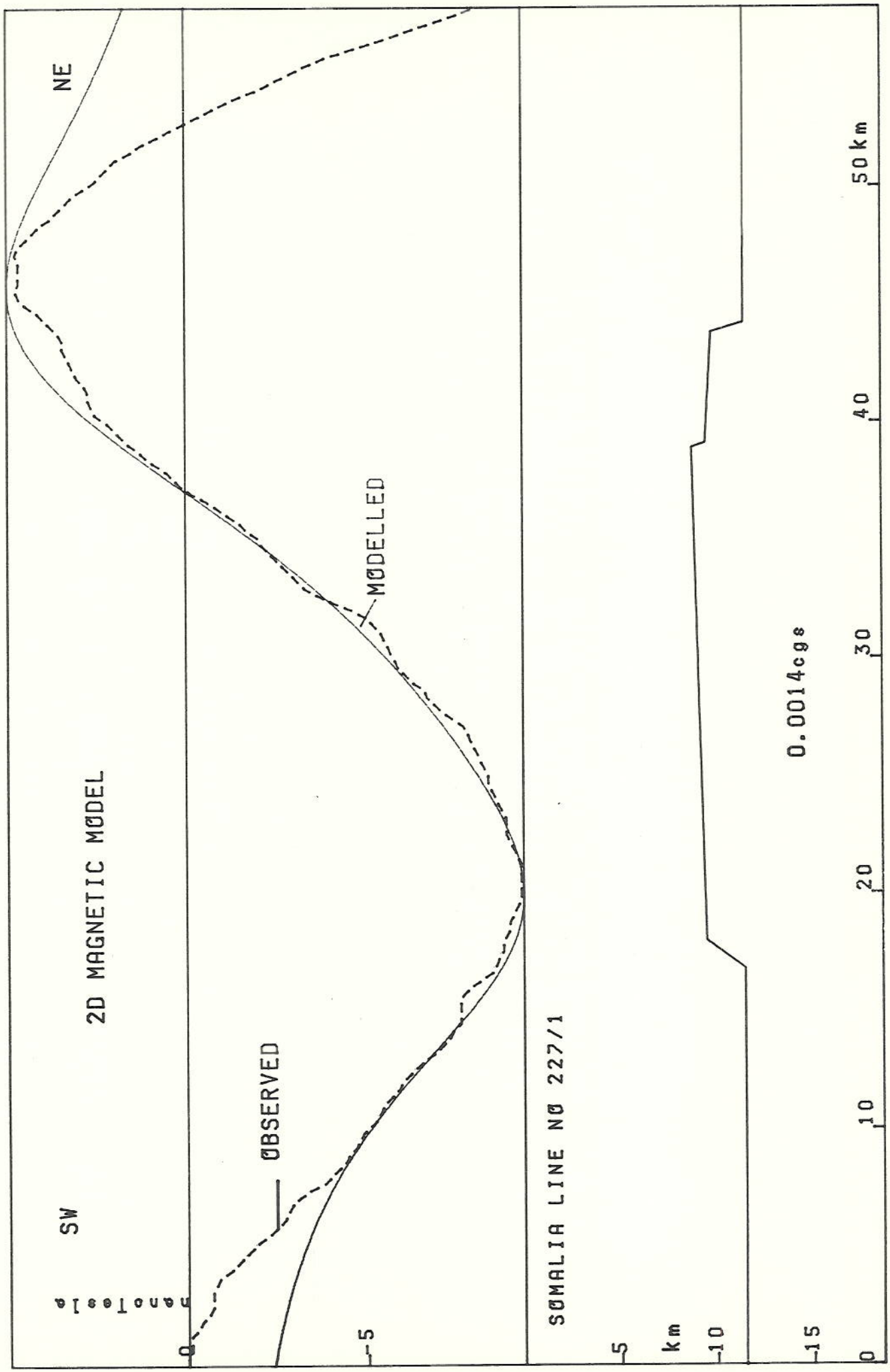
NE
SW
2D MAGNETIC MØDEL
ØBSERVED
MØDELLED
SØMALIA LINE NØ 227/1
0.0014cgs
0
5
10
15
20
30
40
50 km
5
10
km

3D MAGNETIC MODEL - PROFILE E-E'

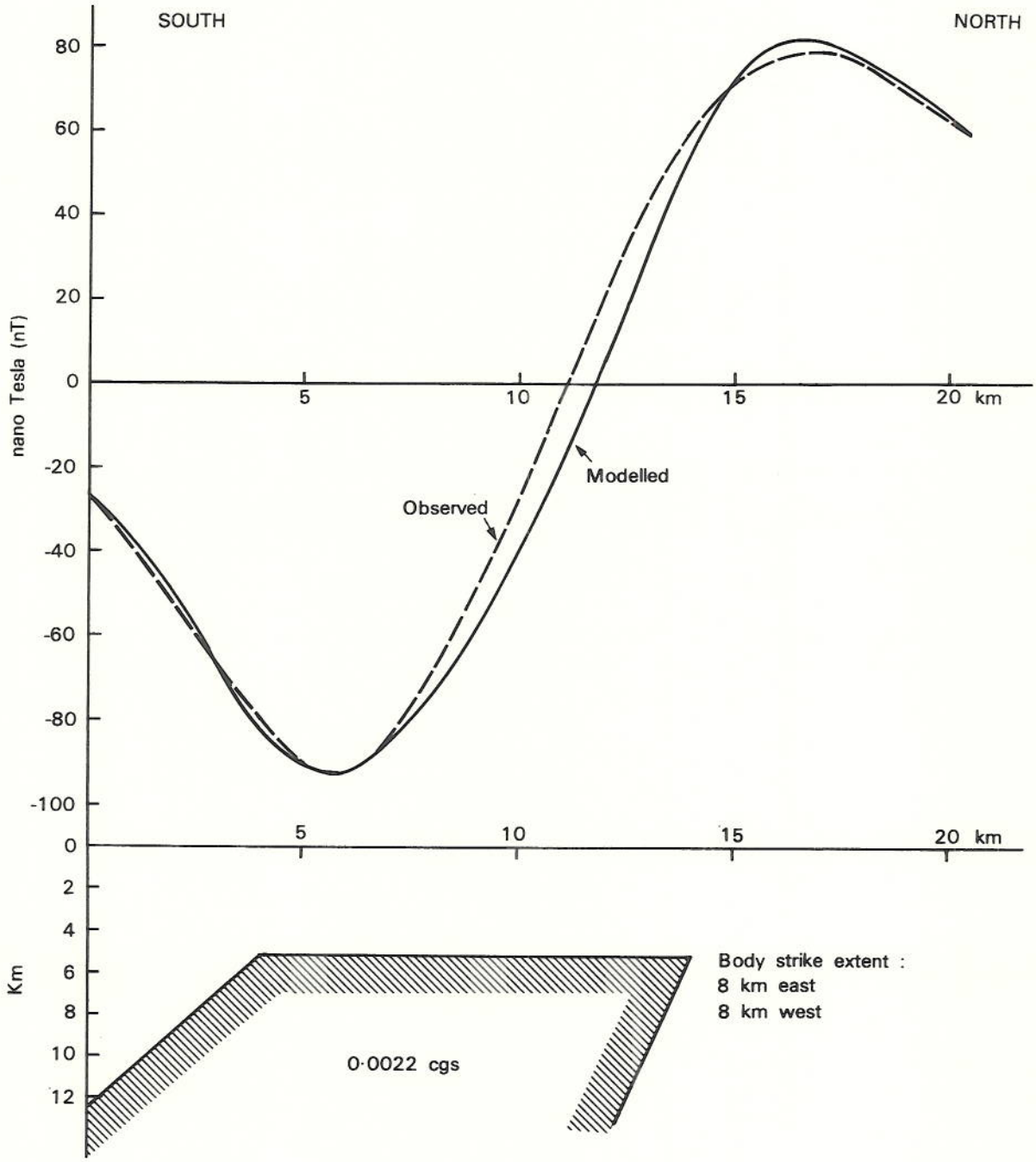

FIGURE 19

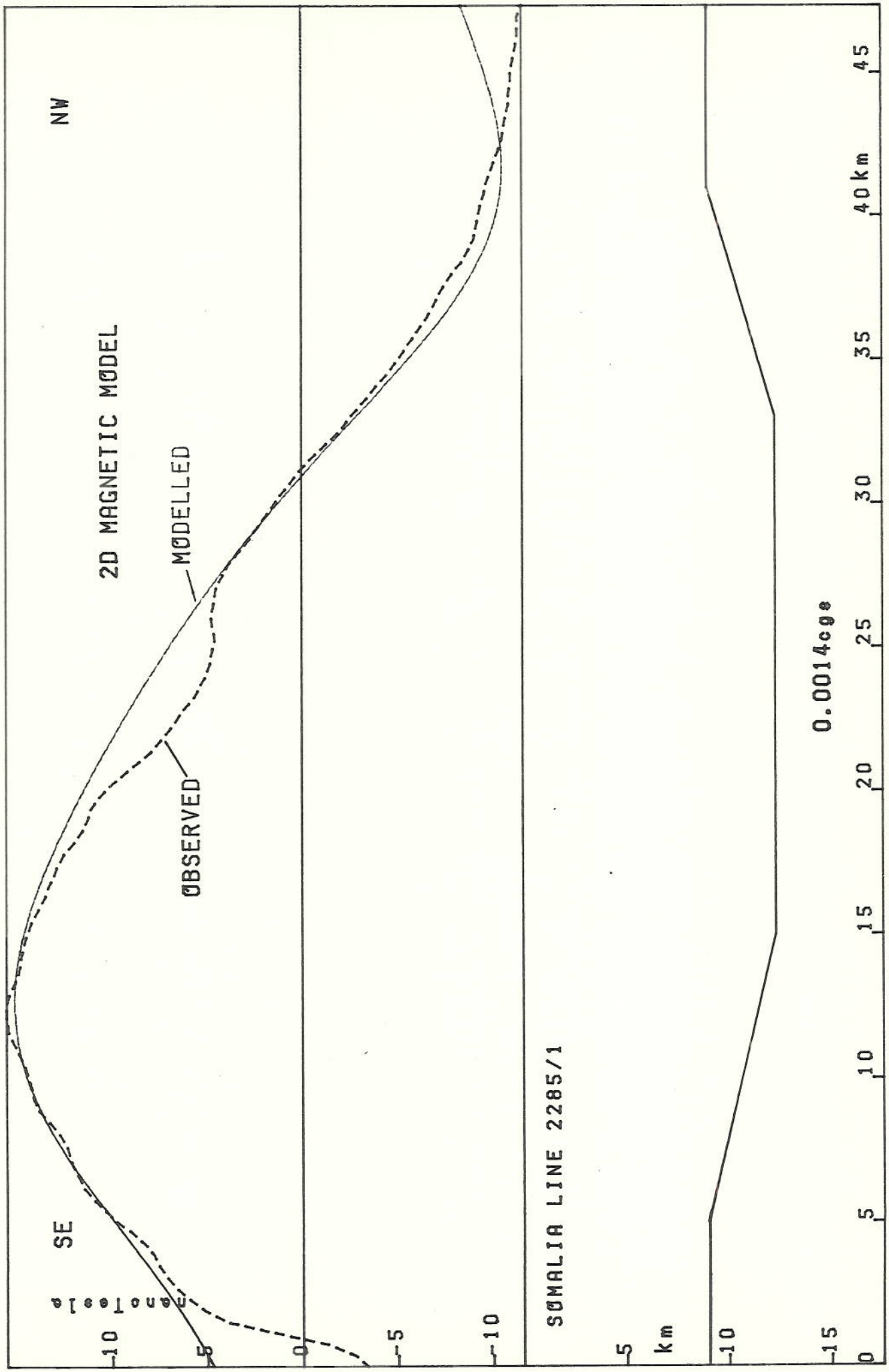
NW
SE
2D MAGNETIC MODEL
MODELLED
OBSERVED
SOMALIA LINE 2285/1
0.0014cgs
nanotesla
km
-10
-5
0
-5
-10
-10
-5
0
5
10
15
20
25
30
35
40km
45

FIGURE 20

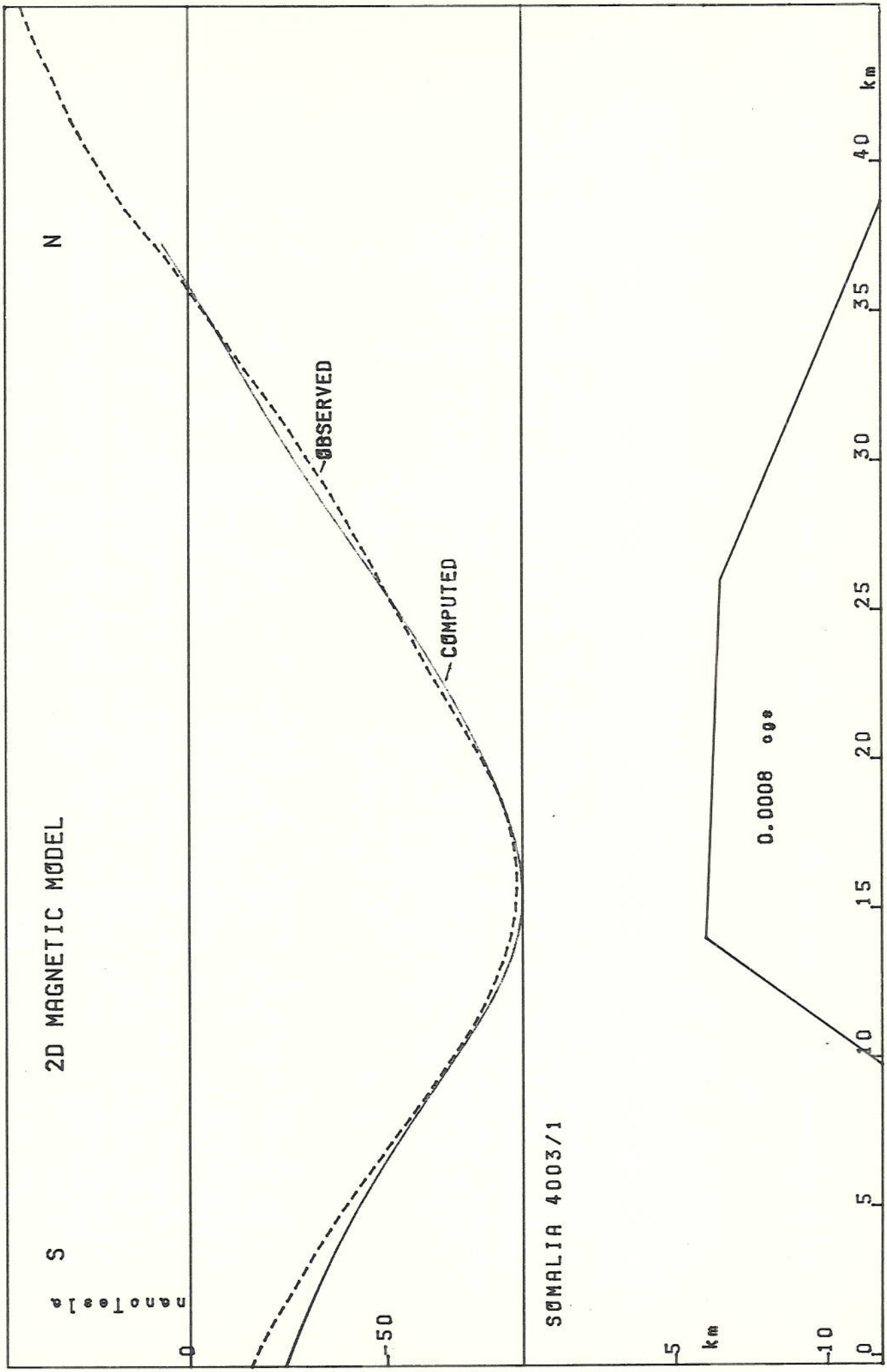
2D MAGNETIC MODEL
S
N
nanoTesla
0
50
OBSERVED
COMPUTED
SOMALIA 4003/1
0.0008 g/cc
5
km
10
0
5
10
15
20
25
30
35
40
km

FIGURE 2

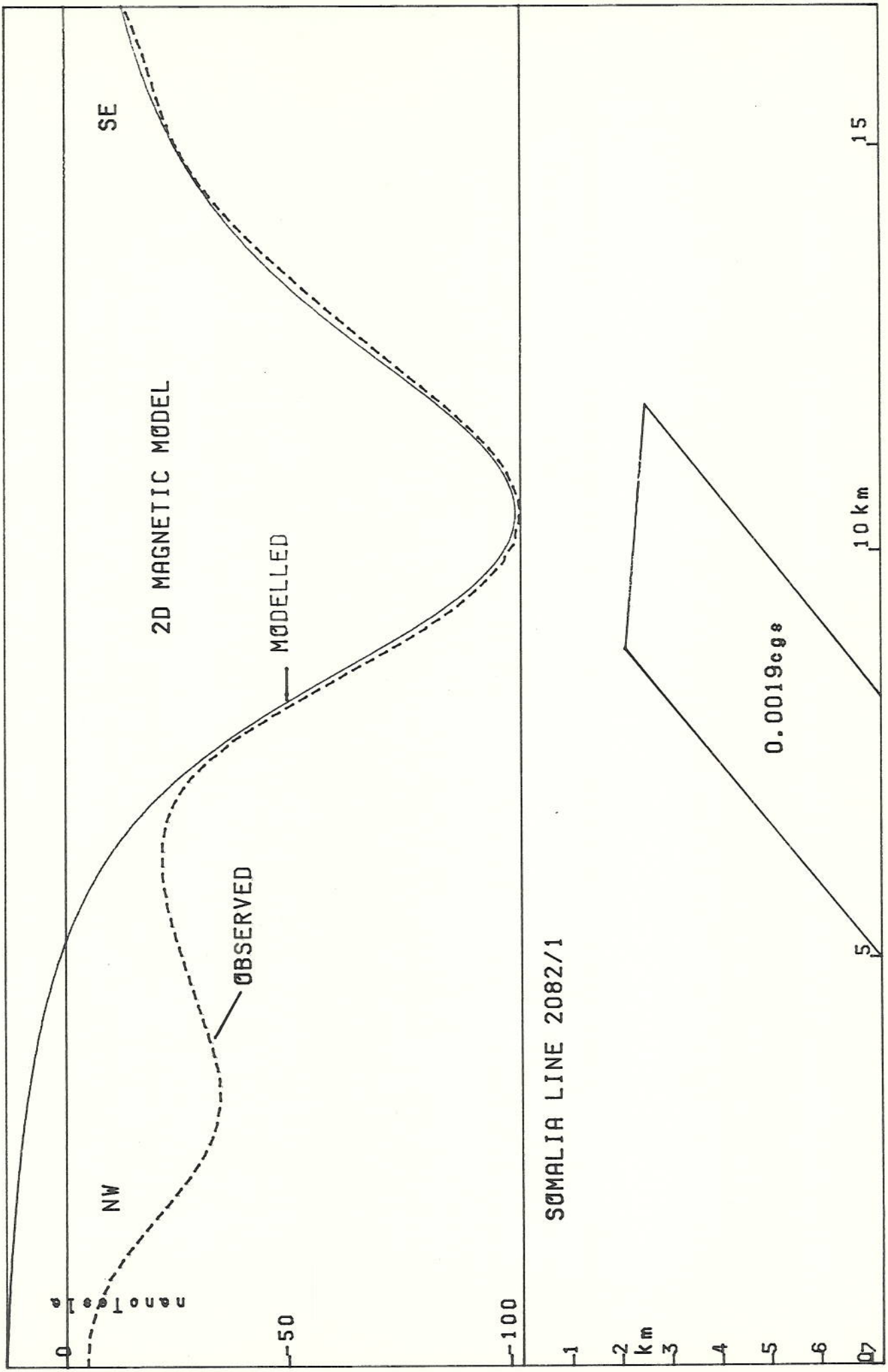
2D MAGNETIC MØDEL
SE
NW
MØDELLED
ØBSERVED
SØMALIA LINE 2082/1
0.0019cgs
10 km
15
5
0
50
100
1
2
3
4
5
6
7
km

3D MAGNETIC MODEL - PROFILE I-I'

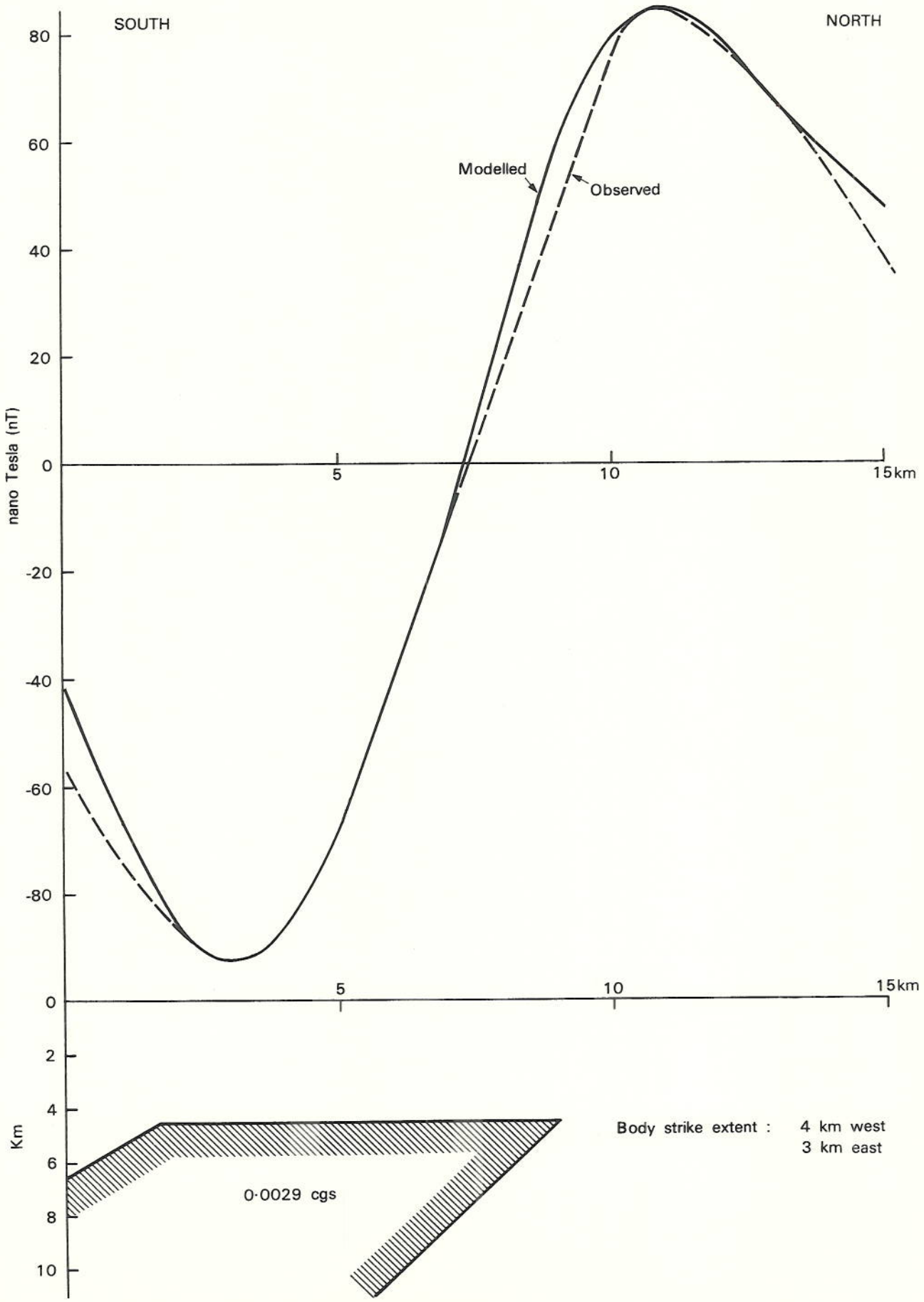

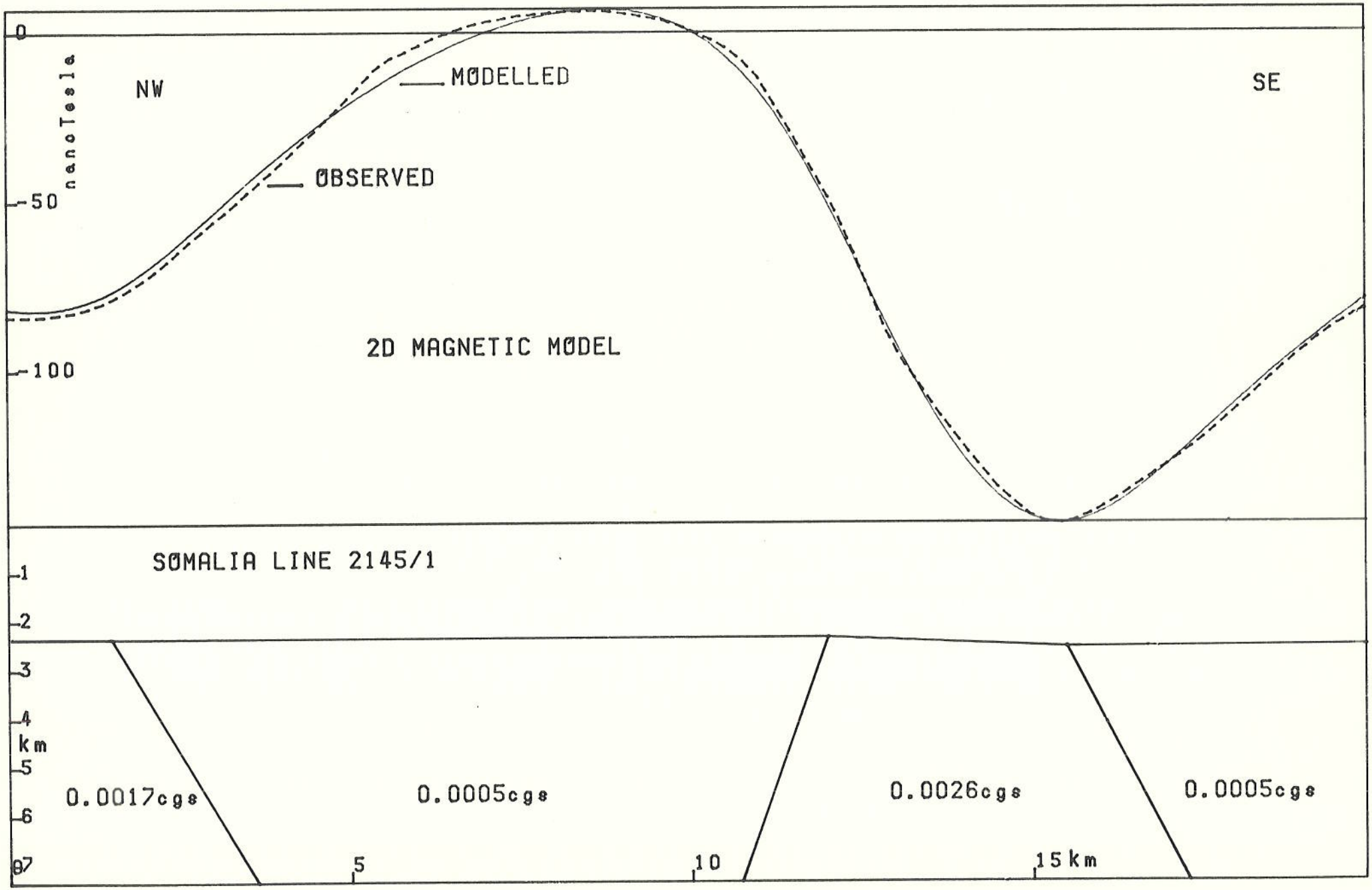
0
-50
-100
nanoTesla
NW
SE
MODELLED
OBSERVED
2D MAGNETIC MODEL
SOMALIA LINE 2145/1
-1
-2
-3
-4
km
-5
-6
-7
0.0017cgs
0.0005cgs
0.0026cgs
0.0005cgs
0
5
10
15 km

FIGURE 23

3D MAGNETIC MODEL - PROFILE H-H'

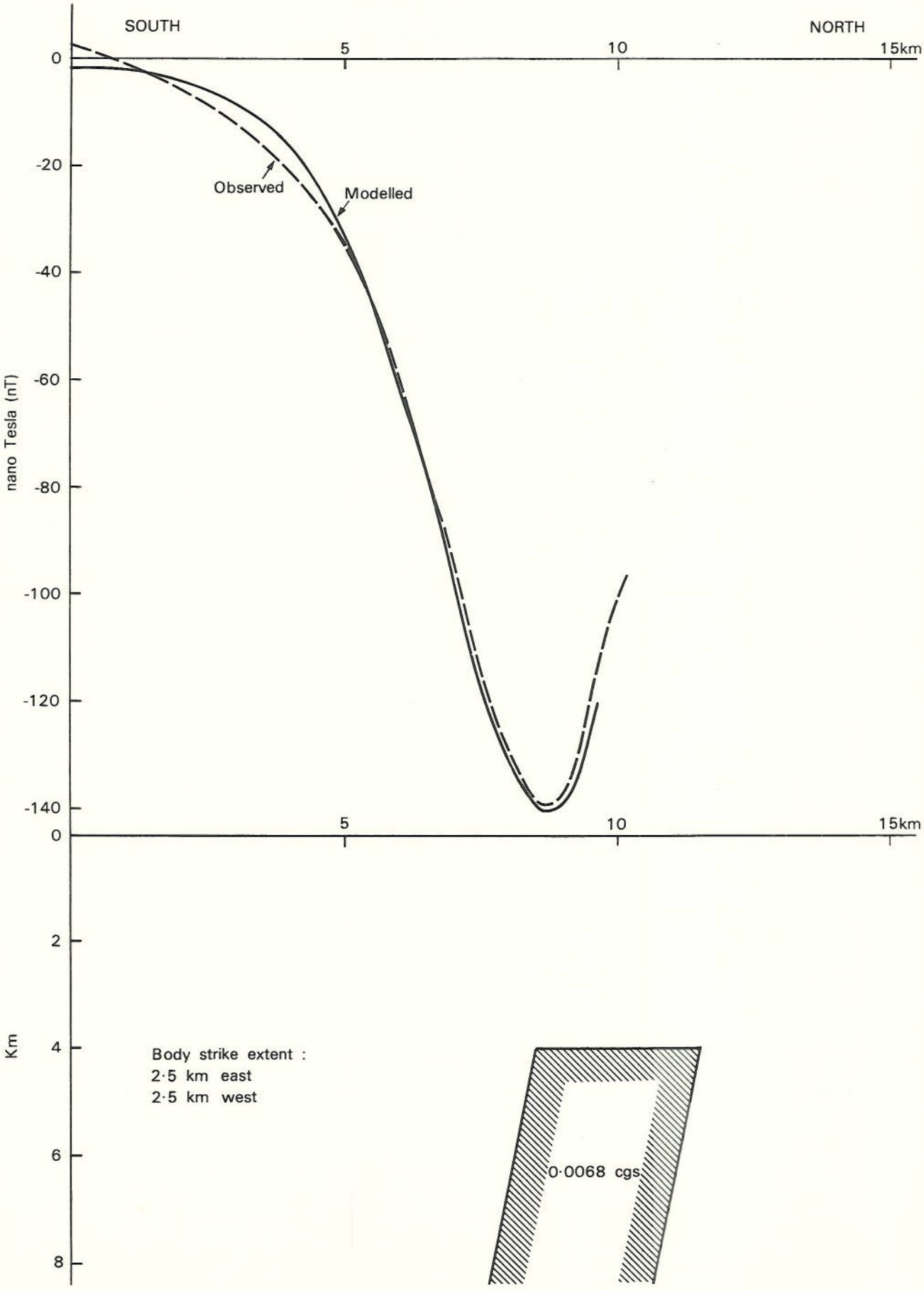

basement depth contours do not exactly confirm this, an explanation may be the general paucity of depth estimates in the region. It is perhaps of some significance that the long arcuate volcanic zone of Block 2 is ultimately truncated by the body B37. Assuming that the arcuate volcanic zone is a result of fissure eruption, the effect of the almost perfectly circular interpreted body B37 may have been to completely relieve crustal stress associated with fissuring as it progressed from the east.

Intrusive bodies exhibiting significant magnetic response are less frequent within the deep basement zone west of the Juba River. This in part may be due to amplitude attenuation caused by greater depth of burial but may also simply reflect a less tectonized basement. Where magnetic evidence of intrusion is indeed observed, (see bodies B42 to B46) these features probably stand proud of the regional basement surface intruding the sedimentary section. Features B42 and B44 are probably the most significant of these intrusive bodies. Three-dimensional computer modelling has been applied to both, along profiles EE' and HH', Figures 18 and 24 respectively.

Modelling along EE' suggests that B42, which lies in the southwest corner of Sheet 49/61, is a broad intrusion of relatively high susceptibility, 0.0022 cgs, dipping to the south and whose apparently flat upper surface lies at a depth of 4.2 km. Although this depth is well above the interpreted level of the surrounding basement, its large 10 by 16 km surface area perhaps dictates that B42 should be reflected in the contours of the estimated basement depths.

The magnetic anomaly corresponding to body B44 is only partially defined lying as it does on the western boundary of Block 2 in Sheet 35/47. Modelling along HH' (Figure 24) is nonetheless possible and suggests that B44 is a relatively narrow intrusion of extremely high susceptibility, 0.0068 cgs, 3 by 5 km in upper surface area, dipping sub-vertically to the south and with a flat upper surface lying at a depth of 3.6 km. Absence of adjacent magnetic bodies (see Figure 24) implies that adjacent basement and sedimentary material are of particularly low magnetic susceptibility. Relative to the very high interpreted value for B44, this of no great surprise. Although other basement depth estimates in the region of B44 are relatively few, the overall indication is that body B44 resides within a region of generally elevated basement.

5.4 Volcanics and Associated Intrusives

Two distinct volcanic zones of quite different ages are recognised from the magnetic data of Block 2.

5.4.1 Tertiary Volcanics - Arcuate Zone

The younger volcanic zone occurs as a relatively narrow, 7-20 km wide, 280 km long, arcuate band of high frequency magnetics across the northern region of the Oddur Arch. This zone, which is the most distinctive magnetic feature of Block 2, closely corresponds in the most part with suboutcrop volcanics and in the west coincides with a

large region of exposed basalts dated as Late Tertiary. The extensive nature of this narrow band suggests that the volcanics were emplaced by a process of fissure eruption. The observed continuity of these volcanics with those of the Western Volcanic Region of Block 1 reinforces this interpretation. Such arcuate fissuring around the northern limits of the Oddur Arch would suggest an association with circumferential fracturing caused by updoming of the arch. The interpreted trough L9 (see Section 5.2.4) coincident with a large proportion of the arcuate volcanic zone, may be largely responsible for containment of volcanics within this zone.

Within the arcuate zone, especially in the west, are numerous narrow high amplitude two-dimensional anomalies whose magnetic response is partially retained within the "deep" filtered version of the magnetic contours. This suggests that these particular features possess a significant depth extent and that they probably represent dykes or indeed the feeders of volcanic extrusives.

The volcanic sub-zones comprising this zone are as follows: V44, V51, V33, V53, V32, V25, V24, V26 and V1 extending out of Block 1. The peripheral sub-zones V45, V46 and V47 lying to the west and south of V44, probably represent thinner sections of volcanics. V44 corresponds largely to the previously mentioned Late Tertiary basalt exposure.

The volcanics within the eastern region of V33 and the western region of V32 appear to underlie two evaporite basins (see unit Klmg UNDP geology map). If the volcanics here are basalt flows (as they indeed are in the Late Tertiary exposure to the west) their position in the section suggests that they pre-date the overlying Lower Cretaceous evaporite. This possibility however is inconsistent with the reasonable assumption that the whole of the arcuate volcanic zone is of the same Late Tertiary age. In short therefore, the volcanics at the base of the two basins are probably Late Tertiary lopolith intrusions, accommodated by upward displacement of the lighter overlying evaporite.

Along the western half of the shallow volcanic zone are many examples of apparently fault controlled volcanic zone boundaries. These are mainly N-S orientated and are no doubt due to the effect of erosion subsequent to reactivation along Oddur Arch related faulting. Notable examples of this occur along faults F227, F228, F215, F210, F185 and F135.

The magnetic data north of the arcuate sub-outcrop band of volcanics shows further evidence of volcanic zones. These zones, the most notable of which are V28, V31 and V34, have relatively subtle magnetic signatures and are best observed in the "shallow" component contour maps. All three zones appear to connect with the arcuate zone and it is suggested that the zones may represent relatively thin, partially eroded basalt deposits, emplaced by northward flows of volcanic material caused by a breach in the palaeo-topographic trough (L9?) which appears to contain the volcanics of the arcuate zone. The boundary of Zone V34 in particular is comprised of numerous straight N-S trending segments. These are undoubtedly the result of reactivations along Oddur Arch related faults followed by a

significant degree of erosion. It is probable that the volcanics north of the arcuate zone were originally much more extensively distributed than they are today.

Lying directly between the arcuate volcanic zones V33 and V34 to the north, lie the interpreted WNW-ESE trending dyke-like intrusions D36, D35 and D34. This general zone of intrusion extends further east via the interpreted ENE-WSW trending intrusions D33 and D32 (between the volcanic zones V34, and V32 and V31). All except D34 show magnetic evidence of northward dip. This is confirmed by computer modelling along profile 2082/1, Figure 21.

Numerous, presumed faulted, N-S trending offsets occur along this zone of intrusion. The most notable of these (Oddur Arch related) faults are F146, F140, F138, F130, F127, F124, F122, F119 and F116 and each have been ascribed a sense of throw consistent with the intrusive dip direction and direction of offset. The resulting pattern of faulting defines a N-S graben-like structure. This structure is the northern continuation of the trough L7 interpreted from the N-S offsets along fault F115 to the south of the arcuate zone. (See Section 5.2.5.)

It is observed that the faults F130 and F124 extend northwards forming N-S boundary segments of the volcanic zone V34. The interpreted westward downthrow of these faults is consistent with the possibility that the present extent of volcanic zone V34 in particular, is due to post-volcanic N-S faulting and subsequent partial erosion. Using the criterion therefore that all N-S boundary segments of the volcanic zones V34 and V31 are due to 'containment' faulting, that is, faults whose down-throw is directed inwards towards the volcanics, the resulting fault pattern also conveniently reinforces the existence of the graben-like feature L7.

The interpreted volcanic zones V48, V49, V52 and V53 are confirmed by corresponding outcrops of Late Tertiary basalt along the eastern bank of the Juba River. V48 and V49 are essentially N-S trending and lie colinearly on the N-S fault F231, which is interpreted from an apparently fundamental magnetic discontinuity within the "deep" component magnetic contours. The curious westward deviation of V48 in the south and V49 in the north is discussed in Section 5.3.

5.4.2 Jurassic Volcanics - Southern Zone

An extensive region of relatively high amplitude, high frequency magnetics occurs directly north of the Bur Acaba basement outcrop. This region is bounded: (i) in the north by the roughly E-W trending interpreted faults F113, F114 and F115, (ii) in the east by the NW-SE trending faults F108 and F110, and (iii) in the west by the large circular feature B37. (See Section 5.3). A similar magnetic response is observed over the Bur Acaba basement outcrop itself (along the reconnaissance doublet lines of Block 3) which would appear to suggest that the magnetic signature north of the outcrop simply reflects the continued presence of shallow basement, perhaps dipping gently northwards along the Oddur Arch axis. Spectral analysis of data, however, within Sheets 4/16 and 5/17 in particular (see Appendix 1) clearly indicates the presence of two significant magnetic horizons.

As the deeper horizon is likely to be basement (assuming it to be significantly magnetic), the second is clearly indicative of an intrasedimentary layer of basic (therefore magnetic) volcanic material.

The magnetic response of this intrasedimentary volcanic zone, or southern volcanic zone (to distinguish from the arcuate zone to the north) is best observed in the "shallow" component filtered magnetic contours. A general uniformity of amplitude and wavelength within this region implies that depth to volcanics does not vary greatly. Spectral analysis of Sheets 4/16 and 5/17 confirms this, indicating in both cases a mean depth to volcanics of 1 km below sensor. According to spectral analysis, therefore, volcanics in this region are sub-outcropping. The deeper segments of both spectral plots suggest basement lying at a depth of about 3.7 km below sensor, that is 2.8 km below sea level. This is consistent with the independantly determined basement depth contours. The numerous distinctive 'holes' within the magnetic contour pattern particularly in Sheet 5/17 (through which longer wavelength basement response is observed) is consistent not with a sill, but with a conformable layer of extrusive volcanics followed by an erosional unconformity. The southern volcanics if they indeed exist, would appear to be of Jurassic age, identical to the age of the sediments in which they appear to reside.

The northern boundary of the southern volcanic zone is observed to closely follow the mapped J3bd/J3an geological boundary (UNDP geological map) within Sheet 4/16 and to a lesser degree within Sheet 5/17. If a conformable intrasedimentary horizon such as a layer of volcanics, shares (or lies in close parallel proximity to) a surface-mapped boundary between two adjacent sedimentary units, the boundary is almost certainly faulted, in this particular case, fault F115 downthrown to the north. This interpretation, which appears to be corroborated by faulting shown on the UNDP geological map within Sheet 4/16, would suggest that the southern volcanic zone continues northwards, deepening abruptly at fault F115 then extending beneath the sub-outcrop volcanics of the Tertiary arcuate zone.

The interpreted E-W fault F168 may represent the southern volcanic zone's southern boundary.

The relatively high amplitude/high frequency anomalies of this region exhibit a change in character either side of a N-S median line through Sheet 4/16, near to the N-S structural axis L7. To the east the "shallow" component magnetic contours show a more uniform volcanic response than to the west where the volcanic response is particularly patchy and interspersed with more extensive dyke-like intrusives. In detail:

(a) East of the Sheet 4/16 median line, the extensive interpreted volcanic zone, though 'holed', is continuous and corresponds to Zone V29. Intrusives, recognized by their generally higher amplitude and strongly retained magnetic response in the corresponding "deep" component contour maps, are relatively numerous and occur mainly in the form of large three-dimensional bodies that is, B20, B21, B22, B24 and B25. D58 and D41 represent the few dyke-like intrusions

which occur in this region. D58 appears to be related to the interpreted 115 km long E-W fault F160. D41 probably possesses remanence and is associated with the fault F159.

(b) West of the Sheet 4/16 median line, a change of emphasis is apparent. Volcanic zones are discontinuous, that is V37, V38, V39, V40, V41, V42 and V57, and dyke-like intrusions are more numerous than three-dimensional intrusive bodies. D59 for example, is an interpreted large semi-elliptical ring dyke, lying within both Sheets 3/15 and 4/16, the magnetic response of which is most easily followed in the "shallow" component magnetic contours. D60 and D61 are dyke-like intrusions lying south of D59 within the volcanic zone V41, perhaps representing the source of the surrounding volcanics. D62, to the southwest at the south of Sheet 3/15, is a broad 40 km long dyke-like zone of intrusion lying partially within the interpreted volcanic zone V57. Like D60 and D61, D62 possibly represents the source of the adjacent volcanics. D62 appears also to form a link between the interpreted intrabasement body B37 in the west and B30 in the east. This association is discussed in Section 5.3. The patchier volcanics west of the Sheet 4/16 median line may merely reflect a more vigorous palaeo-erosional regime, however the higher incidence and greater extent of dyke-like intrusions in the west may in fact reflect a more fundamental difference, that is, one of underlying basement composition.

Fault F115 almost certainly post-dates the proposed volcanic extrusives to the south. As magnetic evidence for volcanics is retained on the upthrown southern side of this fault, the implication is that complete local peneplanation was not attained prior to resumption of marine sedimentation. In consequence, the Jurassic sediments immediately overlying the southern volcanic zone are probably draped over the palaeo-escarpment formed by fault F115. Depending on marine conditions during this period, reef structures may occur in abundance along this fault and indeed further east along faults F114 and F113 and further west along the proposed faulted contact, a direct continuation of fault F115. The appearance at today's surface of faulting along fault F115 (see UNDP geology map) suggests post-Jurassic reactivation.

6. CONCLUSIONS

This survey has succeeded in delineating deep basement target areas and has also contributed significantly to the known geology of the region. The Hiran Graben (L1) in Block 1 and the apparent rift L7 along the Oddur Arch axis are perhaps the most significant of the hitherto unknown tectonic features revealed by this study.

Magnetic interpretation clearly shows the survey area to be complex and subject to a varied tectonic history. Obvious regional hydrocarbon target areas occur as large areas of deep basement either side of the major N-S trending structure, the Oddur Arch. Interpretation suggests that these two deep basement regions are distinctly separate provinces, distinguished by age. Hydrocarbon accumulations, if they exist, are likely to be sourced by Palaeozoic sediments in Block 1 and largely post-Palaeozoic sediments in Block 2. The expectation of particularly thick sediments in the region of the Mandera-Lugh Basin is confirmed. No attempt has been made to assess the thermal histories of the proposed regions of interest.

Various structures throughout the survey area warrant follow-up by seismics and/or gravity. These are described below.

6.1 Block 1

In Block 1 there are perhaps three interpreted structural lows of particular interest:

(i) L2. The base of this sedimentary trough or trench lies at the interpreted depth of 11 km and may have originated in the Palaeozoic as a result of plate subduction. It is possible that L2 retains or at least has 'sourced' adjacent hydrocarbon accumulations, particularly in the west. L4 may be a similar source. The magnetics suggest that NNW-SSE cross-faulting is common in this basin, however, the degree to which faulting extends into the sediments is difficult to assess.

(ii) L1 - the Hiran Graben. This feature is interpreted as at least Cretaceous in age but is probably Palaeozoic. The structural relief associated with L1 appears superimposed upon a relatively steep NE-SW striking basement slope, deepening to the southeast. This slope is interpreted as a northeastward extension of the southern flank of the Bur Acaba Uplift. Although of relatively low structural relief, the basement within L1 appears to lie at between 9 km in the south and 2 km in the north. L1 may therefore harbour hydrocarbon accumulations, particularly in the vicinity of cross-faulting where fault traps may occur. Unfortunately, few if any cross-faults can be recognised magnetically across L1.

(iii) L3. This is the least certain of the potentially interesting Block 1 structures. This uncertainty derives from its attendant lack of direct magnetic response. An

appropriately positioned gravity traverse would probably resolve this uncertainty. The magnetic depth estimates defining this feature suggest nevertheless that sediment may extend to a depth of at least 6 km along its entire length. The proposed Late Jurassic/Cretaceous age suggests that L3 may post-date the intersecting Hiran Graben L1. Reactivated NW-SE faults belonging to L1 may extend into the sediment of L3.

6.2 Block 2

6.2.1 Western Deep Basement

In the deep basement zone of western Block 2, three regions exhibiting significant structural lows are of particular interest:

(i) L10 and L11. Together these troughs form perhaps the most promising sedimentary basin of the whole survey area and indeed corresponds to the long known Mandera-Lugh Basin. Magnetic interpretation suggests that the mainly Jurassic sediment here extends to a depth of at least 9 km (cf. 7.5 km estimated by Merla et al.). Underlying basement shallows rapidly on the eastern flank of the basin along the Juba River and also to the north against the interpreted fault F241 which appears downthrown to the south. The Juba River flank may be a particularly fruitful area for further exploration, assuming that unfavourable reactivations of the nearby N-S fault system, particularly F231, have not occurred.

(ii) L14 and L13. These apparently connected structural lows occur in the south of the region and are interpreted to contain up to 10 km of sediment. This is reinforced by two-dimensional computer modelling along profile 2285/1 across L14. A preview of early seismic data suggests however that in the region of L13 sediment extends to probably less than half the depth calculated to basement by magnetics, perhaps as shallow as the 4.2 km deep upper surface of nearby body B42. Although this observation may not reflect favourably on the estimated depths for the adjacent low L14, L14 unlike L13 is associated with a direct trough-like and duly modelled magnetic response. Sediment within L14 may be intersected by the interpreted NW-SE faults F244 and F242.

(iii) L12. Recognised solely from the contouring of manual estimated depth values rather than direct magnetic response, this trough is somewhat uncertain. The ridge H6 immediately to the south however is interpreted with far greater certainty as it exhibits a strong direct magnetic response and in consequence affords greater probability to the existence of a complementary structural low L12 to the north. A gravity traverse positioned appropriately across L12 would resolve this uncertainty more satisfactorily. Magnetic depth estimates along L12 suggest that magnetic

basement occurs at depths of over 8 km. The interpreted NW-SE faults F237, F243, F244 and possibly F238 and F239, may intersect the sediment within this trough.

6.2.2 Eastern Deep Basement

In the east of Block 2 lies a small region of relatively deep basement, defined by the interpreted NE-SW faulted troughs L6 and L16. Modelled basement depths in both cases exceed 5 km and an indicated shallowing to the southwest suggests that relatively shallow, potentially interesting hydrocarbon accumulations may lie in this direction.

6.2.3 Shallow Basement

Although at present there appears to be little significant sedimentary thickness within the shallow Oddur Arch region of Block 2, far greater historic thickness cannot be precluded. Indeed surface geology suggests that this is highly probable.

The shallow Oddur Arch region may also have been the destination of hydrocarbons migrating from the adjacent major basins. Although a detailed seismic study of the area might lend promise to this suggestion, only drilling would confirm this as a real possibility.

Of the interpreted features likely to be of ancient origin, two or possibly three features are notable:

(i) L7. This broad N-S trending structural low has been interpreted as a possible graben occurring it is thought as a result of rifting along the axis of the developing Oddur Arch. Its N-S orientation makes direct magnetic detection virtually impossible, however indirect evidence is strong. Structural relief across the feature although difficult to determine quantitatively from magnetic evidence, is probably significant. Detailed mapping of the surface counterpart of the intersecting E-W fault F115, particularly dip measurements, may largely resolve this. Hydrocarbon accumulation against fault F115 is a possibility.

(ii) Fault F115. It is suggested that this interpreted E-W fault downthrown to the north has, by its association with volcanic extrusives directly to the south (see Section 5.4.2), experienced a partially sub-marine history. In consequence, reefing along its length is a real possibility. Faults F114 and F113 directly to the east and the faulted contact directly to the west define the full extent of the possible reefing zone.

(iii) L8. This relatively broad N-S structural low has been interpreted in a similar indirect manner as L7. The indirect evidence is however not as extensive and therefore L8 is regarded with a little less certainty. Hydrocarbon accumulation against the intersecting interpreted E-W fault F193 is a possibility.

7. ACKNOWLEDGEMENTS

Hunting Geology and Geophysics Limited would like to express their gratitude to all those Esso personnel involved, both in Somalia and Houston, for their assistance during all stages of this project.

BIBLIOGRAPHY

Am K.	1972	The Arbitrarily Magnetised Dyke: Interpretation by Characteristics. Geoexploration 10, 63-90
Barnes S.U.	1976	Geology and Oil Prospects of Somalia, East Africa. A.A.P.G. Bull. 60(3), 389-413.
Bean R.J.	1966	A Rapid Graphical Solution for the Aeromagnetic Anomaly over a Two-Dimensional Tabular Body. Geophysics 31(5), 963-970
Beltrandi M.D. and Pyre A.	1973	Geological Evolution of Southwest Somalia, in "Bassins sedimentaires du litoral Africain - Sedimentary basins of the African coast" pt. 2., Ass. Serv. Geol. Afr., p.159-178.
Daniels J.L.	1965	A Photogeological interpretation of the Bur Region, Somali Republic. Overseas Geology and Mineral Resources. 9 (4)., 427-436.
Harding T.P.	1984	Graben Occurrences and Structural Style. AAPG Bulletin 68(3), 333-362
Hunting Geology and Geophysics Ltd.		Internal memoranda.
Kent P.	1982	The Somali Ocean Basin and the Continental Margin of East Africa. "The Ocean Basins and Margins" Vol.6 "The Indian Ocean" Plenum Press.
Le Pichon X., Franceteau J., Bonnin J.	1973	Plate Tectonics. Elsevier.
Norton I.O and Sclater J.G	1979	A Model for the Evolution of the Indian Ocean and the Break-up of Gondwanaland. Journal of Geophysical Research, 84(B12), 6803-6830.
Peters L.J.	1949	The Direct Approach to Magnetic Interpretation and its Practical Application. Geophysics, 14(3), 290-320.

Spector A. and Grant F.	1970	Statistical Models for Interpreting Aeromagnetic Data. Geophysics 35(20, 293-302.
Steenland N.C.	1965	Oilfields and Aeromagnetic Anomalies. Geophysics, 30(5), 706-739.
Stefannini G.	1925	Description of Fossils from South Arabia and British Somaliland in: O.H. Little "The Geography and Geology of Makalla (South Arabia)" Egypt Geol. Survey 143-250
Vacquier V., Steenland N.C, Henderson R.G and Zeitz I.	1951	Interpretation of Aeromagnetic Maps. Geological Society of America, Memoir 7.

GEOLOGICAL MAPS

Bianconi et al.	1983	A Geological Map of Somalia. United Nations Development Project.
Canuti P., Fazzuoli M. and Tacconi P.	1980	Memoir and Photogeological Map of the Region between Juba and Webi Shebeli Rivers. Accademia Nazionale dei Lincei International Meeting on "Geodynamic Evolution of the Afro-Arabian Rift System".
Merla G., Abbate E., Azzaroli A., Bruni P., Canuti, P., Fazzuoli M., Sagri M. and Tacconi P.,	1973	A Geological Map of Ethiopia and Somalia (1973) and comment with a map of major Landforms.

A P P E N D I X 1

SHEET BY SHEET SPECTRAL ANALYSIS OF BLOCK 2

AND

SHEET BY SHEET SPECTRAL ANALYSIS CLASSIFICATION

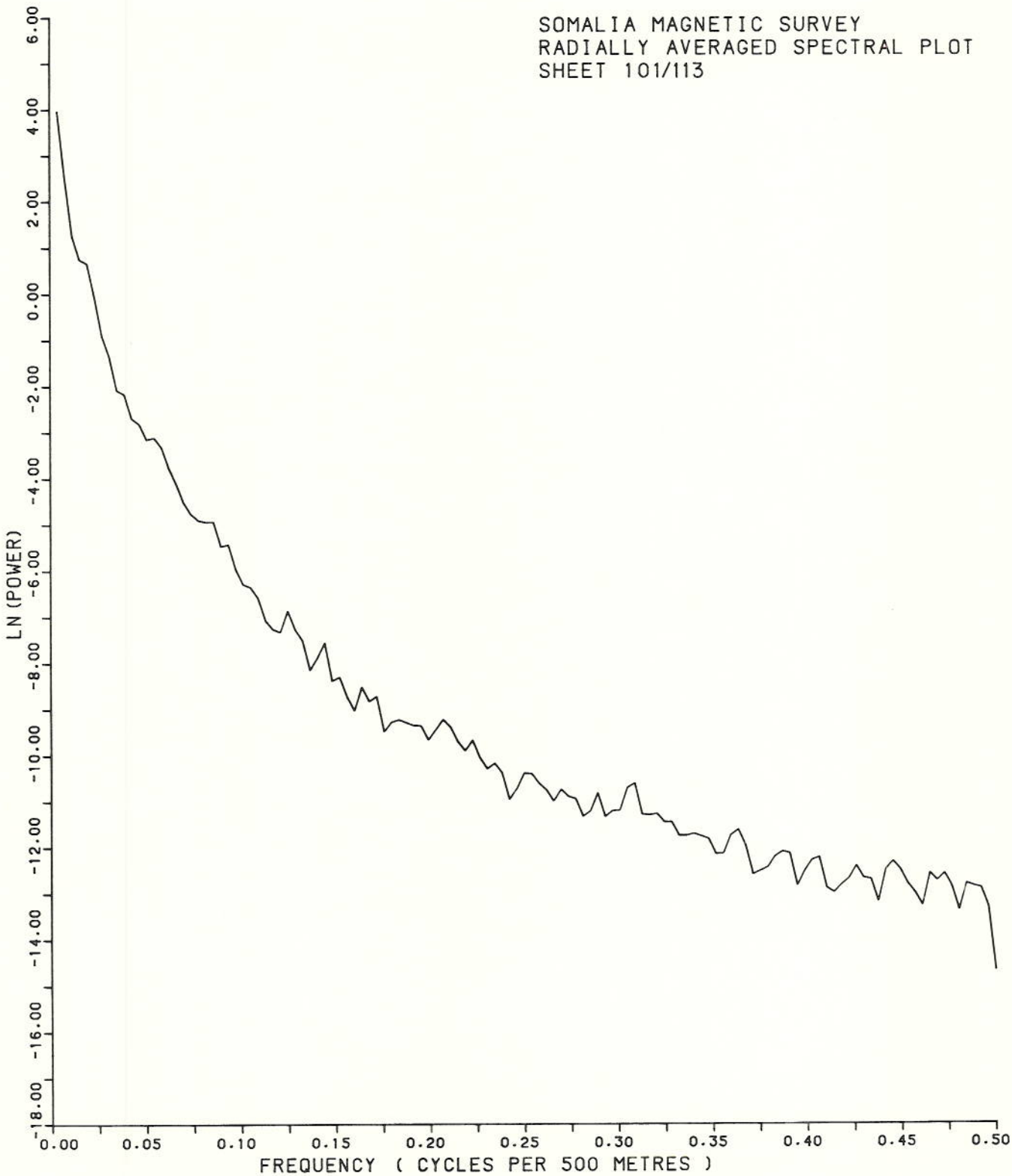
SOMALIA MAGNETIC SURVEY
RADIALLY AVERAGED SPECTRAL PLOT
SHEET 101/113
LN (POWER)
6.00
4.00
2.00
0.00
-2.00
-4.00
-6.00
-8.00
-10.00
-12.00
-14.00
-16.00
-18.00
0.00
0.05
0.10
0.15
0.20
0.25
0.30
0.35
0.40
0.45
0.50
FREQUENCY (CYCLES PER 500 METRES)

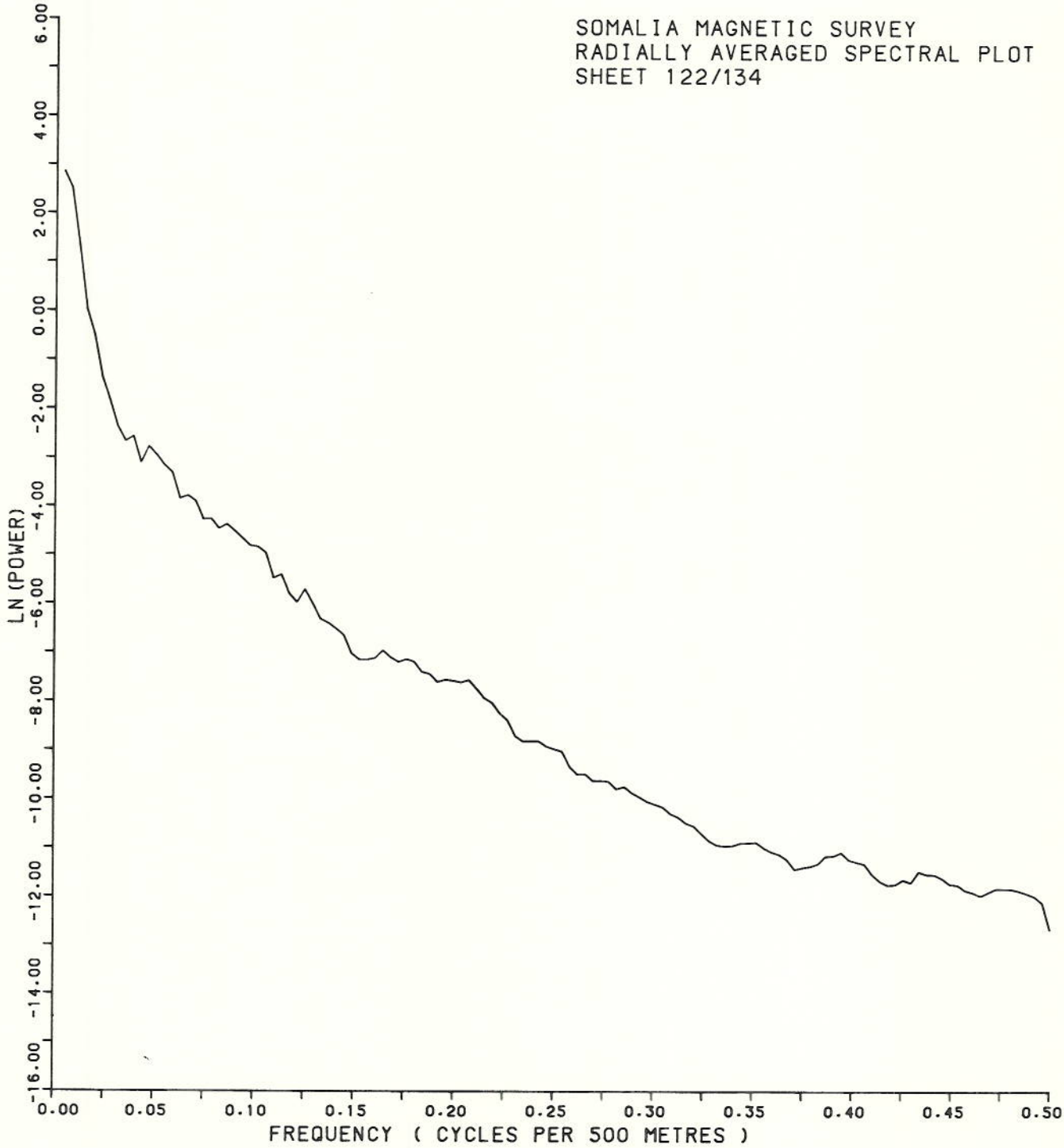
SOMALIA MAGNETIC SURVEY
RADIALLY AVERAGED SPECTRAL PLOT
SHEET 122/134
LN (POWER)
6.00
4.00
2.00
0.00
-2.00
-4.00
-6.00
-8.00
-10.00
-12.00
-14.00
-16.00
0.00
0.05
0.10
0.15
0.20
0.25
0.30
0.35
0.40
0.45
0.50
FREQUENCY (CYCLES PER 500 METRES)

SOMALIA MAGNETIC SURVEY
RADIALLY AVERAGED SPECTRAL PLOT
SHEET 123/135
LN (POWER)
8.00
6.00
4.00
2.00
0.00
-2.00
-4.00
-6.00
-8.00
-10.00
-12.00
-14.00
-16.00
0.00
0.05
0.10
0.15
0.20
0.25
0.30
0.35
0.40
0.45
0.50
FREQUENCY (CYCLES PER 500 METRES)

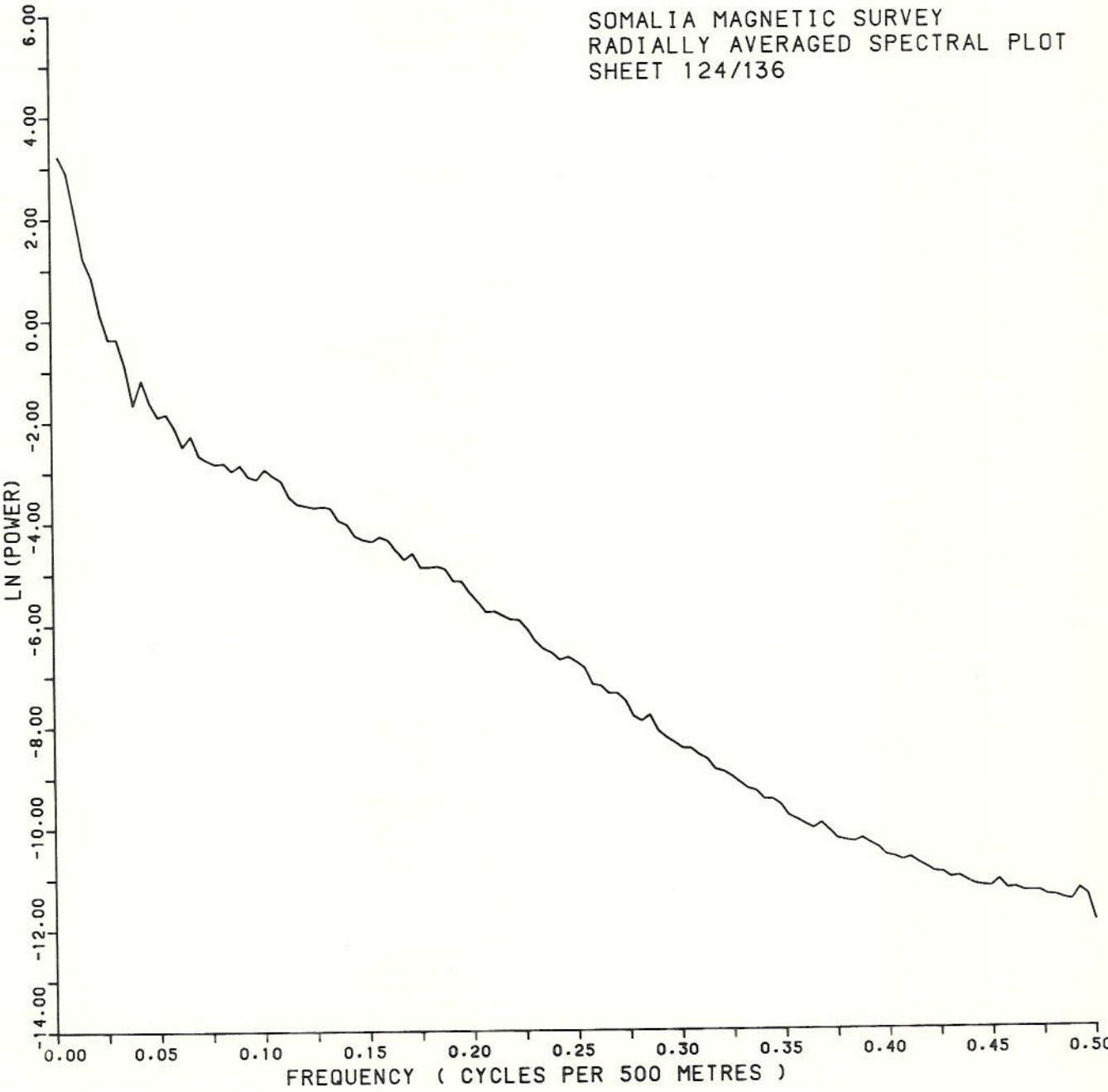
SOMALIA MAGNETIC SURVEY
RADIALLY AVERAGED SPECTRAL PLOT
SHEET 124/136
LN (POWER)
6.00
4.00
2.00
0.00
-2.00
-4.00
-6.00
-8.00
-10.00
-12.00
-14.00
0.00
0.05
0.10
0.15
0.20
0.25
0.30
0.35
0.40
0.45
0.50
FREQUENCY (CYCLES PER 500 METRES)

SOMALIA MAGNETIC SURVEY
RADIALLY AVERAGED SPECTRAL PLOT
SHEET 125/137
LN (POWER)
8.00
6.00
4.00
2.00
0.00
-2.00
-4.00
-6.00
-8.00
-10.00
-12.00
-14.00
-16.00
0.00
0.05
0.10
0.15
0.20
0.25
0.30
0.35
0.40
0.45
0.5
FREQUENCY (CYCLES PER 500 METRES)

SOMALIA MAGNETIC SURVEY
RADIALLY AVERAGED SPECTRAL PLOT
SHEET 126/138
LN (POWER)
8.00
6.00
4.00
2.00
0.00
-2.00
-4.00
-6.00
-8.00
-10.00
-12.00
-14.00
-16.00
0.00
0.05
0.10
0.15
0.20
0.25
0.30
0.35
0.40
0.45
0.50
FREQUENCY (CYCLES PER 500 METRES)

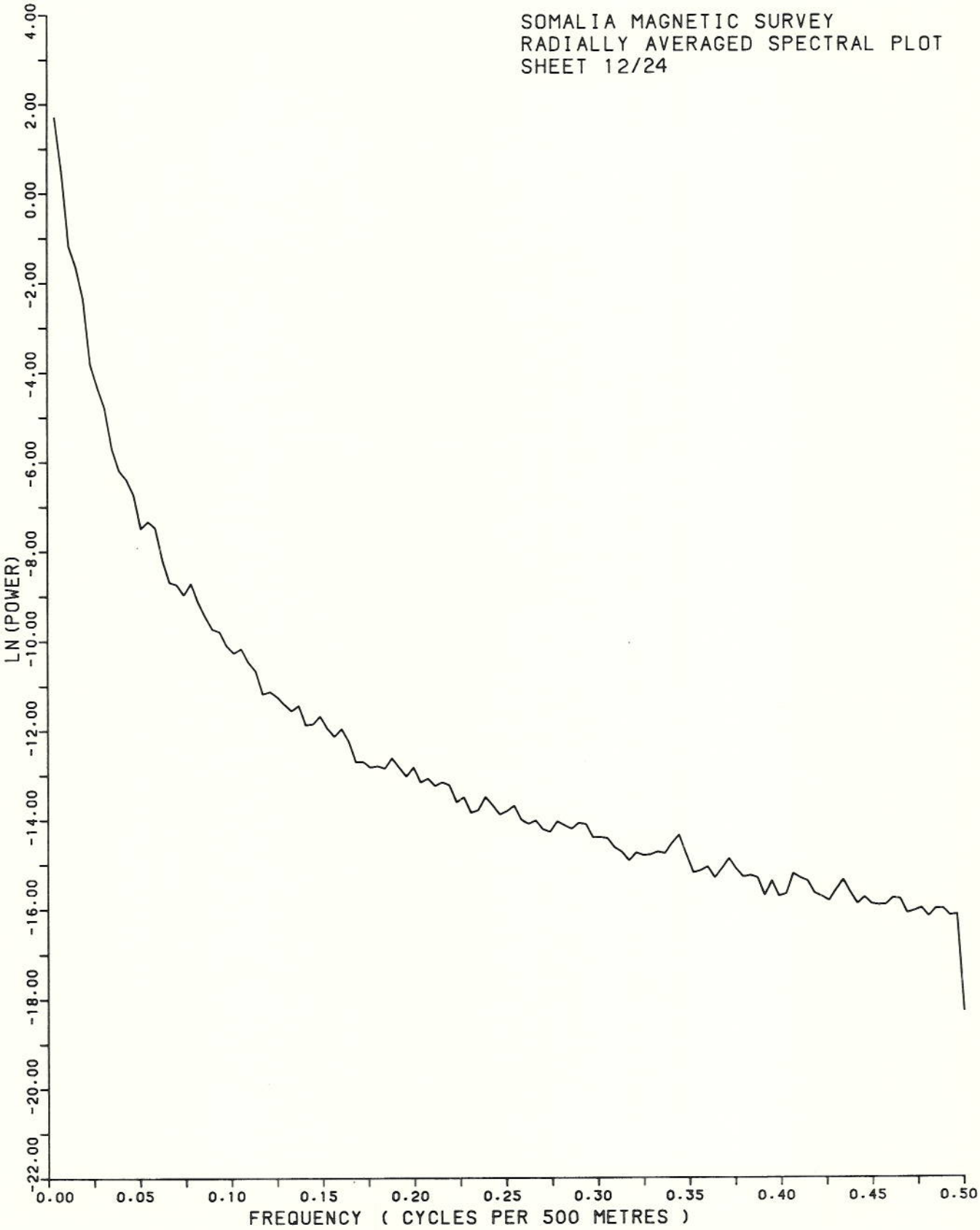
SOMALIA MAGNETIC SURVEY
RADIALLY AVERAGED SPECTRAL PLOT
SHEET 12/24
LN (POWER)
4.00
2.00
0.00
-2.00
-4.00
-6.00
-8.00
-10.00
-12.00
-14.00
-16.00
-18.00
-20.00
-22.00
0.00
0.05
0.10
0.15
0.20
0.25
0.30
0.35
0.40
0.45
0.50
FREQUENCY (CYCLES PER 500 METRES)

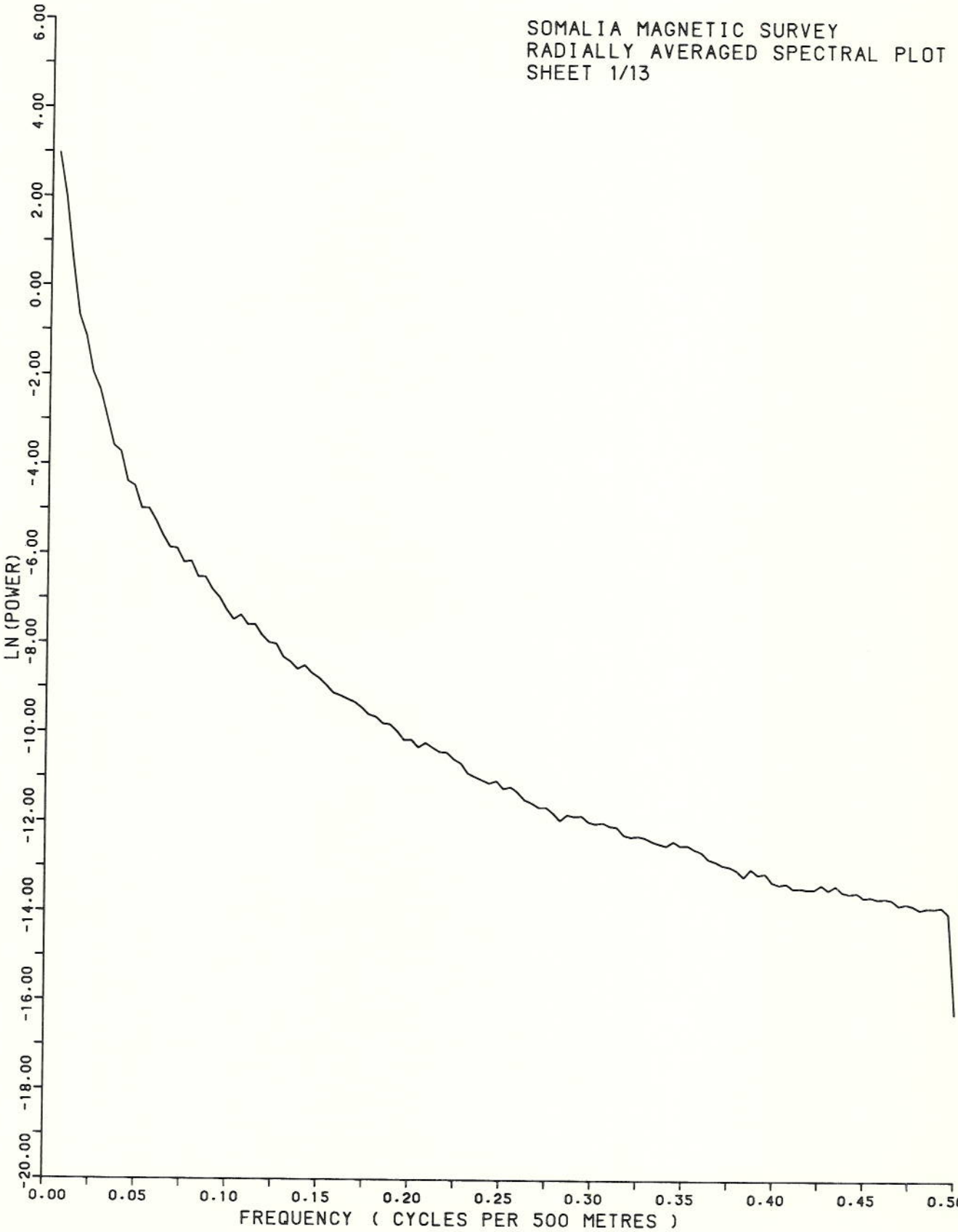
SOMALIA MAGNETIC SURVEY
RADIALLY AVERAGED SPECTRAL PLOT
SHEET 1/13
LN (POWER)
6.00
4.00
2.00
0.00
-2.00
-4.00
-6.00
-8.00
-10.00
-12.00
-14.00
-16.00
-18.00
-20.00
0.00
0.05
0.10
0.15
0.20
0.25
0.30
0.35
0.40
0.45
FREQUENCY (CYCLES PER 500 METRES)

SOMALIA MAGNETIC SURVEY
RADIALLY AVERAGED SPECTRAL PLOT
SHEET 2/14

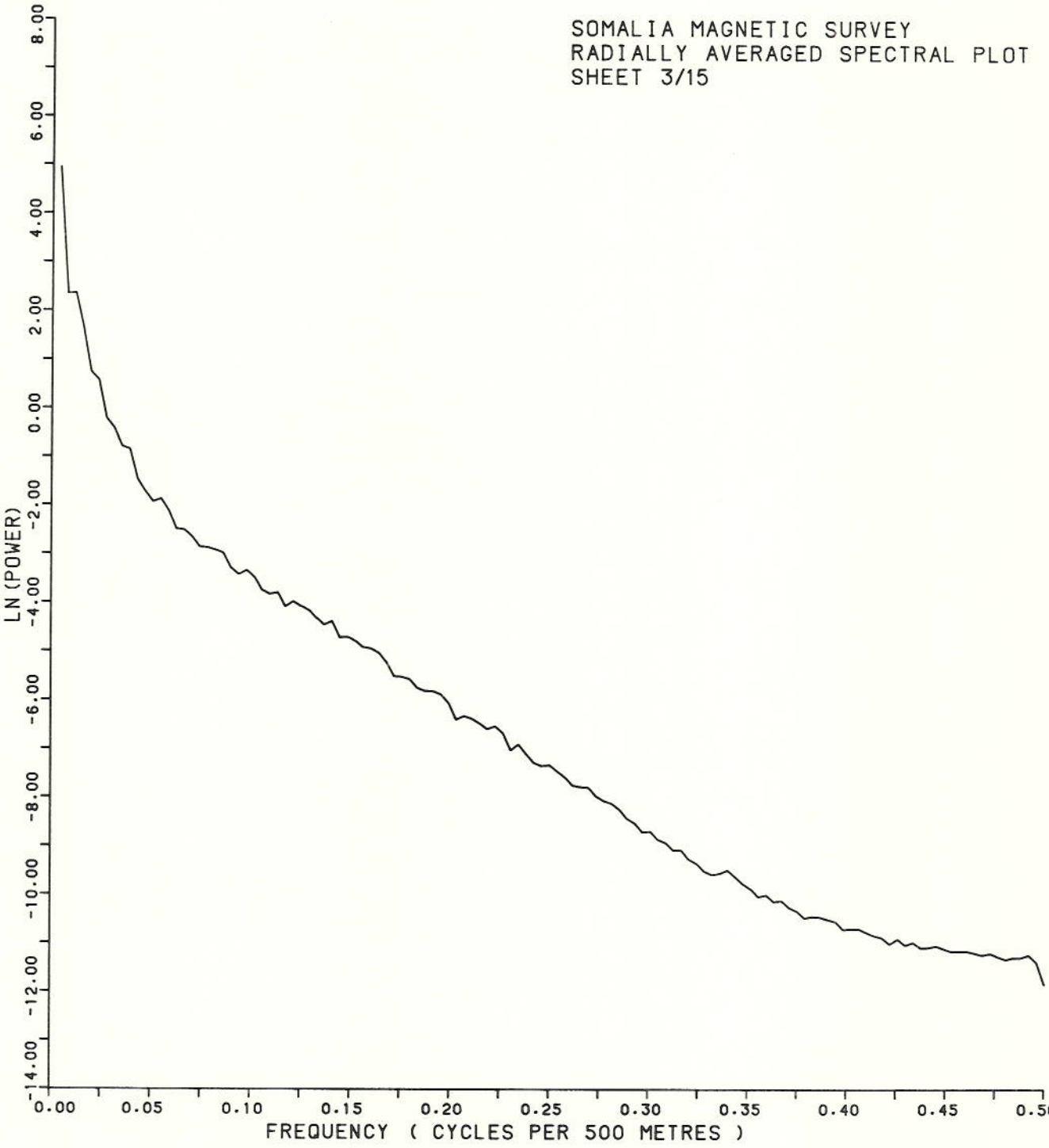
SOMALIA MAGNETIC SURVEY
RADIALLY AVERAGED SPECTRAL PLOT
SHEET 3/15
LN (POWER)
8.00
6.00
4.00
2.00
0.00
-2.00
-4.00
-6.00
-8.00
-10.00
-12.00
-14.00
0.00
0.05
0.10
0.15
0.20
0.25
0.30
0.35
0.40
0.45
FREQUENCY (CYCLES PER 500 METRES)

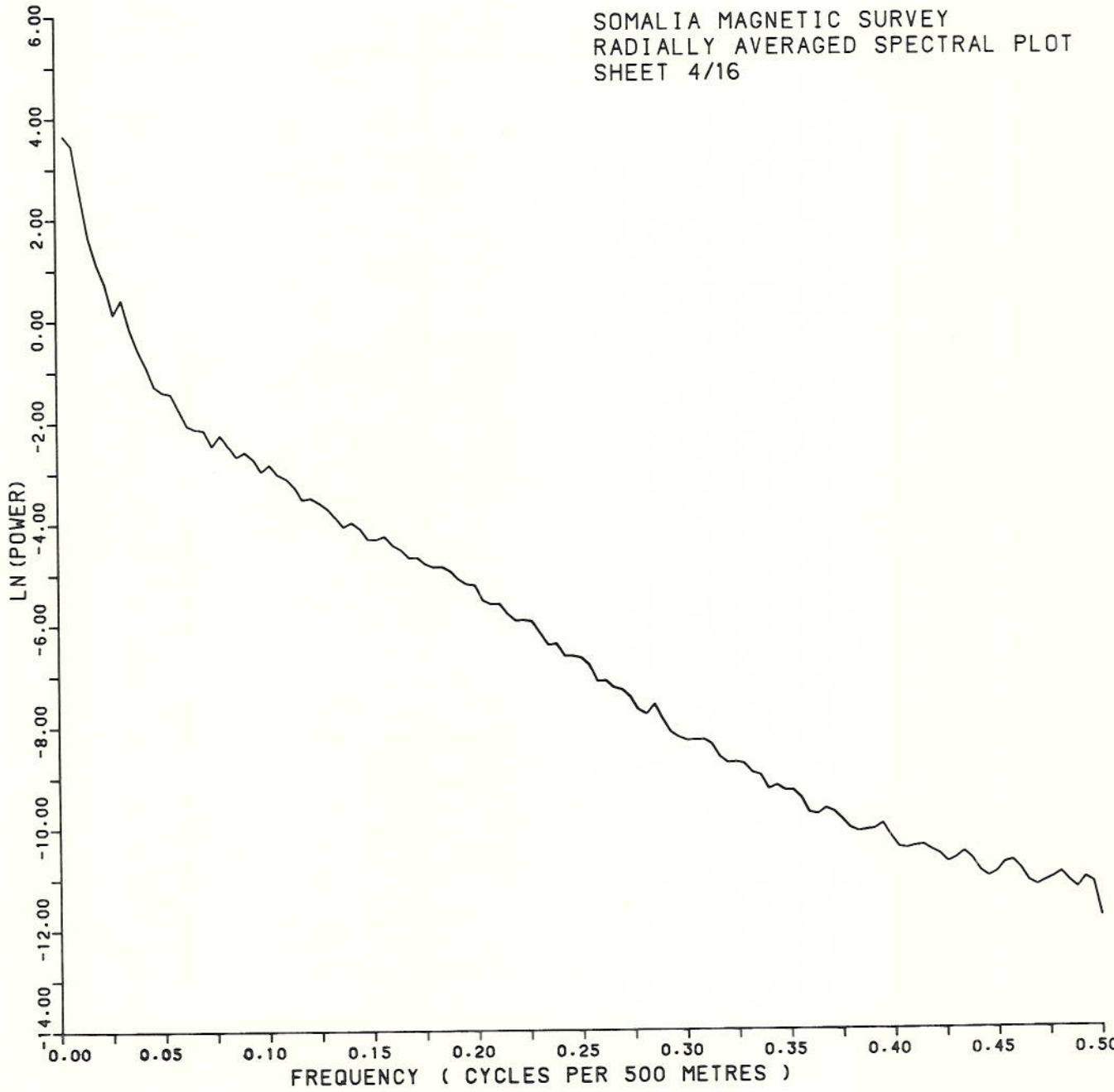
SOMALIA MAGNETIC SURVEY
RADIALLY AVERAGED SPECTRAL PLOT
SHEET 4/16
LN (POWER)
6.00
4.00
2.00
0.00
-2.00
-4.00
-6.00
-8.00
-10.00
-12.00
-14.00
0.00
0.05
0.10
0.15
0.20
0.25
0.30
0.35
0.40
0.45
0.50
FREQUENCY (CYCLES PER 500 METRES)

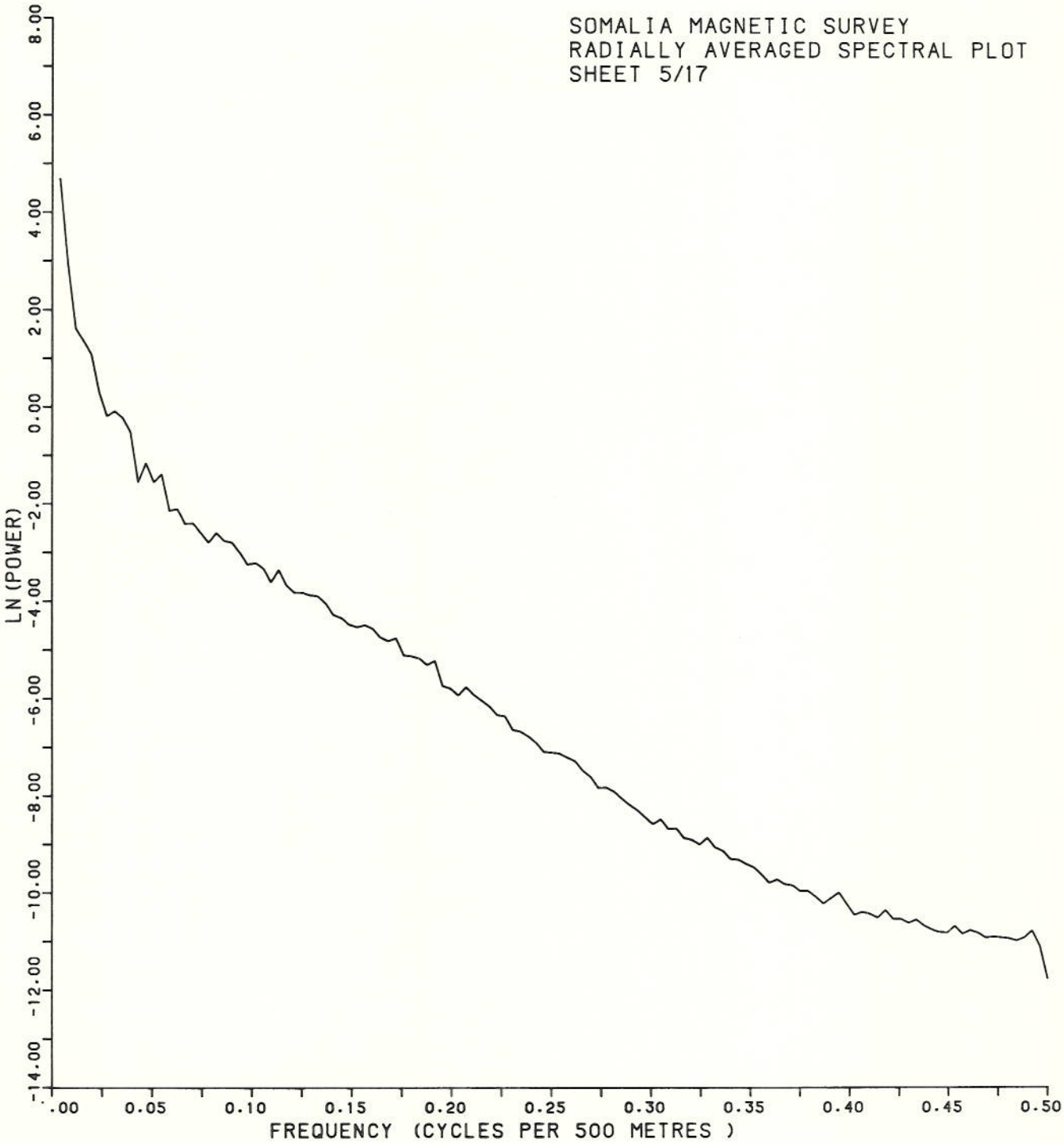
SOMALIA MAGNETIC SURVEY
RADIALLY AVERAGED SPECTRAL PLOT
SHEET 5/17
LN (POWER)
8.00
6.00
4.00
2.00
0.00
-2.00
-4.00
-6.00
-8.00
-10.00
-12.00
-14.00
.00
0.05
0.10
0.15
0.20
0.25
0.30
0.35
0.40
0.45
0.50
FREQUENCY (CYCLES PER 500 METRES)

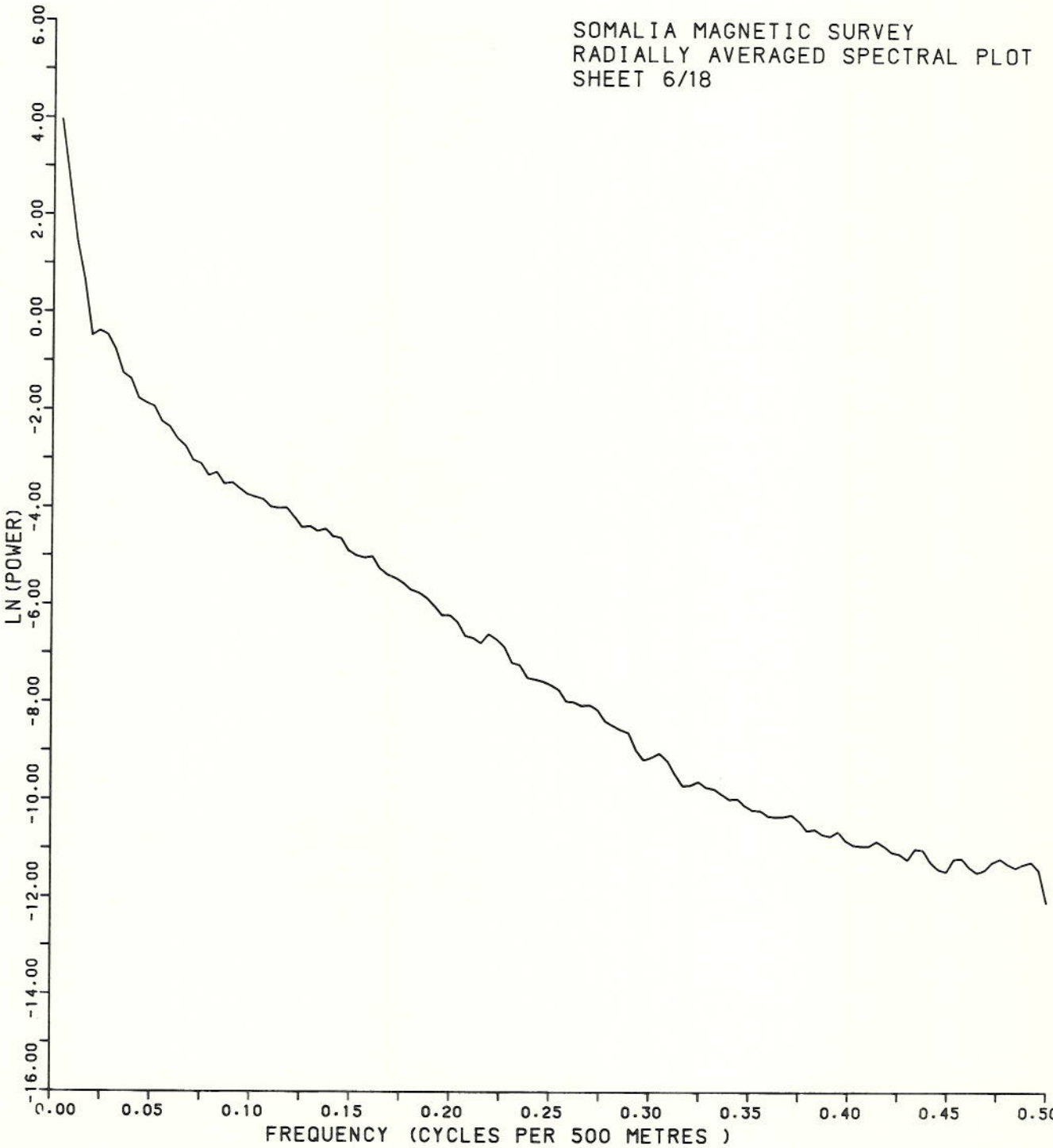
SOMALIA MAGNETIC SURVEY
RADIALLY AVERAGED SPECTRAL PLOT
SHEET 6/18
LN (POWER)
6.00
4.00
2.00
0.00
-2.00
-4.00
-6.00
-8.00
-10.00
-12.00
-14.00
-16.00
0.00
0.05
0.10
0.15
0.20
0.25
0.30
0.35
0.40
0.45
0.50
FREQUENCY (CYCLES PER 500 METRES)

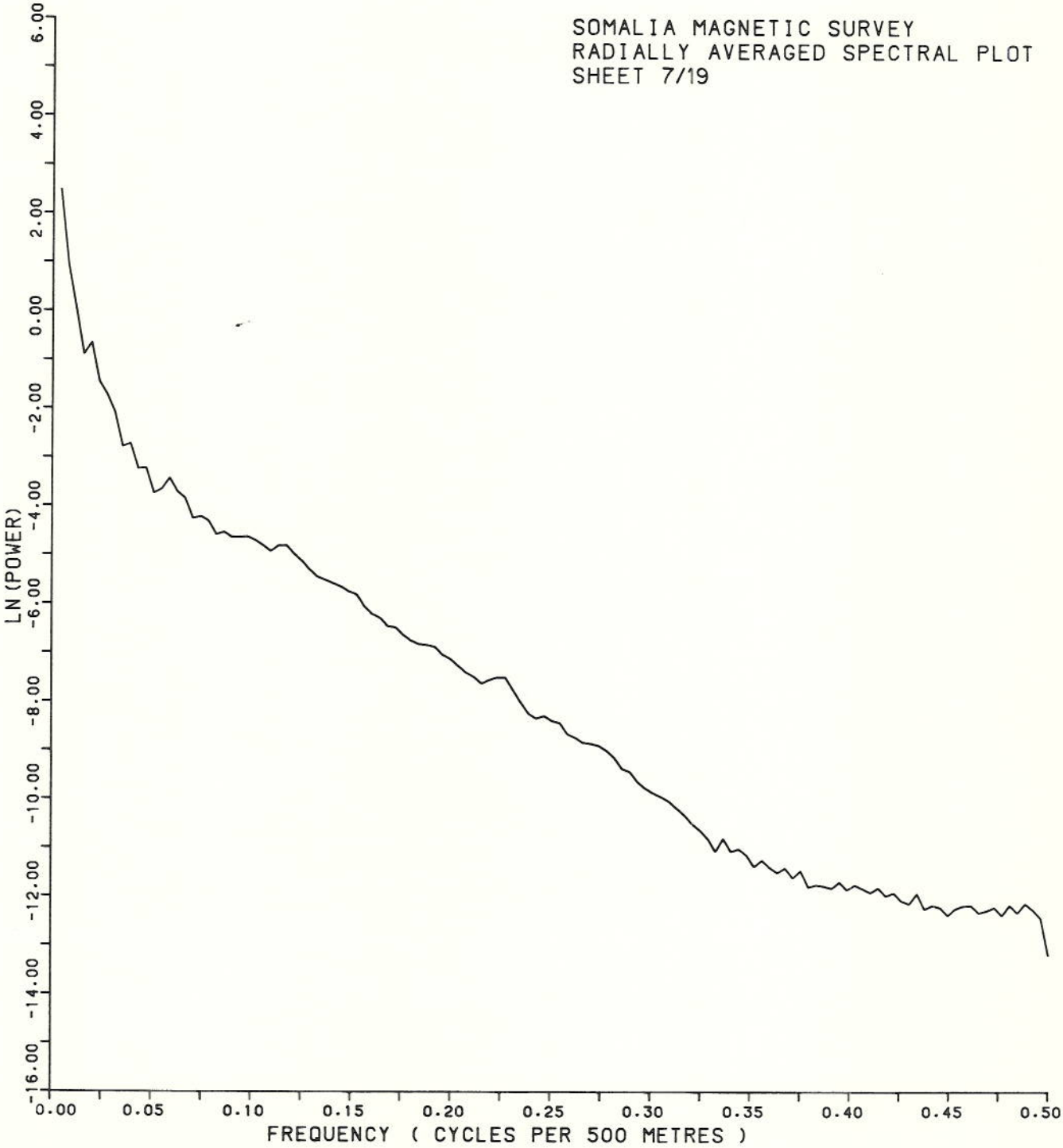
SOMALIA MAGNETIC SURVEY
RADIALLY AVERAGED SPECTRAL PLOT
SHEET 7/19
LN (POWER)
6.00
4.00
2.00
0.00
-2.00
-4.00
-6.00
-8.00
-10.00
-12.00
-14.00
-16.00
0.00
0.05
0.10
0.15
0.20
0.25
0.30
0.35
0.40
0.45
0.50
FREQUENCY (CYCLES PER 500 METRES)

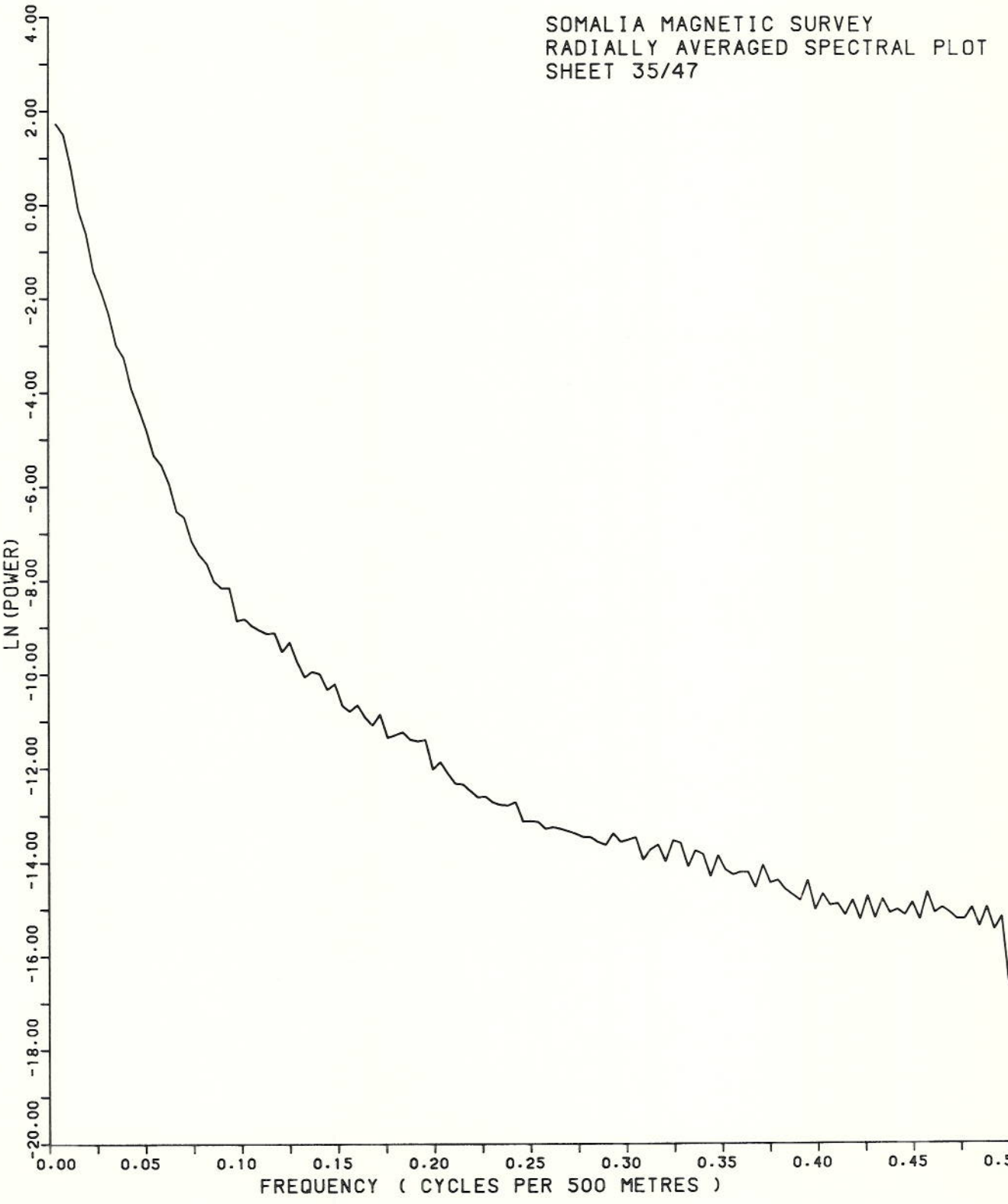
SOMALIA MAGNETIC SURVEY
RADIALLY AVERAGED SPECTRAL PLOT
SHEET 35/47
LN (POWER)
4.00
2.00
0.00
-2.00
-4.00
-6.00
-8.00
-10.00
-12.00
-14.00
-16.00
-18.00
-20.00
0.00
0.05
0.10
0.15
0.20
0.25
0.30
0.35
0.40
0.45
FREQUENCY (CYCLES PER 500 METRES)

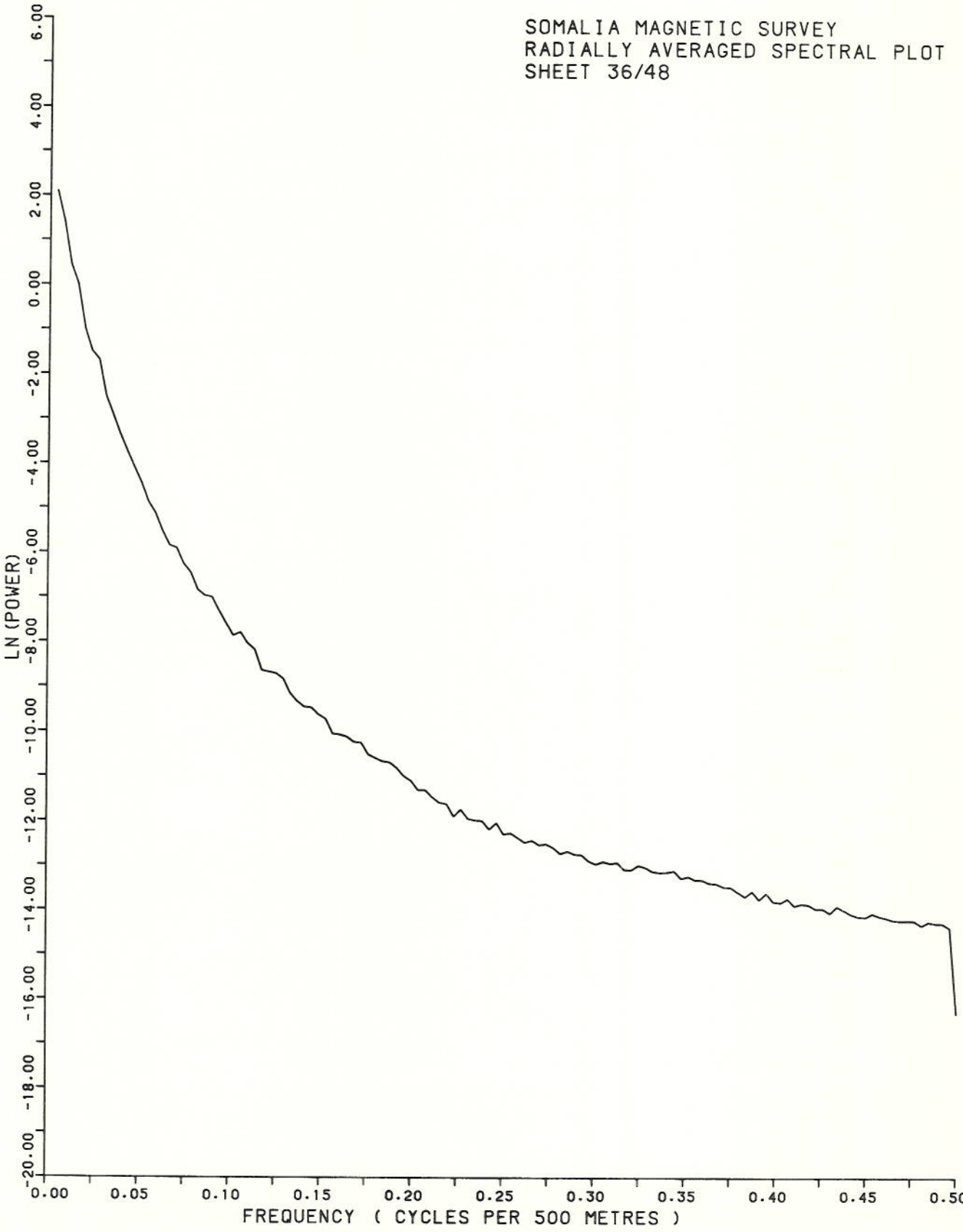
SOMALIA MAGNETIC SURVEY
RADIALLY AVERAGED SPECTRAL PLOT
SHEET 36/48
LN (POWER)
6.00
4.00
2.00
0.00
-2.00
-4.00
-6.00
-8.00
-10.00
-12.00
-14.00
-16.00
-18.00
-20.00
0.00
0.05
0.10
0.15
0.20
0.25
0.30
0.35
0.40
0.45
0.50
FREQUENCY (CYCLES PER 500 METRES)

SOMALIA MAGNETIC SURVEY
RADIALLY AVERAGED SPECTRAL PLOT
SHEET 25/37
LN (POWER)
8.00
6.00
4.00
2.00
0.00
-2.00
-4.00
-6.00
-8.00
-10.00
-12.00
-14.00
-16.00
-18.00
0.00
0.05
0.10
0.15
0.20
0.25
0.30
0.35
0.40
0.45
0.50
FREQUENCY (CYCLES PER 500 METRES)

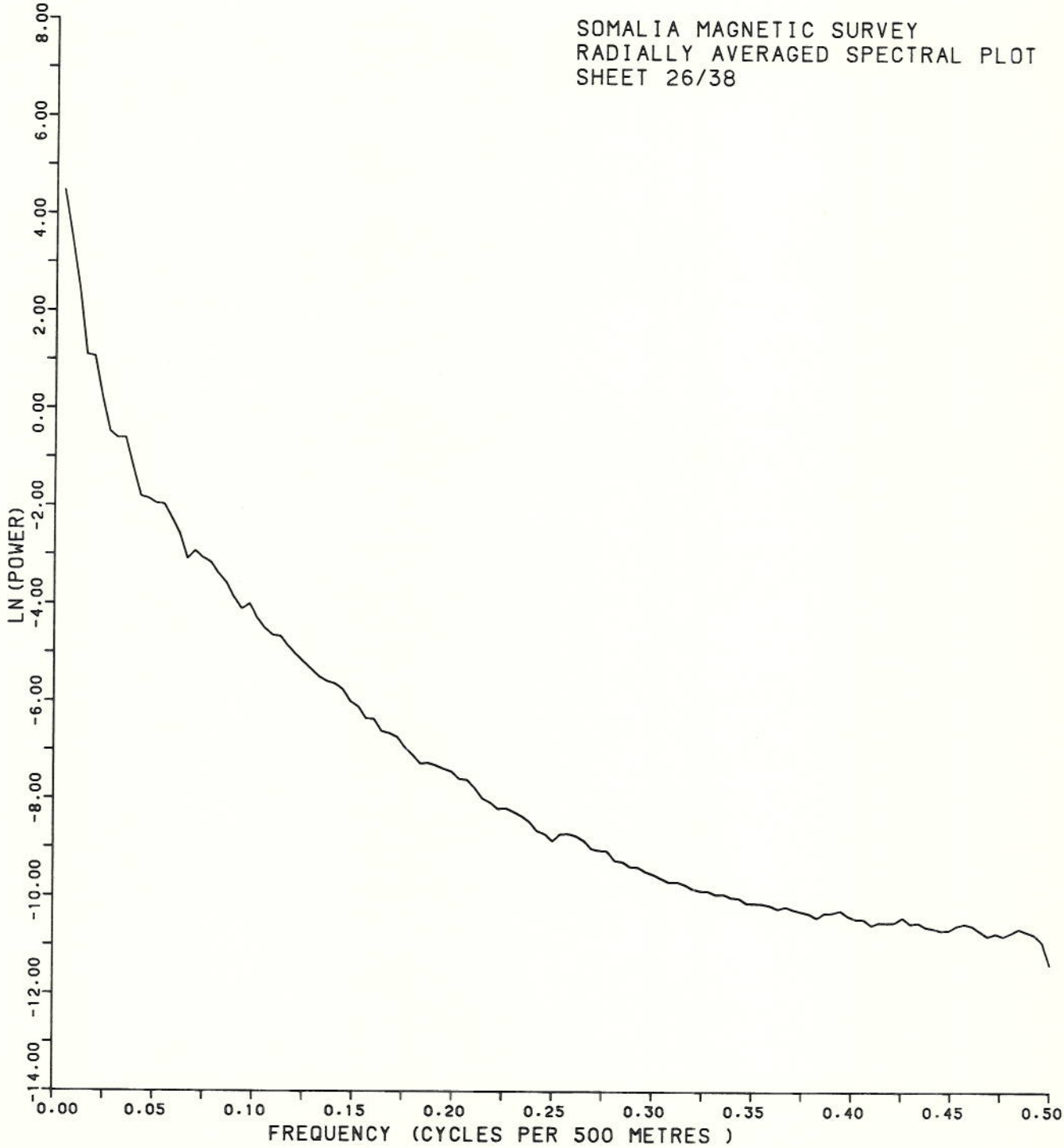
SOMALIA MAGNETIC SURVEY
RADIALLY AVERAGED SPECTRAL PLOT
SHEET 26/38
LN (POWER)
8.00
6.00
4.00
2.00
0.00
-2.00
-4.00
-6.00
-8.00
-10.00
-12.00
-14.00
0.00
0.05
0.10
0.15
0.20
0.25
0.30
0.35
0.40
0.45
0.50
FREQUENCY (CYCLES PER 500 METRES)

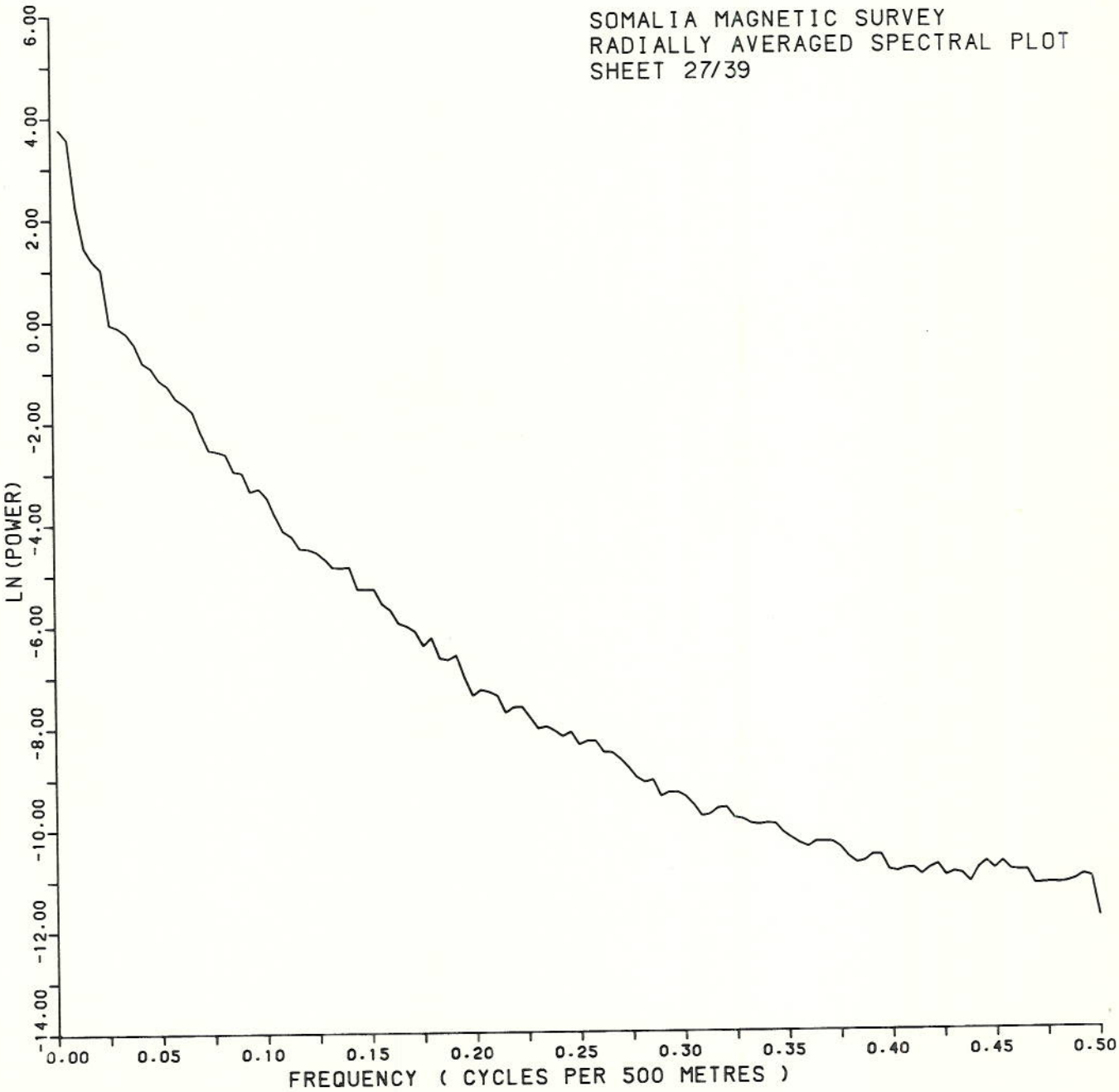
SOMALIA MAGNETIC SURVEY
RADIALLY AVERAGED SPECTRAL PLOT
SHEET 27/39
LN (POWER)
6.00
4.00
2.00
0.00
-2.00
-4.00
-6.00
-8.00
-10.00
-12.00
-14.00
0.00
0.05
0.10
0.15
0.20
0.25
0.30
0.35
0.40
0.45
0.50
FREQUENCY (CYCLES PER 500 METRES)

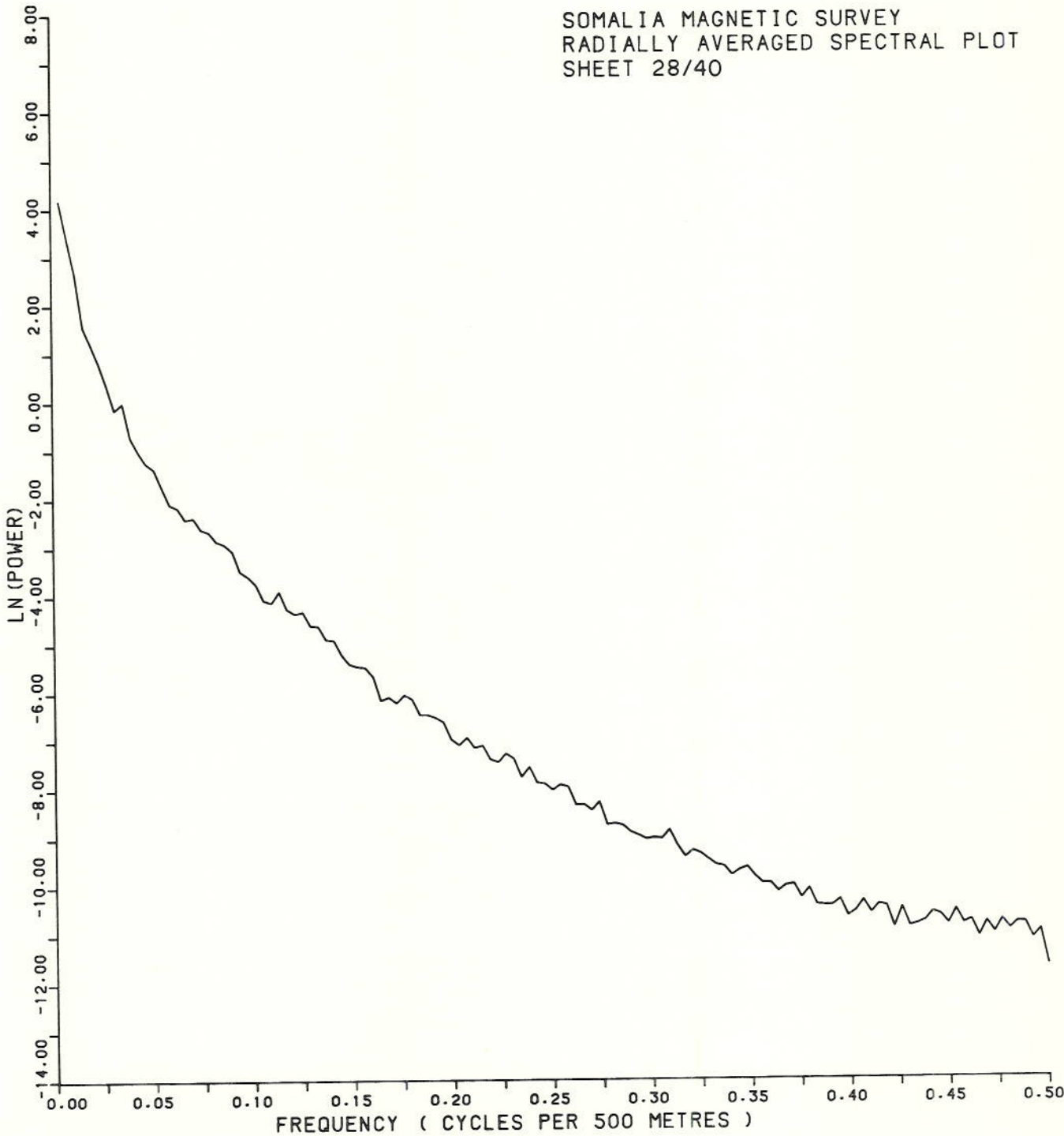
SOMALIA MAGNETIC SURVEY
RADIALLY AVERAGED SPECTRAL PLOT
SHEET 28/40
LN (POWER)
8.00
6.00
4.00
2.00
0.00
-2.00
-4.00
-6.00
-8.00
-10.00
-12.00
-14.00
0.00
0.05
0.10
0.15
0.20
0.25
0.30
0.35
0.40
0.45
0.50
FREQUENCY (CYCLES PER 500 METRES)

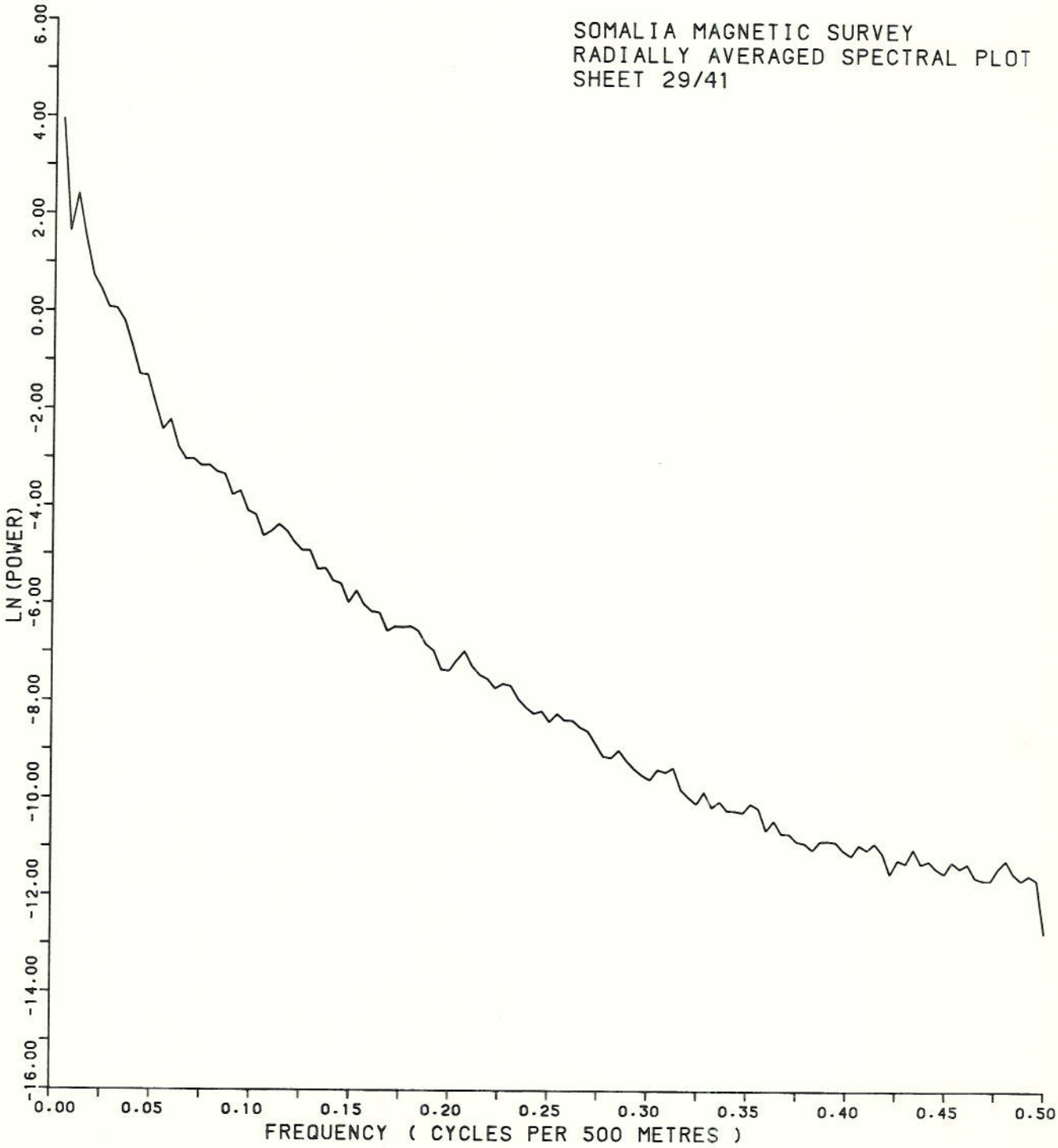
SOMALIA MAGNETIC SURVEY
RADIALLY AVERAGED SPECTRAL PLOT
SHEET 29/41
LN (POWER)
6.00
4.00
2.00
0.00
-2.00
-4.00
-6.00
-8.00
-10.00
-12.00
-14.00
-16.00
0.00
0.05
0.10
0.15
0.20
0.25
0.30
0.35
0.40
0.45
0.50
FREQUENCY (CYCLES PER 500 METRES)

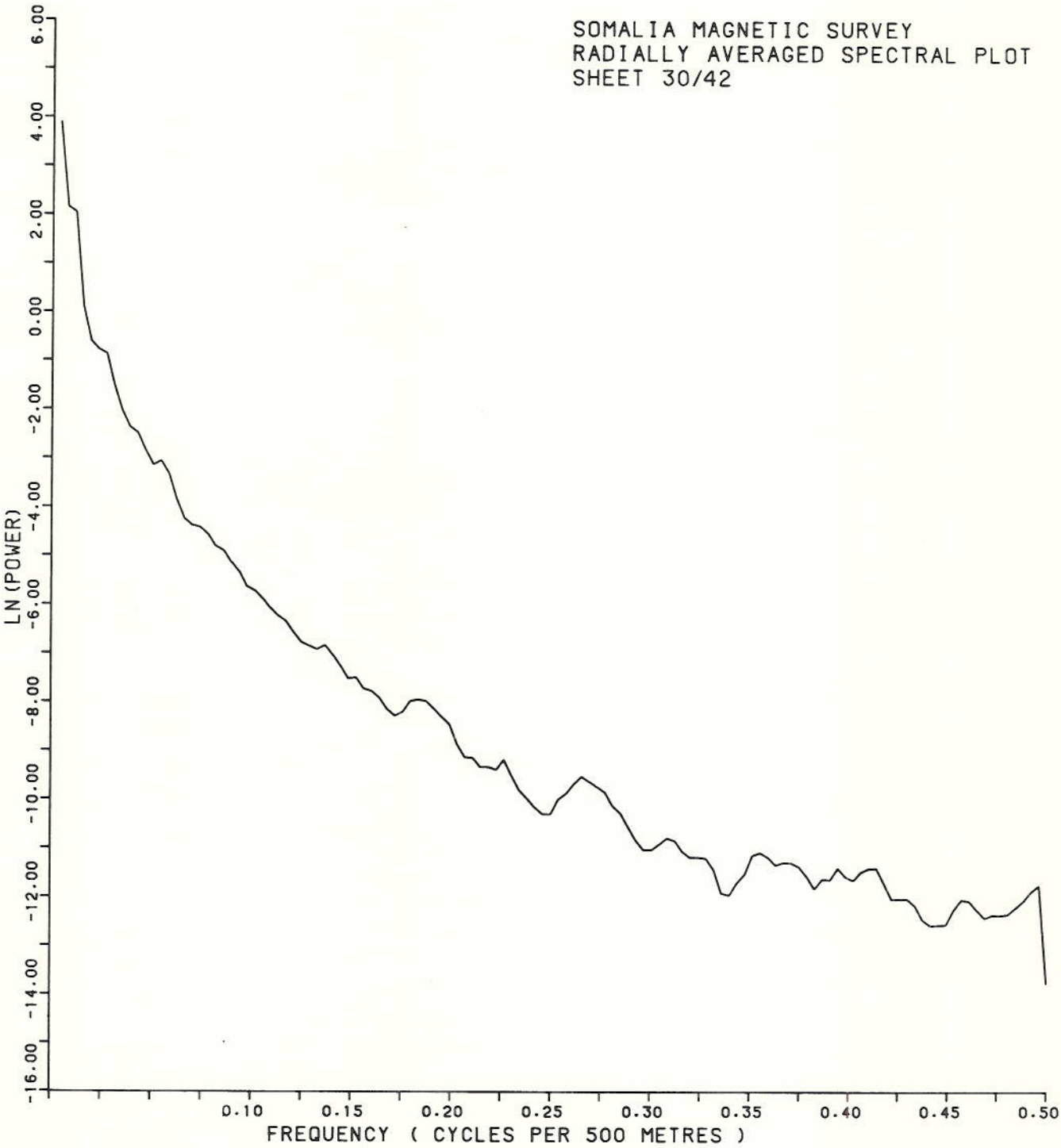
SOMALIA MAGNETIC SURVEY
RADIALLY AVERAGED SPECTRAL PLOT
SHEET 30/42
LN (POWER)
6.00
4.00
2.00
0.00
-2.00
-4.00
-6.00
-8.00
-10.00
-12.00
-14.00
-16.00
0.10
0.15
0.20
0.25
0.30
0.35
0.40
0.45
0.50
FREQUENCY (CYCLES PER 500 METRES)

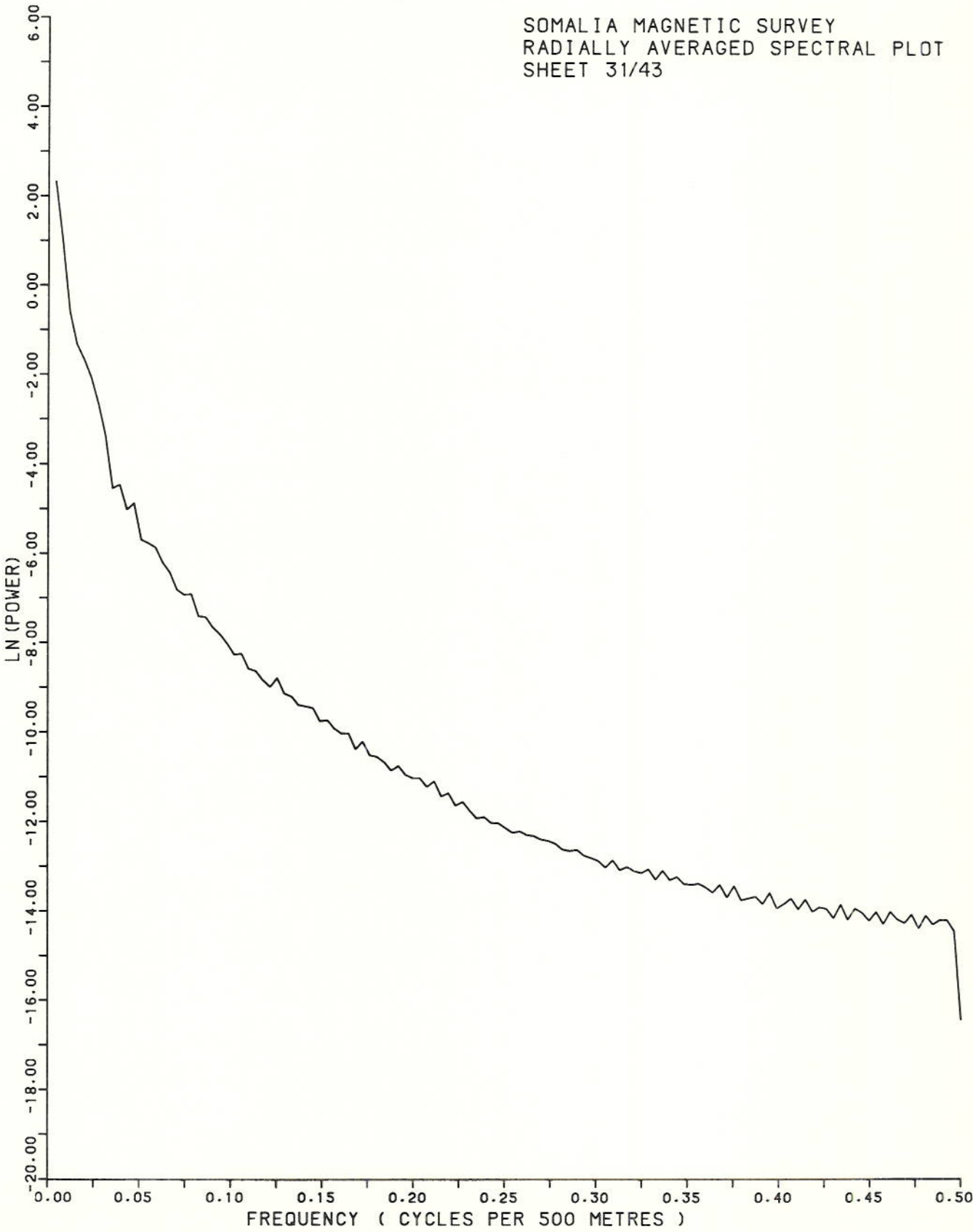
SOMALIA MAGNETIC SURVEY
RADIALLY AVERAGED SPECTRAL PLOT
SHEET 31/43
LN (POWER)
6.00
4.00
2.00
0.00
-2.00
-4.00
-6.00
-8.00
-10.00
-12.00
-14.00
-16.00
-18.00
-20.00
0.00
0.05
0.10
0.15
0.20
0.25
0.30
0.35
0.40
0.45
0.50
FREQUENCY (CYCLES PER 500 METRES)

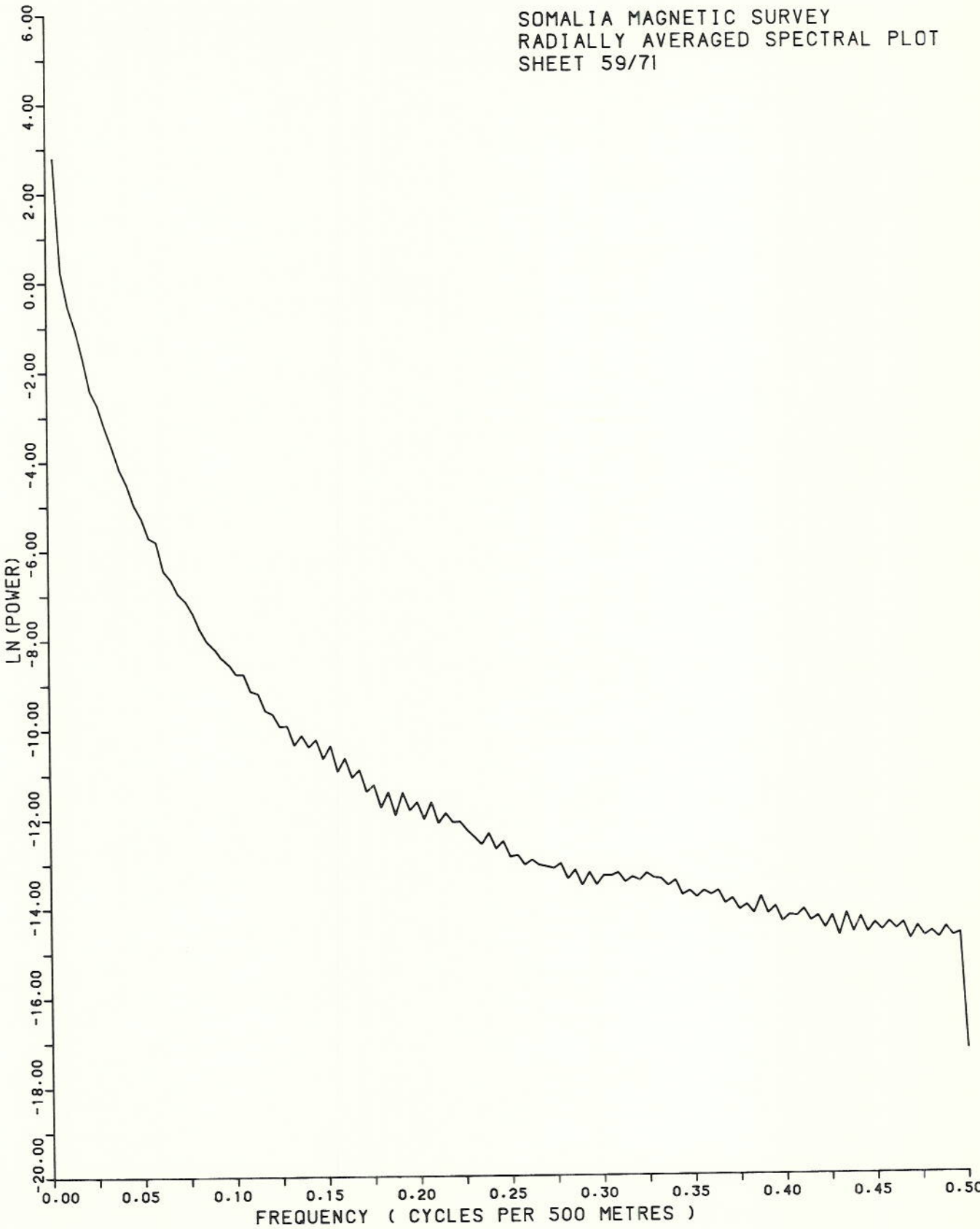
SOMALIA MAGNETIC SURVEY
RADIALLY AVERAGED SPECTRAL PLOT
SHEET 59/71
LN (POWER)
6.00
4.00
2.00
0.00
-2.00
-4.00
-6.00
-8.00
-10.00
-12.00
-14.00
-16.00
-18.00
-20.00
0.00
0.05
0.10
0.15
0.20
0.25
0.30
0.35
0.40
0.45
0.50
FREQUENCY (CYCLES PER 500 METRES)

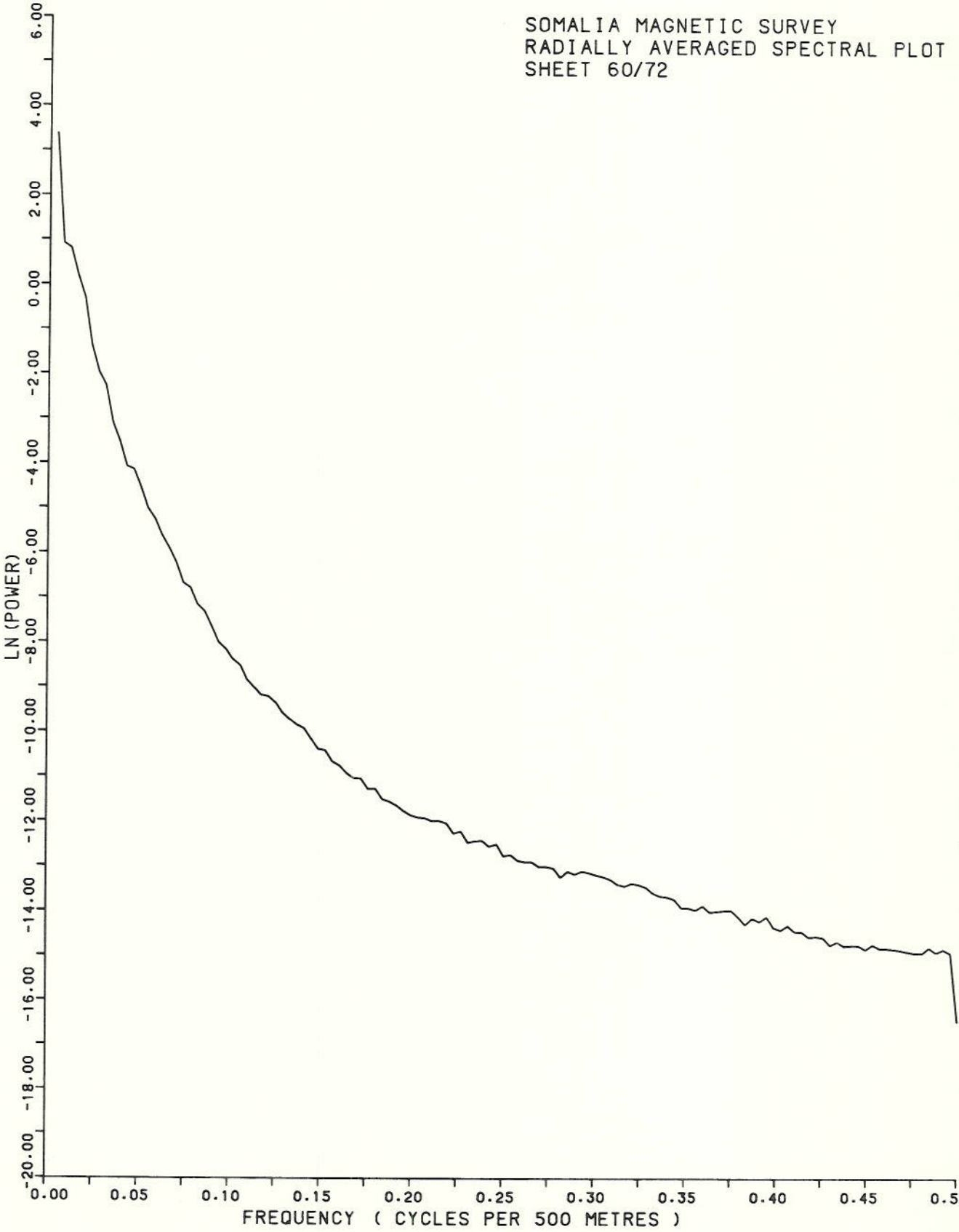
SOMALIA MAGNETIC SURVEY
RADIALLY AVERAGED SPECTRAL PLOT
SHEET 60/72
LN (POWER)
6.00
4.00
2.00
0.00
-2.00
-4.00
-6.00
-8.00
-10.00
-12.00
-14.00
-16.00
-18.00
-20.00
0.00
0.05
0.10
0.15
0.20
0.25
0.30
0.35
0.40
0.45
0.5
FREQUENCY (CYCLES PER 500 METRES)

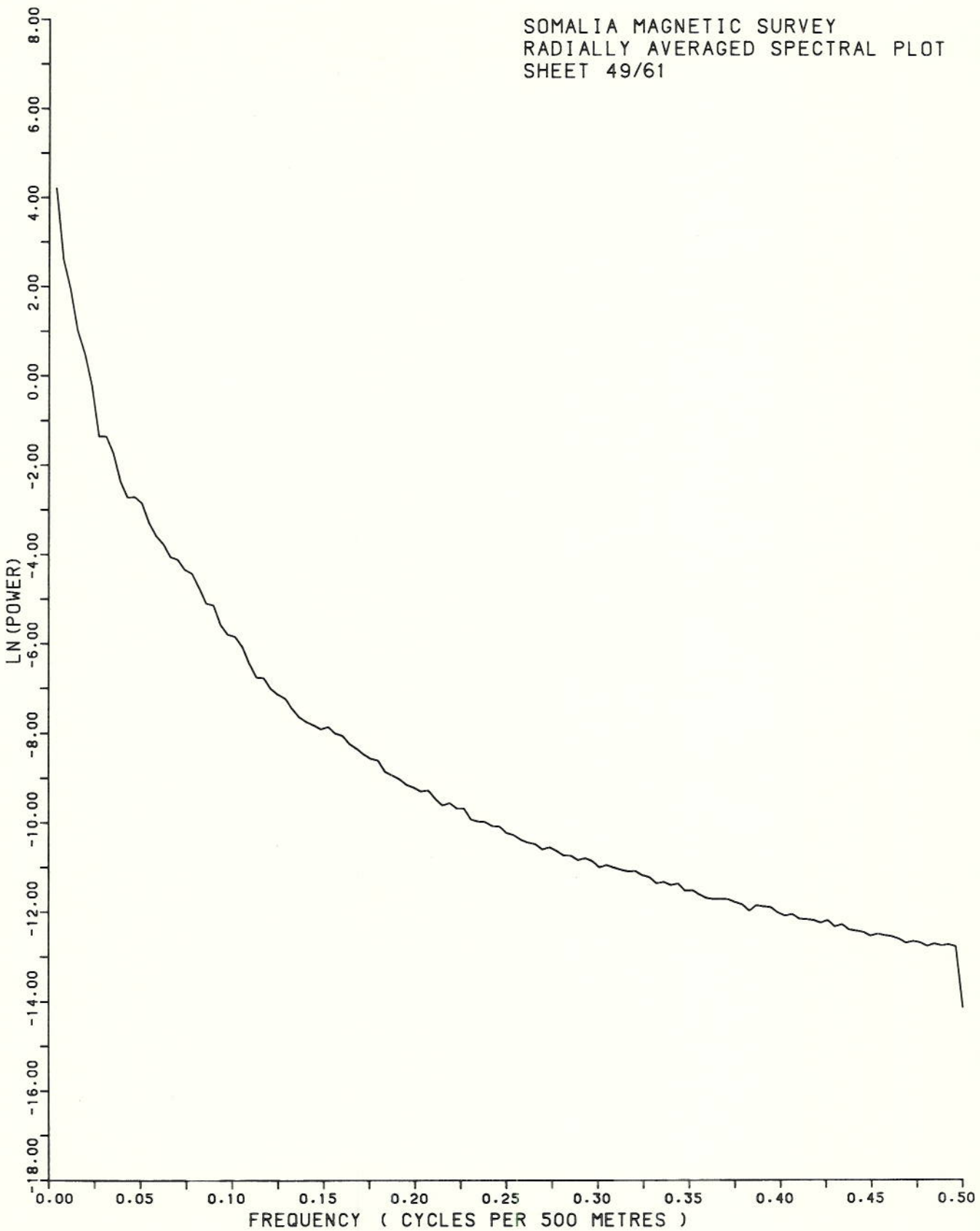
SOMALIA MAGNETIC SURVEY
RADIALLY AVERAGED SPECTRAL PLOT
SHEET 49/61
LN (POWER)
8.00
6.00
4.00
2.00
0.00
-2.00
-4.00
-6.00
-8.00
-10.00
-12.00
-14.00
-16.00
-18.00
0.00
0.05
0.10
0.15
0.20
0.25
0.30
0.35
0.40
0.45
0.50
FREQUENCY (CYCLES PER 500 METRES)

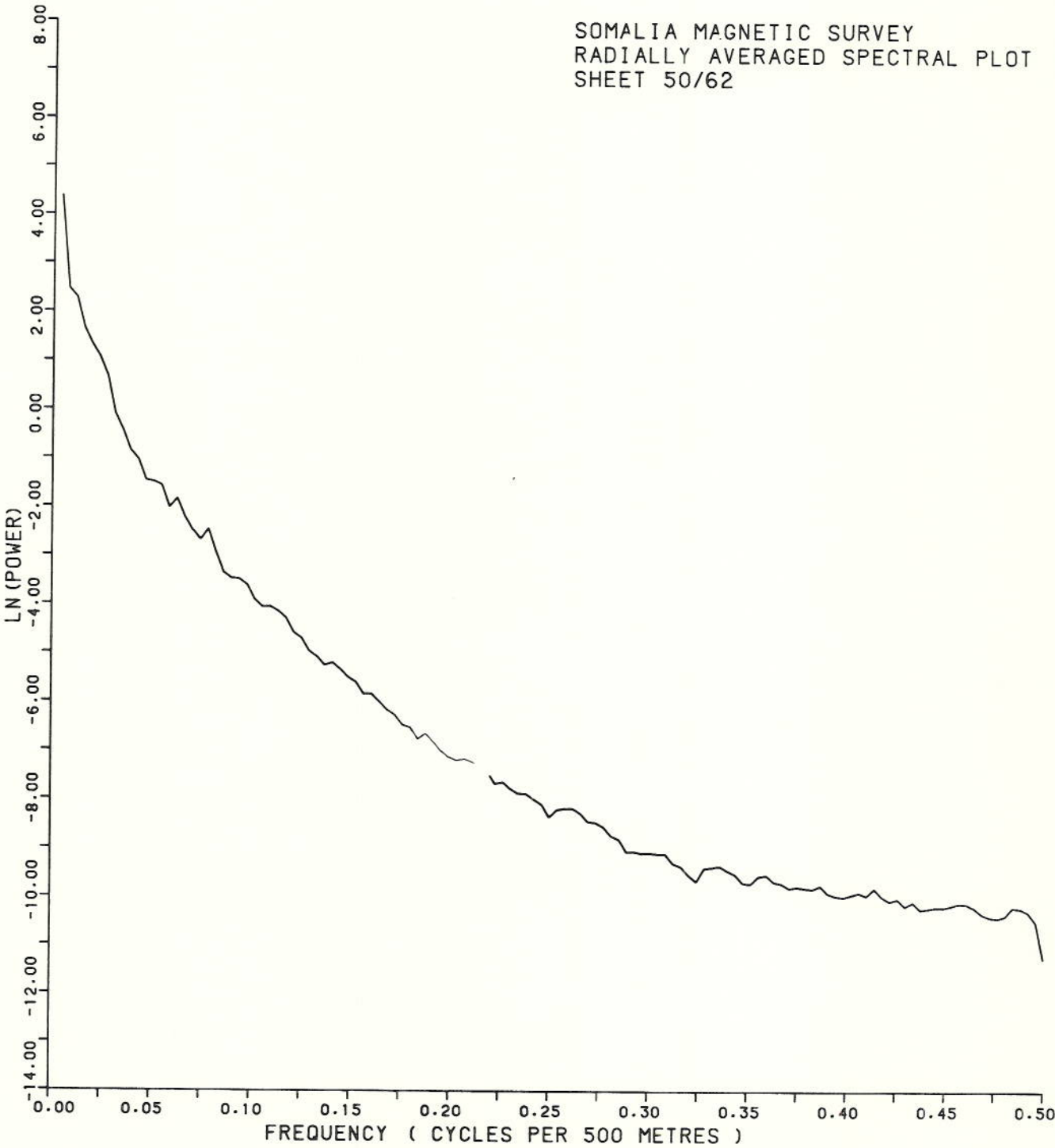
SOMALIA MAGNETIC SURVEY
RADIALLY AVERAGED SPECTRAL PLOT
SHEET 50/62
LN (POWER)
8.00
6.00
4.00
2.00
0.00
-2.00
-4.00
-6.00
-8.00
-10.00
-12.00
-14.00
0.00
0.05
0.10
0.15
0.20
0.25
0.30
0.35
0.40
0.45
0.50
FREQUENCY (CYCLES PER 500 METRES)

SOMALIA MAGNETIC SURVEY
RADIALLY AVERAGED SPECTRAL PLOT
SHEET 51/63
LN (POWER)
8.00
6.00
4.00
2.00
0.00
-2.00
-4.00
-6.00
-8.00
-10.00
-12.00
-14.00
-16.00
0.00
0.05
0.10
0.15
0.20
0.25
0.30
0.35
0.40
0.45
0.50
FREQUENCY (CYCLES PER 500 METRES)

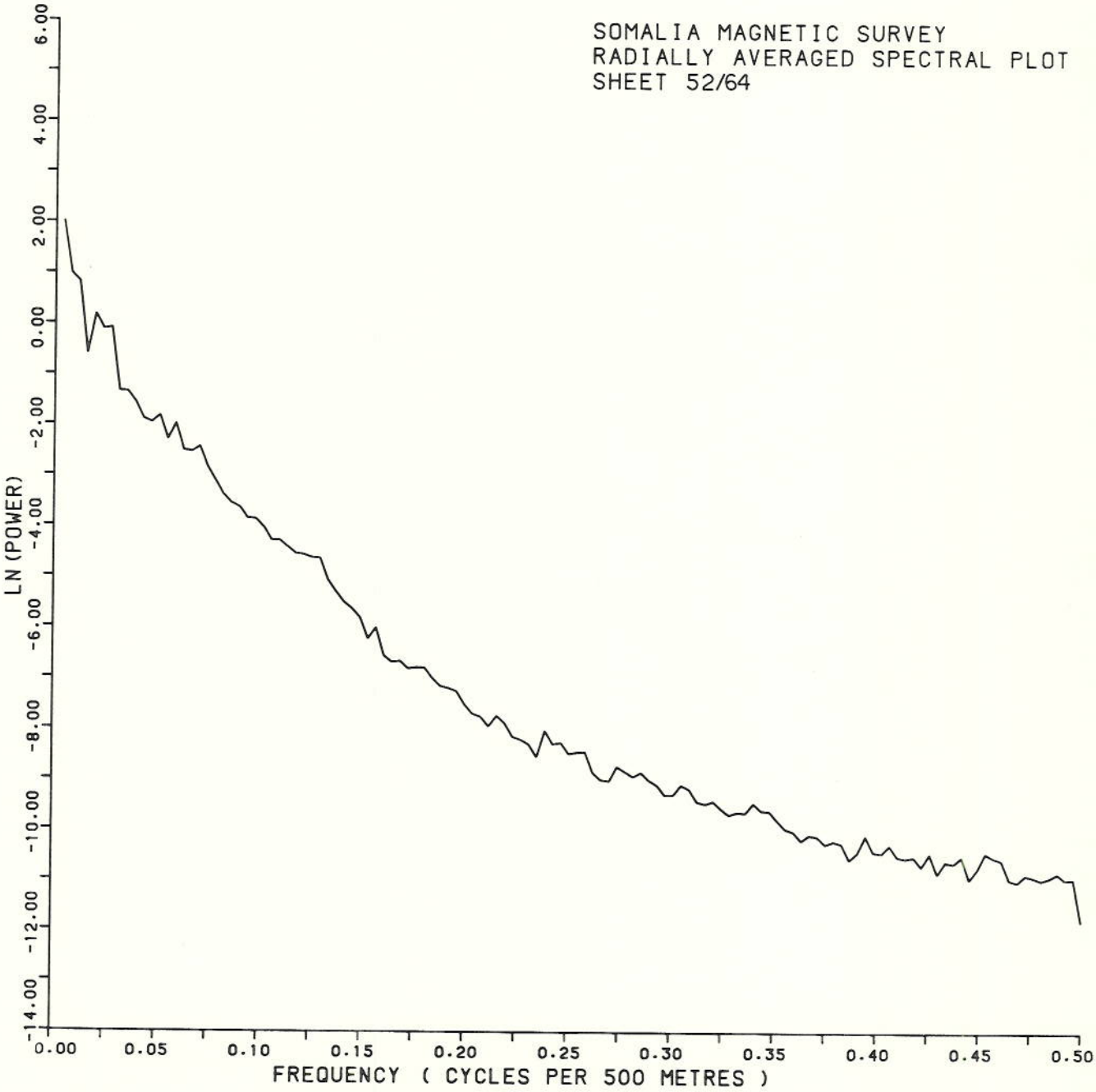
SOMALIA MAGNETIC SURVEY
RADIALLY AVERAGED SPECTRAL PLOT
SHEET 52/64
LN (POWER)
6.00
4.00
2.00
0.00
-2.00
-4.00
-6.00
-8.00
-10.00
-12.00
-14.00
0.00
0.05
0.10
0.15
0.20
0.25
0.30
0.35
0.40
0.45
0.50
FREQUENCY (CYCLES PER 500 METRES)

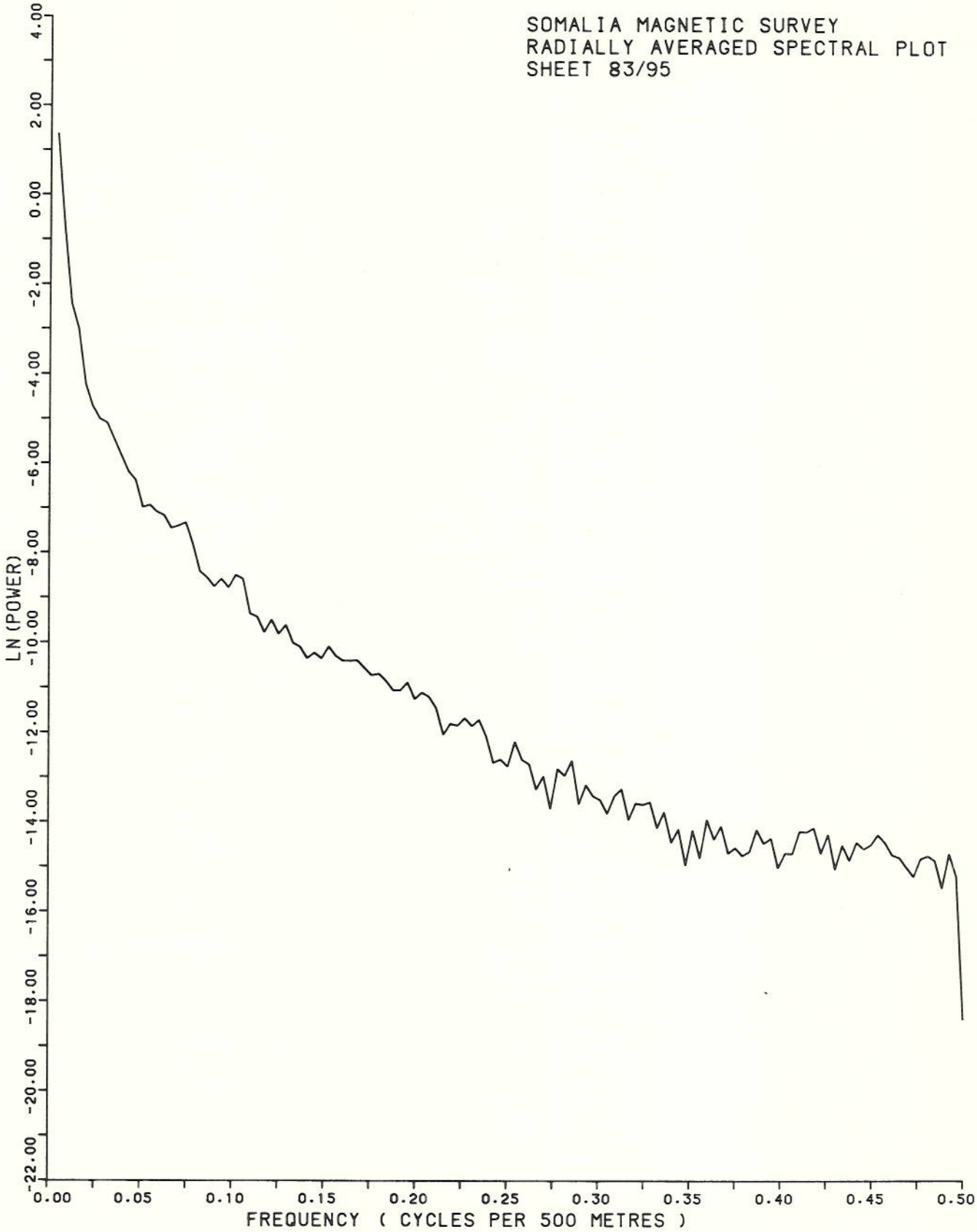
SOMALIA MAGNETIC SURVEY
RADIALLY AVERAGED SPECTRAL PLOT
SHEET 83/95
LN (POWER)
4.00
2.00
0.00
-2.00
-4.00
-6.00
-8.00
-10.00
-12.00
-14.00
-16.00
-18.00
-20.00
-22.00
0.00
0.05
0.10
0.15
0.20
0.25
0.30
0.35
0.40
0.45
0.50
FREQUENCY (CYCLES PER 500 METRES)

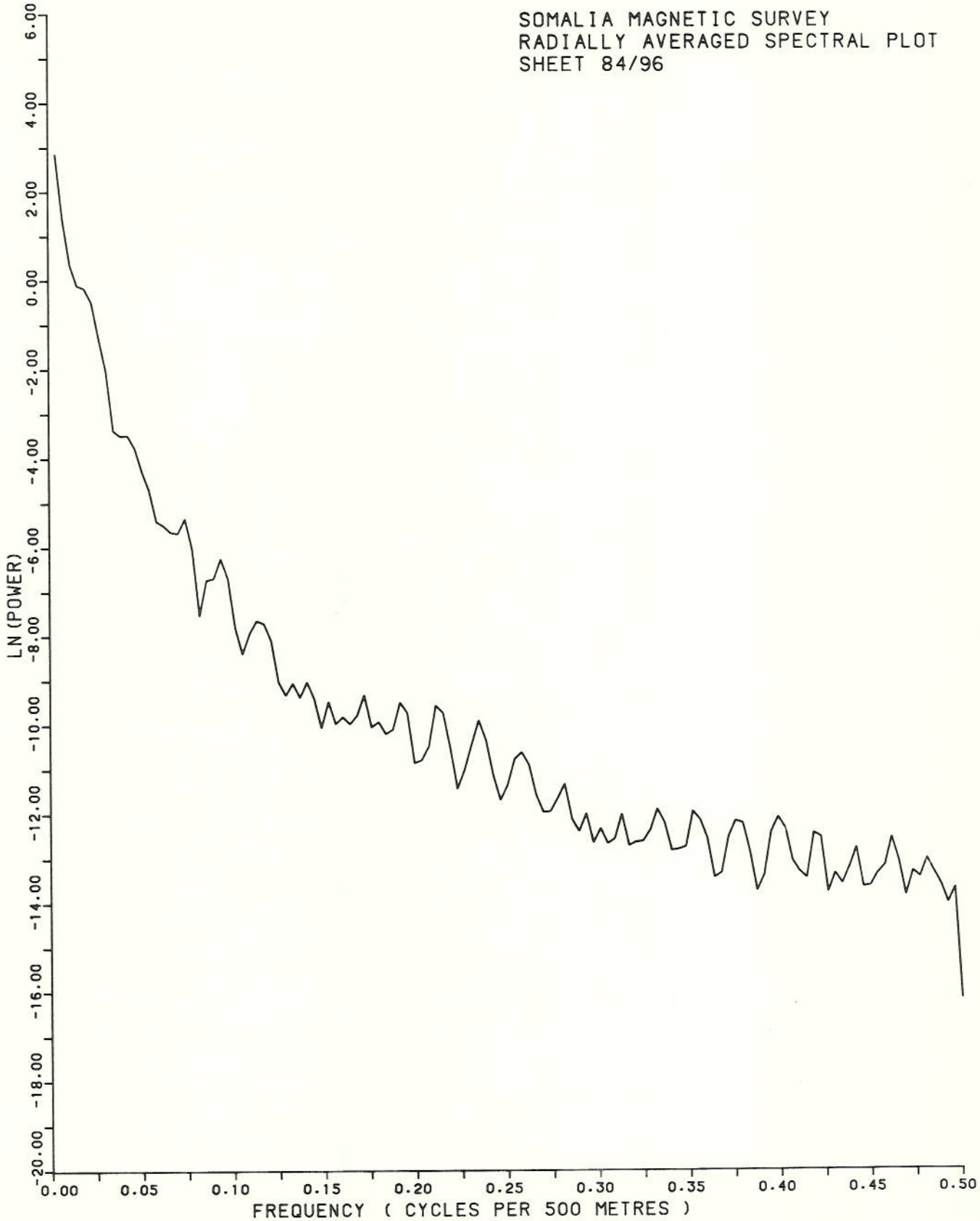
SOMALIA MAGNETIC SURVEY
RADIALLY AVERAGED SPECTRAL PLOT
SHEET 84/96
LN (POWER)
6.00
4.00
2.00
0.00
-2.00
-4.00
-6.00
-8.00
-10.00
-12.00
-14.00
-16.00
-18.00
-20.00
0.00
0.05
0.10
0.15
0.20
0.25
0.30
0.35
0.40
0.45
0.50
FREQUENCY (CYCLES PER 500 METRES)

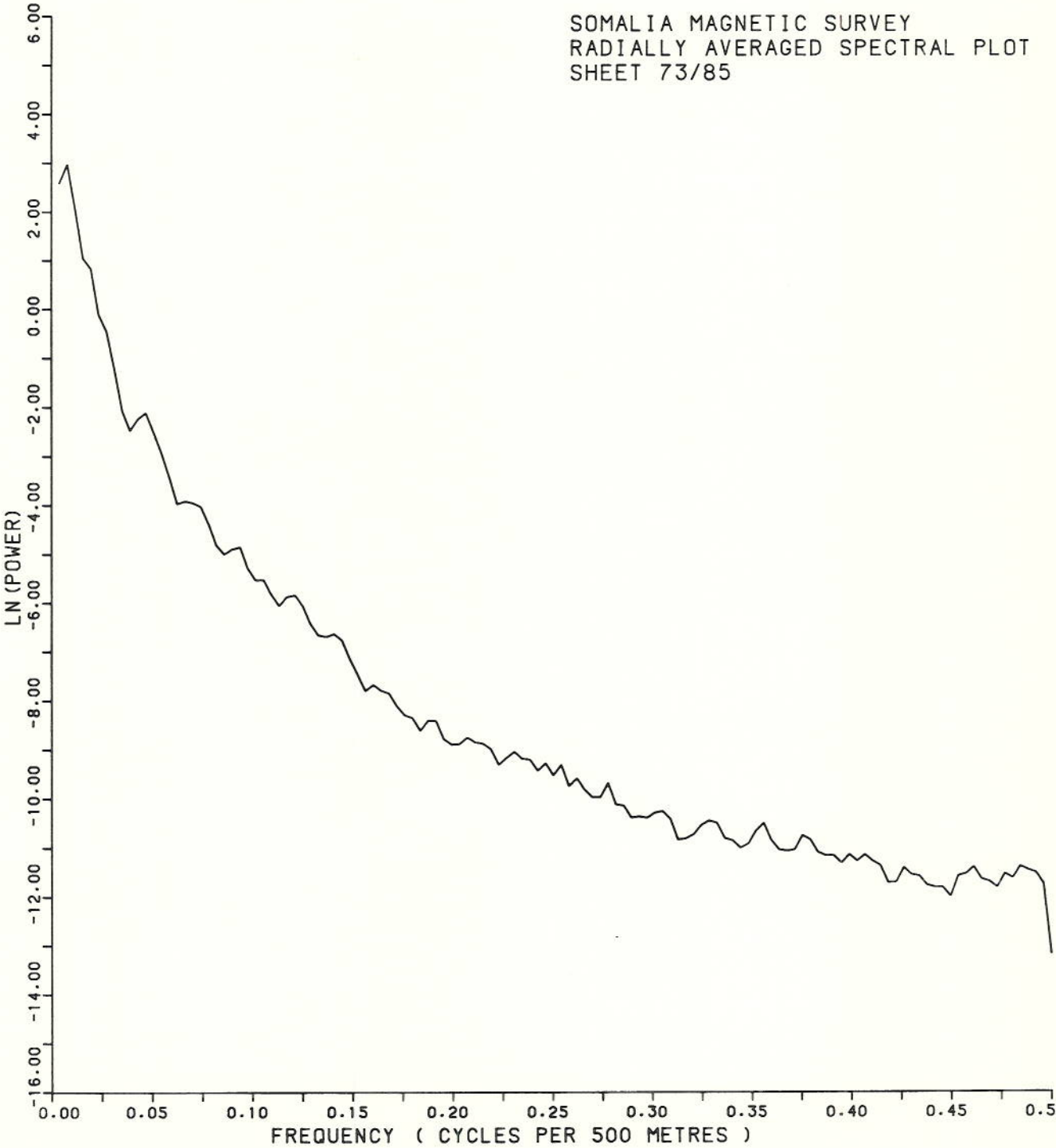
SOMALIA MAGNETIC SURVEY
RADIALLY AVERAGED SPECTRAL PLOT
SHEET 73/85
LN (POWER)
6.00
4.00
2.00
0.00
-2.00
-4.00
-6.00
-8.00
-10.00
-12.00
-14.00
-16.00
0.00
0.05
0.10
0.15
0.20
0.25
0.30
0.35
0.40
0.45
0.5
FREQUENCY (CYCLES PER 500 METRES)

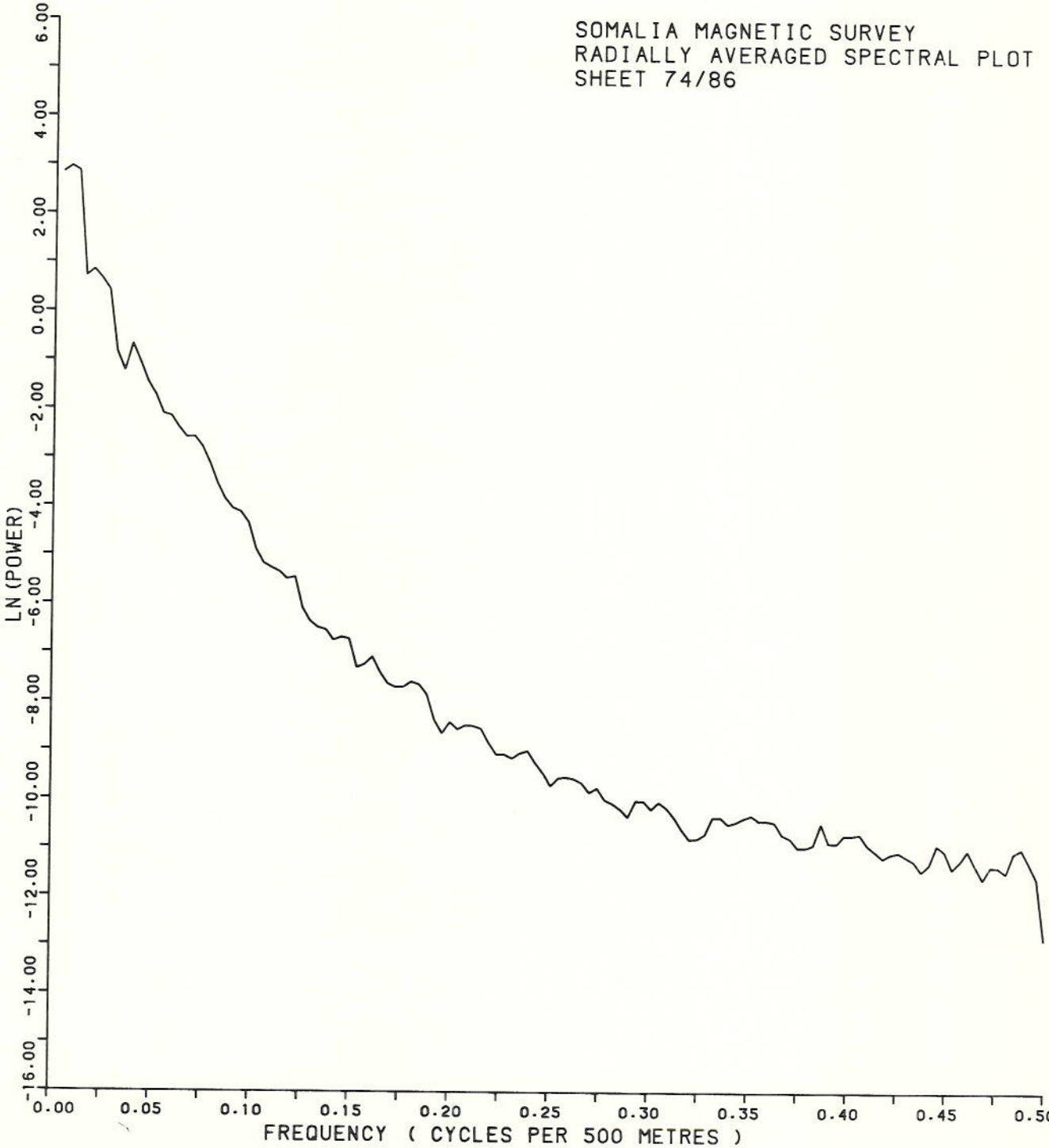
SOMALIA MAGNETIC SURVEY
RADIALLY AVERAGED SPECTRAL PLOT
SHEET 74/86
LN (POWER)
6.00
4.00
2.00
0.00
-2.00
-4.00
-6.00
-8.00
-10.00
-12.00
-14.00
-16.00
0.00
0.05
0.10
0.15
0.20
0.25
0.30
0.35
0.40
0.45
0.50
FREQUENCY (CYCLES PER 500 METRES)

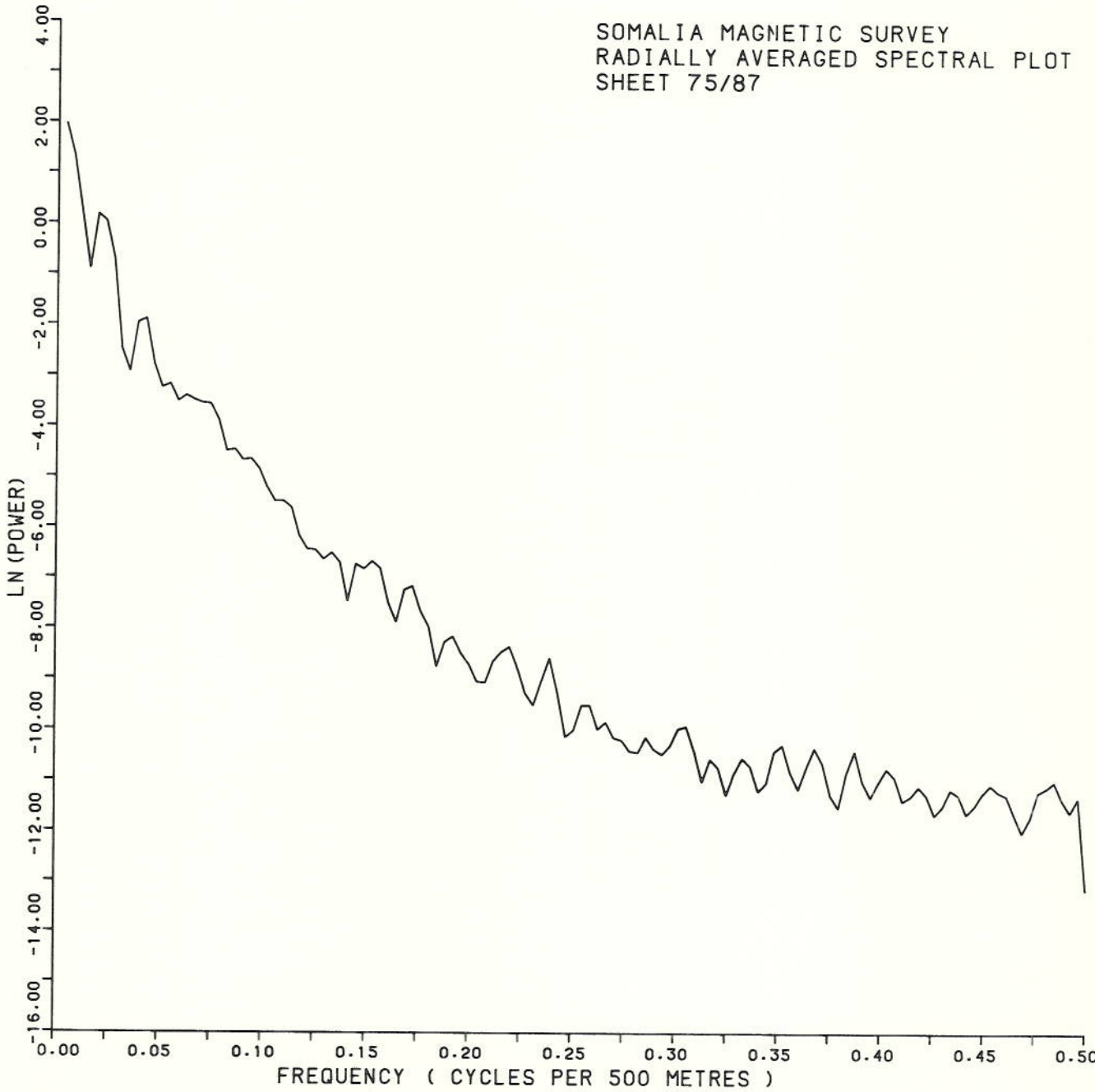
SOMALIA MAGNETIC SURVEY
RADIALLY AVERAGED SPECTRAL PLOT
SHEET 75/87
LN (POWER)
4.00
2.00
0.00
-2.00
-4.00
-6.00
-8.00
-10.00
-12.00
-14.00
-16.00
0.00
0.05
0.10
0.15
0.20
0.25
0.30
0.35
0.40
0.45
0.50
FREQUENCY (CYCLES PER 500 METRES)

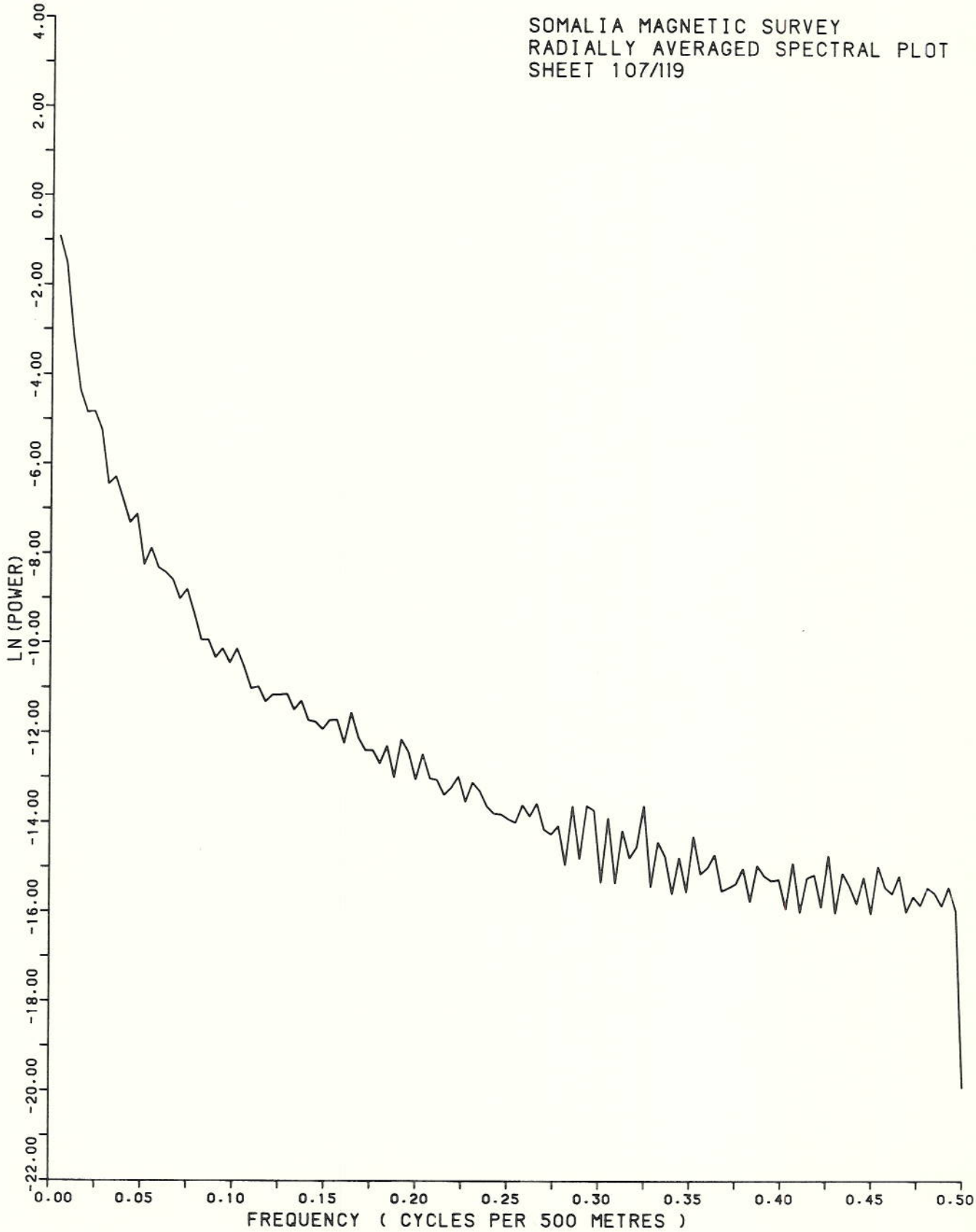
SOMALIA MAGNETIC SURVEY
RADIALLY AVERAGED SPECTRAL PLOT
SHEET 107/119
LN (POWER)
4.00
2.00
0.00
-2.00
-4.00
-6.00
-8.00
-10.00
-12.00
-14.00
-16.00
-18.00
-20.00
-22.00
0.00
0.05
0.10
0.15
0.20
0.25
0.30
0.35
0.40
0.45
0.50
FREQUENCY (CYCLES PER 500 METRES)

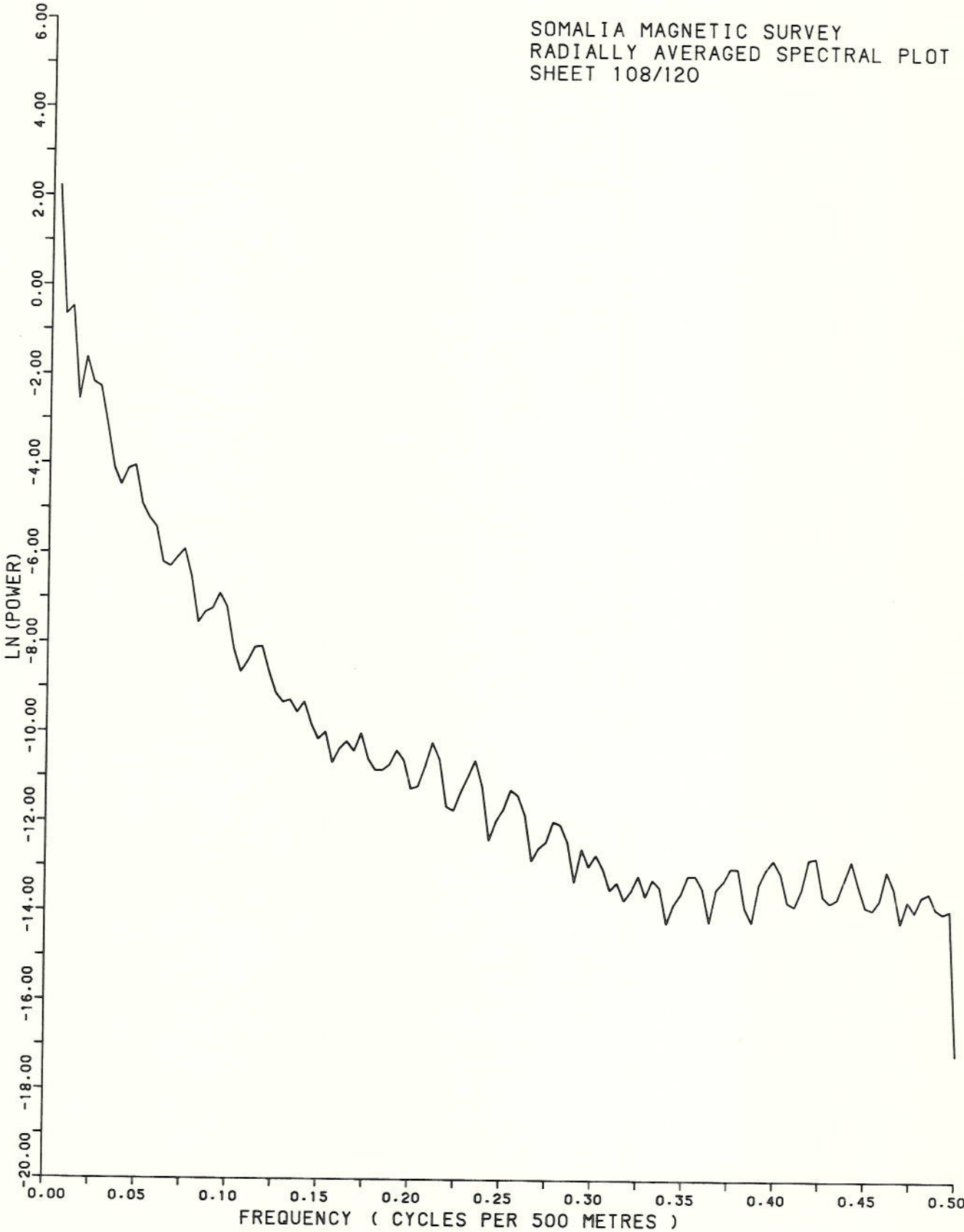
SOMALIA MAGNETIC SURVEY
RADIALLY AVERAGED SPECTRAL PLOT
SHEET 108/120
LN (POWER)
6.00
4.00
2.00
0.00
-2.00
-4.00
-6.00
-8.00
-10.00
-12.00
-14.00
-16.00
-18.00
-20.00
0.00
0.05
0.10
0.15
0.20
0.25
0.30
0.35
0.40
0.45
0.50
FREQUENCY (CYCLES PER 500 METRES)

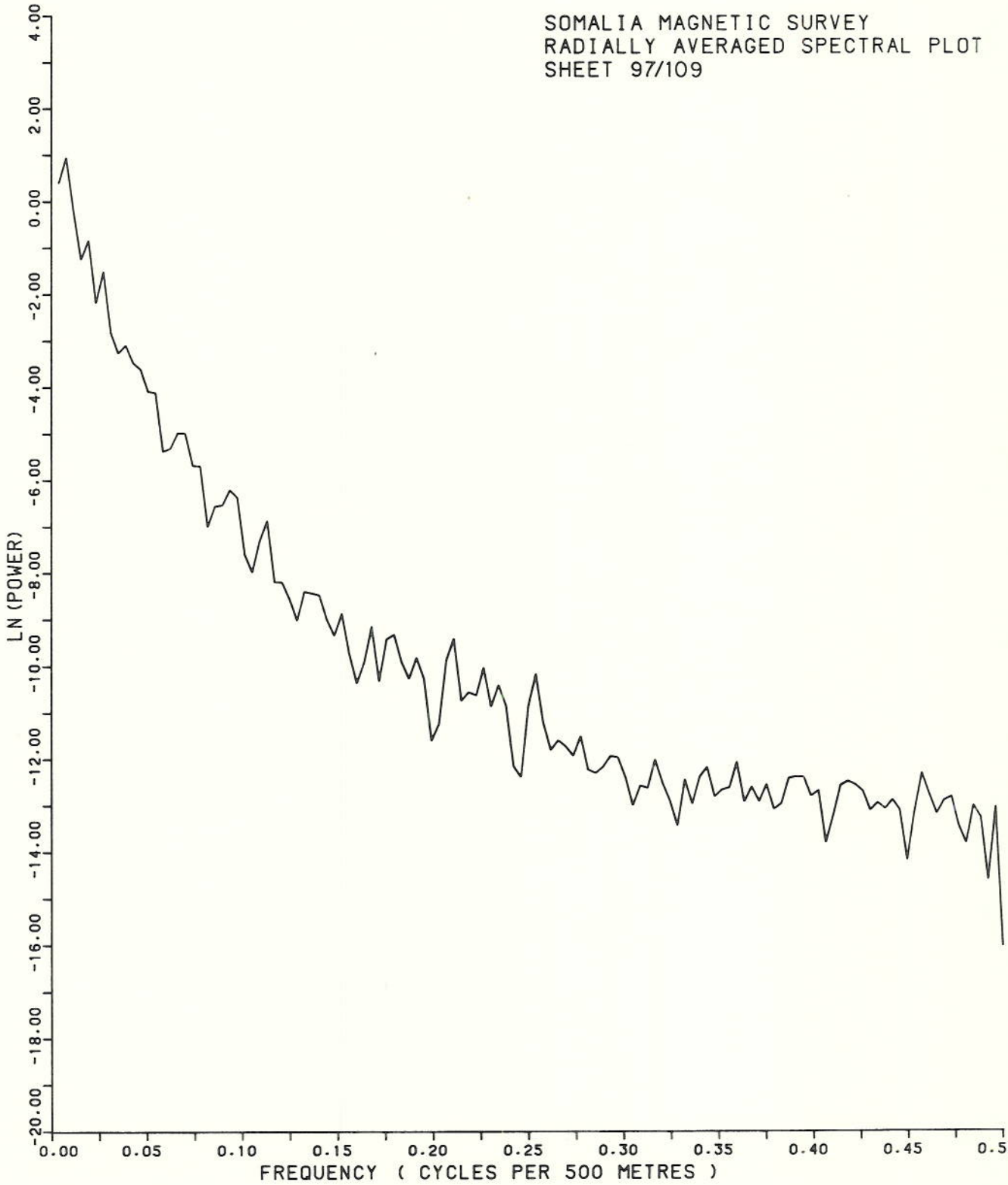
SOMALIA MAGNETIC SURVEY
RADIALLY AVERAGED SPECTRAL PLOT
SHEET 97/109
LN (POWER)
4.00
2.00
0.00
-2.00
-4.00
-6.00
-8.00
-10.00
-12.00
-14.00
-16.00
-18.00
-20.00
0.00
0.05
0.10
0.15
0.20
0.25
0.30
0.35
0.40
0.45
0.5
FREQUENCY (CYCLES PER 500 METRES)

SHEET BY SHEET CLASSIFICATION OF BLOCK 2 SPECTRAL ANALYSIS

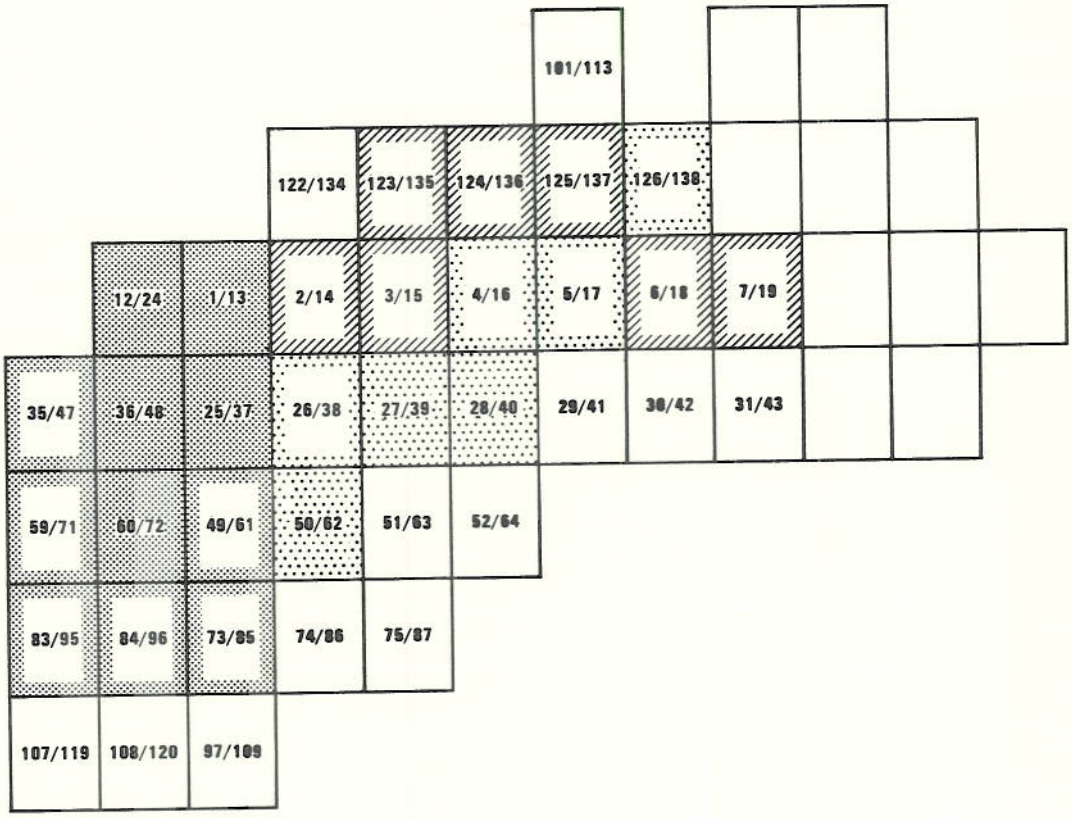

Essentially low frequency magnetics.....

Essentially medium to high frequency magnetics.....

Essentially medium frequency magnetics, superimposed upon which is the high frequency magnetic response of exposed and sub-outcrop volcanics.....
(Sheet 7/19 is in fact essentially low frequency)

Solid Symbol - Only one distinct horizon - basement, appears to exist.
Shallower spectral plot segments are indistinct

Open Symbol - At least two horizons are distinct

Note - Certain peripheral sheets are shown with no symbol.
These have been omitted from this classification due to insufficient data

A P P E N D I X 2

TABULATION OF BUR ACABA BASEMENT ROCK MAGNETIC SUSCEPTIBILITIES

Susceptibility measurements of Bur Acaba basement samples

Sample No.	Description	K (cgs units)
AAH:83:60:a:c	Banded marble	0
AAH:83:71	Quartzose feldspathic gneiss	0.00006
AAH:83:191	Amphibolite gneiss	0.00010
DR:84:84	Granite	0.00088
MJ:83:94-1	Coarse-grained granite	0.00401
MJ:83:95	Quartzite (no iron)	0
MJ:83:121	Biotite gneiss with hornblende	0.00087
MJ:83:134	Amphibolite (small sample only)	0.00022
MJ:84:001	Biotite gneiss	0.00237
MJ:84:49	Iron quartzite	0.00120
MJ:84:63	Medium grained granite	0.00050
MJ:84:097	Dolerite (dyke)	0.00010
MJ:84:200	Microgranite (dyke)	0.00037

Samples were kindly provided by the UNDP, Mogadishu.

OPERATIONS

OPERATIONS REPORT

C O N T E N T S

	PAGE
1. INTRODUCTION	1
2. PERSONNEL	2
3. FLYING OPERATIONS	3
3.1 Aircraft and Operational Base	3
3.2 Flying Specifications and Tolerances	3
3.3 Navigation	3
3.4 Survey Timing and Progress	4
Project Summary	7
4. EQUIPMENT	8
4.1 Magnetometers	8
4.1.1 Airborne Magnetometer	8
4.1.2 Diurnal Ground Magnetometer	8
4.2 Data Acquisition and Recording	8
4.2.1 Airborne Data Acquisition System	8
4.2.2 Analogue Recorders	8
4.2.3 Digital Recorders	9
4.3 Ancillary Equipment	10
4.3.1 Altimeters	10
4.3.2 Tracking Camera	10
4.4 Navigation System	10
4.4.1 Decca Doppler	10
4.4.2 Application and Operational Procedure	11
5. EQUIPMENT TESTS AND SPECIFICATIONS	12
5.1 Airborne Magnetometer	12
5.1.1 Sensitivity and Noise Envelope	12
5.1.2 Heading Test	12
5.2 Ground Magnetometer	12
5.3 Altimeters	13
5.4 Navigation System	13
6. ON-SITE COMPILATION	14

FIGURES

FIGURE		FOLLOWING PAGE
1.	N49401 HEADING EFFECT 21-5-84 (SURVEY START)	12
2.	N49401 HEADING EFFECT 19-8-84 (SURVEY COMPLETION)	12

1. INTRODUCTION

The aeromagnetic survey described in this report was carried out by Hunting Geology and Geophysics Limited on behalf of Esso Exploration Juba S.A., a division of Esso Exploration Incorporated, Houston, Texas. The survey area in Southern Somalia consisted of approximately 150,000 square kilometers over which 76,617 line kilometres of geophysical survey lines were flown. Diagrams showing the survey area and map sheet layout are included as Figures 1A and 1B of the Interpretation Report. Flying commenced on 21st May 1984 and was stopped on 25th May 1984 due to Force Majeure following anti-aircraft fire directed at the survey aircraft. Flying resumed on 24th June 1984 and was completed on 19th August 1984.

The following sections describe in detail the operational aspects of the survey.

2. PERSONNEL

Hunting Geology and Geophysics Limited provided the following personnel:-

V.C.A. Stone	Project Manager/Geophysicist (3.5.84 - 21.7.84)
S.A. Walter	Security liaison/Geophysicist (23.6.84 - 21.7.84)
S.A. Walter	Project Manager/Geophysicist (22.7.84 - 26.8.84)
B.E. Enstone	Senior Data Compiler (12.5.84 - 22.8.84)
D.G. Hampton	Data Compiler (12.5.84 - 22.8.84)
R.E. Westland	Electronics Engineer (14.5.84 - 21.8.84)
L.J.F. Cunningham	Data System Operator (23.6.84 - 22.8.84)

Aerial Surveys (Botswana) Pty Limited provided the following personnel:-

V.B.W. Cook	Chief Pilot/Navigator (22.4.84 - 21.8.84)
P.J. Clark	Pilot/Navigator (14.5.84 - 5.7.84)
C.T. Hill	Pilot/Navigator (14.5.84 - 19.7.84)
R.J. Knight	Pilot (19.7.84 - 9.8.84)
C.P. James	Pilot/Navigator (9.8.84 - 14.8.84)
R.C.T. Williams	Aircraft Engineer (14.5.84 - 21.8.84)

3. FLYING OPERATIONS

3.1 Aircraft

The survey was flown using a Cessna Titan 404, registration number N49401, crewed and supplied by Aerial Surveys Botswana. Throughout the survey this was based at Mogadishu International Airport.

3.2 Flying Specifications and Tolerances

The nominal flying specifications were as follows:-

(a) Blocks 1 and 2

Flight line direction	N147 deg - N327 deg
Flight line spacing	2 kilometres
Flight line spacing tolerance	Spacing not to vary by more than 50% of the specified spacing for a continuous distance greater than 5 km.
Tie line direction	N57 deg - N237 deg
Tie line spacing	6 kilometers. Infilling in part of Block 1 reduced this to 3 km.
Tie line spacing tolerance	Spacing not to vary by more than 1 km or 50% of the specified spacing, whichever is the lesser, for a continuous distance greater than 5 km.
Flying height	Block 1 - 1,500 feet barometric (asl). Block 2 - 3,000 feet barometric (asl).
Flying height tolerance	Not to exceed +/- 100 feet with respect to nominal flying height for a continuous distance greater than 5 km.

(b) Blocks 3 and 4 — Consisting of doublets of length between 25 and 80 km extending south from Block 2, plus two tie lines for control purposes. Flying height 3,000 feet barometric (asl).

3.3 Navigation

The navigation and flight path recovery were visual, based on topographic maps at 1:100 000 scale and assisted by a DECCA Doppler navigation system linked to a TANS computer with digitally recorded output. The Doppler system gives heading and true ground speed information to the pilot through cockpit displays whilst digitally recording x, y co-ordinates computed by the TANS computer. The

aircraft also carried a vertically mounted 35 mm tracking camera which was fired at pre-selected intervals of one to three seconds whilst on line. The tracking film was developed at the aircraft base and the flight path recovered through comparison of the film with the topographic maps. The visual fixes obtained from the tracking film were used in conjunction with the continuous Doppler-recorded flight path to obtain a corrected final flight path which, between those visual fixes obtained at 25 km interval or less, was accurate to well within 100 m.

3.4 Survey Timing and Progress

The following is a diary of events:-

22nd April 1984	Chief pilot V. Cook arrived in Mogadishu as Advance Man.
3rd May	Project Manager/Geophysicist V. Stone arrived in Mogadishu to assist Advance Man.
12th May	Data Compilers B. Enstone and D. Hampton arrived in Mogadishu.
14th May	Survey aircraft N49401 arrived in Mogadishu with crew P. Clark (pilot), C. Hill (pilot), R. Williams (aircraft engineer) and R. Westland (electronics engineer).
15th May	Aircraft, equipment and consumables cleared customs. Problem with water in local AVGAS supply prevented test flight.
16th May	Resolved problem of water in fuel. Test flight performed to assess heading effect and to compensate if necessary.
17th-19th May	Continued difficulty in reducing heading effect determined as being due to imbalance in aircraft magnetic configuration caused by a faulty alternator. A replacement was ordered via Nairobi. Alternator repaired on the 19th May and compensation of magnetometer satisfactorily completed. No flying on the 19th May due to reported Ethiopian MiG fighter incursion.
20th May	No production. Aircraft flown to various military bases within the survey area to ensure familiarity of military personnel with the Hunting operation.
21st-24th May	Production.
25th May	Production curtailed by anti-aircraft fire directed at the survey aircraft from the Somali military base near Bulo Berti. Following consultation with Esso's

	Somalia Manager F. Kroll and Hunting Head Office, Force Majeure was declared.
26th May-2nd June	Force Majeure. Further consultations with F. Kroll and also with Military authorities, American and British Embassies. Instructed by Hunting Head Office to temporarily de-mobilize aircraft to Nairobi and remaining personnel to return to the UK, except for P. Clark who remained in Mogadishu to monitor the security situation. Aircraft departed on the 1st June, remaining personnel 3rd June.
3rd-20th June	Force Majeure continued.
21st June	Force Majeure ended. Survey aircraft returned to Mogadishu.
22nd-23rd June	Remaining personnel returned to Mogadishu. Two additional personnel also arrived: S. Walter (geophysicist/security officer) and L. Cunningham (aircraft data system operator).
24th-29th June	Production.
30th June	Local security liaison officer seconded to the survey operation from the Somali airforce, advised against flying on account of expected Ethiopian airforce activity.
1st-5th July	No flying due to engine trouble. Spare arrived 5th July and repair effected same day. P. Clark (pilot) left the project 5th July.
6th-11th July	Production.
12th July	No production due to magnetic storm followed by magnetometer problem.
13th-14th July	Effectively no production due to magnetic storm.
15th-17th July	Production.
18th July	No production due to bad weather.
19th July	No flying due to change of aircrew. C. Hill (pilot) left the project.
20th-27th July	Production flying. V. Stone left the project on 22nd July and responsibilities of Project Manager assumed by S. Walter.
28th July	Production flying. Equipment operator L. Cunningham reported seeing flashes/smoke from the ground near Garba Harre at 1115 hours. Sortie continued with revised flight plan. Investigations with military failed to confirm any incident.

29th July	Aircrew rest day.
30th-31st July	Production.
1st August	No production due to magnetic storm.
2nd August	Production.
3rd August	No production for security reasons. Decision taken not to fly on Fridays in future on advice of security liaison officer and confirmation of incidents on previous two Fridays.
4th-9th August	Production, including reflies.
10th August	No flying for security reasons. Ethiopian MiG incursion over Borama (Northern Somalia).
11th August	Part production. Sortie aborted at 1040 hours when anti-aircraft batteries at Baidoa trained on survey aircraft. Subsequently military claimed that any anti-aircraft battery activity was only a training exercise.
12th-16th August	Production.
17th August	No flying for security reasons.
18th August	Production.
19th August	Final production sortie. Heading test flown.
20th August	Checking of navigation data.
21st August	Survey aircraft and aircrew departed Mogadishu for base via Nairobi.
22nd August	B. Enstone, D. Hampton and L. Cunningham left Mogadishu.
23rd-25th August	S. Walter remained in Mogadishu to clear final administrative matters, re-export of equipment, etc.
26th August	S. Walter left Mogadishu.

PROJECT SUMMARY

Aircraft days in Somalia	81
Days of productive flying	45
Days lost due to:-	
(a) Aircraft transits, customs delays aircrew changeover/rest days, awaiting permission to de-mobilize pending final navigation check.	10
(b) Tests	1
(c) Magnetic storms	3
(d) Bad weather	1
(e) Equipment/aircraft problems	8
(f) Security problems	6
(g) Force Majeure while aircraft in Somalia (Force Majeure total - 27 days)	7
Total number of aircraft sorties	52
Final line kilometres production	76,617
Mean data acquisition rate for productive days	1,700 lkm per day
Maximum data acquisition rate achieved during course of one day	2,276 lkm
Number of days in which production exceeded 2000 lkm	12 days

4. EQUIPMENT

4.1 Magnetometers

4.1.1 Airborne Magnetometer

This was a Geometrics G813 proton magnetometer which sampled at one second interval. The sensitivity at one second was 0.05 nT. The sensor head and preamplifier were installed in a stinger projecting from the rear of the aircraft. The magnetometer output was recorded digitally and filtered to provide a continuous analogue record.

4.1.2 Diurnal Ground Magnetometer

The ground magnetometer was situated in the grounds of the Taleh Hotel, Mogadishu. Although affected by cultural noise, the use of this site was necessary due to the lack of security elsewhere in Mogadishu. This magnetometer was a rubidium vapour high sensitivity type (0.01 nT) made by Littlemore of Oxford and adapted by Hunting. A second ground magnetometer, located at Afgoi (26 km NW of Mogadishu) was used to obtain a simultaneous diurnal record over the period of one afternoon for comparison purposes. (See Section 5.2).

The ground station was operated continuously throughout the survey period. Analogue records were obtained on a 24 hour basis with digital data being recorded during production sorties.

4.2 Data Acquisition and Recording

4.2.1 Airborne Data Acquisition System

A Geometrics G704 data acquisition system was used to synchronise all recorder fiducial pens, fire the tracking camera, convert analogue data to digital and to sequence the resulting information into a format suitable for digital recording.

The G704 contains a very stable quartz clock which was set to zero at the start of each day's flying. The system was synchronised with the counter mounted in the tracking camera and with a repeater counter in the aircraft cockpit installed for the benefit of the navigator.

4.2.2 Analogue Recorders

One Bryans chart recorder was installed onboard the aircraft to display the output from the magnetometer (at two scales), barometric altimeter, radio altimeter and time fiducials. Full scale deflections (FSD's) and chart speeds were as follows:-

(a) 10 inch chart width, Doppler controlled chart speed to produce analogue records at 1:50,000 scale.
(b) Magnetometer trace, green pen 10 nT FSD and black pen 100 nT FSD over 10 inch width of chart, equivalent to 1 nT/inch and 10 nT/inch respectively.

(c) Barometric altimeter trace, blue pen 500-0-500 feet FSD.
(d) Radar altimeter trace, red pen 0-1000 metres FSD.
(e) Time fiducials every 10 seconds along the chart margin.

An APP48E2 printer was used to produce a numerical printout of Doppler data.

The ground magnetometer output was displayed by a Sekonic single channel chart recorder; the speed was 8 mm/min and the chart scale 10 nT/FSD (1 nT/cm).

4.2.3 Digital Recorders

The information from the G704 airborne data acquisition system was recorded digitally by a Kennedy 7 track tape recorder and a Cristie CS-5 cassette recorder for Doppler data. The ground magnetometer station utilised a second Cristie CS-5 cassette recorder. The data were recorded in serial fashion and formatted as follows:-

Kennedy 7 track - Airborne Magnetometer and Altimeter Data

(Char = character)

Chars 1-3 Day No.	**Chars 4-8** Time in elapsed seconds from midnight	**Char 9** Special character	**Char 10** Sign for radar altimeter	**Char 11-14** Radar altimeter in metres
Char 15 Barometric altimeter polarity	**Char 16-19** Barometric altimeter deviation from datum in feet	**Char 20-26** Magnetic field in 1/100 nT units	**Char 27-36** Doppler info. in 2's complement octal format	

Cristie 1 - Doppler Data

Char 1 'D' for Day No.	**Chars 2-4** Day No.	**Char 5** Aircraft label = 1	**Char 6** 'space'
Char 7 T for time	**Chars 8-9** Hours	**Chars 10-11** Minutes	**Chars 12-13** Seconds
Chars 14-15 'space'	**Char 16** 'N' for northing	**Chars 17-21** Northing in 10 metre units	**Char 22** 'E' for easting

Chars 23-27	Char 28	Char 29
Easting in 10 metre units	Carriage return	Line feed

Cristie 2 - Ground Magnetometer Data

Char 1-3	Char 4	Chars 5-9	Chars 10-16
Day No.	Line feed	Time in seconds elapsed from midnight	Magnetic field in 1/100 nT units

4.3 Ancillary Equipment

4.3.1 Altimeters

The aircraft carried a TRT AHV8 radar altimeter to record the actual ground clearance. A Rosemount barometric altimeter enabled the pilot to maintain the barometric flying height to within +/- 100 feet of the nominal 1500 feet for Block 1, and 3000 feet for Block 2 (and reconnaissance Blocks 3 and 4). Both outputs were recorded digitally and in analogue form.

4.3.2 Tracking Camera

The aircraft's flight track was recorded using a Vinten Mk II 35 mm half-frame tracking camera mounted vertically in the body of the aircraft. The camera was triggered by the G704 data acquisition system and each frame displayed a camera fiducial number related to that of the acquisition system master clock. The firing interval was selected between one and three seconds depending on ground clearance so as to balance film economy with the requirement for adequate forward overlap between successive frames to ensure continuous coverage of the flight track.

4.4 Navigation System

4.4.1 Decca Doppler

The survey aircraft was equipped with a Decca Doppler digital system, controlled through a TANS computer operated by the navigator. The Doppler system requires ground checks to maintain its on-line performance and these were provided through visual updates from the 1:100 000 scale topographic maps used by the navigator. Post-flight location of these ground points was achieved by flight path plotting from the 35 mm film. The outputs from the Doppler system included:-

(a) Digital cassette record at intervals of 1 second of relative UTM co-ordinates together with fiducial time.
(b) Numerical print-out at 10 second intervals of relative UTM co-ordinates together with fiducial time.

Recovery of the flight path was onto 1:100 000 scale topographic maps, initially by plotting recognisable control points from the 35 mm camera. Points intermediate to these were recovered using a suitably programmed HP85 field computer which reconstituted the flight line at an approximate scale of 1:100 000 from the digital Doppler data. This was used as a direct overlay to the visual control points on the topographic maps.

4.4.2 Application and Operational Procedure

After takeoff, the Doppler system is switched on, and the TANS computer initialised by punching in a "grid lock" over a point of known UTM co-ordinates which can be easily recognised visually. Initialisation allows the system to compute relative positional data on an elapsed time basis. A system check is carried out after initialisation.

At the beginning of each line, the theoretical bearing (accurate to 0.1 degrees), the start position of the line and the distance to be flown to the end of the line are entered into the system. In so doing, the navigator can call up on the computer display UTM position, cross track, speed and drift, at any point along the line and thus rectify gross errors of navigation. A left/right meter fed by the Doppler system indicates to the pilot deviations from the theoretical bearing so that minor corrective action can be taken immediately without recourse to computer interrogation.

5. EQUIPMENT TESTS AND SPECIFICATIONS

5.1 Airborne Magnetometer

5.1.1 Sensitivity and Noise Envelope

The Geometrics G813 magnetometer has a sensitivity of 0.05nT at one second sampling. Extreme turbulence was encountered on a number of occasions during the course of the survey and consequently, although the magnetometer noise envelope was usually not more than 0.5 nT, in the worst turbulence it momentarily exceeded 1.0 nT. Interpretation has not been affected by this level of noise due (i) to its insignificant amplitude with respect to anomalies of interest and (ii) to its incoherence across adjacent flight-lines.

5.1.2 Heading Test

Figure 1 shows the result of the heading test performed prior to production flying. This was performed by choosing a point within a relatively magnetically flat area, over which the survey aircraft was flown on the following bearings: N, SW, E, NW, S, NE, W, SE and N. Corrections for diurnal and small lateral gradients showed a peak to trough heading effect of 1.5 nT. Figure 2 shows the result of the heading test performed over the same point at the end of productive flying. The amplitude of the heading effect on this occasion was 3.7 nT.

5.2 Ground Magnetometer

The Littlemore/Hunting rubidium ground magnetometer has a sensitivity of 0.01 nT and consequently enabled any significant diurnal effect to be readily detected and recorded. The diurnal variation was defined as excessive when the variations occurred repeatedly for 5 minutes or more and showed amplitudes in excess of 3 nT over a 3 minute chord. Where the diurnal was found to exceed this tolerance, the decision to re-fly was made according to a sensible assessment of the (geologic) magnetic nature of the line in question. Some reflies were necessary and three days production were lost due to magnetic storms.

A second ground magnetometer station was set up at Afgoi (26 km NW of Mogadishu) in order to obtain a simultaneous diurnal record over a period of one afternoon. The purpose of this was to check the degree of cultural noise and/or enhanced magnetotelluric coastal effect at the Mogadishu base station. Correlation of the two simultaneous records was in general very good. An impending magnetic disturbance (that is, approaching the tolerance of variation allowed) showed virtually equal response. Fifteen percent or so of the lesser variations (above the background noise) were however somewhat disparate. The Afgoi station exhibited little of the very high frequency background noise observed at the Mogadishu site.

HEADING TEST - 21st MAY 1984 (SURVEY START)

SURVEY AIRCRAFT N49401

HEADING EFFECT = 1·5 nT PEAK TO TROUGH

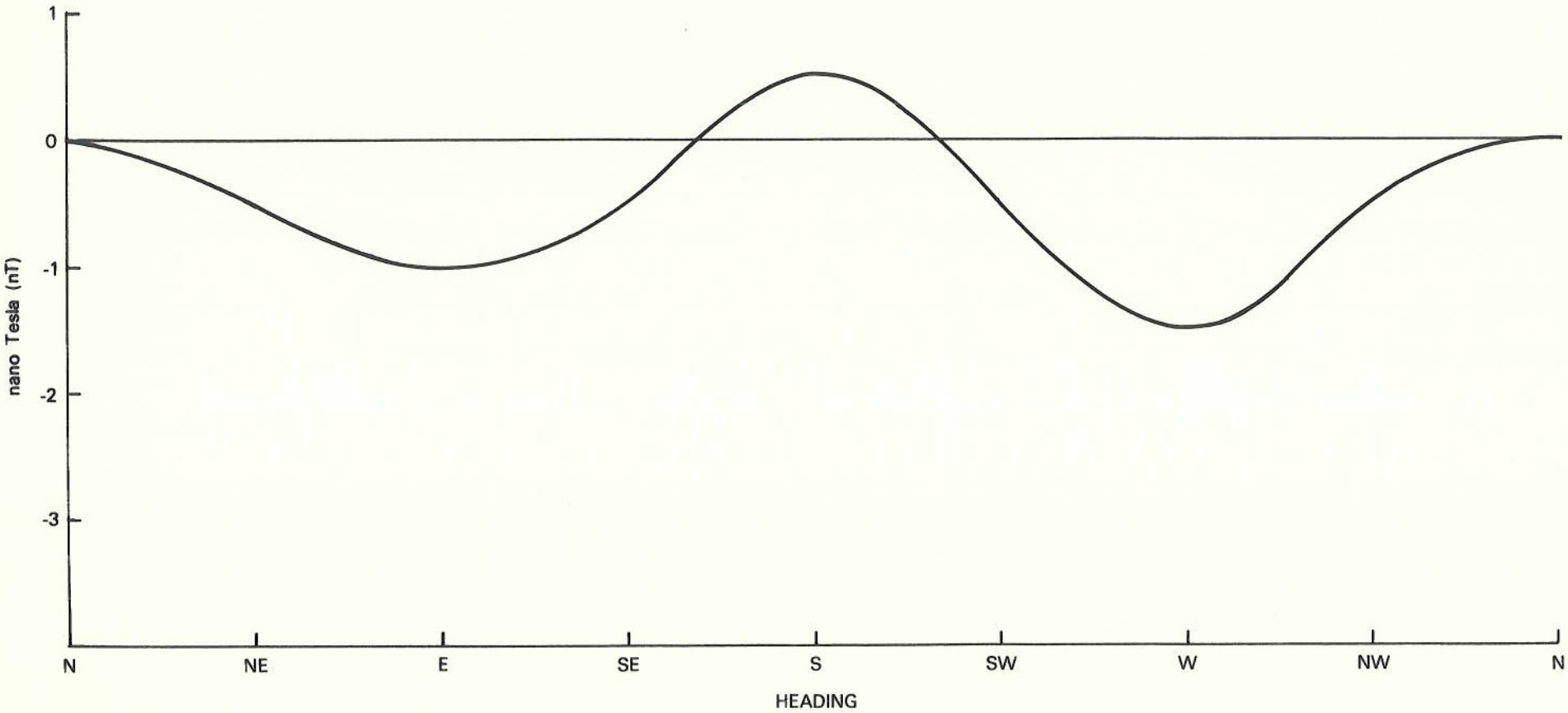

FIGURE 1

HEADING TEST - 19th AUGUST 1984 (SURVEY COMPLETION)

SURVEY AIRCRAFT N49401

HEADING EFFECT = 3·7 nT PEAK TO TROUGH

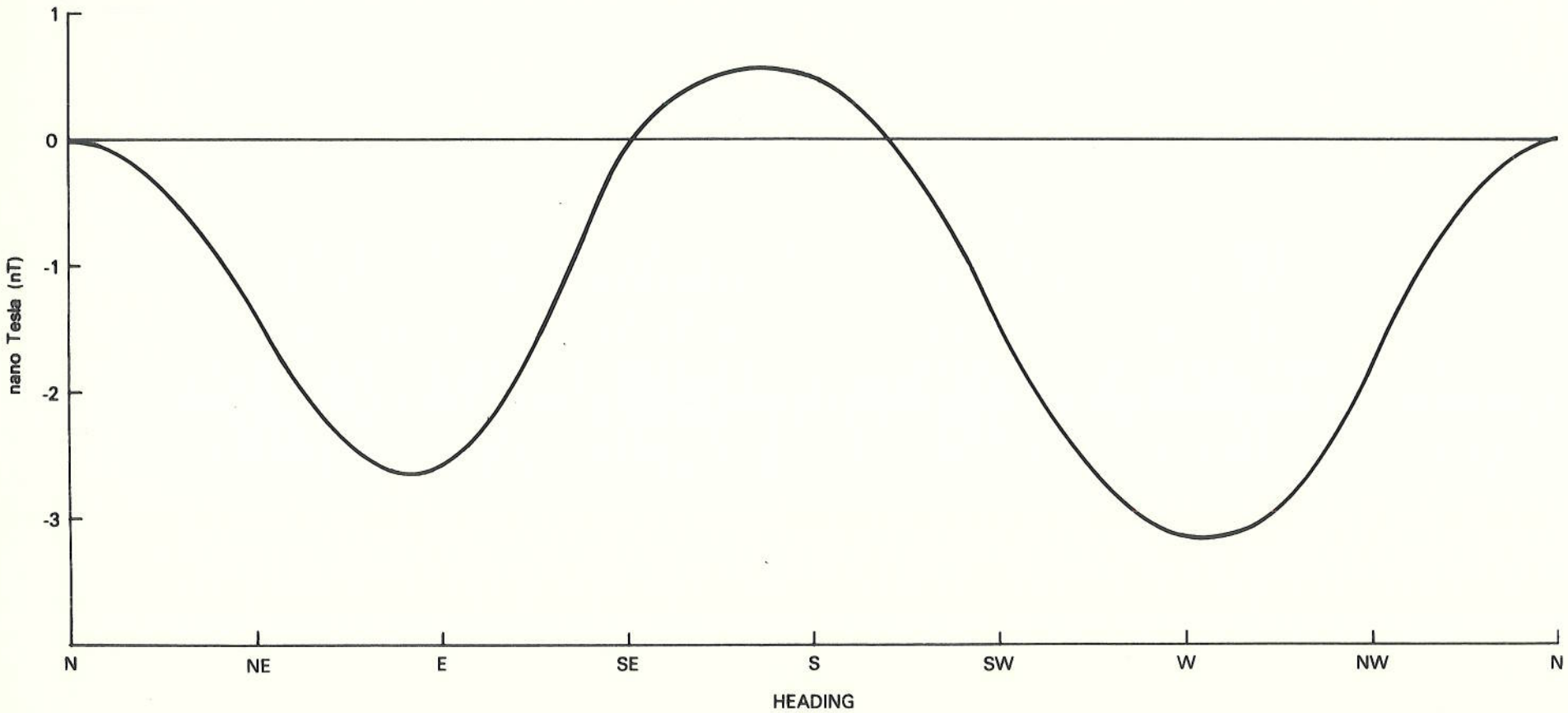

FIGURE 2

5.3 Altimeters

The barometric altimeter was calibrated in conjunction with the radar altimeter each day over the runway at Mogadishu airport or offshore.

5.4 Navigation System

This was calibrated as per Section 4.4.2.

6. ON-SITE DATA COMPILATION

A data compilation office and photographic dark room were set up at the operational base in Mogadishu. Here the 35 mm tracking film was developed and the flight path recovered onto 1:100 000 scale topographic maps as described in Section 4.4.1. The flight path plots were checked for correct tolerances. To enable flight path recovery in regions where insufficient detail existed on the topographic maps, matching of appropriate tracking films enabled accurate determinations of appropriate flight-line and tie-line intersections.

P R O C E S S I N G

PROCESSING REPORT

C O N T E N T S

		PAGE
1.	INTRODUCTION	1
2.	FLIGHT PATH RECOVERY	1
3.	COMPILATION AND PROCESSING OF AEROMAGNETIC DATA	1
	3.1 Data Editing	1
	3.2 Network Adjustment	2
	3.3 IGRF Subtraction	2
	3.4 Total Magnetic Intensity Maps	2
	3.5 Multi-Channel Profiles	2
	3.6 Spectral Analysis and Matched Filtering	3
	3.7 Upward Continuation	3
	3.8 Archiving of Data	3
4.	ITEMS DELIVERED TO CLIENT	4

FIGURES

		FOLLOWING PAGE
1.	OUTLINE FLOWCHART FOR PROCESSING OF AEROMAGNETIC DATA	1

APPENDICES

APPENDIX 1: ARCHIVE TAPE FORMAT

APPENDIX 2: LINE INDEX

1. INTRODUCTION

Hunting Geology and Geophysics Ltd process airborne geophysical data within their own computer department using a Perkin-Elmer 3240 32-bit minicomputer configured with 7 and 9 track tape drives and 900 Mbytes of disc storage. Peripheral devices include VDU terminals, Calcomp plotters and digitisers, Versatec colour electrostatic plotter, and Tektronix and HP graphics terminals.

2. FLIGHT PATH RECOVERY

On receipt of flight path overlays at Hunting's head office they were digitised. This created files on the computer which were checked for errors,edited and loaded into a database ready for processing and merging with the geophysical data.

3. COMPILATION AND PROCESSING OF AEROMAGNETIC DATA

The main stages in compiling the aeromagnetic data (excluding special processing) are shown in the flowchart which forms Figure 1. Field data (airborne magnetics, ground diurnal monitor and Doppler data) were recorded on 7 track tapes and cassettes and these were read, edited and loaded into a specially created database. The following summarises the processing.

3.1 Data Editing

Magnetic data were checked and edited for gaps, noise spikes and any abnormal data. Data for Sortie 1 contained unidirectional spikes caused by avionic effects. Data for all the lines of Sortie 1 were hand smoothed, digitised and loaded into the database.The digitised data were filtered lightly to remove any noise introduced during digitising.The filter used was of Gaussian type with a cutoff wavelength of 3 data spacings (approx 200 metres) All the aeromagnetic data for Block 1 were filtered with a Gaussian filter designed to filter out features up to 2 nT in amplitude and up to 6 data spacings wavelength (approx 400 metres). The purpose of this filter was to remove unwanted noise due to turbulence. Similarly aeromagnetic data for Blocks 2, 3 and 4 were filtered with a Gaussian filter designed to remove features up to 2 nT and up to 18 data spacings in wavelength.

Ground station data were edited and checked for any spurious data. Ground station data were acquired at 4 second intervals. During processing these data were interpolated to 1 second values to conform with the airborne data. Edited ground data without filtering were shown on the multi-channel profiles and included on the archive tape.

FIGURE 1

COMPUTER PROCESSING AEROMAGNETIC DATA OUTLINE FLOWCHART

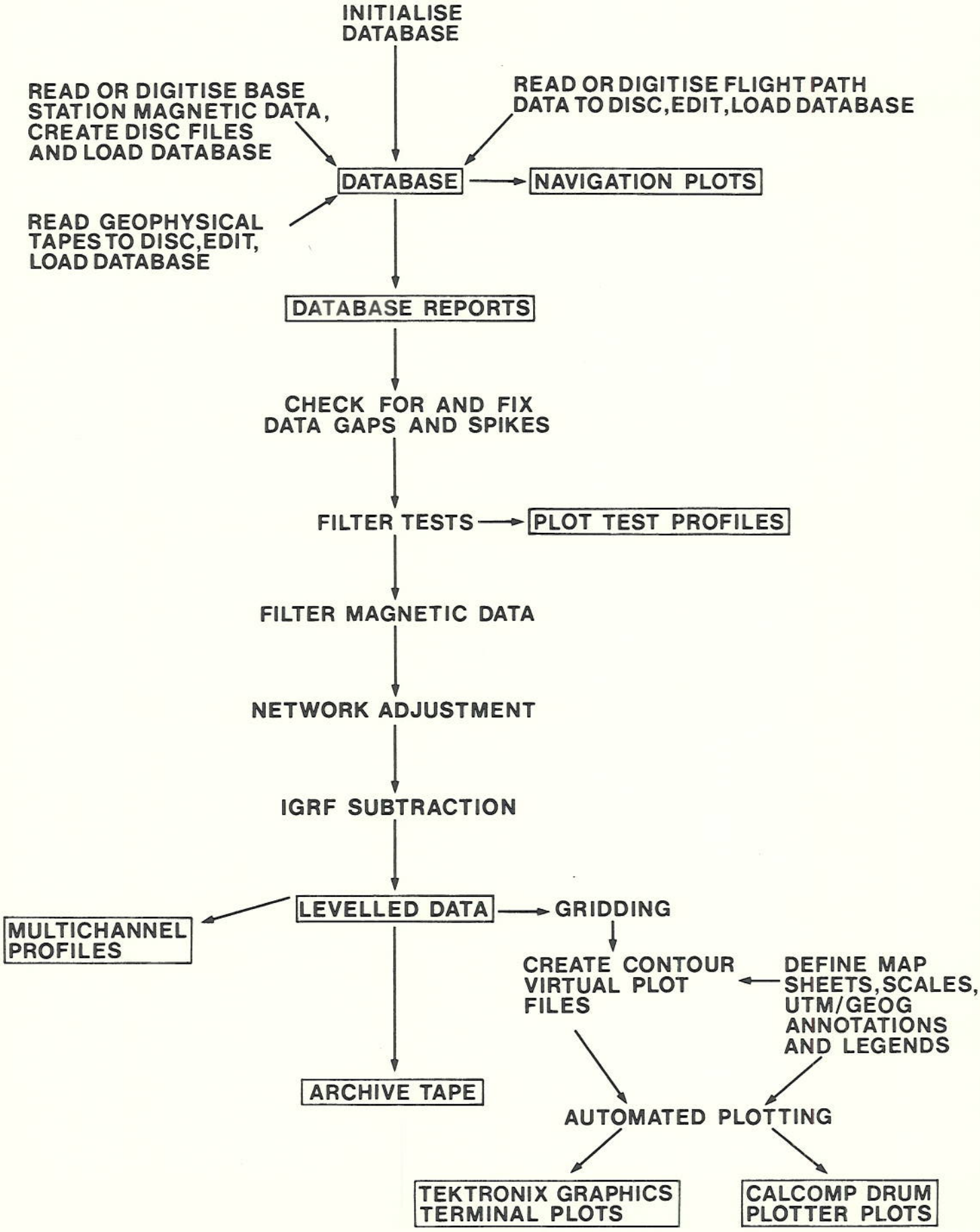

3.2 Network Adjustment

Intersection positions between flight lines and tie lines were computed to form a cross-over file, and the magnetic data at and around the intersections extracted to form a levelling file. The levelling process calculates corrections to minimise the differences between tie line (TL) and flight line (FL) magnetic values at the intersections by an iterative procedure of polynomial fitting to the FL-TL differences. Further corrections were computed by making small adjustments to the computed intersection positions.Finally the FL-TL differences were reduced to zero and the corrections applied to the complete set of magnetic data to produce levelled data.

3.3 IGRF Subtraction

The Earth's regional magnetic field was removed by using the International Geomagnetic Reference Field 1980 (IGRF 1980) corrections for epoch 1984.5 and 457 metres above sea level. (for Block 1) and for 914 metres above sea level for Blocks 2, 3 and 4. A constant of 5000 nT was added to all the data to ensure that all the data were conveniently positive.

3.4 Total Magnetic Intensity Maps

The levelled Total Magnetic Intensity data were gridded and computer contoured to produce preliminary maps at 1:500 000 scale, in biro on paper, and final maps at 1:100 000 scale. The data were gridded with an octant search routine using the flight line and tie-line data. Grid size used was 500 metres with the grid parallel to the flight lines. For Block 1 the raw grid data were filtered with a polynomial filter of radius 2500 metres set to minimise features up to 1 nT. For Blocks 2, 3 and 4 , two stages of grid filtering were used.The first was as for Block 1 but with a radius of 4000 km. The second stage used a polynomial filter with radius 1000 metres. These filters tidy up the final contour maps without removing features of geological significance.

3.5 Multi-Channel Profiles

Multi-channel profiles were produced for all survey lines at a scale of 1:100 000. The data shown comprised:

Total Magnetic Intensity after network adjustment.
At a scale of 5 nT/cm.

Horizontal gradient of the Total Magnetic Intensity
At a scale of 0.20 nT/data spacing/cm.

Base station magnetic data.
At a scale of 5 nT/cm.

Barometric altimeter data.
At a scale of 25 m/cm.

Pseudo-topography (baro.alt - radar alt.) data.
At a scale of 25 m/cm.

For Blocks 2, 3 and 4, filtered aeromagnetic data were also shown at 5 nT/cm. The filter used in this case was of Gaussian type and had a cutoff wavelength of 7.0 km. This filter was applied to the line data. For these three blocks the horizontal gradient was calculated on the filtered data.

3.6 Spectral Analysis and Matched Filtering

The levelled aeromagnetic data were re-gridded on to a N-S/E-W grid with 500 metre mesh size. The data were gridded in sections corresponding to two map sheets , that is, 30 minutes E-W by 40 minutes N-S. Power spectral plots were computed for each area. See Appendix 1 of the Interpretation Report. The spectral plots have been radially averaged to produce plots which are independent of direction. From analysis of the plots a cutoff wavelength of 7.0 km was selected to apply to the gridded data to separate the deeper magnetic features from the shallower features.The filtered grid was contoured to produce the "deep" component set of maps.This filtered grid was subtracted from the unfiltered grid to produce a "shallow" grid. This new grid was contoured to produce the "shallow" component maps. To ensure continuity in the maps, all the grids included overlap between the gridded areas.

3.7 Upward Continuation

The levelled aeromagnetic data for Block 1 were upward continued by 457 metres to simulate the effect of flying at the same barometric level as Block 2 and reconnaissance Blocks 3 and 4. The upward continuation was performed in the space domain on the original grid (used for the lower level maps).

3.8 Archiving of Data

Archive magnetic tapes were created to include selected data channels for all lines.These tapes were created in standard Exxon format. The channels selected were as follows:

Observed Total Magnetic Intensity

Total Magnetic Intensity after network adjustment.

Barometric altitude.

Radar altitude.

Filtered Total Magnetic Intensity.

Magnetic base station data.

Tape format is included in Appendix 1.

4. ITEMS DELIVERED TO CLIENT

4.1 Total Magnetic Intensity maps at 1:100 000 scale. Contours superimposed on limited topographic detail.

One transparency and two dyeline copies.

4.2 Navigation maps at 1:100 000 scale.

One transparency and two dyeline copies.

4.3 Filtered aeromagnetic contour maps at 1:100 000 scale based on matched filtering.These maps comprise two sets:
(a) "deep" component maps.
(b) "shallow" component maps.

4.4 Upward continuation aeromagnetic maps for Block 1.

4.5 Multi-channel profiles produced on gridded paper at a scale of 1:100 000.

One per flight-line and tie-line.

4.6 Six archive tapes of selected data channels for each flight line and tie line.

4.7 Copies of the Interpretation, Operations and Processing reports.

4.8 All original field data and original computer plots.

A P P E N D I X I

ARCHIVE TAPE FORMAT

ARCHIVE TAPE FORMAT

Six archive tapes were produced in EBCDIC at 1600 bpi in standard Exxon format.

No. of characters in record	160
No. of records in block	40

Printouts of the start of each tape are included in this Appendix.

ARCHIVE OF SOMALIA DATA FOR ESSO EXPLORATION
DATA ACQUIRED BY H.G.G. MAY-AUGUST 1984
NOTE: THE VALUE OF 8888 INDICATES NULL DATA
COLS 1-8 = LINE NUMBER;
COLS 9-15 = FIDUCIAL NUMBER
COLS 16-21 = TIME OF RECORD (HHMMSS)
COLS 22-30 = LATITUDE (DECIMAL DEGREES)
COLS 31-40 = LONGITUDE (DECIMAL DEGREES)
COLS 67-74 = OBSERVED MAGNETIC FIELD (GAMMAS),F8.2;
COLS 75-82 = ADJUSTED MAGNETIC FIELD (GAMMAS),F8.2;
COLS 104-108 = BAROMETRIC ALTITUDE (METRES),I 5;
COLS 109-112 = RADAR ALTITUDE (METRES),I 4;
COLS 153-160 = DIURNAL VARIATION (GAMMAS),F8.2;

```
12-999999HUNT21293SOMALIA EXXON        1  457  23 56 71584 85130   31890 91410   33250     BLOCK 1
12  31890 85130  3.31209  45.47680                                34769.38 4912.09                    468 349
12  31891 85131  3.31249  45.47746                                34769.95 4912.84                    467 346
12  31892 85132  3.31288  45.47813                                34771.41 4913.40                    466 344
12  31893 85133  3.31327  45.47880                                34771.27 4913.84                    465 343
12  31894 85134  3.31366  45.47947                                34771.98 4914.29                    463 342
12  31895 85135  3.31405  45.48014                                34772.52 4914.70                    463 340
12  31896 85136  3.31444  45.48081                                34773.29 4915.05                    462 339
12  31897 85137  3.31483  45.48148                                34773.45 4915.32                    462 340
12  31898 85138  3.31522  45.48215                                34773.59 4915.48                    463 342
12  31899 85139  3.31561  45.48282                                34774.02 4915.59                    465 345
12  31900 85140  3.31600  45.48348                                34774.00 4915.64                    467 347
12  31901 85141  3.31640  45.48415                                34774.05 4915.68                    469 349
12  31902 85142  3.31679  45.48482                                34774.16 4915.79                    471 351
12  31903 85143  3.31718  45.48549                                34774.57 4915.93                    472 352
12  31904 85144  3.31757  45.48616                                34774.86 4916.17                    473 352
12  31905 85145  3.31796  45.48683                                34775.23 4916.49                    473 352
12  31906 85146  3.31835  45.48750                                34775.94 4916.85                    473 351
12  31907 85147  3.31874  45.48817                                34776.34 4917.25                    472 349
12  31908 85148  3.31913  45.48884                                34776.95 4917.71                    470 348
12  31909 85149  3.31952  45.48950                                34777.39 4918.32                    468 347
12  31910 85150  3.31991  45.49017                                34777.78 4919.02                    467 347
12  31911 85151  3.32045  45.49078                                34779.73 4920.31                    467 347
12  31912 8515[illegible]  3.32099  45.49139                      34781.41 4921.68                    [illegible] 348
```

ARCHIVE OF SOMALIA DATA FOR ESSO EXPLORATION
DATA ACQUIRED BY H. G. G. MAY-AUGUST 1984
NOTE: THE VALUE OF 8888 INDICATES NULL DATA
COLS 1-8 = LINE NUMBER;
COLS 9-15 = FIDUCIAL NUMBER
COLS 16-21 = TIME OF RECORD (HHMMSS)
COLS 22-30 = LATITUDE (DECIMAL DEGREES)
COLS 31-40 = LONGITUDE (DECIMAL DEGREES)
COLS 67-74 = OBSERVED MAGNETIC FIELD (GAMMAS),F8. 2;
COLS 75-82 = ADJUSTED MAGNETIC FIELD (GAMMAS),F8. 2;
COLS 104-108 = BAROMETRIC ALTITUDE (METRES),I 5;
COLS 109-112 = RADAR ALTITUDE (METRES),I 4;
COLS 153-160 = DIURNAL VARIATION (GAMMAS),F8. 2;

```
10001-999999HUNT21293SOMALIA EXXON        1  457   1327 52184144440   5308015 310   54190     BLOCK 1
10001  53080144440  3. 52044  46. 66098                          34957. 21 4993. 28                          460 282
10001  53081144441  3. 52098  46. 66054                          34956. 80 4993. 24                          460 287
10001  53082144442  3. 52152  46. 66010                          34956. 73 4993. 18                          462 287
10001  53083144443  3. 52206  46. 65965                          34956. 93 4993. 10                          463 287
10001  53084144444  3. 52260  46. 65921                          34957. 34 4993. 06                          464 286
10001  53085144445  3. 52314  46. 65877                          34956. 59 4993. 01                          465 285
10001  53086144446  3. 52368  46. 65833                          34957. 80 4993. 00                          465 284
10001  53087144447  3. 52422  46. 65789                          34957. 71 4992. 95                          465 284
10001  53088144448  3. 52476  46. 65745                          34956. 80 4992. 93                          466 284
10001  53089144449  3. 52530  46. 65701                          34956. 71 4992. 91                          466 282
10001  53090144450  3. 52584  46. 65657                          34957. 10 4992. 86                          466 281
10001  53091144451  3. 52638  46. 65613                          34956. 86 4992. 86                          466 280
10001  53092144452  3. 52692  46. 65569                          34957. 64 4992. 86                          466 280
10001  53093144453  3. 52745  46. 65524                          34957. 03 4992. 87                          466 278
10001  53094144454  3. 52799  46. 65480                          34957. 43 4992. 89                          466 277
10001  53095144455  3. 52853  46. 65436                          34957. 09 4992. 93                          467 276
10001  53096144456  3. 52907  46. 65392                          34957. 55 4992. 95                          467 276
10001  53097144457  3. 52961  46. 65348                          34959. 39 4992. 95                          466 274
10001  53098144458  3. 53015  46. 65304                          34957. 60 4993. 00                          466 271
10001  53099144459  3. 53069  46. 65260                          34957. 71 4993. 02                          466 268
10001  531001445 0  3. 53123  46. 65216                          34958. 02 4993. 03                          466 265
10001  531011     1  3. 53193  46. 65183                          34959. 94 4993. 04                          466 263
```

```
ARCHIVE OF SOMALIA DATA FOR ESSO EXPLORATION
DATA ACQUIRED BY H.G.G.  MAY-AUGUST 1984
NOTE  THE VALUE OF 8688 INDICATES NULL DATA
COLS 1-8 = LINE NUMBER;
COLS 9-15 = FIDUCIAL NUMBER
COLS 16-21 = TIME OF RECORD (HHMMSS)
COLS 22-30 = LATITUDE (DECIMAL DEGREES)
COLS 31-40 = LONGITUDE (DECIMAL DEGREES)
COLS 67-74 = OBSERVED MAGNETIC FIELD (GAMMAS),F8.2;
COLS 75-82 = ADJUSTED MAGNETIC FIELD (GAMMAS),F8.2;
COLS 104-108 = BAROMETRIC ALTITUDE (METRES),I 5;
COLS 109-112 = RADAR ALTITUDE (METRES),I 4;
COLS 145-152 = FILTERED MAGNETIC FIELD (GAMMAS),F8.2;
COLS 153-160 = DIURNAL VARIATION (GAMMAS),F8.2;
```

```
2131-999999HUNT21293SOMALIA EXXON        1  915  51237 818841343 0   493801347 0   49620     BLOCK 2..KRASOVSKY ELLIPSOID 1940
2131  493801343 0  3.38714  45.43068                          34811.14 4921.74                          912 799
2131  493811343 1  3.38679  45.43012                          34811.07 4921.75                          914 805
2131  493821343 2  3.38644  45.42956                          34810.96 4921.69                          916 806
2131  493831343 3  3.38610  45.42899                          34810.82 4921.61                          918 808
2131  493841343 4  3.38575  45.42843                          34810.46 4921.58                          920 810
2131  493851343 5  3.38540  45.42787                          34810.25 4921.52                          922 812
2131  493861343 6  3.38506  45.42730                          34810.30 4921.48                          923 813
2131  493871343 7  3.38471  45.42674                          34810.39 4921.47                          925 815
2131  493881343 8  3.38436  45.42618                          34809.98 4921.46                          926 816
2131  493891343 9  3.38402  45.42561                          34810.05 4921.46                          927 817
2131  49390134310  3.38367  45.42505                          34809.61 4921.45                          927 815
2131  49391134311  3.38332  45.42449                          34809.59 4921.45                          926 813
2131  49392134312  3.38298  45.42392                          34809.60 4921.48                          924 810
2131  49393134313  3.38263  45.42336                          34809.50 4921.48                          921 806
2131  49394134314  3.38228  45.42280                          34809.71 4921.48                          918 803
2131  49395134315  3.38193  45.42223                          34809.63 4921.49                          915 799
2131  49396134316  3.38159  45.42167                          34809.59 4921.50                          912 798
2131  49397134317  3.38124  45.42111                          34809.60 4921.51                          910 797
2131  49398134318  3.38089  45.42054                          34809.48 4921.50                          909 797
2131  49399134319  3.38055  45.41998                          34809.16 4921.49                          908 797
2131  49400134320  3.38020  45.41942                          34808.98 4921.47                          908 799
2131  49401134321  3.37985  45.41885                          34808.80 4921.45                          908 801
2131  49402134322  3.37951  45.41829                          34808.71 4921.44                          909 801
2131  49403134323  3.37916  45.41772                          34808.66 4921.55                          9   802
```

```
ARCHIVE OF SOMALIA DATA FOR ESSO EXPLORATION
DATA ACQUIRED BY H.G.G.  MAY-AUGUST 1984
NOTE: THE VALUE OF 8888 INDICATES NULL DATA
COLS 1-8 = LINE NUMBER;
COLS 9-15 = FIDUCIAL NUMBER
COLS 16-21 = TIME OF RECORD (HHMMSS)
COLS 22-30 = LATITUDE (DECIMAL DEGREES)
COLS 31-40 = LONGITUDE (DECIMAL DEGREES)
COLS 67-74 = OBSERVED MAGNETIC FIELD (GAMMAS),F8.2;
COLS 75-82 = ADJUSTED MAGNETIC FIELD (GAMMAS),F8.2;
COLS 104-108 = BAROMETRIC ALTITUDE (METRES),I 5;
COLS 109-112 = RADAR ALTITUDE (METRES),I 4;
COLS 145-152 = FILTERED MAGNETIC FIELD (GAMMAS),F8.2;
COLS 153-160 = DIURNAL VARIATION (GAMMAS),F8.2;
```

```
20622-999999HUNT21293SOMALIA EXXON        1  915  23147 7158416 630    57990164120    60080      BLOCK 2..KRASOVSKY ELLIPSOID 1940
20622  5799016 630  4.55419  44.67095                                  8888.00 8888.00                          88888888
20622  5799116 631  4.55363  44.67131                                 34766.13 4785.23                           921 542
20622  5799216 632  4.55307  44.67168                                 34765.25 4784.75                           921 544
20622  5799316 633  4.55250  44.67204                                 34765.36 4784.72                           920 542
20622  5799416 634  4.55194  44.67241                                 34765.78 4784.61                           919 539
20622  5799516 635  4.55138  44.67277                                 34764.87 4784.29                           918 537
20622  5799616 636  4.55081  44.67314                                 34764.80 4784.23                           917 536
20622  5799716 637  4.55025  44.67350                                 34764.55 4784.22                           916 536
20622  5799816 638  4.54969  44.67387                                 34763.84 4784.14                           916 534
20622  5799916 639  4.54912  44.67423                                 34763.37 4783.94                           915 532
20622  5800016 640  4.54856  44.67460                                 34763.93 4784.30                           915 533
20622  5800116 641  4.54800  44.67496                                 34764.80 4784.45                           916 533
20622  5800216 642  4.54744  44.67533                                 34764.91 4784.55                           916 534
20622  5800316 643  4.54687  44.67569                                 34764.64 4784.68                           916 536
20622  5800416 644  4.54631  44.67606                                 34764.53 4784.80                           916 535
20622  5800516 645  4.54575  44.67643                                 34764.95 4784.96                           916 535
20622  5800616 646  4.54518  44.67679                                 34764.98 4785.11                           917 536
20622  5800716 647  4.54462  44.67716                                 34764.88 4785.27                           917 536
20622  5800816 648  4.54406  44.67752                                 34765.39 4785.43                           918 536
20622  5800916 649  4.54349  44.67789                                 34765.03 4785.60                           919 538
20622  5801016 650  4.54293  44.67825                                 34765.00 4785.77                           921 541
20622  5801116 651  4.54230  44.67852                                 34764.78 4785.92                           921 543
20622  5801216 652  4.54168  44.67878                                 34765.80 4786.19                           922 543
20622  5801316 653  4.54105  44.67905                                 34765.70 4786.38                           922 542
20622  5801416      4.54042  44.67931                                 34765.91 4786.57                           921 541
```

```
ARCHIVE OF SOMALIA DATA FOR ESSO EXPLORATION
DATA ACQUIRED BY H.G.G.  MAY-AUGUST 1984
NOTE: THE VALUE OF 8888 INDICATES NULL DATA
COLS 1-8 = LINE NUMBER;
COLS 9-15 = FIDUCIAL NUMBER
COLS 16-21 = TIME OF RECORD (HHMMSS)
COLS 22-30 = LATITUDE (DECIMAL DEGREES)
COLS 31-40 = LONGITUDE (DECIMAL DEGREES)
COLS 67-74 = OBSERVED MAGNETIC FIELD (GAMMAS),F8.2;
COLS 75-82 = ADJUSTED MAGNETIC FIELD (GAMMAS),F8.2;
COLS 104-108 = BAROMETRIC ALTITUDE (METRES),I 5;
COLS 109-112 = RADAR ALTITUDE (METRES),I 4;
COLS 145-152 = FILTERED MAGNETIC FIELD (GAMMAS),F8.2;
COLS 153-160 = DIURNAL VARIATION (GAMMAS),F8.2;
```

```
21501-999999HUNT21293SOMALIA EXXON        1  915  46146 81284102154   37314102850   37730     BLOCK 2..KRASOVSKY ELLIPSOID 1940
21501  37314102154  4.08951  43.07768                          34836.52 4989.57                          915 621
21501  37315102155  4.08896  43.07806                          34836.89 4989.75                          916 623
21501  37316102156  4.08841  43.07843                          34837.14 4989.93                          917 624
21501  37317102157  4.08786  43.07881                          34837.62 4990.12                          919 625
21501  37318102158  4.08731  43.07919                          34837.84 4990.33                          920 626
21501  37319102159  4.08676  43.07957                          34836.95 4990.46                          921 629
21501  373201022 0  4.08621  43.07994                          34837.45 4990.77                          921 631
21501  373211022 1  4.08566  43.08032                          34838.05 4991.01                          921 630
21501  373221022 2  4.08511  43.08070                          34838.21 4991.25                          921 629
21501  373231022 3  4.08456  43.08108                          34838.37 4991.46                          921 629
21501  373241022 4  4.08401  43.08145                          34838.69 4991.69                          921 628
21501  373251022 5  4.08346  43.08183                          34838.91 4991.92                          921 627
21501  373261022 6  4.08291  43.08221                          34839.32 4992.15                          922 629
21501  373271022 7  4.08236  43.08259                          34839.00 4992.32                          922 629
21501  373281022 8  4.08181  43.08297                          34839.30 4992.50                          923 629
21501  373291022 9  4.08126  43.08334                          34839.13 4992.67                          923 630
21501  37330102210  4.08071  43.08372                          34839.85 4992.88                          923 630
21501  37331102211  4.08016  43.08410                          34838.94 4992.98                          922 630
21501  37332102212  4.07961  43.08448                          34839.57 4993.14                          922 629
21501  37333102213  4.07906  43.08485                          34839.52 4993.30                          921 627
21501  37334102214  4.07851  43.08523                          34839.36 4993.46                          921 626
21501  37335102215  4.07796  43.08561                          34839.32 4993.60                          920 625
21501  37336102216    07741  43.08599                          34839.80 4993.80                          92   26
```

ARCHIVE OF SOMALIA DATA FOR ESSO EXPLORATION
DATA ACQUIRED BY H. G. G. MAY-AUGUST 1984
NOTE: THE VALUE OF 8888 INDICATES NULL DATA
COLS 1-8 = LINE NUMBER;
COLS 9-15 = FIDUCIAL NUMBER
COLS 16-21 = TIME OF RECORD (HHMMSS)
COLS 22-30 = LATITUDE (DECIMAL DEGREES)
COLS 31-40 = LONGITUDE (DECIMAL DEGREES)
COLS 67-74 = OBSERVED MAGNETIC FIELD (GAMMAS), F8. 2;
COLS 75-82 = ADJUSTED MAGNETIC FIELD (GAMMAS), F8. 2;
COLS 104-108 = BAROMETRIC ALTITUDE (METRES), I 5;
COLS 109-112 = RADAR ALTITUDE (METRES), I 4;
COLS 145-152 = FILTERED MAGNETIC FIELD (GAMMAS), F8. 2;
COLS 153-160 = DIURNAL VARIATION (GAMMAS), F8. 2;

```
22301-999999HUNT21293SOMALIA EXXON        1  915  34326 72784113550   41750114750   42470     BLOCK 2..KRASOVSKY ELLIPSOID 1940
22301  41750113550  2.96476  42.09797                                34603.25 4985.48                          907 551
22301  41751113551  2.96540  42.09752                                34603.55 4985.59                          908 546
22301  41752113552  2.96604  42.09707                                34603.68 4985.68                          910 544
22301  41753113553  2.96668  42.09663                                34603.75 4985.76                          912 545
22301  41754113554  2.96733  42.09618                                34604.04 4985.85                          914 547
22301  41755113555  2.96797  42.09573                                34603.96 4985.92                          915 548
22301  41756113556  2.96861  42.09528                                34603.98 4986.00                          916 548
22301  41757113557  2.96925  42.09483                                34604.34 4986.08                          916 547
22301  41758113558  2.96989  42.09438                                34603.96 4986.14                          915 546
22301  41759113559  2.97053  42.09393                                34604.34 4986.24                          914 544
22301  417601136 0  2.97117  42.09348                                34604.64 4986.32                          913 542
22301  417611136 1  2.97182  42.09303                                34604.64 4986.39                          913 541
22301  417621136 2  2.97246  42.09258                                34605.27 4986.49                          912 542
22301  417631136 3  2.97310  42.09213                                34605.27 4986.58                          912 543
22301  417641136 4  2.97374  42.09168                                34605.39 4986.68                          913 545
22301  417651136 5  2.97438  42.09123                                34605.16 4986.76                          913 548
22301  417661136 6  2.97502  42.09078                                34605.28 4986.86                          913 551
22301  417671136 7  2.97567  42.09033                                34605.96 4986.96                          914 554
22301  417681136 8  2.97631  42.08988                                34606.13 4987.06                          915 557
22301  417691136 9  2.97695  42.08943                                34606.07 4987.15                          915 559
22301  41770113610  2.97759  42.08898                                34606.50 4987.25                          916 562
22301  41771113611  2.97823  42.08853                                34606.21 4987.35                          916 563
22301  41772113612     97887  42.08808                                34606.66 4987.43                          9   563
```

A P P E N D I X 2

LINE INDEX

LINE	BEAR	FLT	DATE	KMS
1/2	57	23	15/ 7/84	124.2
2/2	237	23	15/ 7/84	136.3
3/1	57	22	14/ 7/84	137.0
4/2	57	23	15/ 7/84	136.9
5/1	237	23	15/ 7/84	136.2
6/1	57	23	15/ 7/84	137.4
7/1	237	23	15/ 7/84	136.5
8/1	57	23	15/ 7/84	138.0
9/1	237	23	15/ 7/84	136.6
10/1	57	23	15/ 7/84	136.5
11/1	237	23	15/ 7/84	136.1
12/1	57	23	15/ 7/84	138.1
13/1	237	23	15/ 7/84	137.2
14/1	57	23	15/ 7/84	76.5
14/2	57	24	16/ 7/84	65.0
15/1	237	23	15/ 7/84	77.0
15/2	237	24	16/ 7/84	63.5
16/1	57	24	16/ 7/84	62.0
16/2	57	24	16/ 7/84	77.2
17/1	237	24	16/ 7/84	136.6
18/1	57	24	16/ 7/84	137.1
19/1	237	24	16/ 7/84	76.2
19/2	237	24	16/ 7/84	62.4
20/1	57	24	16/ 7/84	62.5
20/2	57	24	16/ 7/84	76.0
21/1	237	24	16/ 7/84	137.2
22/1	57	25	17/ 7/84	136.9
23/1	237	25	17/ 7/84	137.0
24/1	57	25	17/ 7/84	137.4
25/1	237	25	17/ 7/84	30.5
25/2	237	25	17/ 7/84	47.8
26/1	57	25	17/ 7/84	28.9
27/1	57	25	17/ 7/84	21.8
102/1	57	1	21/ 5/84	61.9
103/1	57	2	22/ 5/84	117.8
104/1	237	1	21/ 5/84	118.4
105/2	57	4	23/ 5/84	119.9
106/1	237	4	23/ 5/84	119.2
107/1	57	5	24/ 5/84	120.2
108/1	237	5	24/ 5/84	62.8
108/2	237	5	24/ 5/84	61.0
109/1	57	11	28/ 6/84	124.4
110/1	237	11	28/ 6/84	120.8
111/1	57	11	28/ 6/84	120.9
112/1	237	11	28/ 6/84	130.5
113/1	57	11	28/ 6/84	142.5
114/1	237	11	28/ 6/84	135.6
115/1	57	11	28/ 6/84	135.4
116/1	237	11	28/ 6/84	136.2
117/1	57	11	28/ 6/84	136.3
118/1	237	11	28/ 6/84	136.9
119/1	57	11	28/ 6/84	50.2
119/2	57	11	28/ 6/84	78.6

120/1	237	11	28/ 6/84	135.6
121/1	57	11	28/ 6/84	136.4
122/1	237	11	28/ 6/84	136.3
123/1	57	12	29/ 6/84	136.8
124/1	237	12	29/ 6/84	135.8
125/1	57	12	29/ 6/84	137.1
126/1	237	12	29/ 6/84	136.2
127/1	57	12	29/ 6/84	135.7
128/1	237	12	29/ 6/84	74.6
128/2	237	14	7/ 7/84	65.7
129/1	57	12	29/ 6/84	136.1
130/1	237	12	29/ 6/84	136.1
131/1	57	12	29/ 6/84	136.2
132/1	237	12	29/ 6/84	137.0
133/1	57	12	29/ 6/84	136.4
134/1	237	12	29/ 6/84	136.2
135/1	237	10	27/ 6/84	45.8
135/3	237	13	6/ 7/84	33.0
136/1	57	10	27/ 6/84	29.5
136/3	57	13	6/ 7/84	28.4
137/2	237	25	17/ 7/84	22.8
138/2	237	25	17/ 7/84	15.4
213/1	237	51	18/ 8/84	16.2
214/1	57	51	18/ 8/84	24.4
215/1	237	51	18/ 8/84	33.7
216/1	57	51	18/ 8/84	47.8
217/1	237	51	18/ 8/84	56.3
218/1	57	37	31/ 7/84	50.5
218/2	57	51	18/ 8/84	66.1
219/1	237	37	31/ 7/84	97.8
219/2	237	51	18/ 8/84	74.8
220/1	57	37	31/ 7/84	112.8
220/2	327	51	18/ 8/84	83.4
221/1	57	38	2/ 8/84	125.4
221/2	147	51	18/ 8/84	89.5
221/3	57	52	19/ 8/84	247.5
222/1	237	38	2/ 8/84	139.6
222/2	327	51	18/ 8/84	101.0
223/1	57	36	20/ 7/84	155.6
223/2	237	52	19/ 8/84	117.1
224/1	237	19	11/ 7/84	57.7
224/2	237	36	20/ 7/84	120.3
224/3	237	36	20/ 7/84	55.6
224/4	57	52	19/ 8/84	70.8
225/1	57	19	11/ 7/84	69.0
225/2	57	19	11/ 7/84	437.8
226/1	237	19	11/ 7/84	508.7
227/1	237	17	9/ 7/84	505.6
228/1	237	14	7/ 7/84	502.7
229/1	57	14	7/ 7/84	472.5
229/2	57	17	9/ 7/84	28.0
230/1	237	15	8/ 7/84	218.7
230/2	237	16	8/ 7/84	279.8
231/1	57	16	8/ 7/84	491.2
232/1	57	17	9/ 7/84	488.0
233/1	237	18	10/ 7/84	482.7

234/1	237	27	20/ 7/84	480.7
235/1	57	27	20/ 7/84	61.7
235/2	237	28	21/ 7/84	415.9
236/1	237	29	22/ 7/84	473.6
237/1	57	29	22/ 7/84	74.9
237/2	237	30	23/ 7/84	399.2
238/1	237	25	17/ 7/84	128.4
238/2	237	44	9/ 8/84	46.2
238/3	237	25	17/ 7/84	295.3
239/1	237	31	24/ 7/84	456.5
240/1	57	31	24/ 7/84	98.4
240/2	237	32	25/ 7/84	44.5
240/3	237	32	25/ 7/84	301.3
241/1	57	25	17/ 7/84	40.3
241/2	237	33	26/ 7/84	392.6
242/1	57	33	26/ 7/84	106.2
242/2	237	34	27/ 7/84	86.0
242/3	237	34	27/ 7/84	235.8
243/1	237	35	28/ 7/84	410.5
244/1	57	35	28/ 7/84	166.8
244/2	147	36	20/ 7/84	239.5
245/1	237	39	4/ 8/84	401.0
246/1	57	39	4/ 8/84	152.5
246/2	237	40	5/ 8/84	253.5
247/1	57	36	20/ 7/84	116.3
247/2	237	38	2/ 8/84	231.4
248/1	237	36	20/ 7/84	190.6
248/2	237	47	13/ 8/84	93.3
249/1	57	36	20/ 7/84	173.5
249/2	57	47	13/ 8/84	76.5
250/1	237	36	20/ 7/84	120.0
251/1	57	36	20/ 7/84	87.8
501/1	57	24	16/ 7/84	105.5
502/1	270	52	19/ 8/84	141.7
503/1	227	37	31/ 7/84	83.1
504/1	270	37	31/ 7/84	107.9
505/1	227	52	19/ 8/84	364.6
506/1	270	52	19/ 8/84	117.3
507/1	90	52	19/ 8/84	109.9
508/1	47	52	19/ 8/84	106.0
1000/1	327	1	21/ 5/84	93.6
1000/2	327	13	6/ 7/84	116.5
1001/1	147	1	21/ 5/84	200.4
1002/1	327	1	21/ 5/84	203.8
1003/1	147	1	21/ 5/84	204.4
1004/1	327	1	21/ 5/84	205.7
1005/1	147	1	21/ 5/84	200.6
1006/1	327	1	21/ 5/84	124.6
1006/2	327	13	6/ 7/84	83.0
1007/1	147	1	21/ 5/84	104.2
1007/3	147	13	6/ 7/84	21.4
1007/4	147	13	6/ 7/84	87.9
1008/1	327	1	21/ 5/84	62.8
1008/3	327	13	6/ 7/84	147.7
1009/1	147	1	21/ 5/84	208.7
1010/1	327	2	22/ 5/84	87.7

1010/2	147	13	6/ 7/84	124.5
1011/1	147	2	22/ 5/84	97.3
1011/2	147	13	6/ 7/84	87.5
1011/3	147	13	6/ 7/84	25.9
1012/1	327	2	22/ 5/84	153.7
1012/2	327	13	6/ 7/84	47.9
1013/1	147	2	22/ 5/84	137.7
1013/2	327	13	6/ 7/84	69.3
1014/1	327	2	22/ 5/84	199.5
1015/1	147	2	22/ 5/84	68.9
1015/2	147	2	22/ 5/84	134.8
1016/1	327	2	22/ 5/84	52.6
1016/2	327	13	6/ 7/84	86.3
1016/3	327	2	22/ 5/84	61.8
1017/1	147	2	22/ 5/84	195.5
1018/1	327	4	23/ 5/84	194.5
1019/1	147	4	23/ 5/84	194.2
1020/1	327	4	23/ 5/84	195.1
1021/1	147	4	23/ 5/84	194.6
1022/1	327	4	23/ 5/84	195.5
1023/1	147	4	23/ 5/84	193.6
1024/1	327	4	23/ 5/84	193.8
1025/1	147	4	23/ 5/84	193.3
1026/1	327	5	24/ 5/84	195.7
1027/1	147	5	24/ 5/84	196.3
1028/1	327	5	24/ 5/84	195.9
1029/1	147	5	24/ 5/84	195.7
1030/1	327	5	24/ 5/84	195.6
1031/1	147	5	24/ 5/84	68.2
1031/2	147	13	6/ 7/84	138.1
1032/1	327	5	24/ 5/84	195.5
1033/1	147	5	24/ 5/84	195.6
1034/1	327	5	24/ 5/84	197.1
1035/1	147	5	24/ 5/84	195.6
1036/1	147	6	25/ 5/84	195.5
1037/1	327	6	25/ 5/84	195.9
1038/1	147	6	25/ 5/84	196.6
1039/1	327	6	25/ 5/84	197.5
1040/1	147	6	25/ 5/84	88.1
1040/2	147	10	27/ 6/84	100.9
1041/1	147	7	24/ 6/84	93.6
1041/2	147	7	24/ 6/84	101.4
1042/1	327	7	24/ 6/84	203.3
1043/1	147	7	24/ 6/84	201.4
1044/2	327	10	27/ 6/84	79.0
1044/3	147	13	6/ 7/84	128.6
1045/1	147	10	27/ 6/84	137.3
1045/2	147	24	16/ 7/84	70.7
1046/1	327	10	27/ 6/84	205.6
1047/1	147	8	25/ 6/84	91.7
1047/2	147	10	27/ 6/84	117.5
1048/1	327	8	25/ 6/84	91.3
1048/2	327	10	27/ 6/84	119.8
1049/1	147	8	25/ 6/84	209.3
1050/1	327	8	25/ 6/84	211.4
1051/1	147	8	25/ 6/84	211.6

1052/1	327	8	25/ 6/84	213.2
1053/1	147	8	25/ 6/84	212.8
1054/1	327	8	25/ 6/84	215.0
1055/1	147	8	25/ 6/84	216.6
1056/1	327	7	24/ 6/84	75.1
1056/2	327	7	24/ 6/84	46.9
1056/3	327	13	6/ 7/84	112.3
1056/4	327	24	16/ 7/84	62.2
1057/1	327	6	25/ 5/84	217.2
1058/1	327	8	25/ 6/84	206.9
1059/1	327	9	26/ 6/84	186.5
1060/1	147	9	26/ 6/84	161.8
1061/1	327	9	26/ 6/84	164.6
1062/1	147	9	26/ 6/84	161.0
1063/1	327	9	26/ 6/84	160.3
1064/1	147	9	26/ 6/84	161.1
1065/1	327	9	26/ 6/84	164.9
1066/1	147	9	26/ 6/84	161.1
1067/1	327	9	26/ 6/84	165.5
2062/2	147	23	15/ 7/84	161.4
2063/2	327	25	17/ 7/84	161.1
2064/1	327	24	16/ 7/84	160.3
2065/1	147	27	20/ 7/84	41.8
2065/2	327	28	21/ 7/84	125.4
2066/1	327	27	20/ 7/84	165.2
2067/1	327	29	22/ 7/84	148.0
2067/4	147	44	9/ 8/84	18.1
2068/1	147	9	26/ 6/84	164.3
2069/1	327	9	26/ 6/84	161.2
2070/1	147	9	26/ 6/84	158.9
2071/1	147	12	29/ 6/84	163.2
2072/1	327	30	23/ 7/84	57.3
2072/3	327	44	9/ 8/84	108.0
2073/1	327	31	24/ 7/84	58.7
2073/2	147	44	9/ 8/84	107.6
2074/1	327	31	24/ 7/84	91.0
2074/2	327	44	9/ 8/84	53.8
2074/3	147	51	18/ 8/84	21.7
2075/1	327	32	25/ 7/84	67.4
2075/2	327	44	9/ 8/84	97.7
2076/1	327	33	26/ 7/84	164.7
2077/1	327	34	27/ 7/84	166.8
2078/1	327	35	28/ 7/84	164.6
2079/1	327	36	20/ 7/84	162.0
2080/1	327	40	5/ 8/84	166.7
2081/1	327	51	18/ 8/84	189.7
2082/1	147	51	18/ 8/84	187.9
2083/1	327	51	18/ 8/84	188.3
2084/1	147	50	16/ 8/84	104.0
2084/2	147	51	18/ 8/84	84.6
2085/1	327	50	16/ 8/84	103.7
2085/2	327	51	18/ 8/84	85.4
2086/1	147	50	16/ 8/84	179.1
2087/1	327	50	16/ 8/84	179.6
2088/1	147	50	16/ 8/84	153.5
2088/2	147	51	18/ 8/84	31.0

2089/1	327	50	16/ 8/84	153.0
2089/2	327	51	18/ 8/84	29.7
2090/1	327	38	2/ 8/84	172.7
2091/1	327	39	4/ 8/84	171.9
2092/1	147	50	16/ 8/84	173.3
2093/1	327	50	16/ 8/84	172.8
2094/1	147	50	16/ 8/84	176.7
2095/1	327	50	16/ 8/84	172.7
2096/1	147	50	16/ 8/84	170.8
2097/1	327	50	16/ 8/84	171.2
2098/1	147	50	16/ 8/84	171.8
2099/1	327	50	16/ 8/84	167.8
2100/1	327	49	15/ 8/84	172.6
2101/1	147	49	15/ 8/84	164.4
2102/1	147	49	15/ 8/84	168.7
2103/1	327	49	15/ 8/84	162.9
2104/1	147	49	15/ 8/84	168.2
2105/1	327	49	15/ 8/84	165.7
2106/1	147	49	15/ 8/84	170.5
2107/1	327	49	15/ 8/84	170.1
2108/1	147	49	15/ 8/84	169.4
2109/1	327	49	15/ 8/84	168.1
2110/1	147	49	15/ 8/84	45.7
2110/2	147	49	15/ 8/84	110.6
2111/1	327	49	15/ 8/84	100.2
2111/2	327	49	15/ 8/84	46.6
2112/1	147	48	14/ 8/84	104.0
2112/2	327	49	15/ 8/84	45.4
2113/1	327	48	14/ 8/84	111.1
2113/2	147	49	15/ 8/84	46.2
2114/1	327	48	14/ 8/84	160.7
2115/1	147	48	14/ 8/84	160.6
2116/1	327	48	14/ 8/84	183.7
2117/1	147	48	14/ 8/84	184.2
2118/1	147	48	14/ 8/84	163.1
2119/1	327	48	14/ 8/84	162.3
2120/1	147	48	14/ 8/84	162.3
2121/1	327	48	14/ 8/84	155.3
2122/1	147	48	14/ 8/84	155.0
2123/1	327	48	14/ 8/84	155.0
2124/1	147	48	14/ 8/84	156.0
2125/1	327	48	14/ 8/84	189.6
2126/1	147	47	13/ 8/84	166.9
2126/2	147	48	14/ 8/84	23.4
2127/1	327	47	13/ 8/84	130.3
2127/2	327	48	14/ 8/84	23.6
2128/1	147	47	13/ 8/84	150.1
2129/1	327	47	13/ 8/84	152.3
2130/1	327	47	13/ 8/84	152.2
2131/1	147	47	13/ 8/84	94.6
2131/2	147	47	13/ 8/84	60.5
2132/1	147	47	13/ 8/84	152.8
2133/1	327	47	13/ 8/84	117.4
2133/2	327	47	13/ 8/84	39.8
2134/1	147	47	13/ 8/84	150.1
2135/1	327	47	13/ 8/84	82.9

2135/2	327	47	13/ 8/84	99.6
2136/1	147	47	13/ 8/84	99.5
2136/2	147	47	13/ 8/84	83.0
2137/1	327	47	13/ 8/84	150.2
2138/1	147	46	12/ 8/84	150.1
2139/1	327	46	12/ 8/84	148.0
2140/1	147	46	12/ 8/84	150.4
2141/1	327	46	12/ 8/84	149.2
2142/1	147	46	12/ 8/84	148.2
2143/1	327	46	12/ 8/84	148.3
2144/1	327	46	12/ 8/84	182.9
2145/1	147	46	12/ 8/84	179.9
2146/1	147	46	12/ 8/84	139.4
2147/1	327	46	12/ 8/84	139.3
2148/1	327	46	12/ 8/84	137.2
2149/1	147	46	12/ 8/84	137.6
2150/1	147	46	12/ 8/84	31.1
2150/2	147	46	12/ 8/84	93.0
2151/1	327	46	12/ 8/84	94.4
2151/2	327	46	12/ 8/84	30.3
2152/1	147	45	11/ 8/84	135.4
2153/1	327	44	9/ 8/84	65.9
2153/2	327	45	11/ 8/84	116.6
2154/1	147	44	9/ 8/84	180.0
2155/1	327	44	9/ 8/84	136.0
2156/1	147	43	8/ 8/84	46.4
2156/2	147	44	9/ 8/84	94.2
2157/1	327	43	8/ 8/84	45.3
2157/2	327	44	9/ 8/84	93.8
2158/1	147	43	8/ 8/84	136.7
2159/1	327	43	8/ 8/84	136.9
2160/1	147	43	8/ 8/84	136.8
2161/1	327	43	8/ 8/84	137.0
2162/1	147	43	8/ 8/84	145.7
2163/1	327	43	8/ 8/84	195.4
2164/1	147	43	8/ 8/84	196.2
2165/1	147	43	8/ 8/84	147.2
2166/1	327	43	8/ 8/84	145.7
2167/1	147	43	8/ 8/84	147.9
2168/1	327	43	8/ 8/84	147.6
2169/1	327	43	8/ 8/84	148.2
2170/1	147	42	7/ 8/84	65.1
2170/2	327	43	8/ 8/84	87.6
2171/1	327	42	7/ 8/84	63.0
2171/2	147	43	8/ 8/84	87.6
2172/1	327	42	7/ 8/84	199.8
2173/1	147	42	7/ 8/84	199.3
2174/1	147	42	7/ 8/84	147.5
2175/1	327	42	7/ 8/84	146.5
2176/1	327	42	7/ 8/84	146.0
2177/1	147	42	7/ 8/84	153.1
2178/1	147	42	7/ 8/84	152.8
2179/1	327	42	7/ 8/84	153.9
2180/1	147	42	7/ 8/84	153.5
2181/1	327	41	6/ 8/84	207.6
2182/1	147	41	6/ 8/84	207.2

2183/1	327	42	7/ 8/84	136.5
2184/1	147	42	7/ 8/84	136.8
2185/1	327	42	7/ 8/84	137.8
2186/1	327	41	6/ 8/84	159.1
2187/1	147	41	6/ 8/84	159.4
2188/1	327	41	6/ 8/84	159.0
2189/1	147	41	6/ 8/84	159.4
2190/1	327	41	6/ 8/84	216.9
2191/1	147	41	6/ 8/84	218.7
2192/1	327	41	6/ 8/84	161.5
2193/1	147	41	6/ 8/84	161.0
2194/2	327	41	6/ 8/84	161.2
2195/1	147	40	5/ 8/84	161.6
2196/1	327	40	5/ 8/84	160.8
2197/1	147	40	5/ 8/84	159.0
2198/1	327	40	5/ 8/84	158.9
2199/1	147	40	5/ 8/84	159.7
2200/1	327	40	5/ 8/84	222.0
2201/1	147	40	5/ 8/84	222.2
2202/1	147	39	4/ 8/84	49.9
2202/2	327	40	5/ 8/84	113.0
2203/2	147	40	5/ 8/84	114.0
2203/3	147	44	9/ 8/84	50.4
2204/1	327	39	4/ 8/84	160.4
2205/1	147	39	4/ 8/84	160.0
2206/1	147	39	4/ 8/84	159.5
2207/1	327	39	4/ 8/84	159.2
2208/1	147	39	4/ 8/84	159.5
2209/1	327	38	2/ 8/84	88.6
2209/2	327	39	4/ 8/84	135.7
2210/1	147	38	2/ 8/84	37.7
2210/2	147	39	4/ 8/84	135.4
2210/3	147	38	2/ 8/84	58.1
2211/1	147	38	2/ 8/84	112.9
2211/2	327	39	4/ 8/84	31.9
2212/1	327	38	2/ 8/84	110.8
2212/2	147	39	4/ 8/84	32.7
2213/1	147	38	2/ 8/84	112.2
2213/2	327	39	4/ 8/84	32.1
2214/1	327	38	2/ 8/84	112.2
2214/2	147	39	4/ 8/84	31.4
2215/1	327	36	20/ 7/84	152.7
2216/1	147	36	20/ 7/84	152.2
2217/1	147	35	28/ 7/84	138.7
2217/2	327	36	20/ 7/84	14.9
2218/1	327	35	28/ 7/84	163.8
2219/1	147	35	28/ 7/84	229.4
2220/1	327	35	28/ 7/84	230.2
2221/1	147	34	27/ 7/84	61.4
2221/2	147	35	28/ 7/84	103.1
2222/1	327	34	27/ 7/84	68.2
2222/2	327	35	28/ 7/84	101.8
2223/1	147	34	27/ 7/84	169.4
2223/2	147	38	2/ 8/84	27.3
2224/1	327	34	27/ 7/84	106.0
2224/2	147	38	2/ 8/84	69.0

2225/1	147	34	27/ 7/84	169.2
2226/1	327	34	27/ 7/84	176.5
2227/1	147	34	27/ 7/84	179.2
2228/1	327	34	27/ 7/84	230.1
2229/1	147	34	27/ 7/84	223.1
2230/1	327	34	27/ 7/84	63.5
2230/2	147	35	28/ 7/84	123.6
2231/1	147	33	26/ 7/84	76.9
2231/2	327	34	27/ 7/84	110.5
2232/1	327	33	26/ 7/84	78.2
2232/2	147	34	27/ 7/84	49.4
2232/3	147	34	27/ 7/84	62.6
2233/1	147	33	26/ 7/84	189.1
2234/1	327	33	26/ 7/84	186.2
2235/1	147	33	26/ 7/84	187.9
2236/1	327	33	26/ 7/84	188.5
2237/2	147	33	26/ 7/84	219.6
2238/1	147	32	25/ 7/84	74.2
2238/2	327	33	26/ 7/84	99.7
2238/3	327	38	2/ 8/84	15.5
2238/4	327	33	26/ 7/84	40.6
2239/1	327	32	25/ 7/84	76.2
2239/2	147	33	26/ 7/84	100.3
2239/3	147	38	2/ 8/84	15.4
2240/1	147	32	25/ 7/84	184.5
2241/1	327	32	25/ 7/84	183.0
2242/1	147	32	25/ 7/84	183.1
2243/1	327	32	25/ 7/84	186.5
2244/1	147	32	25/ 7/84	183.8
2245/1	327	32	25/ 7/84	185.3
2246/1	147	32	25/ 7/84	182.2
2246/2	327	31	24/ 7/84	44.4
2247/1	147	31	24/ 7/84	224.7
2248/1	327	31	24/ 7/84	188.0
2249/1	147	31	24/ 7/84	182.7
2250/1	327	31	24/ 7/84	181.5
2251/1	147	31	24/ 7/84	185.2
2252/1	327	31	24/ 7/84	185.5
2253/1	147	31	24/ 7/84	135.1
2253/2	327	32	25/ 7/84	53.1
2254/1	147	30	23/ 7/84	185.6
2255/1	327	30	23/ 7/84	223.1
2256/1	147	30	23/ 7/84	217.5
2257/1	327	30	23/ 7/84	180.2
2258/1	147	30	23/ 7/84	77.0
2258/2	147	30	23/ 7/84	106.0
2259/1	147	29	22/ 7/84	101.2
2259/2	327	30	23/ 7/84	83.4
2260/1	327	29	22/ 7/84	98.9
2260/2	147	30	23/ 7/84	81.9
2261/1	147	29	22/ 7/84	180.4
2262/1	327	29	22/ 7/84	180.9
2263/1	147	29	22/ 7/84	180.7
2264/1	327	29	22/ 7/84	218.2
2265/1	147	29	22/ 7/84	159.4
2265/2	327	30	23/ 7/84	19.8

2265/3	327	30	23/ 7/84	44.4
2266/1	147	28	21/ 7/84	179.2
2267/1	147	28	21/ 7/84	178.6
2268/1	327	28	21/ 7/84	178.8
2269/1	147	27	20/ 7/84	175.3
2270/1	327	28	21/ 7/84	177.7
2271/1	327	27	20/ 7/84	175.6
2272/1	147	27	20/ 7/84	177.0
2273/1	327	27	20/ 7/84	175.3
2274/1	147	27	20/ 7/84	172.7
2275/1	327	25	17/ 7/84	172.0
2276/1	327	27	20/ 7/84	68.6
2276/2	147	28	21/ 7/84	104.2
2277/1	147	25	17/ 7/84	39.6
2277/2	147	25	17/ 7/84	105.0
2277/3	327	36	20/ 7/84	20.4
2277/4	147	36	20/ 7/84	31.8
2278/1	327	19	11/ 7/84	41.7
2278/2	147	25	17/ 7/84	126.2
2279/1	147	19	11/ 7/84	166.1
2280/1	327	19	11/ 7/84	165.7
2281/1	147	19	11/ 7/84	156.7
2282/1	327	19	11/ 7/84	151.3
2283/1	147	19	11/ 7/84	147.0
2284/1	327	19	11/ 7/84	142.6
2285/1	147	18	10/ 7/84	138.7
2286/1	327	18	10/ 7/84	134.6
2287/1	147	18	10/ 7/84	132.1
2288/1	327	18	10/ 7/84	126.9
2289/1	147	18	10/ 7/84	121.6
2290/1	327	18	10/ 7/84	118.0
2291/1	147	18	10/ 7/84	114.5
2292/1	327	18	10/ 7/84	108.0
2293/1	147	18	10/ 7/84	103.2
2294/1	327	18	10/ 7/84	100.3
2295/1	147	17	9/ 7/84	40.6
2295/2	147	18	10/ 7/84	56.0
2296/1	327	17	9/ 7/84	90.6
2297/1	147	14	7/ 7/84	49.0
2297/2	147	17	9/ 7/84	40.9
2298/1	327	14	7/ 7/84	85.1
2299/1	147	14	7/ 7/84	75.7
2300/1	327	14	7/ 7/84	69.9
2301/1	147	14	7/ 7/84	69.2
2302/1	327	14	7/ 7/84	64.3
2303/1	147	14	7/ 7/84	58.0
2304/1	327	14	7/ 7/84	56.5
2305/1	147	14	7/ 7/84	50.1
2306/1	327	14	7/ 7/84	45.8
2307/1	147	14	7/ 7/84	39.4
2308/1	327	14	7/ 7/84	32.5
2309/1	147	14	7/ 7/84	31.5
2310/1	327	14	7/ 7/84	25.8
2311/1	147	14	7/ 7/84	25.6
2312/1	327	14	7/ 7/84	18.8
2313/1	147	14	7/ 7/84	19.9

4000/1	180	37	31/ 7/84	49.3
4001/1	360	37	31/ 7/84	48.3
4002/1	360	37	31/ 7/84	43.9
4003/1	180	37	31/ 7/84	44.1
4004/1	360	37	31/ 7/84	43.8
4005/1	180	37	31/ 7/84	44.4
4006/1	360	37	31/ 7/84	47.1
4007/1	180	37	31/ 7/84	47.2
4008/2	180	37	31/ 7/84	47.7
4009/2	360	37	31/ 7/84	46.8
4010/1	360	37	31/ 7/84	47.0
4011/1	180	37	31/ 7/84	47.8

TOTAL = 76616.8